Development of Dendritic Cells in the Intestine

Tamsin Florencia Pamela Zangerle Murray

BSc., MRes.

A thesis submitted to the College of Medicine, Veterinary and Life Sciences, University of Glasgow in fulfilment of the requirements for the degree of Doctor of Philosophy.

May 2016

Institute of Infection, Immunity and Inflammation
University of Glasgow
120 University Place
Glasgow, G12 8TA

Acknowledgements

If there is anything in life that makes you appreciate the support you have, it is doing a PhD…oh and losing a parent! These last few years would not have been possible without the people mentioned below, as well as many more that have given a few words of encouragement along the way. And so, to begin with I must thank Allan Mowat, my supervisor – it was a slow start for both of us, but I think we got there in the end! Thank you for all of your advice and support, the amount of your time spent reading and correcting this thesis, and for all of the encouragement you have given. I realise that your support will continue for years to come, and I just hope that I have been an acceptable final PhD student!

Thank you to 'The Mowlings' (Mowats & Millings) both past and present. Simon Milling, thank you for being my supervisor in waiting and operating an open doors policy for when I ever needed to speak to you. Charlie, thank you for passing me the reins, if a little reluctantly, in the final year of your PhD – I learnt a lot from your determination and drive. You set me up in the lab and were there for me when I needed it (most memorably after my first lab meeting). Also, many thanks for reading over my SIRPα chapter. Calum, you pocket genius! There was never a moment where you failed to bring a smile to my face, be it with words of encouragement, making me remember how to compensate properly, crazy mad jokes, or putting up with my singing. Your patience and guidance will not go unnoticed in the future. Thanks also for reading Chapter 5! Alberto, gracias por su apoyo y amabilidad; y para la comprensión de mis emociones Latina! Thank you to Vuk, Carolyn, Stephanie and Pamela for reading over my chapters and for all of your support over the years, and thank you Carolyn for getting me through some tough times. Ashley Gilmore, Lizzie, Hannah, Ashok, Jennifer, Lotta, Verena, Johannes and Anika, thank you for making everyday a fun day.

Thanks to everyone in the department, especially Megan MacLeod, for your advice and words of wisdom, as well as giving me courage in meeting speakers and not fearing that I would talk about my dreams! Thanks to all the CRF staff for looking after my timed breeders, as I know they were a bit of a headache. Thank you Diane

Vaughan for all of your help in the Flow Facility and putting me forward for the amazing opportunity to go to BD, Erembodegem for the Aria III training course. Thank you Oliver Pabst for the opportunity to do some lovely histology in your lab, though sadly I could never get the technique quite as nice in Glasgow. Thanks also to Lindsay Hall and Christoph Muller for providing me with mice, and thank you Joanne Konkel for employing me as a post-doc before getting the PhD, as well as for your patience over the last few months.

I am indebted to Darren Monkton and Olwyn Byron for seeing potential in me and for their continued support as I carried out my Wellcome Trust (to whom I am also grateful) funded PhD. Thank you also to Bill Cushley, for all of our chats and pep talks. You have been a great help through these years. Also, many thanks to the BSI for providing me with the travel grant that got me my job!!

Now to the family: Mum, you are the strongest person I know. Thank you for supporting me through the emotional rollercoaster that has been the last five years. If losing Dad so tragically on the day I was awarded this PhD wasn't bad enough, then the continued battle with grief and the stress of the PhD really did test me, but you were there every step of the way, unwavering and supportive, but more than happy to give me a kick up the bum when it was required. Papá, te haces un lío con esto bueno y adecuado para mí, pero creo que estaría orgulloso de lo que he logrado en su ausencia. Carise, thank you for being a great little sister! And to all of my Aunties, Uncles and Cousins and Abuela, both in Europe and Argentina, knowing you are all there for me has kept me going. Thanks to the Kennys and Brian as well.

Thank you to all of my friends: Hannah Kelly, my best of friends for your beautiful cynicism and a bed in London when I had conferences to attend, Katie Percival for your charming and sunny smile, Siubhan MacDonald for your calming elegance, and all of my other University of Bristol friends. Matthew Lakins and Amy Sawtell, thank you for everything. Hannah Wessel, your love has been invaluable; Lizzie Mann, the laughs too much; Ruth McCartney, you are wise beyond your years; and Pamela Wright, you are a star! Thank you also to Marcia Blagg – your friendship has been treasured, and thanks for your help with my introduction figures. I am sure I have

forgotten people, but to you all, I am forever in your debt for giving me the strength to finish the PhD.

And finally, Michael Kenny: Thanks for the gin! No really, thank you Mike for putting up with me over the last few years. It can't have been easy and it must take the patience of a saint to deal with me, even on a good day! You know how much you mean to me and although we have had our own stresses to deal with, you have never stopped supporting or loving me, and for that I am truly grateful. There are no words to thank you enough, so instead of rambling on any further I will leave it there.

And now to learn some Spanish, a promise I have made to mi Papa…

Table of Contents

List of Tables and Figures

Author's declaration

I declare that all the experimental data contained in this thesis are the result of my own work, with the following exceptions of the microarray experiments which were carried out by Dr Charlotte Scott (University of Glasgow and VIB, Ghent) and analysed by Drs Marc Dalod (CIML, Marseille) and Carolyn Thomson (University of Glasgow); the initial experiment on Trem-1$^{-/-}$ mice was performed by Dr Leslie Saurer in Professor Christoph Mueller's group at the University of Bern, while the microbiome analysis of germ free mice by 16S RNA sequencing was carried out by Dr Suparna Mitra at the Institute of Food Research/University of East Anglia, Norwich. No part of this thesis has been previously submitted for any other degree at the University of Glasgow or any other institution.

Signature..... Printed Name.....

Publication

Scott, C.L., **Zangerle Murray, T.F.P.**, Beckham, K., Douce, G., Mowat, A.M., 2014b. Signal regulatory protein alpha (SIRPα) regulates the homeostasis of CD103+CD11b+ DCs in the intestinal lamina propria. European Journal of Immunology 44, 3658-3668

List of Abbreviations

7-AAD	7-amino-actinomycin D
Abx	antibiotics
AF	Alexafluor
-APC	allophycocyanin
APC	antigen presenting cell
BatF	basic leucine zipper transcription factor, ATF-like
BM	bone marrow
BV	brilliant violet
CD	cluster of differentiation
cDC	conventional dendritic cell
CDP	common dendritic cell progenitor
cMLN	colonic draining mesenteric lymph node
CMP	common myeloid progenitor
CNS	central nervous system
CSF	colony stimulating factor
Cy7	cyanine 7 dye
DC	dendritic cell
DEAB	diethylaminobenzaldehyde
DNA	deoxyribonucleic acid
EDTA	ethylenediaminetetraacetic acid
FACS	fluorescence activated cell sorting
FCS	foetal calf serum
fDC	follicular dendritic cell
FITC	fluorescein isothiocyanate
flt3	*fms*-like tyrosine kinase 3
flt3L	*fms*-like tyrosine kinase 3 ligand
FoxP3	forkhead box P3
FSC	forward scatter
GALT	gastrointestinal associated lymphoid tissue
GF	germ free
GFP	green fluorescent protein
GM-CSF	granulocyte macrophage colony-stimulating factor
GMP	granulocyte/macrophage precursor
HBSS	Hank's buffered salt solution
HSC	haematopoietic stem cell
IBD	inflammatory bowel disease
ID	inhibitor of DNA binding
IDO	indoleamine-2,3-deoxygenase
IEL	intra-epithelial lymphocyte
IFN	interferon
Ig	immunoglobulin

IL	interleukin
ILC	innate lymphoid cell
ILF	isolated lymphoid follicle
i.p.	intraperitoneal
IRF	Interferon regulatory transcription factor
i.v.	intravenous
KO	knock out
LP	lamina propria
LPS	lipopolysaccharide
LT	lymphotoxin
M cell	microfold cell
MDP	macrophage and dendritic cell precursor
Mϕ	macrophage
MFI	mean fluorescence intensity
MHC	major histocompatibility complex
MLN	mesenteric lymph node
MP	mononuclear phagocyte
MPS	mononuclear phagocyte system
Mt	mutant
MyD88	myeloid differentiation factor 88
NK	natural killer
NLR	Nod-like receptor
NO	nitric oxide
NOD	nucleotide-binding oligomerisation domain
OVA	ovalbumin
PAMP	pathogen associated molecular pattern
PBS	phosphate buffered solution
PCR	polymerase chain reaction
pDC	plasmacytoid dendritic cell
PE	phycoerythrin
PerCP	Peridinin-chlorophyll-protein
PG	prostaglandin
PFA	paraformaldehyde
PLN	peripheral lymph node
PMA	phorbol 12-myristate 13-acetate
PP	Peyer's patches
PPAR	peroxisome proliferator-activated receptor
Pre-DC	DC-committed progenitor
PRR	pattern recognition receptor
RA	retinoic acid
RPMI	Roswell Park Memorial Institute-1640 medium
RT-PCR	reverse transcriptase polymerase chain reaction
SA	streptavidin

SD	standard deviation
SI	small intestine
SIRP	signal regulatory protein
SFB	segmented filamentous bacteria
sMLN	small intestinal draining mesenteric lymph node
SPF	specific pathogen free
SSC	side scatter
STAT	signal transducer and activator of transcription
TED	transepithelial dendrites
TGF	transforming growth factor
TRAF	TNF receptor activated factor
TREM	triggering receptor expressed by myeloid cells
TH1	T helper 1
TH2	T helper 2
TH17	T helper 17
TLR	Toll-like receptor
TNF	tumour necrosis factor
TSLP	thymic stromal lymphopoietin
T_{Reg}	regulatory T cell
VEGF	vascular endothelial growth factor
VIP	vasoactive intestinal peptide
WT	wild type
Zbtb46	zinc finger and BTB containing 46

Summary

The intestinal tract is exposed to a large variety of antigens such as food proteins, commensal bacteria and pathogens and contains one of the largest arms of the immune system. The intestinal immune system has to discriminate between harmless and harmful antigens, inducing tolerance to harmless antigens and active immunity towards pathogens and other harmful materials. Dendritic cells (DC) in the mucosal lamina propria (LP) are central to this process, as they sample bacteria from the local environment and constitutively migrate to the draining mesenteric lymph nodes (MLN), where they present antigen to naïve T cells in order to direct an appropriate immune response. Despite their crucial role, understanding the function and phenotype of LP DC has been hampered by the fact that they share phenotypic markers with macrophages (mϕ), which are the dominant population of mononuclear phagocyte (MP) in the LP. Recent work in our own and other laboratories has established gating strategies and phenotyping panels that allow precise discrimination between intestinal DC and mϕ using the mϕ specific markers CD64 and F4/80. In this way four *bona fide* DC subsets with distinct functions have been identified in adult LP based on their expression of CD11b and CD103 and a major aim of my project was to understand how these subsets might develop in the neonatal intestine.

At the beginning of my PhD, the laboratory had used these new methods to show that signal regulatory protein α (SIRPα), an inhibitory receptor expressed by myeloid cells, was expressed by mϕ and most DC in the intestine, except for those expressing CD103 alone. In addition, mice carrying a non-signalling mutation in SIRPα (SIRPα mt) had a selective reduction in $CD103^{+}CD11b^{+}$ DC, a subset which is unique to the intestinal LP. This was the basis for the initial experiments of my project, described in Chapter 3, where I investigated if the phenotype in SIRPα mt mice was intrinsic to haematopoietic cells or not. To explore this, I generated bone marrow (BM) chimeric mice by reconstituting irradiated WT mice with SIRPα mt BM, or SIRPα mt animals with WT BM. These experiments suggested that the defect in $CD103^{+}CD11b^{+}$ DC was not replicated in DC derived from BM of SIRPα origin. However as this seemed inconsistent with other data, I considered the possibility that

the phenotype may have been lost with age, as the BM chimeric mice were considerably older than those used in the original studies of SIRPα function. However a comparison of DC subsets in the intestine of WT and SIRPα mt mice as they aged provided no conclusive evidence to support this idea.

As these experiments did show age-dependent effects on DC subsets, in Chapter 4, I went on to investigate how the DC populations appeared in the intestine and other tissues in the neonatal period. These experiments showed there were few $CD103^+CD11b^+$ DC present in the LP and migratory DC compartment of the MLN in the neonate and that as this population gradually increased in proportion with age, there was a reciprocal decrease in the relative proportion of $CD103^-CD11b^+$ DC. Interestingly, most of the changes in DC numbers in the intestine were found during the second or third week of life when the weaning process began. To validate my findings that there were few $CD103^+CD11b^+$ DC in the neonate and that this was not merely an absence of CD103 upregulation, I examined the expression of CD101 and Trem-1, markers that other work in the laboratory had suggested were specific to the $CD103^+CD11b^+$ DC lineage. My work showed that CD101 and Trem-1 were co-expressed by most $CD103^+CD11b^+$ DC in small intestine (SI) LP, as well as a small subset of $CD103^-CD11b^+$ DC in this tissue. Interestingly, Trem-1 was highly specific to the SI LP and migratory DC in the MLN, but absent from the colon and other tissues. CD101 expression was also only found on $CD11b^+$ DC, but showed a less restricted pattern of distribution, being found in several tissues as well as the SI LP.

The relative timing of their development suggested there might be a relationship between $CD103^+CD11b^+$ and $CD103^-CD11b^+$ DC and this was supported by microarray analysis. I hypothesised that the $CD103^-CD11b^+$ DC that co-expressed CD101 and Trem-1 may be the cells that developed into $CD103^+CD11b^+$ DC. To investigate this I analysed how CD101 and Trem-1 expression changed with age amongst the DC subsets in SI LP, colonic LP (CLP) and MLN. The proportion of $CD101^+$Trem-1^+ cells increased amongst $CD103^+CD11b^+$ DC in the SI LP and MLN with age, while amongst $CD103^+CD11b^+$ DC in the CLP this decreased. This was not the same in $CD103^-CD11b^+$ DC, where CD101 and Trem-1 expression was more varied with age in all tissues. CD101 and Trem-1 were not expressed to any great extent on $CD103^+CD11b^-$ or $CD103^-CD11b^-$ DC. The phenotypic development of the

intestinal DC subsets was paralleled by the gradual upregulation of CD103 expression, while the production of retinoic acid (RA), as assessed by the Aldefluor™ assay, was low early in life and did not attain adult levels until after weaning. Thus DC in the neonatal intestine take some time to acquire the adult pattern of phenotypic subsets and are functionally immature compared with their adult counterparts.

In Chapter 5, I used CD101 and Trem-1 to explore the ontogeny of intestinal DC subsets in CCR2$^{-/-}$ and SIRPα mt mice, both of which have selective defects in one particular group of DC. The selective defect seen amongst CD103^{+}CD11b^{+} DC in adult SIRPα mt mice was more profound in mice at D7 and D14 of age, indicating that it may be intrinsic to this population and not highly dependent on environmental factors that change after birth. The expression of CD101 and Trem-1 by both CD103^{+}CD11b^{+} and CD103^{-}CD11b^{+} DC was reduced in SIRPα mt mice, again indicating that this entire lineage was affected by the lack of SIRPα signalling. However there was also a generalised defect in the numbers of all DC subsets in many tissues from early in life, suggesting there was compromised development, recruitment or survival of DC in the absence of SIRPα signalling. In contrast to the findings in SIRPα mt mice, more CD103^{+}CD11b^{+} DC co-expressed CD101 and Trem-1 in CCR2$^{-/-}$ mice, while there were no differences in the expression of these molecules amongst CD103^{-}CD11b^{+} DC. This may suggest that CCR2^{+} CD103^{-}CD11b^{+} DC are not the cells that express CD101 and Trem-1 that are predicted to be the direct precursors of CD103^{+}CD11b^{+} DC. I also examined the expression of DC growth factor receptors on DC subsets from mice of different ages, but no clear age or subset-related patterns of the expression of mRNA for *Csf2ra*, *Irf4*, *Tgfbr1* and *Rara* could be observed. Next, I investigated whether Trem-1 played any role in DC development. Preliminary experiments in Trem-1$^{-/-}$ mice show no differences between any of the DC subsets, nor were there any selective effects on individual subsets when DC development from Trem-1$^{-/-}$ KO and WT BM was compared in competitive chimeras. However these experiments were difficult to interpret due to viability problems and because I found an unexpected defect in the ability of Trem-1$^{-/-}$ BM to generate all DC, irrespective of whether they expressed Trem-1 or not.

The final experiments I carried out were to examine the role of the microbiota in driving the differentiation of intestinal DC subsets, based on the hypothesis that this could be one of the environmental factors that might influence events in the developing intestine. To this end I performed experiments in both antibiotic treated and germ free adult mice, both of which showed no significant phenotypic differences amongst any of the DC subsets. However the study of germ free mice was compromised by recent contamination of the colony and may not be the conclusive answer.

Together the data in this thesis have shown that the population of $CD103^{+}CD11b^{+}$ DC, which is unique to the intestine, is not present at birth. These cells gradually increase in frequency over time and as this occurs there is a reciprocal decrease in the frequency of $CD103^{-}CD11b^{+}$ DC. Along with other results, this leads to the idea that there may be a linear developmental pathway from $CD103^{-}CD11b^{+}$ DC to $CD103^{+}CD11b^{+}$ DC that is driven by non-microbial factors that are located preferentially in the small intestine. My project indicates that markers such as CD101 and Trem-1 may assist the dissection of this process and highlights the importance of the neonatal period for these events.

Chapter 1

General Introduction

1.1 Introduction

From the beginning of time, selective pressures such as competition for nutrients and space have allowed for the evolution of systems of protection and survival. Even as early as the sponge, there is evidence of cell specialisation and pattern recognition, as well as recognition of self and non-self, elements we associate with the immune system. Fast-forward several hundred million years and mammals have evolved a complex system of discrimination between harmful materials such as pathogens and innocuous agents such as 'self' tissues, commensal bacteria or food proteins. Harmful or infectious organisms must be eradicated, and the immune system does this efficiently via two lines of defence, namely innate and adaptive immunity. The innate immune system acts rapidly, but is hard wired, is not antigen specific and does not show memory. In contrast, adaptive immunity takes longer to develop, needing to expand antigen specific cells, but is long-lived and generates faster responses upon re-encounter of the same antigen (memory). As well as generating active responses, the immune system must also tolerate the presence of commensal organisms, dietary proteins and other harmless environmental antigens. As the intestinal immune system encounters more foreign antigens than any other part of the body from the moment of birth, it is particularly crucial that immune responses in this tissue are highly regulated. Dendritic cells (DC) are crucial for surveying the intestinal environment, migrating to the draining mesenteric lymph nodes (MLN) with sampled antigen, and presenting this to naïve T cells. The T cells then proliferate and differentiate accordingly into gut homing effector or regulatory T cells, allowing for active immunity or tolerance to be induced.

1.1.1 The gastrointestinal tract

The gastrointestinal (GI) tract is made up of several "systems" with different biological functions, which have evolved alongside one another to create an integrated efficient organ. The GI tract consists of the stomach, small intestine and large intestine and develops from the embryological midgut (stomach, small intestine (SI)) and hindgut (caecum, large intestine/colon, rectum). An enteric nervous system develops in parallel, providing sensory and motor activities essential for intestinal function. Local neuroendocrine cells also develop in the intestine, releasing

hormones to help regulate digestion. The GI tract has several layers with different functions. The outermost layer is the mucosa, made up of the surface epithelium, the underlying lamina propria (LP) and the muscularis mucosae. Under the mucosa is the submucosa, a dense layer of connective tissue containing vasculature, lymphatics and nerves. The muscularis externa is the outer muscle layer responsible for peristalsis. Lastly there are the adventitia and serosa, which are the outermost layers of the GI tract and are made up of connective tissue separating the intestinal tissues from the peritoneal cavity. This also contains the mesentery that houses the veins and arteries that supply the intestine, as well as the lymphatics draining from the intestinal wall to the MLN.

The primary function of the GI tract is to move and process foodstuffs, absorbing essential nutrients and water from the small intestine and colon respectively. It does this via a single epithelial layer that is the largest mucosal surface of the body and is bombarded constantly by antigens and other external agents. As a result, it has evolved an enormous and elaborate immune system. The size and fragility of the epithelium means there is a high risk of invasion by pathogens. Meanwhile, the gut also provides a home to trillions of symbiotic commensals and is in regular contact with dietary antigen, both of which require immunological hyporesponsiveness to be maintained to prevent inflammatory disorders such as coeliac disease and inflammatory bowel disease (IBD) (A. Mowat, 2003). The immune apparatus of the intestine consists of organised lymphoid tissues such as the Peyer's patches (PPs), isolated lymphoid follicles (ILFs), appendix and the MLN, where immune responses are initiated (Chirdo et al., 2005; A. Mowat, 2003). Many immune cells are also found scattered throughout the wall of the intestine, where lymphocytes, plasma cells, macrophages (mϕ), DC, innate lymphoid cells (ILCs) and eosinophils form the effector arm of the local immune system.

1.1.2 The intestinal immune system

The SI and colon form a continuous tube from the outlet of the stomach to the rectum. The SI is made up of three segments, the duodenum, jejunum and ileum, while the colon comprises the ascending, transverse and descending colon. The caecum forms the first part of the large intestine separated from the ileum by the ileocaecal valve.

Along the length of the SI, the surface area of the already extensive structure is increased by the presence of finger-like projections known as villi that extend into the lumen. These are longest in the duodenum and jejunum becoming shorter as the ileum is reached. The caecum and colon have a flat luminal surface due to the absence of the villi. The function of the SI is to digest and absorb nutrients from food, whereas the colon is designed to reabsorb water, remove undigested foodstuffs and provide a home to a huge array of different commensal bacteria. The immune system in these sites reflects these anatomical and physiological differences.

1.1.3 Peyer's patches and isolated lymphoid follicles

In 1677, Johann Conrad Peyer described lymphoid aggregates found along the anti-mesenteric axis of the SI, after which they were known as Peyer's patches (PP). In mice, the development of PP begins before birth with colonisation by lymphoid tissue inducer (LTi) cells that aggregate to form primordial PP around embryonic day 16.5 (E16.5) (Veiga-Fernandes et al., 2007). By two days *post partum*, $CD11c^+$ cells are present in the periphery of the PP anlagen and these are thought to help the structural compartmentalisation of the PP (Hashi et al., 2001). It is still to be established whether these are *bona fide* DC or mϕ. The general structure of PP is that of large B cell follicles with intervening T cell areas, together with an overlying subepithelial dome (SED) region, which is rich in a variety of immune cells including DC. Overlying the PP is a single layer of columnar epithelial cells that have only low levels of the brush border found on other intestinal epithelial cells, and is known as the follicle associated epithelium (FAE) (A. Mowat, 2003). This differs from the conventional villus epithelium in that it contains microfold (M) cells which are specialised enterocytes lacking surface microvilli and the thick layer of mucus found elsewhere in the intestine (Hamada et al., 2002). M cells have distinct oligosaccharides on their surface allowing for the adhesion and invasion of pathogens (Neutra et al., 1996). Microbes and other particulate materials taken up by M cells are transported to neighbouring DC in the SED for presentation to local T and B cells (Newberry and Lorenz, 2005). Recent evidence suggests that some of these DC are also capable of migrating to the draining MLN to present antigen (Houston et al., 2015). The exact role of PP in the intestinal immune response remains ambiguous, as some reports have shown normal tolerance to fed proteins in mice lacking PP and M

cells, while others have shown opposite results (Alpan et al., 2001; Fujihashi et al., 2001).

ILFs are found throughout the length of both the SI and colon. They are microscopic lymphoid aggregates and are similar to PP in that they have FAE and M cells but consist of a single B cell follicle with a few T cells and DC. The ILFs are thought to contribute to the regulation of bacterial colonisation in the intestine via the production of immunoglobulin A (IgA) (Eberl and Lochner, 2009). Unlike PP, ILFs develop postnatally in response to factors produced by the microbiota (Eberl and Lochner, 2009).

1.1.4 Mesenteric lymph nodes

The MLN are a chain of lymph nodes that drain the SI and colon. Consistent with the antigenic load in the intestine, the MLN are the largest lymph nodes in the body and are thought to be the principal site for induction of most immune responses in the gut. Although the MLN consists of linked nodes, each of these drains anatomically distinct parts of the SI or colon. This compartmentalisation was first described over 40 years ago (Carter and Collins, 1974; Tilney, 1971), but has been largely forgotten until recently, when two studies showed that not only are there anatomically distinct drainage routes (Houston et al., 2015; Van den Broeck et al., 2006), but that the characteristics of the T cells primed in either the SI draining lymph node (sMLN) or the colonic draining lymph node (cMLN) are distinct (Houston et al., 2015). The MLN are compartmentalised in the same way as other secondary lymphoid tissues, with B cell follicles in the outer cortex surrounding T cell zones in the paracortical region. It is this highly organised structure of the lymph nodes that allows for the efficient priming of T cells (Sainte-Marie, 2010) by migrating DC, which I will discuss later. During my project, I investigated whether or not the DC populations migrating to the segments of the MLN draining either the SI or the colon were phenotypically similar.

1.1.5 Intestinal epithelial cells

Epithelial cells in the intestine are highly specialised, consisting of a number of different cell types including absorptive enterocytes, enteroendocrine cells, mucus secreting goblet cells and antimicrobial peptide (AMP) secreting Paneth cells, each of which has a distinct role in the function of the epithelium. The epithelial layer is constantly renewed by fresh cells that are transported in a conveyor belt-like process from the crypts where they divide, to the tips of the villi from where they are shed every 4-5 days (A. Mowat, 2003). The microvilli on the luminal surface of SI epithelial cells (brush border) are embedded with nutrient transporters and enzymes required for the digestion of dietary components. The long length of the duodenal villi enhances this absorptive effect and, as the length of the villi shortens towards the ileum, so do the levels of brush border enzymes (A. M. Mowat and Agace, 2014; Sansonetti, 2004; Turner et al., 1997). The colon lacks villi and a brush border, consistent with its role in water reabsorption rather than digestion.

Although there are regional differences between the epithelial layer of the SI and the colon, throughout its length it acts as a physical barrier against penetration of microorganisms, and it is an important first line component of the innate immune system. Epithelial cells are connected by tight junctions that contain proteins such as occludins and claudins, as well as other junctional adherence proteins, that keep the cells firmly attached to one another and maintain the polarity of the epithelial layer; this creates an highly effective barrier (M. E. Delgado et al., 2015). Conventional epithelial cells express pattern recognition receptors (PRRs), thus allowing innate responses via Toll-like receptors (TLRs) and the resulting production of cytokines and chemokines.

Paneth cells are found in the SI, mostly in the ileum and they are found at the base of the crypts, where they produce AMPs and maintain crypt stem cell activity. They are not present in the colon, where large numbers of goblet cells are present instead. Goblet cells produce mucus that coats the mucosa with a layer known as the glycocalyx, thickest in the colon, where it consists of an inner dense layer and an

outer loose layer (also found in the SI). Although bacteria can be found in the outer layer of mucus, the inner layer is impenetrable to bacteria (Johansson et al., 2011; 2008). Mucus production is controlled by immune mediators such as interferon-γ (IFNγ), IL-9 and IL-13 (Bancroft et al., 1998; Steenwinckel et al., 2009), and it plays an important antimicrobial role by forming a highly charged gel layer that acts as a physical barrier. Mucin glycoproteins are directly microbicidal, and the mucus also provides a scaffolding for secreted antibodies and AMPs to adhere to (Johansson et al., 2011).

A number of immune cells including intra epithelial lymphocytes (IELs), DC and mϕ are also present whithin the epithelium, or in close proximity to it. IELs are mostly $CD8^+$ T cells that express CD103, the α_E chain of $\alpha_E\beta_7$ integrin. They can be divided into two major groups. So-called "natural" IELs can express either an αβ or γδ TCR together with a CD8αα homodimer. These IELs are believed to leave the thymus early in development and undergo a terminal selection process in the epithelium itself. "Induced" IELs are conventional $TCR\alpha\beta^+$ $CD8\alpha\beta^+$ T cells that are primed by cognate antigen in the PP or MLN and have returned to the intestine as effector cells, where they act as cytotoxic T lymphocytes (CTLs) or produce IFNγ (Gangadharan et al., 2006; Hayday and Gibbons, 2008; Steege and Buurman, 1997).

1.1.6 Lamina Propria

The LP is made up of loosely packed connective tissue immediately beneath the epithelium and contains blood vessels, lymphatics and nerve cells, as well as many immune cells. The LP is connected to the draining MLN via afferent lymphatics and is one of most varied of any immune site, containing lymphocytes, mononuclear phagocytes (DC and mϕ), eosinophils and ILCs. Along with classical $TCR\alpha\beta$ $CD4^+$ and $CD8^+$ T cells, there are γδ T cells, NKT cells and plasma cells which produce vast quantities of immunoglobulin A (IgA) (Mayrhofer et al., 1983). IgA is the most abundant immunoglobulin isotype in the body, being secreted as a J chain-linked dimer by LP plasma cells, from where it is transferred into the lumen after binding to polymeric Ig receptors (pIgR) on the basolateral surface of the epithelial cells. The complex is then transported across the cell and released into the lumen as secretory

IgA (SIgA), where it binds to the mucus layer. SIgA contributes to the local immune system by trapping and neutralising microorganisms and can help to keep in check the bacterial communities of the intestine (Cerutti and Rescigno, 2008).

The T cells of the LP are mostly effector/memory type cells and are derived from naïve T cells that have migrated to the LP after activation in the PP or MLN (van Wijk and Cheroutre, 2009). TCR$\alpha\beta^+$ $CD4^+$ cells in the LP consist of a mixture of IFNγ-producing Th1, IL-17/IL-22 producing Th17 cells and $FoxP3^+$ Tregs, although the relative proportions of the different subsets vary along the length of the GI tract (Denning et al., 2011). Th17 cells are most predominant in the SI, whilst Tregs are increasingly frequent towards the colon. The composition of the $CD4^+$ T cell population of the LP is also highly dependent on the presence of the microbiota, with Th17 cells being decreased in germ free (GF) mice or after treatment with antibiotics, despite no overall difference in the total number of CD4 T cells (Ivanov et al., 2008). Segmented filamentous bacteria (SFB) are particularly associated with the generation of Th17 cells in the SI (Ivanov et al., 2009). Th17 cells produce IL-17A and IL-17F along with IL-22, which together play important role in intestinal homeostasis. IL-17A and IL-17F are both capable of inducing production of the antimicrobial peptide (AMP), β-defensin, by epithelial cells, while IL-22 induces the production of the Reg family of AMPs and also enhances tight junction formation between epithelial cells (A. M. Mowat and Agace, 2014).

Potentially damaging immune responses to harmless dietary and commensal antigens are normally prevented by regulatory T cells (Tregs) (Asseman et al., 2003). Tregs are divisible into $FoxP3^+$ natural Tregs (nTregs) that are thymically derived and recognise self antigens, together with two populations of inducible Tregs (iTregs) that, as their name suggests are induced in response to self and foreign antigen in the periphery. These can be $FoxP3^+$ or $FoxP3^-$, with the $FoxP3^-$ subset being characterised by the production of IL-10 (Barnes and Powrie, 2010; Kamanaka et al., 2006; Maynard et al., 2007).

1.1.7 Intestinal microbiota

Normal intestinal function and immune responses are dependent on the presence of a large and diverse microbiota that lives in close symbiosis with the host, exploiting the nutrient rich niche of the intestine. This has been shown in experiments with germ free (GF) mice, which have very poor immune responses and smaller LNs than their SPF counterparts (Hooper and Macpherson, 2010; Hooper et al., 2001). The two main phyla found in the intestine are Bacteroidetes (~16%) and Firmicutes (~66%) (Ley et al., 2008). One of the major roles of intestinal bacteria is to break down complex dietary polysaccharides that escape digestion in the SI and it is this function that is thought to have driven such close evolution of the host and its microbiota. Short-chain fatty acids such as butyrate, acetate and palmyrate produced by this digestion are essential for epithelial cell renewal (Maslowski et al., 2009) and stimulation of AMP production by Paneth cells (Hooper and Macpherson, 2010; Sonnenburg et al., 2005). Butyrate also drives Tregs via HDAC and modification of the FoxP3 locus(Barbi et al., 2014). The microbiota can also influence other aspects of intestinal physiology such as angiogenesis (Hooper et al., 2003; Stappenbeck et al., 2002).

A further crucial property of commensal bacteria is that they are essential for protection against harmful pathogens. This partly reflects their ability to compete for nutrients and space, as well as modulation of the host immune response. An example of this is during *Salmonella* typhimurium infection which is limited by the activation of TLRs by the commensals on host immune cells (Stecher et al., 2005). This effect extends to more complex pathogens such as *Toxoplasma gondii,* where activation of DC by commensals induces the production of protective pathways (Benson et al., 2009). Similarly, the ability of certain families of bacteria, such as SFB, to skew the CD4 T cell repertoire towards Il-17 production can provide protection from *Citrobacter rodentium* infection (Ivanov et al., 2009).

1.1.8 Active immunity versus tolerance in the intestine

Pathogens have evolved to gain entry to the LP where they come into contact with many innate immune cells including the largest population of

mϕ in the body, as well as eosinophils and ILCs; neutrophils are recruited readily in response to infection. Granulocytes and mϕ engulf and kill invading organisms and produce pro-inflammatory cytokines. ILCs can produce cytokines such as IL-22 that further drives the release of AMPs and strengthens the epithelial barrier (Cella et al., 2008; Sanos et al., 2009; Sonnenberg et al., 2011). The LP and PP/ILF are also rich in DC, which can acquire microbes, process the associated antigens and present the peptides to T and B cells in the PPs and MLN. This begins the cascade of the antigen specific adaptive immune response, discussed in more detail below.

As discussed above, the intestinal immune system is exposed to many other antigens that are not pathogenic, but are not "self" either. These are dietary proteins and antigens from commensal organisms, all of which are continuously sampled from the lumen by mϕ and DC. Under normal conditions, the consequence of exposure to these materials is the induction of antigen-specific tolerance. "Oral tolerance" is the phenomenon by which dietary proteins induce tolerance of both the systemic and local immune systems (Pabst and A. M. Mowat, 2012). This is believed to reflect the generation of Tregs in the MLN (Thomson and Knolle, 2010). In contrast, tolerance to commensal bacteria is restricted to the mucosal immune system, as these antigens normally do not spread beyond the MLN and the systemic immune system remains ignorant of their presence. Furthermore substantial amounts of intestinal sIgA are generated against commensal bacteria, but not food proteins (Pabst and A. M. Mowat, 2012).

When there is a failure to induce tolerance, inappropriate immune responses generated against both dietary and commensal antigens can lead to intestinal pathology such as food allergies, coeliac disease and the inflammatory bowel diseases, ulcerative colitis (UC) and Crohn's disease (CD). It remains unclear what factors lead to a breakdown in these tolerance mechanisms, but it seems reasonable to suggest that it may involve the way antigens are presented to naïve T cells by local DC, as they are the principal cells that can discriminate between innocuous and harmful antigen. Thus, there is considerable interest in understanding the nature and functions of intestinal DC and their subsets, which is the main focus of this thesis.

1.2 The neonatal intestine

At the moment of birth, the embryonic intestine is introduced to the non-sterile outside world, ingesting a large amount of bacteria during passage along the birth canal and with this, a new microbial eco-system is born. Shortly afterwards the newborn mammal begins to ingest food in the form of the mother's milk and at around 14 days in mice, this is supplemented with solid food, before becoming fully weaned around 20-21 days.

The GI tract expands in size from the neonatal period into adulthood, with the mature villus-crypt architecture developing slowly during the first three weeks of life. Epithelial cell turnover is low until the time of weaning (Clevers, 2013), when there are marked increases in crypt length and decreases in villus length (Mowat, unpublished data). In parallel the epithelial layer is much less well developed in the neonate than in the adult with low levels of digestive enzymes, as well as few Paneth cells (Bry et al., 1994), explaining the very low amounts of AMPs that are found until around D9 after birth (Hornef and Fulde, 2014). Epithelial cell expression of PRR also changes during neonatal development, with most TLR being found at low levels at birth, increasing thereafter. It has been suggested that this may be a strategy aimed at allowing efficient colonisation by the arriving microbiota (Hornef and Fulde, 2014; Pott et al., 2012). In contrast, Nod1/2 and components of the inflammasome do not change (Gribar et al., 2009). Goblet cells are also reduced in the neonatal GI tract, resulting in a reduced thickness in mucus layer compared with the adult (Birchenough et al., 2013; Kim and Ho, 2010).

As already mentioned, in mice PP are present from as early as E15.5. Around E17.5, lymphoid tissue inducer cells are recruited in a VCAM-1 dependent manner (Hashi et al., 2001; Jung et al., 2010) and this leads to recruitment of mature lymphocytes to the PP anlagen within the first few days of postnatal life. As a result PP are almost fully formed in the early postnatal period. ILF on the other hand, are not present at birth and require interaction with commensal bacteria for their development (Eberl and Lochner, 2009; Hamada et al., 2002). Like PP, MLN appear in the embryo between E10.5 and E15.5, requiring the function of a specific subset of $CD4^{+}CD3^{-}$ IL-$7R\alpha^{+}$ lymphoid tissue inducer cells that are required for the development of the MLN

(Mebius et al., 1996). Another important mechanism of protection against the onslaught by new antigens in the early days of neonatal development is that a large amount of IgA is present in the infant GI tract. As the neonatal intestine has few mature B cells (Adkins et al., 2004; Torow et al., 2015), this IgA is derived from the mother through ingestion of colostrum and milk (Macpherson et al., 2001). The ability of this IgA to recognise commensal organisms is thought to help regulate microbial colonisation of the neonatal intestine (Kramer and Cebra, 1995) (Macpherson et al., 2001). Maternal IgA also seems to suppress development of the host immune response, perhaps because it limits access to the microbiota, and mice suckled for longer than usual are unable to generate IgA plasma cells efficiently (Kramer and Cebra, 1995).

$CD4^+$ T cells accumulate in the neonate LP within the first two days after birth and then increase again after weaning. However those that are present early in development are immature and unable to secrete IL-17, IFNγ, IL-10 or IL-22 (Torow et al., 2015). The entry of immature T cells into PP, MLN and LP is dependent on their expression of β7 integrin, which recognises mucosal adressin cell adhesion molecule 1 (MAdCAM-1) on the vasculature of the LP, PP and MLN. The expression of MAdCAM-1 is partly driven by the microbiota. It has been suggested that the immaturity of gut lymphocytes in the neonate may reflect active suppression, and that this provides a window in the neonatal period that favours the development of tolerance again commensals (Torow et al., 2015).

Although some studies have described an increase in DC in the neonate intestine (A. M. Williams et al., 2006), to my knowledge no work has been carried out on how the intestinal DC subsets develop in this early period, and thus a principal aim of my thesis was to understand the population dynamics of DC from birth until adulthood.

1.3 Dendritic cells

DC are specialised antigen presenting cells of myeloid origin and are the crucial link between innate and adaptive immunity. They were first described by Ralph Steinman and Zanvil Cohn in 1973 based on their morphology and appearance in lymphoid organs (Steinman and Cohn, 1973). They are found in all tissues of the body, and in

non-lymphoid organs, DC sample large amounts of material from the local environment through macropinocytosis, endocytosis and phagocytosis. After uptake of antigen, DC process the protein, present the resulting peptides on the cell surface with class I or II major histocompatibility complex (MHC) molecules and migrate to the draining lymph nodes, where they interact with naïve T cells. This induces proliferation of antigen specific T cells, and depending on the circumstances, they differentiate into effector or regulatory T cells and are imprinted with the ability to home back to the tissue from where the DC arrived. Although other cells such as mϕ and B cells can present antigen with MHC, DC are unique in their ability to carry antigen to lymph nodes and to prime naïve T cells. This is particularly crucial for MHC II-restricted presentation by DC; hence DC are essential for $CD4^+$ T cells activation and consequently most adaptive immune responses.

1.3.1 How to identify a DC

DC are classified along with macrophages and monocytes as mononuclear phagocytes. The mononuclear phagocyte system (MPS) was first described in 1972 as a system of phagocytic cells located in reticular connective tissue arising from a common bone marrow (BM) progenitor via blood monocytes (Bain et al., 2014). Although now known to be more complex than this, the concept of the MPS still underpins much of our current understanding of DC and mϕ ontogeny.

Discriminating between DC and mϕ has been a problem for some time, because of the overlap in their phenotype and function. Like other leucocytes, DC express CD45, but lack lineage markers found on B and T cells, erythrocytes, granulocytes and NK cells (Merad et al., 2013). In mice, they were classically defined by their co-expression of MHC II and the integrin CD11c and usually this is sufficient to identify DC in secondary lymphoid organs. However it is now clear that this is not suitable in non-lymphoid tissues, where other cells such as mϕ, eosinophils and T cells can express CD11c (Bain et al., 2012; Tamoutounour et al., 2012). This is a particular problem in the intestine, where all mϕ express MHC II and CD11c (Schraml and Reis e Sousa, 2015) and therefore more specific markers have to be used. Previous work in the lab had applied rigorous testing of several phenotypic markers (Table 1.1) to the intestine for the first time, allowing *bona fide* DC to be identified. In line with this, I

have used the expression of MHC II along with CD11c to identify all MP, before differentiating between DC and mϕ based on the expression of CD64 or F4/80. This approach has been validated by additional markers, including CD24 and zbtb46 specifically in DC as well as MERTK and CD26 in mϕ (Bain et al., 2012; Scott et al., 2014b).

Table 1.1: Phenotype of murine MP

Surface Marker	CD8α⁺ DC cDC1	CD11b⁺ DC cDC2	pDC	mϕ
CD45	+	+	+	+
MHC II	++	++	+	+++
CD11c	++	++	+	+
CD64	-	-	-	+
F4/80	-	-	-	+
CD8a	+	-	+/-	+
CD4	-	+/-	+	+
CD11b	-	+	-	+
CD103	+	+/-	-	-
SIRPα (CD172a)	-	+	-	+
Ly6C	-	-	++	+
CD205	++	+	-	-
CD209	-	+/-	++	ND
Clec9a (DNGR1)	++	-	+	-
XCR1	+	-	-	-
CD24	++	+/-	ND	-
CX3CR1	-	+/-	-	+++
MERTK	-	-	-	+

- Marker not expressed; **+** marker expressed; **+/-** expressed on a subset; **ND** not determined

1.3.2 Dendritic cell subsets

There are two main lineages of DC – plasmacytoid (pDC) and conventional (cDC). Although derived from the same precursor, these are quite distinct, with pDC showing little APC activity and producing copious amounts of type-1 IFNs. cDC were traditionally separated into "myeloid" and "lymphoid" derived subsets, although we now know that they are all generated from a myeloid progenitor (see below). Nevertheless, there are clearly distinct subsets of cDC. DC subsets were first identified in mouse lymphoid organs, where one expressed CD11b or CD4 and lacked

the expression of CD8α (CD11b$^+$ DC), whereas the other expressed CD8α but lacked CD4 or CD11b (CD8$^+$ DC). In non-lymphoid tissues, CD8α expression largely overlaps with the expression of the a_E integrin CD103 (Ginhoux et al., 2009a), except in the intestine, where a large population expresses both CD103 and CD11b (Bogunovic et al., 2009; Denning et al., 2011; Varol et al., 2009)(see below). Cd11b/CD8α based DC subsets also differ in the expression of other surface markers (Table 1.1) and this can be useful in defining some functional properties of DC. Although the individual surface markers vary, analogous populations exist in other species, and recently an attempt at consensus has been made based on common phenotypic markers, dependence on transcription factors, functions and anatomical localisation (Cerovic et al., 2014a; Geissmann et al., 2010; Miller et al., 2012; Schraml and Reis e Sousa, 2015; Steinman and Idoyaga, 2010). These have been labelled as cDC1 and cDC2 (Guilliams et al., 2014).

1.3.2.1 cDC1

Initially described as CD11b$^-$CD8α$^+$(CD103$^+$) in mice, the cDC1 subset was difficult to assign in other species, where CD8 is not expressed on DC and CD103 expression had not been characterised fully. However, recent work has shown that the chemokine receptor XCR1 and DC NK lectin group receptor-1 (DNGR1, also called CLEC9A) are expressed by this subset in all species (Bachem et al., 2010; 2012; Sancho et al., 2009; 2008). Resident cDC1 in secondary lymphoid organs are CD103$^-$, but those in non-lymphoid tissues, or those that have migrated from there to lymphoid tissues express CD103. In humans, this subset can also be identified by expression of CD141. This subset of DC also expresses a unique set of transcription factors, including IRF8 (Edelson et al., 2010a; Ginhoux et al., 2009b; Schraml and Reis e Sousa, 2015), the basic leucine zipper transcription factor ATF-like 3 (Batf3) (Edelson et al., 2010b) and inhibitor of DNA-binding 2 (Id2) (Jackson et al., 2011), and its development in mice is dependent on these factors. Finally, the absence of the DC specific transcription factor zDC skews DC development towards CD103$^+$ CD8$^+$ DC (Meredith et al., 2012; Satpathy et al., 2012). Although cDC1 are able to carry out all classical DC functions, they have the unique ability to cross-present exogenous antigen to CD8$^+$ T cells in the context of MHC I.

1.3.2.2 cDC2

cDC2 are CD11b$^+$CD8α^- and also CD4$^+$ in mice, but again, CD11b is not a useful marker in other species. The defining feature of cDC2 is the expression of and dependence on the transcription factor interferon regulatory factor 4 (IRF4). In the absence of IRF4 signalling there are reduced populations of CD11b$^+$ DC in most tissues, including the spleen, lung and intestine (Persson et al., 2013b; Schlitzer et al., 2013). Although it was originally thought that IRF4 was involved in development of these DC (Suzuki et al., 2004), more recent work suggests it may also be important for their survival or migration from tissues to LN (Bajana et al., 2012; Persson et al., 2013b).

Other factors involved in cDC2 development or maintenance include Notch2 signalling (Lewis et al., 2011), RelB and TRAF6 (Kobayashi et al., 2003; Wu et al., 1998). However, the CD11b$^+$ DC subset in mice is clearly heterogeneous, as not all are depleted in the absence of IRF4 or Notch2 signalling and there is evidence that ESAM$^+$ DC in the spleen (Lewis et al., 2011) and CD103$^+$CD11b$^+$ DC in the intestine (Satpathy et al., 2013) are more affected in these circumstances. Another factor involved in cDC2 commitment is Kruppel-like factor 4 *(Klf4),* which appears to induce IRF4 expression in DC precursors, and the absence of *Klf4* leads to reduced CD11b$^+$ DC in the skin and lung as well as reduced CD103$^+$CD11b$^+$ DC the intestine (Tussiwand et al., 2015).

Although cDC2 may contribute to CD8 T cell priming in some circumstances (Fujimoto et al., 2011), their main role appears to be in activation of CD4$^+$ T cells. The reduction of cDC2 in IRF4 KO mice is associated with a defect in Th2 generation (Vander Lugt et al., 2013; J. W. Williams et al., 2013), although as described later, the selective absence of CD103$^+$CD11b$^+$ DC in the intestine leads to reduced differentiation of Th17 cells (Lewis et al., 2011; Persson et al., 2013b; Schlitzer et al., 2013). The equivalent subset in humans can be identified as CD1c$^+$ while SIRPα appears to be a conserved marker of cDC2 in all species (Barclay, 2009; Saito et al., 2010).

1.3.2.3 SIRPα expression on mononuclear phagocytes

SIRPα (CD172a) is a transmembrane receptor expressed on myeloid cells including cDC2 and mϕ. SIRPα has three extracellular immunoglobulin domains and an intracellular region with two immunoreceptor tyrosine-based inhibitory motifs (ITIMs). Recognition of its ubiquitously expressed ligand, CD47, results in ITIM phosphorylation and recruitment of the phosphatases, SHP-1 and SHP-2, which inhibit several kinase pathways (Fortin et al., 2009; Sato-Hashimoto et al., 2011). The role of the SIRPα/CD47 pathway in the immune system is still poorly understood, with both positive and inhibitory functions having been described (Matozaki et al., 2009; Yrlid et al., 2006). Recognition of CD47 on red blood cells or other cells by SIRPα on mϕ inhibits phagocytosis, and acts as a "don't eat me" signal (Ishikawa-Sekigami et al., 2006). In addition, ligation of SIRPα has been shown to regulate pro-inflammatory cytokine production by DC (Latour et al., 2012; Smith, 2003), stimulate the migration of several cell types (Hagnerud et al., 2006; Ogura et al., 2012; Stefanidakis et al., 2008) and promote eosinophil homeostasis (Verjan Garcia et al., 2011).

1.3.2.4 Plasmacytoid DC

pDC, although originating from a similar lineage to cDC are quite different. Morphologically they resemble more of a plasma cell, as their name would suggest. Their surface phenotype also differs from that of cDC as they express B220, Ly6C, CCR9 and SIGLEC-H along with lower levels of CD11c and MHC II (Table 1.1) (Nakano et al., 2001). The main function of pDC is to respond to viral infections by rapidly producing type 1 IFN to viral nucleic acid and inducing cDC maturation by their release of type 1 IFN and TNFα (Fonteneau et al., 2004; Tang et al., 2010). However, these DC are not the focus of this study and are therefore not considered further.

1.3.3 Dendritic cell functions

In non-lymphoid tissues such as the intestine, DC continuously sample their local environment, take up antigens, and reconnoitre for danger and invasive organisms using pattern recognition receptors such as Toll-like receptors (TLR). They then

migrate constitutively to local draining lymph nodes where they interact with and cause differentiation of recirculating naive T cells.

1.3.3.1 Antigen acquisition

The cDC that arrive as precursors in non-lymphoid tissues are referred to as immature and they have a huge capacity for the uptake of antigen, via the processes of phagocytosis, receptor mediated endocytosis or fluid phase macropinocytosis. The volume of fluid the DC can take up via the latter mechanism is estimated to be 1000 – 1500 mm^3 per hour, similar to the volume of the cell itself (Sallusto et al., 1995). This environmental sampling can go on for several days without affecting DC behaviour markedly, but in the presence of a pathogen, tissue damage or an other source of inflammation, the DC undergo maturation. This is driven by families of innate immune receptors on the DC (PRRs) that recognise pathogen associated molecular patterns (PAMPs) which are conserved molecules found on microorganisms and not on mammalian cells. The best understood are the Toll-like receptors (TLRs), of which there are ten and thirteen in humans and mice respectively (T. Kawai and Akira, 2009). TLRs recognise PAMPs on the surface or in the nucleic acid of viral, bacterial and protozoal organisms. Other PRRs include surface C-type lectins and cytosolic molecules such as retinoic acid-inducible gene-I (RIG-I)-like receptors (RLRs) and nucleotide-binding oligomerisation domain (NOD)-like receptors (NLRs) (O. T. Kawai and Akira, 2009; Medzhitov, 2001). As well as recognising PAMPs on microbes, some of these PRRs can also detect the products of damaged cells such as uric acid or ATP, and their effects are enhanced by proinflammatory cytokines such as TNFα. Maturation of DC in response to these signals leads to a number of changes in the cell including stabilisation of the MHC II – peptide complex due to reduced recycling of MHC II (Sallusto et al., 1995), together with upregulation of the costimulatory molecules CD80 (Larsen et al., 1992), CD86 and CD40 (Lenschow et al., 1993), and reduced macropinocytotic activity. They are now ready to interact with and stimulate naïve T cells.

1.3.3.2 Migration of dendritic cells

One of the main consequences of DC maturation is the induction of locomotor activity and the up-regulation of CCR7 expression which allows the DC to migrate to the draining LN in afferent lymph (Dieu et al., 1998; Sallusto et al., 1998; Sozzani et al., 1998; Yanagihara et al., 1998). CCR7 has two ligands, one being CCL21 that is constitutively produced by fibroblastic reticular cells in the T cell rich areas of secondary lymphoid tissues, while CCL19 is produced by stromal cells and mature DC in the T cell areas. Although it is not entirely clear how DC enter afferent lymphatics in tissues, it is believed to be in a CC21 dependent manner (Tal et al., 2011), with the DC initially crawling actively along the lymphatics, before being carried along passively (Tal et al., 2011). On entering the LN via the sub-capsular sinus, the DC are then attracted to the T cell rich areas by CCL19. It is thought that DC in these regions are also able to present or produce CCL19, thus further increasing the chemokine gradient towards the T cells (Alvarez et al., 2008). For these reasons the priming of immune responses by DC is entirely dependent on CCR7. Prostaglandin E2 (PGE2) produced by epithelia, fibroblasts and recruited inflammatory cells is shown to promote the migration of DC to the MLN through increased sensitivity of CCR7 to CCL19 and CCL21 (Kalinski, 2012; Yen et al., 2008).

The "migratory" DC that have taken up antigen in tissues and have arrived in draining lymph nodes via afferent lymph can be distinguished from resident DC that enter lymphoid tissues directly from the bloodstream by the levels of CD11c and MHC II expression. While resident DC are $CD11c^{+}$ MHC II^{int}, migratory DC are $CD11c^{+}$ MHC II^{hi} (Cerovic et al., 2013; Henri et al., 2001; Houston et al., 2015). Migratory DC were originally thought to only comprise the $CD11b^{+}$ $SIRP\alpha^{+}$ subset in mice, but more recently it has become clear that the $CD8\alpha^{+}$ $XCR1^{+}$ subset can also migrate from non-lymphoid tissues and these are characterised by expression of CD103 (Ginhoux et al., 2009b). Lymph nodes contain both migratory and resident DC, whereas other lymphoid tissues such as the spleen and thymus only contain resident DC, as they lack an afferent lymph supply (Bogunovic et al., 2009; Denning et al., 2011).

1.3.3.3 Priming of naïve lymphocytes by dendritic cells

Once the DC have arrived in the T cell area of draining LN they contact naïve T cells that are in constant flux through this region after arriving through high endothelial venules (HEVs). The crucial events for initiating virtually all immune responses are the priming, proliferation, maturation and polarisation of naïve MHC II restricted $CD4^+$ T cells. Mature DC are uniquely able to do this because of their high levels of stable MHC II and expression of costimulatory molecules, as well as their production of factors that drive T cell differentiation. This process involves DC forming immune synapses with cognate T cells, in which addressin molecules form a ring-like structure that holds the TCR, peptide-MHC (pMHC), costimulatory molecules and signalling molecules in a stable manner that allows the TCR to signal. As a result the naïve T cell up regulates IL-2 and the IL-2 receptor and begins the process of clonal expansion by entering cell cycle (Guermonprez et al., 2003; Mellman and Steinman, 2001; Théry and Amigorena, 2001). After several rounds of cell division, the T cells differentiate into one or other type of effector T cell, appropriate to the type of immune response that is required. $CD4^+$ T cells can differentiate into several T helper (Th) subsets, namely Th1, Th2, Th17 or T follicular helper (Tfh) cells as well as Tregs, and this fate determination is controlled by the nature of the costimulatory molecules and cytokines expressed by the DC. In turn, the environment from which the DC has emigrated, determines this.

IFNγ producing Th1 cells are generated in response to the IL-12 heterodimer produced by ligation of TLRs and CD40 on DC (Gubler et al., 1991; Urbain et al., 1998), and their differentiation requires the transcription factor T-bet (Szabo et al., 2000). IFNγ produced by Th1 cells activates mϕ to kill intracellular pathogens and stimulates the production of nitric oxide, TNFα and other pro-inflammatory mediators by mϕ, as well as causing B cells to produce IgG2a (Snapper et al., 1988b). Thus, Th1 cells are important drivers of inflammation. A different cocktail of DC cytokines generates IL-17 and IL-22 producing Th17 effector cells. IL-1β, IL-6 and TGF-β, largely from DC and mϕ, initiate the differentiation of Th17 cells, and induce the expression of IL-23R on these cells, which allows DC derived IL-23 to stabilise the generation of Th17 cells (Aggarwal et al., 2003; Bettelli et al., 2006; Mangan et al., 2006; Veldhoen et al., 2006).

Th17 cells require the transcription factor RORγt (Ivanov et al., 2006) and are involved in controlling infection by extracellular bacteria and fungi (Happel et al., 2005), as well as being implicated in several forms of inflammatory disease (Park et al., 2005). The largest population of Th17 cells in healthy animals is found in the intestine (see below). The generation of Th2 cells require the presence of IL-4,and given that DC do not produce this cytokine themselves, it remains unclear exactly how DC drive Th2 differentiation. IL-4 may come from other T cells, basophils, eosinophils or NKT cells (O'Garra, 1998). IL-4 induces the transcription factors GATA-3, STAT-6 and c-MAF in T cells (Agarwal and Rao, 1998; Zhang et al., 1997; Zheng and Flavell, 1997), and Th2 cells produce IL-4, IL-5, IL-9 and IL-13 which can act upon naïve B cells to induce class switching generating IgE and IgG1. The role of Th2 cells is to respond to and clear extracellular nematodes, but they also play a part in allergy and asthma (Finkelman et al., 1988; Katona et al., 1991; Snapper et al., 1988a). Tfh cells are the most recently described T cells. They express Bcl6 and IL-21, provide B cell help by promoting class switching, and do this by acquiring CXCR5 in the thymus-dependent area and migrating into the germinal centres of lymphoid tissues (Crotty, 2011; Fazilleau et al., 2009).

In addition to driving $CD4^+$ T cell responses, DC are also needed to initiate $CD8^+$ T cell responses. $CD8^+$ T cells differentiate into CTLs that are capable of killing cells that are infected with viruses and other intracellular pathogens. DC present exogenous antigen to $CD8^+$ T cells in an MHC I restricted manner in a process known as cross presentation.

1.3.3.4 Dendritic cells and the induction of tolerance

DC that have acquired antigen in the tissues in the absence of “danger signals” from PRR can still mature to some extent and migrate to the draining LN. However, because they do not express high levels of costimulatory molecules these “semi-mature” DC cannot induce the differentiation of effector T cells, even though they can present antigen to naïve cognate T cells. In contrast, this leads to the induction of tolerance in the T cell. One mechanism of this is anergy, in which the T cell is unable to undergo clonal expansion and becomes blocked in a non-functional state.

Alternatively the T cells become inducible FoxP3$^+$ T regs due to the production of IL-10 or RA by the DC, and/or the presence of TGFβ.

DC are also important for the induction of central tolerance that prevents responses to self antigen via clonal deletion of self-reactive T cells in the thymus, or by the induction of natural FoxP3$^+$ Tregs (nTregs). There are two ways this is thought to occur; firstly by expression of autoimmune regulator (AIRE) on medullary thymic epithelial cells (mTECs) which drives the expression of peripheral antigens in the thymus for thymic cDC to take up and present (Gallegos and Bevan, 2004; Hubert et al., 2011). Alternatively, cDC1 and cDC2 may carry self-antigen from the periphery to the thymus and directly induce clonal deletion in T cells (Bonasio et al., 2006).

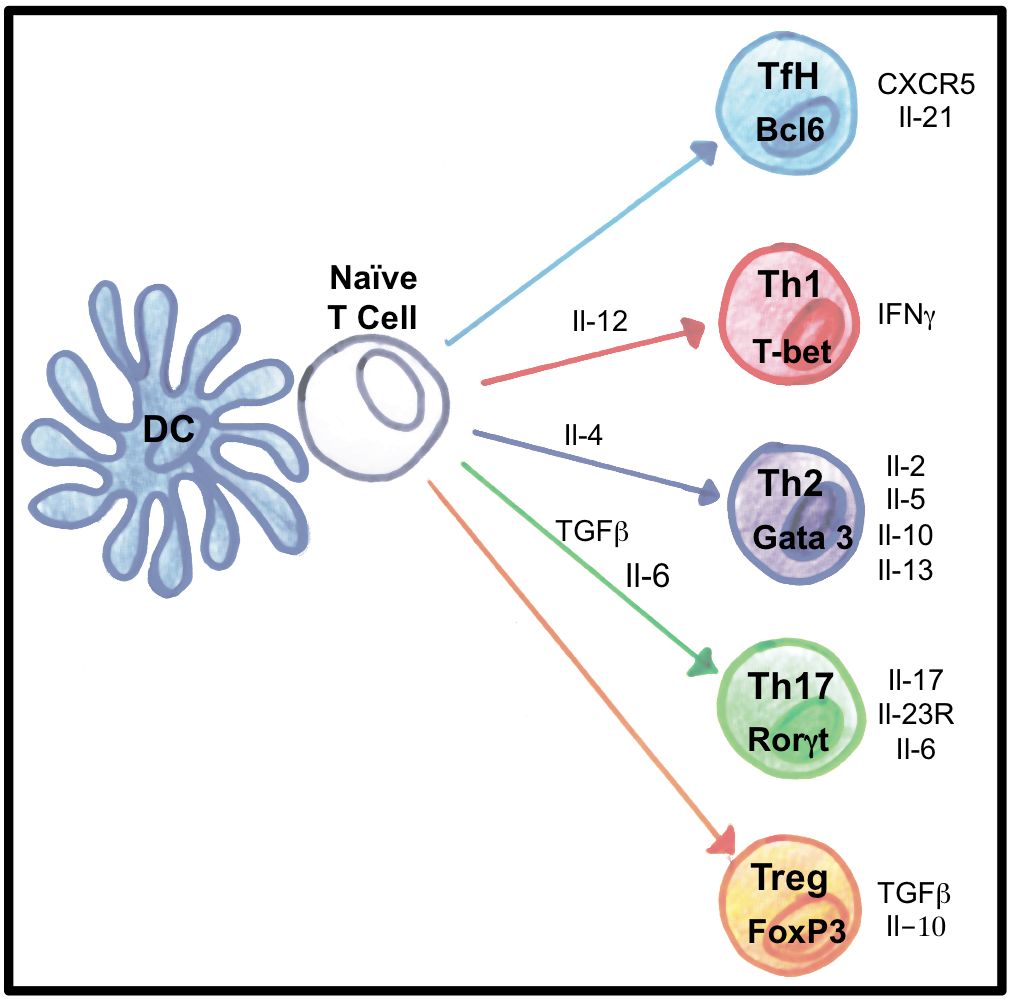

Figure 1.1: DC – T cell interactions. DC produce a number of different cytokines in response to acquired antigen. These polarise naïve T cells to become effector T cells or Tregs. Each of the T cell subsets is under the influence of a specific transcription factor.

1.4 Development of dendritic cells

Haematopoiesis develops in two waves. The initial phase begins in mice at approximately embryonic day 7 (E7) in the yolk sac of the embryo. This primitive phase gives rise to mϕ progenitors from the primitive ectoderm, which then seed many tissues directly. Definitive haematopoiesis begins at around E10.5, when haematopoietic stem cells (HSCs) formed in the yolk sac move to the foetal liver, expanding and producing erythrocytes, lymphocytes and myeloid cells. Just before birth, HSCs colonise the BM, which is then the source of haematopoiesis throughout adult life.

The generation of the individual types of haematopoietic cells involves a linear series of precursors, each of which becomes increasingly committed to a specific lineage (FIGURE 1.2). In myelopoeisis, HSC give rise to the common myeloid progenitor (CMP), which develops into the granulocyte/mϕ progenitor (GMP), followed by the mϕ/DC progenitor (MDP) that can generate both these populations. The MDP is characterised by the expression of CX3CR1, CD135 (Flt3), CD115 and CD117, but lacks MHCII and lineage markers for B cells, T cells, erythrocytes and NK cells (Fogg et al., 2006). The MDP then diverges to produce pro-monocytes ($CD117^{-}$ $CX3CR1^{+}$ $CD115^{+}$ $CD135^{-}$ $CD11b^{+}$ $Ly6C^{hi}$) or $CD117^{lo}$ $CX3CR1^{+}$ $CD115^{+}$ $CD135^{+}$ common DC precursors (CDP) (Onai et al., 2007) (also termed pro-DC (Naik et al., 2007)), that can give rise to both cDC and pDC. Pro-monocytes give rise to two subsets of monocytes; $Ly6C^{hi}$ and $Ly6C^{lo}$. It was originally believed that $Ly6C^{hi}$ monocytes were "inflammatory" monocytes that gave rise to mϕ in inflammation, while $Ly6C^{lo}$ monocytes were thought to be precursors of mϕ in steady state tissues. However, it is now clear that $Ly6C^{lo}$ monocytes are derived from $Ly6C^{hi}$ monocytes and are specialised cells that persist in the bloodstream to monitor the vasculature (Yona et al., 2012). In addition, $Ly6C^{hi}$ monocytes are known to give rise to mϕ in healthy tissues such as the gut (Bain et al., 2014; Tamoutounour et al., 2012), dermis (Ginhoux et al., 2006) and heart (Heidt et al., 2014) and are now referred to as "classical monocytes". The exact contribution of monocytes to resident mϕ populations in different parts of the body is currently controversial, as mϕ in the adult brain (Ajami et al., 2007), lung (Guilliams et al., 2013), epidermis (Hoeffel et al., 2012)

and liver (Bain et al., 2014) are derived from self-renewal of embryonic precursors generated in either the yolk sac or foetal liver (Yona et al., 2012).

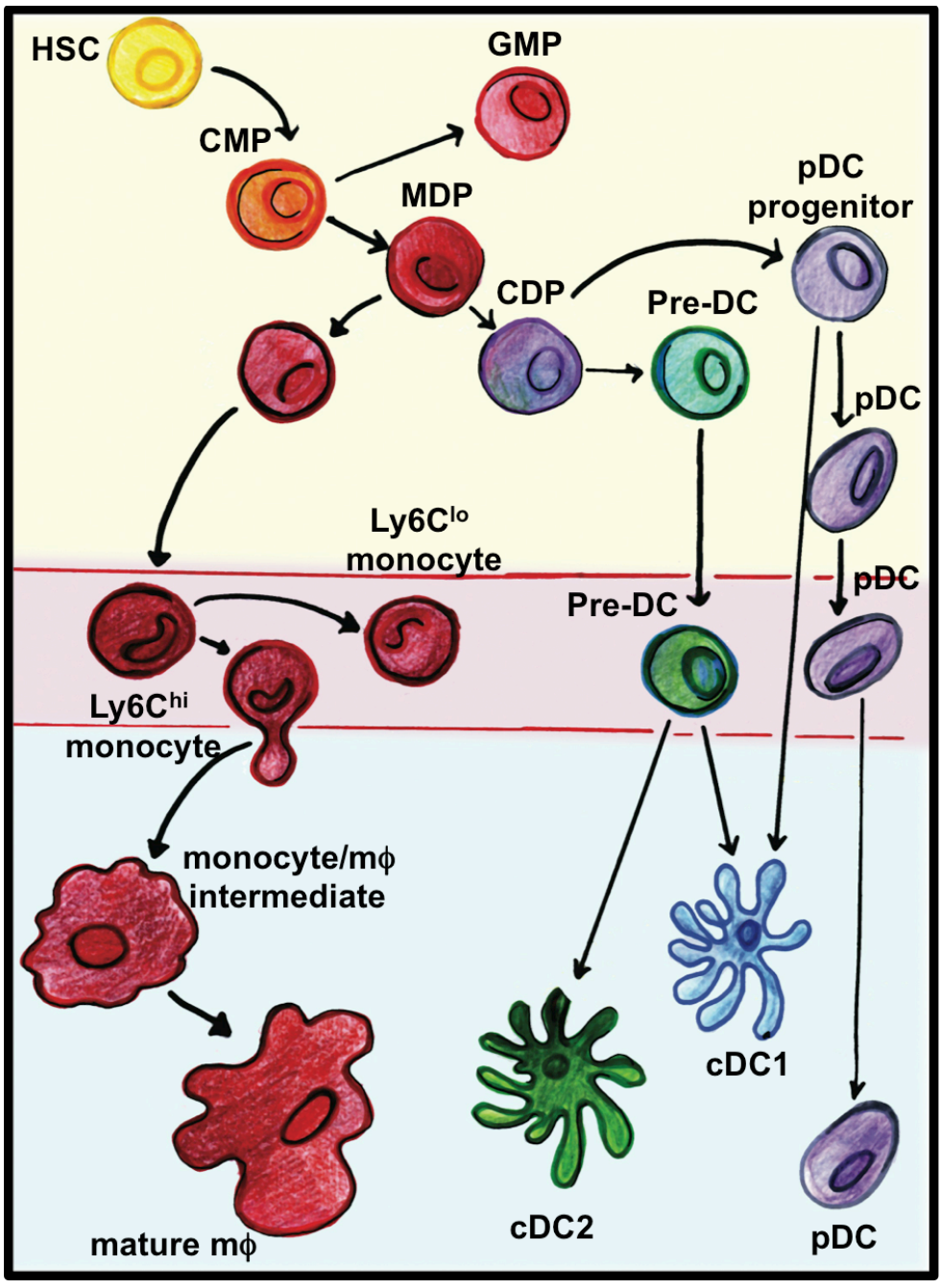

Figure 1.2: Myelopoeisis. DC progenitors arise from the bone marrow HSCs. HSCs give rise to CMPs that differentiate into GMPs or MDPs from which monocytes or CDPs are derived. Monocytes enter the blood stream after which they can enter the peripheral tissues and give rise to mature mϕ. CDPs give rise to a pDC progenitor, which goes on to generate pDC, or the pre-DC, which can enter tissues and immediately differentiate into CD8+ cDC1 and CD11b+ cDC2.

1.4.1 Dendritic cell ontogeny and development

After differentiation from MDP, CDP lose the potential to enter the monocyte/mϕ lineage and instead can develop into either CD117^{-} CX3CR1^{-} CD135^{+} CD115^{-} CCR9^{+} CD11c^{+} B220^{+} Ly6C^{+} pDC or CD117^{-} CX3CR1^{+} CD135^{+} CD115^{-} CD11c^{int} CD11b^{-} precursors of conventional DC (pre-cDC) (Naik et al., 2007). pDC mature fully in the BM before exiting into the circulation, whereas pre-cDC leave the BM as immature cells and migrate in the bloodstream to peripheral tissues where they undergo further differentiation *in situ* to become mature DC (Liu et al., 2009). It is not clear whether or not individual pre-DC can generate all mature DC subsets, or whether there are pre-committed precursors for each subset. Recent work has suggested that the pre-DC population itself is heterogeneous for expression of CD24, and that this might identify distinct precursors for CD8^{+} and CD11b^{+} DC, suggesting that there may be some degree of lineage commitment before exit of pre-cDC from the BM (Naik et al., 2007; 2006). It has also been suggested that pre-cDC may exhibit some degree of tissue specificity with evidence that pre-cDC expressing α4β7 integrin may seed the gut preferentially (Zeng et al., 2012). However, others have proposed that these CCR9^{-} B220^{+} CD11c^{int} α4β7^{+} DC may be a plastic progenitor with some characteristics of pDC; but with the potential to develop into pDC and cDC (Schlitzer et al., 2012; 2011).

1.4.1.1 Transcriptional and Growth factors in DC development

As mentioned previously, cDC subsets are under the control of specific factors. The cDC1 require IRF8 and Batf3, whilst cDC2 require IRF4, Notch and ID2 signalling. However, prior to commitment to any specific DC subset, there are a number of growth factors involved in the development of DC. Fms-like tyrosine kinase -3 (Flt-3; CD135) is expressed by several haematopoietic progenitors, but whereas others down-regulate its expression, DC retain Flt3 throughout their development (Karsunky et al., 2003; Liu et al., 2009). Mice that lack expression of Flt-3 or ligand (Flt3L$^{-/-}$) have a profound defect in all tissue DC, although those that remain are functional (McKenna et al., 2000). Conversely, mice injected with Flt3 ligand (Flt-3L) have expanded DC in tissues due to greater *in situ* proliferation (Maraskovsky et al., 1996; Scott et al., 2014a; Waskow et al., 2008).

Another growth factor involved in DC development, maturation and maintenance is granulocyte-macrophage colony-stimulating factor (GM-CSF; CSF-2). It was the first growth factor used to generate DC from mouse BM or human monocyte precursors *in vitro* (Inaba et al., 1992; Sallusto and Lanzavecchia, 1994), although it is now known that this procedure also produces mϕ and other myeloid cells. In addition *in vivo* administration of CSF-2 or overexpression in transgenic mice only increases DC to a small extent (Maraskovsky et al., 1996; Vremec et al., 1997). Absence of CSF-2 or CSF-2R has little effect on DC populations in lymphoid tissues, but it leads to a selective defect in $CD103^+CD8a^+$ DC in non-lymphoid tissue such as the lung, liver, kidney and dermis, as well as in $CD103^+CD11b^+$ DC in the intestine (Bogunovic et al., 2009; Greter et al., 2012; King et al., 2010; Varol et al., 2009). These effects are not simply because CSF-2 directly induces the expression of CD103, but reflects a generalised defect in their lineage (Greter et al., 2012). Unlike monocytes and mϕ, DC are independent of mϕ colony stimulating factor (M-CSF; CSF-1) or its receptor CSF-1R (CD115), for their maintenance.

1.5 Intestinal mononuclear phagocytes

Both DC and mϕ are highly abundant in the intestine, where they play important roles in the balance between tolerance and immunity. DC can be found in the LP, PP, ILF and MLN, as well as in the LP and in the afferent lymph that drains the intestine (Cerovic et al., 2013). Large numbers of $CD64^+$ mϕ are also present throughout the small and large intestinal LP, where they are sessile, tissue resident cells. The possibility that functionally distinct DC subsets exist in the intestine has generated much interest in recent years, and as noted above, work in our lab has elucidated methods for discriminating mucosal DC from mϕ and for characterising the cells present within each group. When I started my project, this work had shown that tissue resident mϕ expressed high levels of CD64 and CX3CR1 and are derived from 'classical' $Ly6C^{hi}$ monocytes in a CSF-1 dependent manner (Bain et al., 2012; Tamoutounour et al., 2012). In contrast, $CD11c^+$ $MHCII^+$ DC express zbtb46 (zDC) but not F4/80 or CD64. cDC derive from pre-DC and rely on Flt3L and GM-CSF for their development as well as having a rapid turnover *in vivo* of around 6-7 days (Bogunovic et al., 2009; Scott et al., 2014a; Varol et al., 2009).

1.5.1 Intestinal DC subsets

The conclusion of earlier work was that all intestinal DC could be defined by their expression of CD103 and that this was a homogeneous population. However when it became possible to distinguish DC and mϕ more precisely, it was clear that intestinal $CD103^+$ DC were heterogeneous and that there were also $CD103^-$ subsets of genuine DC. As a result the current view is that four subsets of genuine intestinal DC can be found based on the expression of CD11b and CD103 (TABLE 1.2). Notably, these include substantial numbers of $CD103^+CD11b^+$ DC, not found in other tissues. All of these are derived from pre-DC, require Flt3L for development, migrate constitutively from mucosa to MLN, express DC-specific markers and genes shown in Table 1.1 and can prime naïve T cells.

The function of CD103 on DC is unknown, although one of its ligands is known to be E-cadherin expressed by intestinal epithelial cells. This interaction may be involved in the maintenance of $CD103^+$ T cells and DC in intestine (Siddiqui and Powrie, 2008), although it has never been shown to influence DC behaviour directly. Once believed to be uniformly tolerogenic in nature, it is now clear that all intestinal DC can induce a variety of T cell functions depending on the circumstances. However, the exact role of each DC subset *in vivo* is still being elucidated.

Table 1.2: Intestinal DC subsets

MP Subset	Phenotype	Location	Growth Factor
$CD103^+CD11b^+$	CD11c+, MHCII+, F4/80-, CX3CR1-, SIRPα+, XCR1-	SI LP >> CLP	Flt3L, CSF-2
$CD103^+CD11b^-$	CD11c+, MHCII+, F4/80-, CX3CR1-, SIRPα-, XCR1+	SI LP << CLP	Flt3L
$CD103^-CD11b^+$	CD11c+, MHCII+, F4/80-, CX3CR1+, SIRPα+, XCR1-	SI LP < CLP	Flt3L
$CD103^-CD11b^-$	CD11c+, MHCII+, F4/80-, CX3CR1-, SIRPα+/-, XCR1-	SI LP = CLP	Flt3L

1.5.1.1 CD103$^+$ CD11b$^+$ DC

This is the most numerous population in the SI and unlike CD103$^+$ DC in other, non-lymphoid tissues, these are CD8α^- and are largely unique to the GI tract (Fujimoto et al., 2011; Sun et al., 2007), although they can be found in small numbers in the lung (own observations). They are also present in the colon, but in lower numbers than in the SI and indeed their relative frequency decreases progressively going down the SI from duodenum to ileum (Denning et al., 2011). They can also be isolated from intestinal afferent lymph and the migratory compartment of the MLN. As well as Flt3, CD103$^+$CD11b$^+$ DC require CSF-2 for their development (Bogunovic et al., 2009; Greter et al., 2012), together with IRF4 (Persson et al., 2013b), Notch2 (Lewis et al., 2011), IkkB (Mancino et al., 2013), vitamin A (Agace and Persson, 2012) and SIRPα (Scott et al., 2014b). Originally held to be responsible for induction of tolerance and Tregs *in vivo* (Coombes et al., 2007), they can drive the generation of FoxP3 Tregs *in vitro* (Siddiqui and Powrie, 2008). However, *in vivo* studies show that mice lacking CD103$^+$CD11b$^+$ DC have normal numbers of Tregs in the intestine, but have defects in the generation of Th17 cells (Welty et al., 2013) and in Th17 mediated responses towards *Citrobacter rodentium* infection (Denning et al., 2011; Fujimoto et al., 2011; Lewis et al., 2011; Scott et al., 2014b). It has been suggested that this reflects the ability of CD103$^+$CD11b$^+$ DC to produce IL-6 that drives Th17 generation (Persson et al., 2013b). Conversely, it has also been reported that IRF4 dependent CD103$^+$CD11b$^+$ DC are required for the generation of Th2 responses in the intestine, as they are able to clear *Citrobacter rodentium* infection, but succumb to *Schistosoma mansoni* infection (Tussiwand et al., 2015). Furthermore, CD103$^+$CD11b$^+$ DC are thought to be responsible for TLR5-mediated induction of IgA producing B cells, as well as antigen specific Th17 and Th1 cells after TLR5 stimulation with flagellin (Cerovic et al., 2013; Uematsu et al., 2008).

1.5.1.2 CD103$^+$ CD11b$^-$ DC

CD103$^+$CD11b$^-$ DC are found in the SI LP, CLP, PP, lymph and both the resident and migratory compartment of the MLN (Cerovic et al., 2014b; Houston et al., 2015). DC with this phenotype in the intestine also express CD8α, XCR1 and DNGR1, but not SIRPα and they appear to be conventional, cross-presenting DC. They are present

throughout the GI tract and their frequency is similar between the duodenum an ileum. However, they make up the majority of DC in the colon (Denning et al., 2011). As in other parts of the body, $CD103^+CD11b^-$ DC in the intestine require BATF3 for their development. Mice with a selective defect in $CD103^+CD11b^-$ DC have normal numbers of Tregs in the intestine, whilst mice lacking both subsets of $CD103^+$ DC do have reduced numbers of these T cells, suggesting that there is redundancy amongst the two subsets of DC (Welty et al., 2013).

1.5.1.3 $CD103^-CD11b^+$ DC

Until the improved strategies for characterising intestinal MP, this subset was usually included amongst mϕ, based on their failure to express CD103. This was further complicated by the fact that genuine $CD103^-CD11b^+$ DC express some CX3CR1, the marker usually associated with monocytes and mϕ (Cerovic et al., 2014a). The relative frequency of $CD103^-CD11b^+$ DC increases from the SI to the colon (Denning et al., 2011), but although it is clearly similar to conventional $CD11b^+$ $SIRP\alpha^+$ DC in other tissues, the exact role of this subset in the intestine is unknown, as is their relationship to the more abundant $CD103^+CD11b^+$ DC. They are also largely unaffected in CD11c-cre $IRF4^{fl/fl}$ and SIRPα mt mice, despite the fact that there is a defect in the conventional $CD11b^+$ $SIRP\alpha^+$ DC subset in other tissues. This subset also appears to be heterogeneous in the intestine, as recent work in our lab has shown that some of them are absent in CCR2 KO mice and a proportion of them express CCR2, again usually thought to be a feature of the monocyte/ mϕ lineage. However, these CCR2 expressing $CD103^-CD11b^+$ DC are derived from Flt3 dependent pre-DC and do not express CD64 or F4/80. They appear to have an even greater ability to drive Th17 cell differentiation in vitro when compared to $CCR2^-CD103^-CD11b^+$ DC (Scott et al., 2014a).

1.5.1.4 $CD103^-CD11b^-$ DC

This subset of DC lacks CD11b and CD103 expression and is the smallest in the intestine. Although they migrate to the MLN, their nature is unclear. They are heterogeneous for DC markers such as SIRPα and it is thought that this population could contain DC precursors that become $CD103^+CD11b^-$, $CD103^-CD11b^+$, or

$CD103^+CD11b^+$ DC. Their relative frequency does not change much from the SI to the colon (Denning et al., 2011).

Although much has been learnt about intestinal DC subsets in recent years, their biology is not yet fully understood. It is clear that there is a certain amount of redundancy amongst the DC subsets, which may account for the conflicting results seen in the literature. However unknown, and to my knowledge unexplored, is why there are $CD103^+CD11b^+$ DC in the intestine in the first place when they are not present at other mucosal and epithelial sites, and at what stage in development they appear. This becomes the main focus of this thesis.

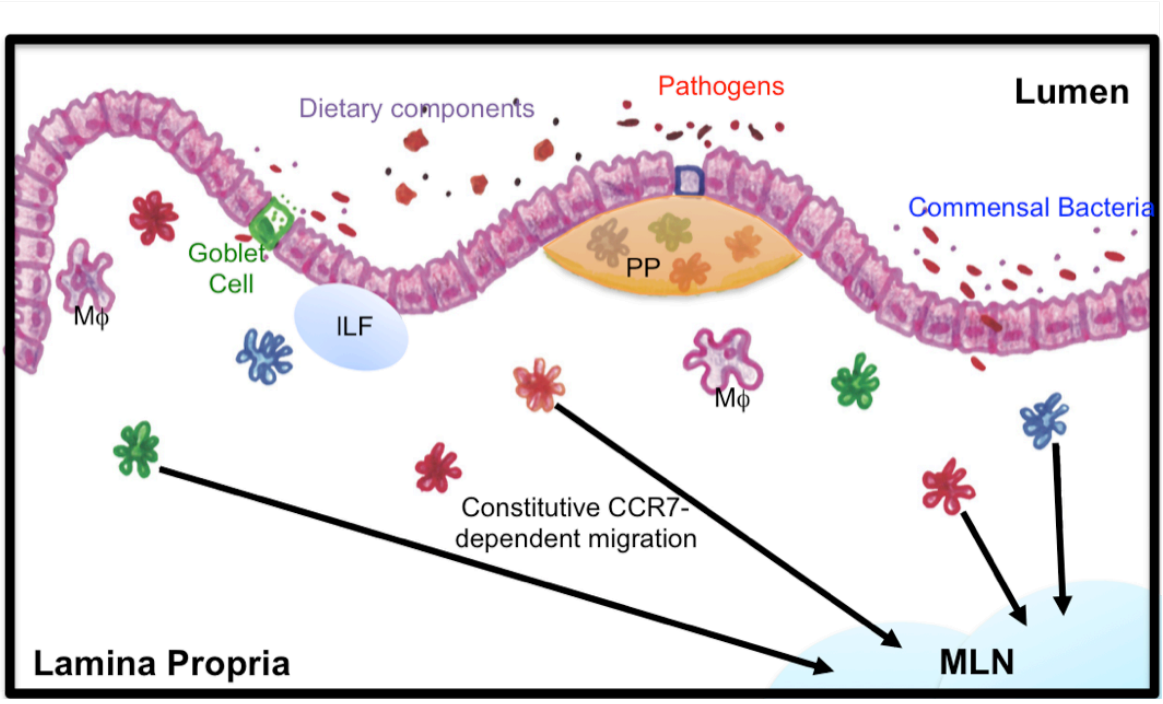

Figure 1.3: Schematic representation of the LP and associated lymphoid tissue. DC in the LP constitutively migrate to the MLN via afferent lymphatics where they interact with T cells in order to generate an effector or regulatory immune response. $CD103^+CD11b^+$ DC, $CD103^-CD11b^+$ DC, $CD103^+CD11b^-$ DC, $CD103^-CD11b^-$ DC.

1.5.2 Functions of Intestinal DC

The main function of DC is to take up antigen and migrate to the draining LNs to present antigen to naïve T cells. There are several sites where antigen acquisition may occur in the intestine, including via M cells in ILFs or PP. Although DC also

clearly appear to be loaded with intestinal antigen in the LP villus, it remains unknown how this occurs. One possibility is direct access of soluble antigen across or between epithelial cells. It has also been suggested that there may be M cells in the epithelium of conventional villi in the SI (Jang et al., 2004). Early work using in vivo microscopy suggested that a population of $CX3CR1^{+}MHC\ II^{+}$ "DC" could extend dendrites across the epithelium to capture luminal bacteria (Chieppa et al., 2006; Niess et al., 2005; Rescigno et al., 2001). However, these were never proved to be DC or to present antigen to T cells and even if this phenomenon could be replicated, it now seems more likely that mϕ were the cells involved (Schulz et al., 2009). More recent twin-photon microscopy work using $CD11c^{+/YFP}$ x $CX3CR1^{+/GFP}$ transgenic mice, suggested that goblet cell associated antigen passages (GAPs) could allow the passage of soluble dextran and proteins to underlying DC. However, this route was shown to be ineffective for the passage of particulate antigens >0.2μm and thus would be unlikely to account for the uptake of bacteria (McDole et al., 2012). Other work using twin-photon microscopy found no role for GAPs, but did report the presence of $CD103^{+}$ DC in the epithelia itself that could extend dendrites into the lumen and sample bacteria (Farache et al., 2013). A further mechanism that has been suggested is that soluble antigens may be taken up initially by $CX3CR1^{+}$ mϕ before being passed on to $CD103^{+}$ DC via connexin 43^{+} gap junctions. This process was shown to be important for the induction of oral tolerance to protein antigen (Mazzini et al., 2014). Thus a number of routes have been proposed to account for antigen acquisition by DC in the LP, but there may be contradictions and the lack of reproduction of some of these data mean that more work is required to understand the exact modus operandi.

As elsewhere in the body, DC migrate from the intestine in a CCR7 dependent manner and this involves all the subsets based on CD103 and CD11b (Jang et al., 2006; Worbs et al., 2006). Studies using pseudo afferent lymph from mesenteric lymphadenectomised mice, show that the relative proportions of each subset in lymph correspond to those seen in mucosal LP and in the migratory compartment of MLN (Cerovic et al., 2013). The migration of intestinal DC in lymph is a constitutive process, even in steady state. The mechanisms involved are unknown though it requires MyD88, but not TLRs and is intact in GF mice, although can be enhanced by LPS or TNFα. Importantly, recent work in our laboratories has been unable to

confirm a recent report that CX3CR1$^+$ mϕ might migrate in intestinal lymph, even during infection, and it appears that this study did not distinguish mϕ from CX3CR1$^+$ DC properly (Diehl et al., 2013). DC migrating to the MLN have been shown to carry both soluble and bacterial antigen (Bogunovic et al., 2009; Jaensson et al., 2008; Macpherson and Uhr, 2004) and this is essential for the development of both tolerance and immunity in the intestine, with oral tolerance to proteins being entirely dependent on CCR7 driven migration of DC (A. Mowat, 2003; Worbs et al., 2006). DC migrating in lymph do not go further than the MLN, as few are present in the thoracic duct before mesenteric lymphadenectomy (Cerovic et al., 2013), and commensal bacteria that are taken up by intestinal DC are never found in other tissues in the presence of intact MLN (Yrlid et al., 2006).

After arrival in the MLN, a unique feature of intestinally derived DC is their ability to generate retinoic acid (RA) from dietary vitamin A, inducing the expression of gut homing markers CCR9 and $\alpha_4\beta_7$ integrin on naïve T cells (Annacker et al., 2005; Johansson-Lindbom et al., 2005). This ensures that the T cells primed in the MLN return to the intestinal mucosa to express their effector functions (Iwata et al., 2004). All intestinal DC express the *Aldh1a1* and *Aldh1a2* enzymes necessary for producing RA, although the CD103$^+$ subsets are particularly effective in this respect (Coombes et al., 2007). Firstly, vitamin A is oxidised to retinaldehyde by ALDH and then further oxidised to RA by RALDH (Duester, 2001; Maden, 2002). The production of RA by DC is restricted to the small intestine and is not found in the colon or systemic lymphoid organs, although a recent study has suggested that CD103$^+$ and CD103$^-$ DC subsets from the lung can produce RA and induce T cell homing to the intestine (Ruane et al., 2013). It is unclear whether DC are the only source of RA in the intestine and it is likely that epithelial and stromal cells also produce it. The only source of vitamin A in mammals is the diet and it is delivered to the mucosa directly, or from the liver stores also shown to generate RA from vitamin A, with the potential to enhance RA production by DC, or imprinting gut homing properties on T cells (Agace and Persson, 2012; Annacker et al., 2005).

Under steady state conditions, RA induces the generation of FoxP3$^+$ Treg cells from naïve CD4$^+$ T cells (Sun et al., 2007), thus favouring the induction of tolerance to

harmless antigens in the intestine. The generation of FoxP3$^+$ Tregs also requires collaboration with TGF-β, that can be produced by many cells in the intestine such as mϕ and DC themselves. However TGF-β is synthesised in an inactive form and must be cleaved to be biologically active (Annes et al., 2003). One molecule that can do this is αvβ8 integrin, which is expressed by CD103$^+$CD11b$^-$ DC, and mice that lack αvβ8 expression on CD11c$^+$ cells have reduced numbers of FoxP3 Tregs and develop spontaneous inflammation. Tregs also express αvβ8; when they lack its expression, mice succumb to IBD (Travis et al., 2007; Worthington et al., 2012; 2015).

Although earlier studies suggested that CD103$^+$ DC had a selective role in the generation of gut homing Tregs and tolerance, many were performed before it was known that there were two subsets of intestinal CD103$^+$ DC, and the population responsible was not identified. As mentioned earlier, Batf3$^{-/-}$ mice have a selective defect in CD103$^+$CD11b$^-$ DC, but have normal numbers of FoxP3$^+$ Tregs in the intestine (Edelson et al., 2010b), as do mice with reduced CD103$^+$CD11b$^+$ DC due to a mutation in SIRPα (Scott et al., 2014b). Some of these studies did not distinguish between thymically derived nTregs (which make up a large proportion of intestinal Tregs (Cebula et al., 2013; Weiss et al., 2012)) and inducible iTregs, which would be the ones that would be expected to require gut DC for their generation. However other work in CD11c-cre IRF4$^{fl/fl}$ mice that also have a selective reduction in CD103$^+$CD11b$^+$ DC, found normal numbers of both iTregs and nTregs (Persson et al., 2013b). Similar results were obtained in human-langerin diphtheria toxin (hu-Langerin DTR) transgenic mice that lack CD103$^+$CD11b$^+$ DC, but ablation of both CD103$^+$ DC subsets did lead to a reduction in both types of Tregs, suggesting there may be redundancy between these DC populations (Welty et al., 2013).

Redundancy amongst DC subsets in their ability to produce RA and to migrate to the MLN may also explain the apparently contradictory data reported by different groups examining the ability of DC subsets to imprint T cell responses. Although the CD103$^+$CD11b$^-$CD8α$^+$ subset appears to be the only one that can cross present antigen to CD8$^+$ T cells (Cerovic et al., 2014b; Fujimoto et al., 2011)), both CD103$^+$CD11b$^+$ and CD103$^+$CD11b$^-$ DC can drive IFNγ production by CD4$^+$ T cells (Fujimoto et al., 2011). Both CD103$^+$CD11b$^+$ and CD103$^-$CD11b$^+$ DC have also been

reported to polarise T cells towards Th17 effector cells *in vitro* (Denning et al., 2011; Fujimoto et al., 2011; Lewis et al., 2011; Persson et al., 2013b; Schlitzer et al., 2013). However, as noted above, depletion of $CD103^{+}CD11b^{+}$ DC *in vivo* leads to reduced Th17 cells in the gut despite normal numbers of the other subsets (Cerovic et al., 2013; Scott et al., 2014a). As the DC subsets express distinct patterns of TLR and other PRR, this could mean that the population involved in any response may be dependent on the environment and that there is substantial plasticity amongst the subsets.

1.5.3 Local conditioning of intestinal dendritic cells

While there has been one report that there may be distinct pre-cDC that give rise to intestinal DC (Zeng et al., 2012), it seems more likely the unusual properties of these cells is due to local factors that condition the local differentiation of pre-DC once they arrive in the intestine. There are a number of possible candidates for producing such effects.

1.5.3.1 Epithelial cell derived mediators

IECs can produce several immunoregulatory factors that can affect DC development including thymic stromal lymphopoeitin (TSLP), TGF-β and prostaglandin E2. TSLP is the best studied of such factors and is expressed constitutively by IEC in an NFκB dependent manner and is further up regulated in response to infection, inflammation and tissue injury (Allakhverdi et al., 2007; Bogiatzi et al., 2007; Rimoldi et al., 2005). Specific deletion of NFκB in IEC leads to dysregulation of cytokine production in DC leading to intestinal inflammation. TSLP has been shown to condition human monocyte derived DC to drive Th2 anti-inflammatory responses and upregulate CD103 on DC which can then drive Treg generation *in vitro* (Iliev et al., 2009a; 2009b; Spadoni et al., 2012). TSLP produced by Hassal's corpuscles in the thymus has also been suggested to support the differentiation of DC that drive the local development of nTregs (Watanabe et al., 2005). Furthermore, deletion of TSLP in mice leads to overexpression of IL-12/IL-23p40 in DC and the inability to generate Th2 responses against *Trichuris muris* infection (Zaph et al., 2007). DC themselves may also produce TSLP in response to MyD88 signalling (Spadoni et al., 2012). Other DC regulatory

factors produced by IEC include TGF-β that conditions intestinal DC to generate Treg differentiation. Other cell types can also drive the production of TGF-β *in vivo*, such as $CD4^+$ T cells and mϕ (Fukaura et al., 1996; Gonnella et al., 1998; Weber et al., 2011).

1.5.3.2 Intestinal microbes

Given the close proximity of intestinal DC to the microbiota, it would seem obvious that their behaviour might be influenced by microbial products. This is supported by the findings that commensal bacteria such as *Bacteroides* and *Bifidobacteria* can induce monocyte-derived DC to acquire tolerogenic properties *in vitro* (Baba et al., 2008). Furthermore, the ability of polysaccharide A derived from *Bacteroides fragilis* to promote IL-10 producing Tregs in the colon induces interaction with $CD11c^+$ cells (Mazmanian et al., 2005), as do the Th17 inducing effects of SFB (Ivanov et al., 2009). However the exact mechanisms by which the bacteria do this are unclear. The normal intestine also contains commensal fungal populations and zymosan from yeast cell walls can induce both IL-10 production and *Aldh1a2* expression in DC that then favour the generation of $FoxP3^+$ Treg cells. These effects are TLR2 and the C-type lectin, dectin-1 dependent (Dillon et al., 2006). MyD88 dependent TLR1 and TLR2 signals are required for RA synthesis, suggesting that ligation of these receptors by the microbiota may be at least partly responsible for the ability of DC to produce RA and the resultant imprinting of gut homing T cells (Wang et al., 2011).

Despite these clues, the role of the microbiota on the development and functions of intestinal DC remains to be elucidated in full and has not been studied using the recently improved means of analysing these cells. In this thesis I therefore explored the effects of antibiotics and a germ free environment on DC in the intestine.

1.5.3.3 Dietary constituents

DC in the intestine are constantly encountering dietary constituents and some of these may play a role in the conditioning of local DC. Most studied is vitamin A, which is acquired purely via the diet in mammals. As well as being important for the characteristic effector functions of intestinal DC, RA also conditions their properties. A vitamin A deficient diet leads to reduced numbers of $CD103^+CD11b^+$ DC in the SI LP,

and the remaining $CD103^+$ DC are impaired in their ability to generate Tregs and imprint gut homing T cells in the MLN (Klebanoff et al., 2013). The source of RA may be DC themselves, or epithelial and stromal cells (Agace and Persson, 2012) although it has also been shown that bile is a source of retinol that induces RA receptor-dependent retinol metabolising activity in $CD103^+$ DC (Jaensson-Gyllenbäck et al., 2011). This imprinting of $CD103^+$ DC in the SI may explain the fact that $CD103^+CD11b^+$ DC are more frequent in the duodenum.

1.5.3.4 Neuroendocrine pathways

The GI tract is highly innervated and produces large amounts of neurotransmitters that are essential for physiological functions of the intestine such as peristalsis, digestion, fluid secretion and appetite control. Many immune cells express high levels of receptors for neurotransmitters, and the best described neural regulator of immune function is vasoactive intestinal peptide (VIP). It is produced by intestinal enteroendocrine cells, where it acts as a vasodilator and regulator of epithelial permeability (Bellinger et al., 1996). VIP has potent anti-inflammatory effects in the immune system and has been shown to inhibit mϕ function as well as DC maturation and migration via an ability to suppress LPS-induced CCR7 expression (Weng et al., 2007). VIP can also induce the differentiation of IL-10 and TGF-β producing Tregs, and they promote the induction of tolerance rather than active immunity in the intestine (Gonzalez Rey and M. Delgado, 2006).

1.6 Triggering receptor on myeloid cells – 1 (Trem-1)

Triggering receptor on myeloid cells – 1 (Trem-1) is one of a number of innate immune receptors of the Trem and Trem-like family that are thought to amplify or dampen TLR signals in neutrophils, monocytes, mϕ, DC, osteoclasts and microglia.

1.6.1 The Trem family

All the proteins of the Trem family are structurally related and are found on mouse chromosome 17C and human chromosome 6p21.1 (Ford and McVicar, 2009). The Trem genes encode mRNA for Trem-1, Trem-2 and Trem-3 (mouse only) surface

proteins, along with the Trem-like family genes for Trem-like transcript (TLT) -1 and TLT-2. They are all members of the immunoglobulin superfamily and are highly conserved throughout vertebrate evolution (Klesney-Tait et al., 2006). Trem-1, Trem-2 and Trem-3 all associate with the DAP12 adaptor protein that contains an immunoreceptor tyrosine-based activation motif (ITAM) which is phosphorylated by Src kinases on ligation of Trem-1 leading to downstream signalling via the protein tyrosine kinase Syk. TLT-1 does not associate with DAP12 and instead has a cytoplasmic domain containing ITIMs, which recruit SHP-1, and SHP-2 phosphatases.

Trem-1 is the best characterised of the Trem and Trem-like family, and consists of an extracellular Ig V-type domain, a transmembrane region and a short cytoplasmic portion involved in the recruitment of DAP12. Trem-1 is an amplifier of inflammatory responses, increasing the levels of cytokines produced after TLR signalling (Bouchon et al., 2000; 2001) and expression is upregulated in response to LPS (Dower et al., 2008). Ligation of Trem-1 leads to increased inflammatory responses during sepsis and these effects can be reduced by treatment with an inhibitory peptide of Trem-1 (Bouchon et al., 2001; Gibot et al., 2004). As a result it is thought that Trem-1 may reduce the threshold at which microbial threats are detected. Trem-1 is expressed by blood neutrophils and monocytes, but it decreases with maturation of monocytes and mϕ (Bouchon et al., 2001; 2000).

Unlike Trem-1, Trem-2 has been proposed to be a negative regulator of inflammation. Initial experiments showed that Trem-2 ligation could suppress TNFα and IL-6 production by mϕ (Turnbull et al., 2006), and subsequent work indicated that blockade of Trem-2 led to more severe experimental autoimmune encephalomyelitis (EAE), a mouse model for multiple sclerosis (Piccio et al., 2007). Trem-2 also has a role in osteoclastogenesis, as evidenced by the bone cysts seen in Nasu-Hakola disease, which is due to a loss of function mutation in DAP12 or Trem-2 (Klesney-Tait et al., 2006). There is little known about Trem-3 and its functions, as its expression has only been observed at the transcript level in mouse mϕ cell lines. In humans it is a pseudogene (Ford and McVicar, 2009). TLT-1 and TLT-2 promote cellular activation but do not associate with DAP12. TLT-1 can prevent platelet aggregation (Ford and McVicar, 2009) whereas TLT-2 has more widespread effects being

expressed on T- and B- lymphocytes as well as myeloid cells and has been shown to enhance CD3-mediated, IL-2 and IFNγ production by T cells (Hashiguchi et al., 2008).

Most of the Trem family members bind bacterial components directly (Cannon et al., 2012), but the ligand for Trem-1 has been unclear until recently when it was suggested that neutrophil peptidoglycan recognition protein 1 (PGLYRP1) may be involved (Read et al., 2015). Peptidoglycan (PGN) is a macromolecular component of the bacterial cell wall and binds to PGLYRP1 found in the tertiary granules of neutrophils, where it induces production of reactive oxygen species (Dziarski et al., 2003). Although PGN can also be sensed by TLR2 and NOD1/2, it is proposed that Trem-1 mediated recognition of the PGLYRP1:PGN complex released by neutrophils may be an important mechanism of PGN sensing by myeloid cells (Read et al., 2015). The role of Trem-1 in DC is largely unknown, although it has been shown to be upregulated on monocyte derived DC when they are exposed to hypoxic conditions (Bosco et al., 2010).

1.6.2 Trem-1 in the intestine

Trem-1 has been examined in the intestine mostly in the context of monocytes and macrophages, although early studies suggested that it was not expressed by these cells in steady state (Schenk et al., 2005). It was postulated that this might reflect down-regulation of Trem-1 by local IL-10 and TGF-β thus helping to prevent overactive responses to bacterial PAMPs (Schenk et al., 2005). However, it is important to note that these experiments failed to find monocytes and early stage mϕ now known to be present in the healthy intestine, and the cells that might be expected to respond to bacteria. Indeed, increased Trem-1^{+} mϕ were found in the mucosa of patients with IBD and during experimental colitis in mice. Treatment with the antagonistic blocking peptide based on the extracellular domain of Trem-1, led to reduced levels of serum TNF and to less intense intestinal pathology in experimental colitis (Schenk et al., 2007). More recent work reported that Trem1$^{-/-}$ mice were normal under homeostatic conditions, but they were resistant to dextran sodium sulphate (DSS) colitis and had attenuated disease (Weber et al., 2014), although it was not clear whether this reflected the absence of Trem-1 on mϕ or neutrophils. The

expression and role of Trem-1 in intestinal DC has not been investigated and this was one aim of my thesis.

1.7 Thesis aims

Dendritic cells are crucial for determining whether active immunity or tolerance is generated in the intestine. Recent work has established methods for characterising mucosal DC precisely and has revealed unusual properties and heterogeneity amongst these cells. However much remains to be learnt about the specific functions of the various DC subsets found in the intestine, as well as of the factors controlling their development in early life.

The overall goal of this thesis was to explore the processes that might be involved in the development of intestinal DC under steady state conditions. To achieve this, my first specific aim was to describe the dynamics of intestinal DC development from birth onwards and then to investigate the role of SIRPα in determining DC subset development. Next, I aimed to identify markers that were specific to the intestine-restricted subset of $CD103^+CD11b^+$ DC and use them to interrogate the development of this population in greater depth in wild type mice. Lastly, I aimed to exploit these insights to investigate the role of different molecular mechanisms, and the microbiota in shaping intestinal DC population development.

In Chapter 3, I introduced the DC subsets, and showed that intestinal $CD103^+CD11b^+$ DC are reduced in adult SIRPα mt mice but not in bone marrow chimeric mice. I went on to test the hypothesis that the defect seen in adult SIRPα mt mice was related to their age. This showed a greater defect in four-week old mice, which led me to carry out a more detailed analysis of how intestinal DC subsets changed from birth until adult life in Chapter 4. I established CD101 and Trem-1 as markers for dissecting the differentiation of $CD103^+CD11b^+$ DC in more detail. I then used these to extend my analysis of DC development from birth onwards. From these findings, I predicted that intestinal DC function developed with age, which I showed by using RA metabolism as a readout. Lastly, in Chapter 5 I explored some of the factors that might control the development of intestinal DC, examining how the expression of transcription factors and growth factor receptors changed. I then exploited Trem-1 and CD101 to

investigate how SIPRα, CCR2 and the microbiota influenced the appearance of the DC subsets.

Chapter 2

Materials and Methods

2.1 Mice

All mice were maintained under specific pathogen free (SPF) conditions at the Central Research Facility (CRF) or the Veterinary Research Facility (VRF), University of Glasgow. They were used between 6 and 12 weeks of age, unless otherwise specified. Table 2.1 details the mouse strains used throughout these studies. All strains were on the C57/Bl6 background and were CD45.2^{+} unless stated otherwise. All procedures were carried out in accordance with UK Home Office regulations.

Table 2.1: Mice Strains

Strain	Source
C57Bl/6	Harlan Olac (Bicester, Oxfordshire)
C57Bl/6.SJL (CD45.1^{+})	Kindly provided by Prof. W. Agace (Lund University, Sweden)
CD45.1^{+}/CD45.2^{+}	Generated by crossing C57Bl/6 with C57Bl/6.SJL
SIRPα Mutant	Provided by Prof. P.A. Oldenburg (Umeå University, Sweden) with kind permission from Prof. T. Matozaki (University of Tokyo, Japan) (Inagaki, Yamao et al. 2000)
CCR2$^{-/-}$	Kindly provided by Prof. Robert Nibbs (University of Glasgow) ("Impaired monocyte migration and reduced type 1 (Th1) cytokine responses in C-C chemokine receptor 2 knockout mice.," 1997)
Trem-1$^{-/-}$	Bones kindly sent by Prof. C. Mueller (University of Bern, Switzerland)
Germ Free C57Bl/6	Kindly allowed to perform experiments with Dr. L. Hall (University of East Anglia, Norwich, UK)

2.1.1 Treatment of mice with antibiotics

Mice received 1 mg/ml Cefoxitin (Santa Cruz Biotechnology), 1 mg/ml Gentamicin (Sigma), 1 mg/ml Metronidazol (Roche), and 1 mg/ml Vancomycin (Hospira, UK Limited) in their drinking water, with the addition of artificial sweetener (Sweetex, Reckitt Benckiser Household, UK) for two weeks. Control mice received sweetener only for two weeks. Antibiotic solutions were made up on the day of issue and replaced every two days. Mice weights were recorded everyday.

2.1.2 Analysis of germ free mice

All experiments done on germ free (GF) mice were performed in Dr Lindsay Hall's lab at the Institute of Food Research, University of East Anglia, Norwich, UK. In order to assess the GF status, in-house testing of ceacal contents from GF mice was carried out. FACS analysis was using a BD FACSAria II (BD Biosciences).

2.2 Genotyping Mice

2.2.1 Genomic DNA Isolation

Tail tips from SIRPα mutant (mt) and CD47KO mice were stored at -20°C until use. DNA was isolated using the DNeasy Blood and Tissue Kit (Qiagen) as per the manufacturer's guidelines. Briefly, 25mg of each tail tip was digested overnight at 56°C with Proteinase K. The following day, DNA was purified by binding to the spin column membrane provided, washed and eluted in the elution buffer supplied. Genomic DNA was frozen and stored at -20°C until needed.

2.2.2 Genotyping

DNA from tail tips was diluted 1:2 prior to polymerase chain reaction (PCR) and analysed using the primers (Integrated DNA Technologies, IDT) detailed in Table 2.2. Each PCR mixture had a final volume of 20μl, containing 1μl of diluted genomic DNA, 0.2μl each of 10μM sense and anti-sense primers, 0.4μl of 10μM dNTPs (25mM), 0.1μl of 5U/ml Go Taq polymerase, 4μl of 5X reaction buffer and 14.1μl nuclease free water (all Life Technologies, Paisley, UK). The PCR entailed one cycle of 5 minutes at 95°C,

thirty-five cycles of 1 minute at 95°C, annealing at 58 °C and elongation at 72°C for 2 minutes, followed by one more cycle of elongation at 72°C for 10 minutes.

The products of the PCR were visualised by electrophoresis on a 2% agarose gel (Sigma-Aldrich, Poole, UK) in 1X TAE with 5μl ethidium bromide (Life Technologies) per 100ml gel. 10μl of the PCR reaction, along with 2μl of 6X loading dye (Life Technologies) were loaded onto the gel with 5μl of DNA ladder (Life Technologies) and 1μl of 6X loading dye. Gels were run in 1X TAE for approximately 1 hour at 100mV, before being visualised under a UV light.

Table 2.2 Primers for Genotyping

Gene	Sense	Antisense
Sirpa wt	ATACCATTGGCTGAGCCCACTGGGAA AGAA	TAGTACAGACCACAGCCCCATTCACTTCCT
Sirpa mt	TCGTGCTTTACGGTATCGCCGCTCCCG AAT	TAGTACAGACCACAGCCCCATTCACTTCCT

2.3 Isolation of Leukocytes from Tissues

2.3.1 Intestinal Lamina Propria Cells

The small intestines (SI) from adult mice were excised and soaked in PBS (Gibco, Life Technologies). After removal of Peyer's patches and fat, the intestines were opened longitudinally. Faeces were removed by washing in calcium/magnesium free (CMF) Hank's balanced salt solution (HBSS; Gibco) supplemented with 2% foetal calf serum (FCS; Gibco) and the intestines were cut into approximately 0.5cm segments. Tissues were shaken in HBSS/2% FCS and supernatant removed by passing tissue and supernatant through Nitex mesh (Cadisch and Sons, London, UK) followed by collection of the tissue sections remaining on the mesh. To remove the epithelial layer, tissues were incubated at 37°C whilst shaking in 10ml pre-warmed HBSS supplemented with 2mM EDTA (Sigma-Aldrich, Poole, UK) for 20 minutes. The tubes were shaken again, supernatants discarded and the tissues washed in pre-warmed

HBSS before a second incubation in HBSS/2mM EDTA for a further 20 minutes. Following a repeat of the wash step, the tissues were digested with 1mg/ml collagenase VIII (Sigma) in 10ml pre-warmed complete RPMI (RPMI 1640 containing 50mM 2-β-mercaptethanol, 2mM L-glutamine, 100μg/ml penicillin, 100μg/ml streptomycin, 1.25μg/ml Fungizone, and 10% FCS; all Gibco) by incubation at 37°C with shaking for 20-30 minutes. The tubes were shaken vigorously every 5 minutes to increase digestion. Following this, the cell suspensions were passed through an 100μm filter (BD Falcon), followed by a 40μm filter (BD Falcon), then washed twice in complete RPMI to remove any residual enzyme, resuspended in complete RPMI, counted and kept on ice until use. Absolute numbers were calculated by multiplying the cell count by the percentage population of interest, as a proportion of live cells.

Adult colonic LP (CLP) cells were isolated in a similar fashion, except that the two HBSS/2mM EDTA incubations were performed for 15 minutes and 30 minutes, while digestion was carried out for 30-45 minutes using 0.625mg/ml collagenase D (Roche; Roche Diagnostics GmbH, Mannheim, Germany), 0.425mg/ml collagenase V (Sigma), 1mg/ml dispase (Gibco), and 30U/ml DNase (Roche) diluted in complete RPMI.

Neonatal intestines were treated in the same manner, except that it was not always possible to open the intestine longitudinally, or remove the Peyer's patches; digestion times were also reduced and were determined by continuous observation of how much intact tissue remained in the digest mix.

2.3.2 Lymph Node and Spleen Cells

Lymph nodes and/or spleens were excised from mice and fat removed. The tissues were washed in HBSS and cut into small pieces. When lymphocytes were required, the tissues were mashed through an 100mm filter in complete RPMI, counted and left on ice until use. To isolate DC, tissues were digested by incubating at 37°C with shaking in HBSS supplemented with 1mg/ml collagenase D for 40 minutes. After the digestion, cell suspensions were passed through an 100mm filter, washed twice in complete RPMI to remove any residual enzyme, resuspended in complete RPMI, counted and left on ice until use. Red blood cells in spleen preparations were lysed by incubation for 6 minutes on ice with ammonium chloride/EDTA solution (0.8%

NH_4Cl/0.1mM EDTA, Stem Cell Technologies, Grenoble, France) prior to resuspension in complete RPMI and counting.

2.3.3 Liver Leukocytes

CO_2-euthanised mice were perfused by intra-cardiac injection of 10ml PBS and the livers were removed. They were then cut into small pieces (<2mm) and placed in HBSS supplemented with 2% FCS. Tissues were shaken vigorously in HBSS/2% FCS and the supernatant removed by pouring through Nitex mesh. The livers were then digested in complete RPMI supplemented with an enzyme cocktail containing 0.75mg/ml collagenase D, 0.425mg/ml collagenase V, 1mg/ml dispase, and 30U/ml DNase at 37°C with shaking for 20 minutes. After digestion, the cell suspensions were passed through a 40μm filter, washed twice in complete RPMI to remove residual enzymes and red blood cells were lysed by incubation for 6 minutes on ice with ammonium chloride/EDTA solution, before being resuspended in complete RPMI, counted and kept on ice until use.

2.3.4 Lung Leukocytes

CO_2-euthanised mice were perfused by intra-cardiac injection of 10ml PBS and the lungs were excised. These were then cut into small pieces (<2mm) and digested in complete RPMI supplemented with an enzyme cocktail containing 0.625mg/ml collagenase D (Roche; Roche Diagnostics GmbH, Mannheim, Germany), 0.45mg/ml collagenase V (Sigma), 1mg/ml dispase (Gibco), and 30U/ml DNase (Roche) at 37°C with shaking for 45 minutes. Following digestion, the cell suspensions were passed through a 40μm filter, washed twice in complete RPMI to remove any residual enzyme, and red blood cells were lysed by incubation for 6 minutes on ice with ammonium chloride/EDTA solution before being resuspended in complete RPMI, counted and kept on ice until use. The same protocol was used for the isolation of leucocytes from the kidney and heart.

2.3.5 Peripheral Blood Leukocytes

Whole blood was obtained from mice by cardiac puncture and collected into heparin. Red blood cells (RBCs) were lysed by incubating on ice with ammonium

chloride/EDTA solution for 10 minutes and washed twice in PBS. Cells were counted and left on ice until use.

2.3.6 Bone Marrow Cells

Femurs and tibiae were isolated from mice and the bone marrow was flushed out using RPMI 1640 and filtered through Nitex. For flow cytometric analysis, RBCs were lysed and the cells were washed twice in FACS buffer (PBS/2% FCS/ 2mM EDTA). Cells were then counted and left on ice until required.

2.4 Flow Cytometry

2.4.1 Cell Surface Staining

Freshly isolated cells were resuspended in FACS buffer and 2.5-5x10^6 cells were added to 12x75mm polystyrene tubes (BD Falcon). Non-specific binding of antibodies to Fc receptors was prevented by incubation of cells with anti-CD16/CD32 ('Fc Block'; BD Biosciences) at 4°C for 10-20 minutes. Cells were then washed in FACS buffer and incubated with the required antibodies or isotype controls (Table 2.4) at a dilution of 1:200 unless otherwise specified by the manufacturer at 4°C for 20 minutes. Cells were then washed and if biotinylated antibodies had been used, were incubated with streptavidin conjugates at 4°C for a further 20 minutes and washed once more. Just prior to analysis, 15μl of 7-aminoactinomycin D (7-AAD; Biolegend) was added to the cells to allow dead cell discrimination. Cells were acquired on BD LSRII, BD FACSAriaI or BD FACSAriaIII flow cytometers with Diva software and analysed using FlowJo Software (Treestar Inc., USA).

2.4.2 Intracellular Staining

When staining for intracellular cytokines or transcription factors, the staining protocol was adapted slightly to be compatible with the fixable dead cell exclusion dyes used. 4x10^6 cells were incubated in complete RPMI for 4.5 hrs in 5ml polystyrene tubes in the presence of phorbol 12-myristate 13-acetate (PMA) and ionomycin (Cell stimulation cocktail plus protein transport inhibitors, eBioscience) to restimulate the cells. After culture, the cells were washed in PBS and then incubated

for 20 minutes protected from light at 4°C with LIVE/DEAD® fixable dead cell stain (eBioscience) as per the manufacturer's guidelines. Cells were then washed in FACS buffer, incubated with purified anti-CD16/CD32 and stained with the appropriate antibodies for cell surface antigens as described above, before being washed three times in FACS buffer. After being fixed and permeabilised using the eBioscience Flow Kit according to manufacturer's instructions, the cells were then incubated with purified anti CD16/CD32 and stained with antibodies to stain for intracellular cytokines or transcription factors in permeabilisation buffer for 20 mins at 4°C protected from light. They were then washed in permeabilisation buffer, resuspended in FACS buffer and analysed by flow cytometry as described above.

2.4.3 Fluorescence Activated Cell Sorting

Cells were prepared for FACS as described above but under sterile conditions, before being sorted using a BD FACSAria I or BD FACSAria III cell sorter and were typically 94-99% pure.

2.4.4 Aldefluor assay

Aldehyde dehydrogenase activity was assessed using the aldefluor™ kit, as per the manufacturer's instructions (Stemcell Technologies, Manchester, UK). The cells were digested as explained above and then incubated with the aldefluor™ reagent or its inhibitor diethylaminobenzaldehyde (DEAB). Cells were then washed and stained for flow cytometry.

Table 2.3: Antibodies and Isotype Controls

Antibody	Clone	Isotype	Source
B220	RA3-6B2	Rat IgG2a	Biolegend
CCR2	475301	Rat IgG2b	R & D Systems
CD3	145-2C11	Hamster IgG	Biolegend
CD4	GK1.5	Rat IgG2b	Biolegend
CD8	53-6.7	Rat IgG2a	Biolegend
CD11b	M1/70	Rat IgG2b	Biolegend
CD11c	HL3	Hamster IgG1	BD Biosciences
CD11c	N418	Hamster IgG	Biolegend
CD19	1D3	Rat IgG2a	BD Biosciences
CD45	30-F11	Rat IgG2b	Biolegend
CD45.1	A20	Mouse IgG2a	Biolegend
CD45.2	104	Mouse IgG2a	Biolegend
CD64	X54-5/7.1	Mouse IgG1	Biolegend
CD101	Moushi101	Rat IgG2a	eBioscience
CD103	M2/90	Rat IgG2a	BD Biosciences
CD103	2E7	Hamster IgG	Biolegend
F4/80	BM8	Rat IgG2a	eBioscience
FoxP3	FJK-16s	Rat IgG2a	eBioscience
IFNγ	XMG1.2	Rat IgG1	BD Biosciences
IL17a	TC11-18H10.1	Rat IgG1	Biolegend
Ly6C	AL-21	Rat IgM	BD Biosciences
Ly6G	1A8	Rat IgG2a	BD Biosciences
MHC II (IA-IE)	M5/114.15.2	Rat IgG2b	eBiosciences
SIRPα (CD172a)	P84	Rat IgG1	BD Biosciences
TNFα	MP-6XT22	Rat IgG1	BD Biosciences
TREM-1 (CD354)	TR3MBL1	Rat IgG2a	eBiosciences
Streptavidin BV605			Biolegend
Streptavidin QDot 605			Molecular Probes

2.5 Transcriptional Analysis of Cell Populations

2.5.1 RNA Extraction

Cells were sorted directly into 500 μL RLT buffer (Qiagen) and RNA was then isolated using the RNeasy Micro kit (Qiagen) according to the manufacturer's guidelines. Contaminating genomic DNA was removed on the column during RNA isolation with the RNase-free DNase Set (Qiagen) according to the manufacturer's instructions. The RNA was quantified using a nanodrop spectrophotometer (Amersham Biosciences) and RNA was stored at –20°C until use.

2.5.2 cDNA Synthesis

cDNA was reverse transcribed from DNase-treated RNA using Superscript III Reverse Transcriptase (RT) (Life Technologies) according to the manufacturer's instructions. Briefly, 10ng of RNA, 1μl Oligo(dT)$_{12\text{-}18}$ (500μg/ml; Life Technologies), 1μl dNTP mix (25mM each; Life Technologies), and nuclease-free water were added to a nuclease-free microcentrifuge tube (ABgene, Surrey, UK) in a total volume of 10μl. The mixture was heated at 65˚C for 5 minutes, and then chilled on ice. 4μl 5X First-Strand Buffer, 2μl 0.1M DTT, and 1μl RNaseOUT (40 units/ml) (Life Technologies) were added and incubated at 42˚C for 2 minutes. 1μl (200 units) Superscript III RT was then added and the RNA was reverse transcribed at 42˚C for 50 minutes. The Superscript III RT was inactivated by heating at 70˚C for 15 minutes and RNA was degraded using *Escherchia coli* RNase H (10units) (Life Technologies) at 37°C for 20 minutes. Negative control samples were incubated in the absence of Superscript III and all cDNA was stored at –20˚C until use.

2.5.3 Real-Time PCR

Gene expression was assayed by quantitative reverse transcription PCR (qRT-PCR) using Brilliant III Ultra Fast SYBR qPCR master mix (Agilient Technologies) on the 7900HT Fast system (Applied Biosystems). Primers (Table 2.5) were designed using Primer Express software (Applied Biosystems, Life Technologies) and purchased from IDT (Iowa, USA). cDNA samples were assayed in triplicate and gene expression

levels were normalised to TATA binding protein (TBP) as a housekeeping gene. The mean relative gene expression was calculated using the $2^{-\Delta\Delta C(t)}$ method.

Table 2.4: Primers for qRT-PCR

Gene	Sense	Antisense
TBP	TCCACAGCCTATTCAGAACACC	CTACTGCCTGCTGTTGTTGC
Rara	CTTCGAGCACCACAGGACAT	GTTAAGCGGTCCTGGGAGAC
Csf2ra	CGTGGCGCGATGCAT	TCACGACCAAGTAGGCCTCACT
Tgfbr1	TTGCACTTATGCTGATGGTCT	AGTGATGGATCCTCTTCATTT
Irf4	TCTCTGAGGGTCTGGAAACT	GCCCAAGCTAGAAAG

2.6 Generation of BM Chimeras

8 week old C57Bl/6.SJLxC57Bl/6 ($CD45.1^+/CD45.2^+$) mice were irradiated with 2 doses of 5 Gy 2 hours apart. Mice then received $1x10^6$ BM cells from WT ($CD45.1^+$) and TREM1 KO ($CD45.2^+$) mice or SIRPa (CD45.2) mice. Recipient mice were left for 8 weeks to allow BM engraftment.

2.7 Statistical analysis

Results are presented as means ±1 standard deviation unless stated otherwise stated and normally distributed groups were compared using a Student's t-test or for multiple groups, a one-way or two-way ANOVA followed by a Bonferroni post test using Prism Software (GraphPad Software Inc., USA). Values of less than $p<0.05$ were considered to be statistically significant.

Chapter 3

Characterisation of intestinal dendritic cells in SIRPα mt mice

3.1 Introduction

Signal regulatory protein α (SIRPα) is an inhibitory receptor expressed by several different myeloid cells, and has been suggested to control the behaviour of $CD11b^+$ DC in the spleen and skin (Iwamura et al., 2011; Saito et al., 2010). At the outset of my PhD, the laboratory had obtained evidence that although SIRPα was expressed by mϕ and most DC in the intestine, mice carrying a non-signalling mutation in SIRPα (SIRPα mt) had a selective reduction in $CD103^+CD11b^+$ DC. Subsequently, the initial aim of my PhD was to extend this work and to investigate the effects of aging on the phenotype.

3.2 Effects of defective SIRPα signalling on myeloid cells in the intestinal lamina propria and MLN

When I began in the laboratory, much groundwork had established methods for isolating and characterising DC and mϕ from the lamina propria. Furthermore, recent evidence had shown that CD11b, CD11c and MHC II were insufficient to distinguish between DC and mϕ. To address this problem, previous members of the lab devised a rigorous gating strategy that allowed mϕ and distinct subsets of *bona fide* DC to be identified. I adopted this approach to examine MPs in SIRPα mt mice (Fig. 3.1A). In this protocol single, live $CD45^+$ leukocytes were first identified amongst enzymatically-digested samples of SI LP, and MPs were then defined as $CD11c^+$ MHC II^+. CD64, restricted to tissue mϕ in mice, was used to identify $CD11c^+$ MHC II^+ $CD64^+$ mϕ (Fig. 3.1B) (Bain et al., 2013; Tamoutounour et al., 2012). B220 was used to exclude pDCs and the remaining $CD11c^+$ $B220^-$ $CD64^-$ cells could then be subdivided into four distinct populations based on expression of CD11b and CD103 (Fig. 3.1B). Our own work, alongside that of other groups (Persson et al., 2013a; Tamoutounour et al., 2012), has confirmed that all these four subsets are genuine conventional DC, as defined by their ability to migrate via lymph to the draining MLN and present antigen to naïve T cells, and to express DC specific markers such as Zbtb46 and Flt3 (Cerovic et al., 2013). The $CD103^+CD11b^+$ DC population, which is unique to the intestine (Denning et al., 2011), makes up the biggest subset in SI LP (~40% of all DC), followed by the $CD103^-CD11b^+$ subset and then smaller numbers of $CD103^+CD11b^-$

and CD103$^-$CD11b$^-$ subsets (Fig. 3.1B). The intestinal DC subsets expressed varying levels of SIRPα, with the CD103$^+$CD11b$^+$ and CD103$^-$CD11b$^+$ DC expressing high levels, whereas CD103$^+$CD11b$^-$ DC were SIRPα$^-$. The DC that lacked expression of CD103 and CD11b were heterogeneous for the expression levels of SIRPα, while CD64$^+$ mϕ expressed the highest levels of SIRPα (Fig. 3.1C). Replicating the results of a former PhD student, I found that mice carrying a non-functional mutation in the cytoplasmic domain of the SIRPα molecule had significantly reduced frequencies and numbers of CD103$^+$CD11b$^+$ DC compared with WT controls (Fig. 3.2A). In parallel there was an increased frequency of CD103$^+$CD11b$^-$ DC in the SIRPα mt SI LP, although their absolute numbers were not significantly different to WT mice. No differences in the proportions or numbers of CD103$^-$CD11b$^+$ or CD103$^-$CD11b$^-$ DC subsets were observed. Although mϕ also expressed SIRPα, the frequencies of MHC II$^+$ CD11b$^+$ CD64$^+$ mϕ were not significantly different in the SI LP of SIRPα mt mice, although the absolute numbers were significantly reduced (Fig. 3.2B).

The effect of the SIRPα mutation on SI LP DC was mirrored amongst migratory DC in the draining MLN. Migratory DC having arrived in the MLN from the LP can be identified as CD11c$^+$MHC II^{hi} whereas those "resident" DC that are derived directly from the bloodstream are CD11c^{hi} MHC II^{int} (Henri et al., 2001)(Fig. 3.3A). The total numbers and frequencies of both migratory and resident DC were severely reduced in the MLN of SIRPα mt mice compared with their WT counterparts. This observation translated into a significant reduction in the numbers of all DC subsets in SIRPα mt MLN. Consistent with their origin in the LP, there was a significant reduction in the relative proportion of CD103$^+$CD11b$^+$ DC amongst the migratory population in SIRPα mt MLN, while the proportion of migratory CD103$^+$CD11b$^-$ DC was increased (Fig. 3.3B). In contrast to what I found in the SI LP, the relative proportions of CD103$^-$ CD11b$^+$ DC were also reduced amongst migratory DC in the SIRPα mt MLN (Fig. 3.3B). CD103$^+$CD11b$^+$ DC were rare amongst resident DC in WT MLN and there were only a few CD103$^+$CD11b$^-$ DC. The relative proportions of both these subsets and of CD103$^-$ CD11b$^-$ DC were actually significantly increased in the SIRPα mt MLN, reflecting a severe reduction in resident CD103$^-$CD11b$^+$ DC in the SIRPα mt MLN. Consistent with previous findings, the proportions and numbers of CD11b$^+$ DC were also reduced in

the spleen of SIRPα mt mice, with a parallel increase in the proportion of CD11b$^-$ DC (Fig. 3.4) (Saito et al., 2010; Washio et al., 2015).

3.3 Requirement for SIRPα signalling on haematopoietic cells

Whilst these initial experiments confirmed previous findings in the lab that SIRPα mt mice have a defect in intestinal CD103$^+$CD11b$^+$ DC, they could not determine if this effect was intrinsic to haematopoietic cells or not. To explore this, I generated bone marrow chimeric mice by reconstituting irradiated (CD45.1$^+$ CD45.2$^+$) WT mice with CD45.2$^+$ SIRPα mt BM, or by reconstituting CD45.2$^+$ SIRPα mt animals with CD45.1$^+$ BM (Fig. 3.5A). After eight weeks, the SI LP was harvested, and engraftment of donor BM assessed by examining the expression of CD45.1 and CD45.2 on leukocyte populations. Approximately 95% of CD45$^+$ DC in the SI LP of WT recipients were of SIRPα mt origin whilst 96% were of WT origin in the SIRPα mt SI LP, confirming the virtually complete replacement of DC by precursors of donor origin (Fig 3.5B).

Somewhat surprisingly, analysis of the live leukocyte populations in the SI LP revealed few differences in the frequencies or cell numbers of the DC subsets between the two groups of chimeras, apart from a significantly higher frequency of CD103$^+$CD11b$^-$ DC in SIRPα mt -> WT chimeras compared with the WT -> SIRPα mt mice, similar to what was seen in intact SIRPα mt mice (Fig 3.5C). However it is important to note that the percentage of CD103$^+$CD11b$^+$ DC appeared to be lower in both groups of chimeras (~ 30%) compared with what I had found in intact WT mice (~ 40%) (Fig 3.2B). In parallel, the proportion of CD103$^+$CD11b$^-$ DC appeared to be higher in the chimeras. In light of this observation, it was difficult to interpret the DC subset data in the chimeric mice. This was compounded further by the fact that I had insufficient mice to set up WT -> WT or SIRPα mt -> SIRPα mt chimeras, which would have provided controls for the generic effects of BM reconstitution on DC populations. There were no significant differences in the frequencies or absolute numbers of mϕ in the SI LP of the two groups of chimeras (Fig. 3.6).

The total numbers of DC were low in the MLN of both chimeras and this was especially true for the SIRPα mt -> WT mice, suggesting that the defect in these cells in the intact SIRPα-expressing (WT) mouse was intrinsic to haematopoietic cells.

There was a trend towards a reduction in the frequency and absolute number of both total migratory and resident MLN DC in the SIPRα mt -> WT mice, similar to what was seen in the intact SIRPα mt MLN. However, insufficient sample size prevented statistical analyses of these data (Fig 3.7A). Despite identical populations of $CD103^+CD11b^+$ DC in the SI LP of the two sets of chimeras (~ 30%), this subset was reduced amongst migratory DC in the MLN of SIRPα mt -> WT mice (~ 18%) compared with WT -> SIRPα mt chimeric mice (~ 25%). Again this mirrored the intact SIRPα mt mouse, although the frequencies of both were lower than in the intact WT or SIRPα mt (Fig 3.3B). Similarly there was also a trend towards an increased frequency of $CD103^+CD11b^-$ DC in SIRPα mt -> WT MLN. However, unlike intact SIRPα mt MLN, there was no decrease in $CD103^-CD11b^+$ DC amongst the SIRPα mt -> WT migratory DC (Fig. 3.7B). Analysis of the subsets of DC in the resident compartment of the chimeric MLN showed the presence of $CD103^+CD11b^+$ DC in the SIRPα mt -> WT MLN. As this observation differs from that seen in intact mice, it may indicate that the gating strategy for distinguishing resident and migratory DC may not be reliable after irradiation and BM transfer. However, $CD103^+CD11b^+$ DC resident MLN DC were rare in WT -> SIRPα mt chimeras. Unlike intact SIRPα mt MLN, there were no differences in the proportion of $CD103^-CD11b^+$ resident DC in the SIRPα mt -> WT and WT -> SIRPα mt mice. The frequencies of $CD103^+CD11b^-$ DC and $CD103^-CD11b^-$ DC appeared to be reduced in the SIRPα mt -> WT chimeras compared with WT -> SIRPα mt MLN, although again, I was unable to analyse these differences statistically (Fig 3.7C).

I next analysed the spleen of the chimeric mice using CD4 as an additional marker that can define two subsets of splenic $CD11b^+$ DC (Miller et al., 2012) (Fig. 3.8A). Rather strikingly, the spleen of SIRPα mt -> WT mice had a profound defect in the frequency and number of both $CD11b^+CD4^+$ and $CD11b^+CD4^-$ DC (and thus total $CD11b^+$) populations compared with those from WT -> SIRPα mt mice. By contrast, the $CD11b^-$ DC population significantly increased (Fig. 3.8B). These findings are therefore similar to the behaviour of splenic $CD11b^+$ DC in the intact SIRPα mt mice (Fig 3.4).

These data suggest that the systemic DC defect in SIRPα mt mice may reflect an intrinsic effect on the haematopoietic compartment. However the lack of phenotype in the SI LP of the SIRPα mt -> WT chimeras means that it was impossible to assess the cell type responsible for the effect in the intestine.

3.4 Effects of age on dendritic cells in SIRPα mt mice

One possible explanation for the lack of a DC phenotype in the SIRPα mt BM chimeras was that it could reflect an effect of age. This is because the recipients of BM were eight weeks old when irradiated and were then left for a minimum of eight weeks before being analysed, meaning they were approximately twice the age of the intact SIRPα mt mice I had examined earlier. To explore whether there might be a selective loss of the intestinal DC phenotype in intact SIRPα mt mice with age, I analysed the SI LP, MLN and spleen of WT and SIRPα mt mice from four until 24 weeks of age. Furthermore, I examined how SI LP T cell populations changed with age to determine the relationship between T cells and DC subsets in this model, in which a selective defect in Th17 cells has been reported (Scott et al., 2014b).

The frequency of $CD103^+CD11b^+$ DC in the SI LP remained constant throughout the time course in both WT and SIRPα mt mice, and the degree of the defect in the SIRPα mt SI LP remained relatively constant (Fig. 3.9A). The numbers of $CD103^+CD11b^+$ DC in the SI LP were not significantly different between the two strains at any age, although they were generally lower in the SIRPα mt mice. This difference appeared most apparent at four weeks of age when there was approximately a 50% reduction in numbers in SIRPα mt mice (Fig. 3.9A).

As I had found previously in eight week old mice, the frequency of SI LP $CD103^-CD11b^+$ DC was not significantly different between the WT and SIRPα mt mice at four, eight or 24 weeks of age, although it was significantly decreased in the SIRPα mt SI LP at 16 weeks of age (Fig 3.9B). Absolute numbers of $CD103^-CD11b^+$ DC were reduced in SIRPα mt mice at four weeks, but not at the later time points (Fig. 3.9B). $CD103^+CD11b^-$ DC were significantly increased in frequency in the SIRPα mt SI LP at all ages, as was their absolute number at eight weeks of age, similar to my previous

experiments (Fig. 3.9C). Lastly, the $CD103^{-}CD11b^{-}$ DC were not significantly different in the SI LP of WT and SIRPα mt mice in frequency or absolute number, except for a slightly reduced frequency in 16 week old SIRPα mt mice (Fig. 3.9D). There were no differences in the frequency or absolute numbers of Th1 or Th17 cells in the SI LP of 24-week-old SIRPα mt or WT mice, suggesting that the reported defect in Th17 cells may have resolved by 24 weeks of age (Fig. 3.10).

The proportions and numbers of migratory $CD103^{+}CD11b^{+}$ MLN DC were significantly reduced in SIRPα mt mice at four and eight weeks of age (Fig. 3.11A), but at later times there was a marked reduction in the proportion of $CD103^{+}CD11b^{+}$ DC in WT MLN which meant that the difference in DC frequency could be seen between the strains (Fig. 3.11A). The frequency and numbers of migratory $CD103^{-}CD11b^{+}$ DC were significantly reduced in the SIRPα mt MLN at all time points (Fig. 3.11B). The frequency of $CD103^{+}CD11b^{-}$ DC was increased in the SIRPα mt at both four and eight weeks of age, but this was not apparent at later times (Fig. 3.11C). Although absolute numbers of $CD103^{+}CD11b^{-}$ DC in SIRPα mt mice were significantly reduced at both four and eight weeks of age, this also resolved by 16 weeks of age (Fig. 3.11C). There were no significant differences between the frequencies of migratory $CD103^{-}CD11b^{-}$ DC in WT and SIRPα mt MLN at any age, although the numbers were reduced in SIRPα mt mice at all times (Fig. 3.11D).

As I found previously in young adult mice, all subsets of resident MLN DC were very scarce in number in SIRPα mt mice throughout the time course, especially after four weeks of age and they were significantly lower than in WT MLN at all times. Despite this generalised effect the relative frequency of $CD103^{-}CD11b^{+}$ DC was markedly reduced amongst resident MLN from SIRPα mt mice at all ages (Fig. 3.12A), while the proportions of $CD103^{+}CD11b^{-}$ DC were always higher in the SIRPα mt MLN (Fig. 3.12B). The frequency of resident $CD103^{-}CD11b^{-}$ DC was significantly higher in SIRPα mt MLN at four and eight weeks of age, but was then similar to that in the WT mice thereafter (Fig. 3.12C).

The frequency and number of $CD11b^{+}$ DC in the spleen of SIRPα mt were profoundly reduced compared with WT mice at all times, while the proportion of $CD11b^{-}$ DC was

reciprocally higher at all ages. However, the absolute numbers of CD11b$^-$ DC in SIRPα mt spleen were similar to those in WT mice, except for a significant increase at 16 weeks (Fig. 3.13).

3.5 Summary

In this chapter, I first confirmed previous findings in the laboratory that had shown that although SIRPα was expressed by several intestinal DC subsets and mϕ, there was a selective reduction in the number of CD103$^+$CD11b$^+$ DC in the small intestine of SIRPα mt mice. This effect was phenocopied amongst migratory DC in the draining MLN, while the population of CD103$^-$CD11b$^+$ DC was reduced in both resident MLN DC and in the spleen, where proportions of CD103$^+$CD11b$^-$ DC were significantly increased. Despite their expression of SIRPα, there were no differences in frequency or number of mϕ in the intestine.

Based on these observations I investigated whether the reduction of these DC subsets was due to an intrinsic defect within the haematopoietic compartment by generating SIRPα mt -> WT and WT -> SIRPα mt BM chimeras. After eight weeks of reconstitution with donor BM, there were no differences in the frequency or number of DC subsets or mϕ in the SI LP or MLN between the two groups of chimeras. Interestingly, the defect in CD11b$^+$ DC in the spleen was present in SIRPα mt -> WT chimeras, suggesting this phenomenon was distinct from that affecting intestinal DC. I considered the possibility that the loss of phenotype in the intestine of either group of chimeric mice might have been due to the age of the animals, as the mice were approximately twice the age of those in which the phenotype was first described. To investigate this, I analysed the SI LP, MLN and spleen of four to 24 week old mice. This showed that the selective CD103$^+$CD11b$^+$ DC defect in SIRPα mt mice did not diminish with age in the SI LP. There were no consistent changes with age in the numbers or frequencies of CD103$^-$CD11b$^+$ DC, while the frequencies of CD103$^+$CD11b$^-$ DC generally increased in the SI LP, although they were reduced in number amongst all MLN DC at all times.

By 24 weeks there were no differences in the SI LP Th1 or Th17 populations in SIRPα mt and WT mice, although the defect in CD11b$^+$ DC in the spleen was found in

SIRPα mt mice of all ages. While these results suggest that the DC phenotype in SIRPα mt mice may be age dependent in the intestine but not in the spleen, it should be noted that many of the effects of age were not consistent and I was not able to carry out many replicate experiments, especially in older mice. Furthermore, I did not have access to SIRPα mt -> SIRPα mt or WT -> WT BM chimeras that would be necessary to interpret the apparent absence of an age dependent loss of phenotype in the intestine of SIRPα mt -> WT chimeras. In the next chapter, I went on to investigate how DC subsets develop from the neonate in order to gain a better understanding of the dynamics of DC subsets over time.

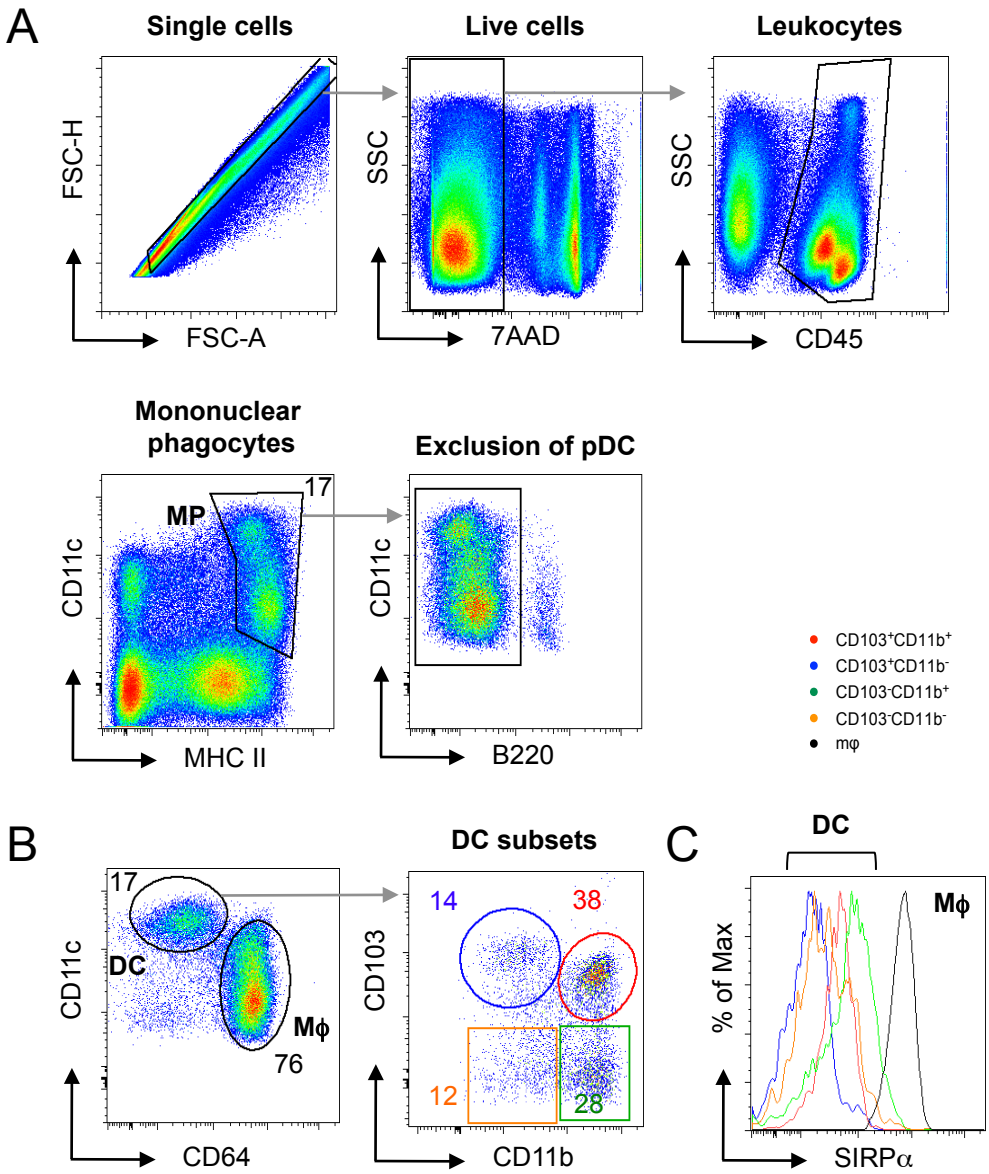

Figure 3.1: Gating strategy for identifying mononuclear phagocytes in small intestinal lamina propria

A SI LP cells were isolated from WT mice by enzymatic digestion and after identifying single cells based on FSC-A and FSC-H, mononuclear phagocytes (MP) were identified amongst live 7AAD$^-$ CD45$^+$ leukocytes as MHC II$^+$ CD11c$^+$. After B220$^+$ CD11c$^+$ plasmacytoid DC (pDC) were excluded, **B** conventional DC were then identified as CD11c$^+$ CD64$^-$, while mϕ are CD11c$^+$ CD64$^+$**.** The DC were then subdivided into four populations based on expression of CD103 and CD11b. **C** Expression of SIRPα by DC populations and CD64$^+$ mϕ. Results are representative of at least 10 individual experiments.

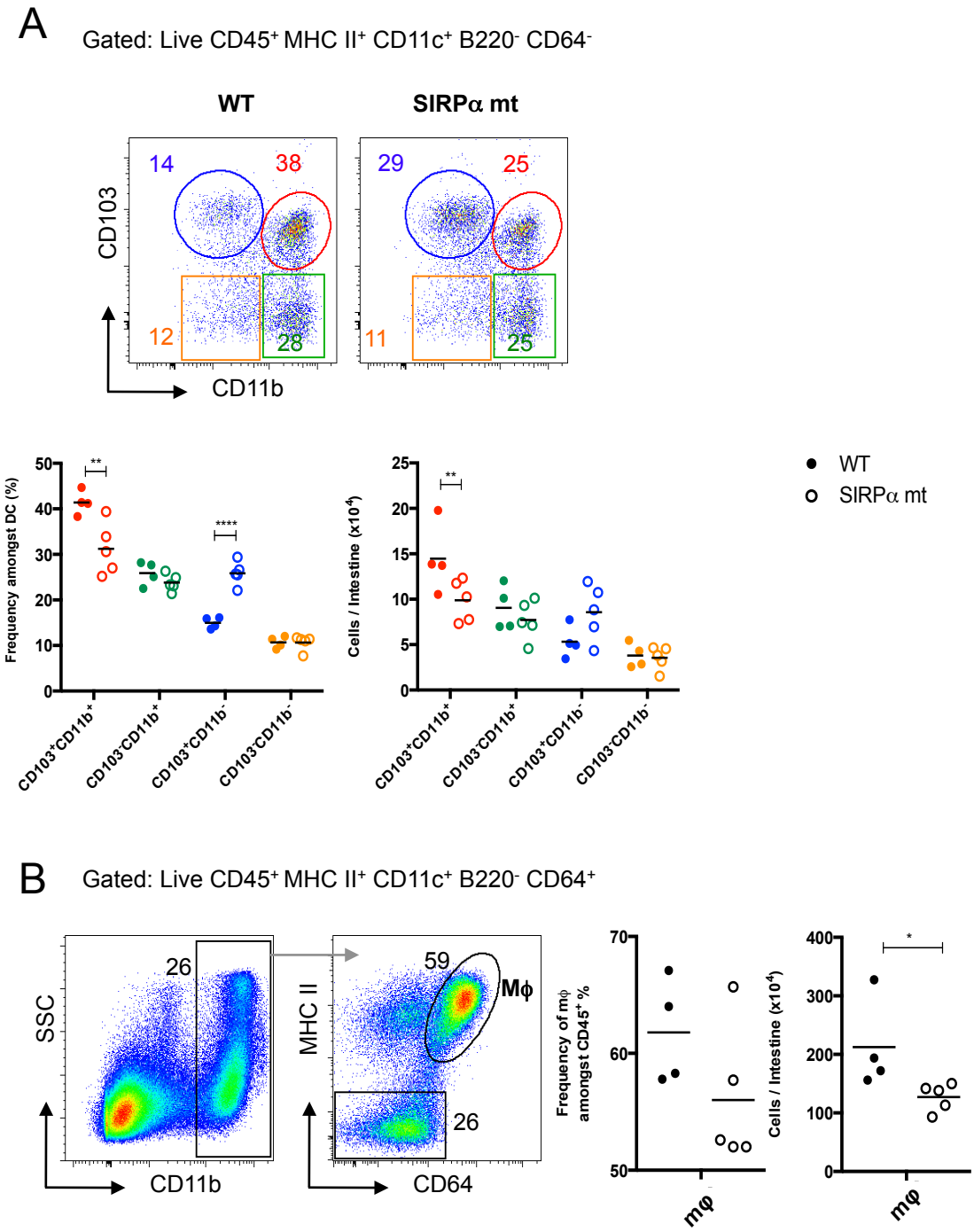

Figure 3.2: Mononuclear phagocytes in the small intestinal lamina propria of SIRPα mt mice

A Representative dot plots showing DC subsets amongst live (7-AAD$^-$) CD11c$^+$ MHC II$^+$ CD64$^-$ B220$^-$ leukocytes isolated from SI LP of WT or SIRPα mt mice (top panels). Frequencies amongst total DC (left) and absolute numbers of DC subsets (right) are shown (bottom panels). **B** Total mϕ were identified as live (7-AAD$^-$) CD45$^+$ CD11b$^+$ MHC II$^+$ CD64$^+$ B220$^-$ cells and the frequency amongst CD11b$^+$ cells and absolute numbers are shown. Data are from a single experiment with n=4-5. *p<0.05, **p<0.01, ****p<0.0001 Student's t-test.

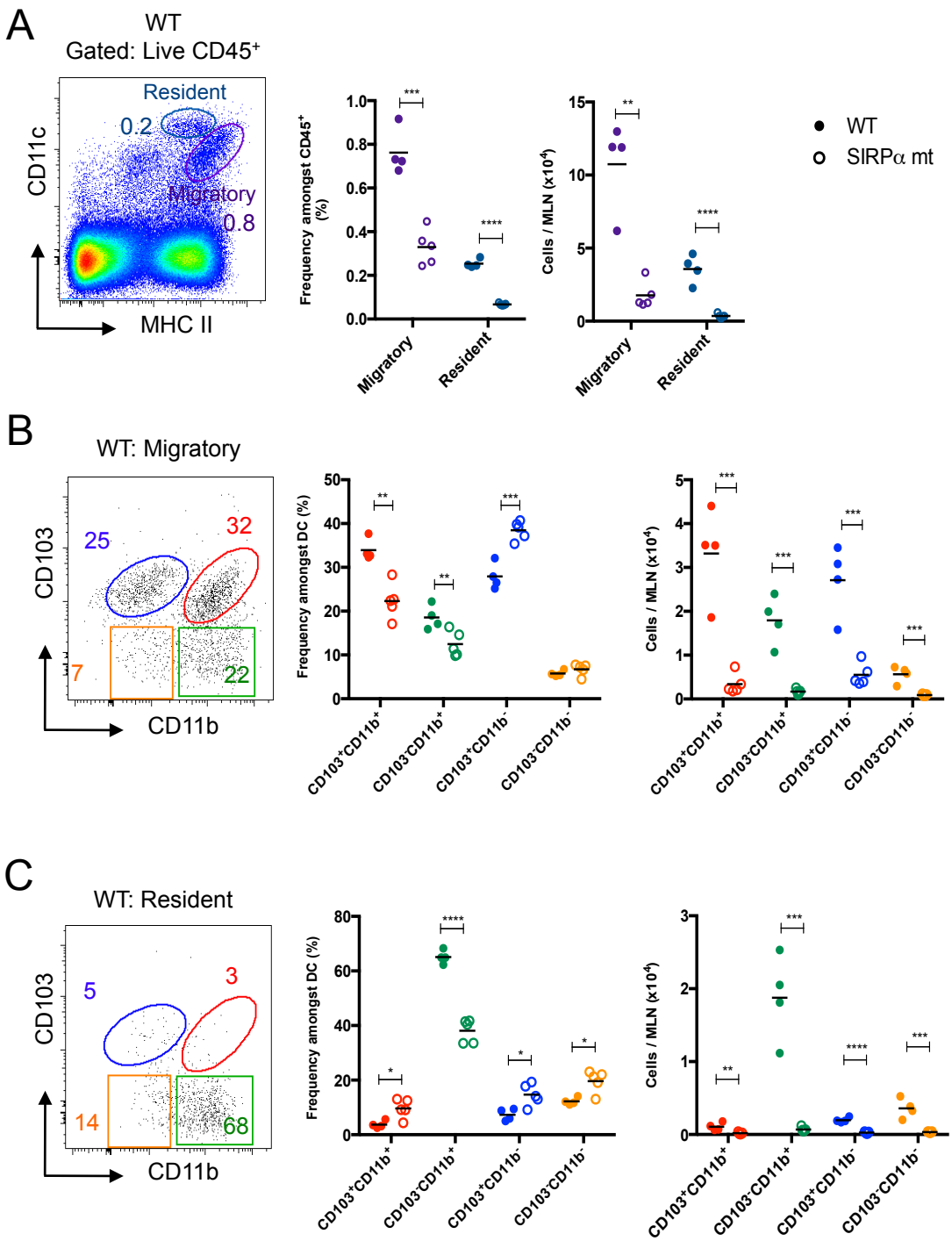

Figure 3.3: Dendritic cells in the MLN of SIRPα mt mice

A MLN cells were isolated from WT and SIRPα mt mice and migratory ($MHCII^{hi}$ $CD11c^{+}$) and resident ($MHCII^{int}$ $CD11c^{+}$) DC were identified amongst $7AAD^{-}$ $CD45^{+}$ leukocytes (representative dot plot; left). The graphs show the frequency (centre) and absolute numbers (right) in WT and SIRPα mt MLN. **B** Frequency (centre) and absolute numbers (right) of DC subsets amongst migratory MLN DC based on expression of CD103 and CD11b (representative dot plot; left). **C** Frequency (centre) and absolute numbers (right) of DC subsets amongst resident MLN DC based on expression of CD103 and CD11b (representative dot plot; left). Data are from a single experiment with n=4-5. *p<0.05, **p<0.01, ***p<0.001, ****p<0.0001 Student's t-test.

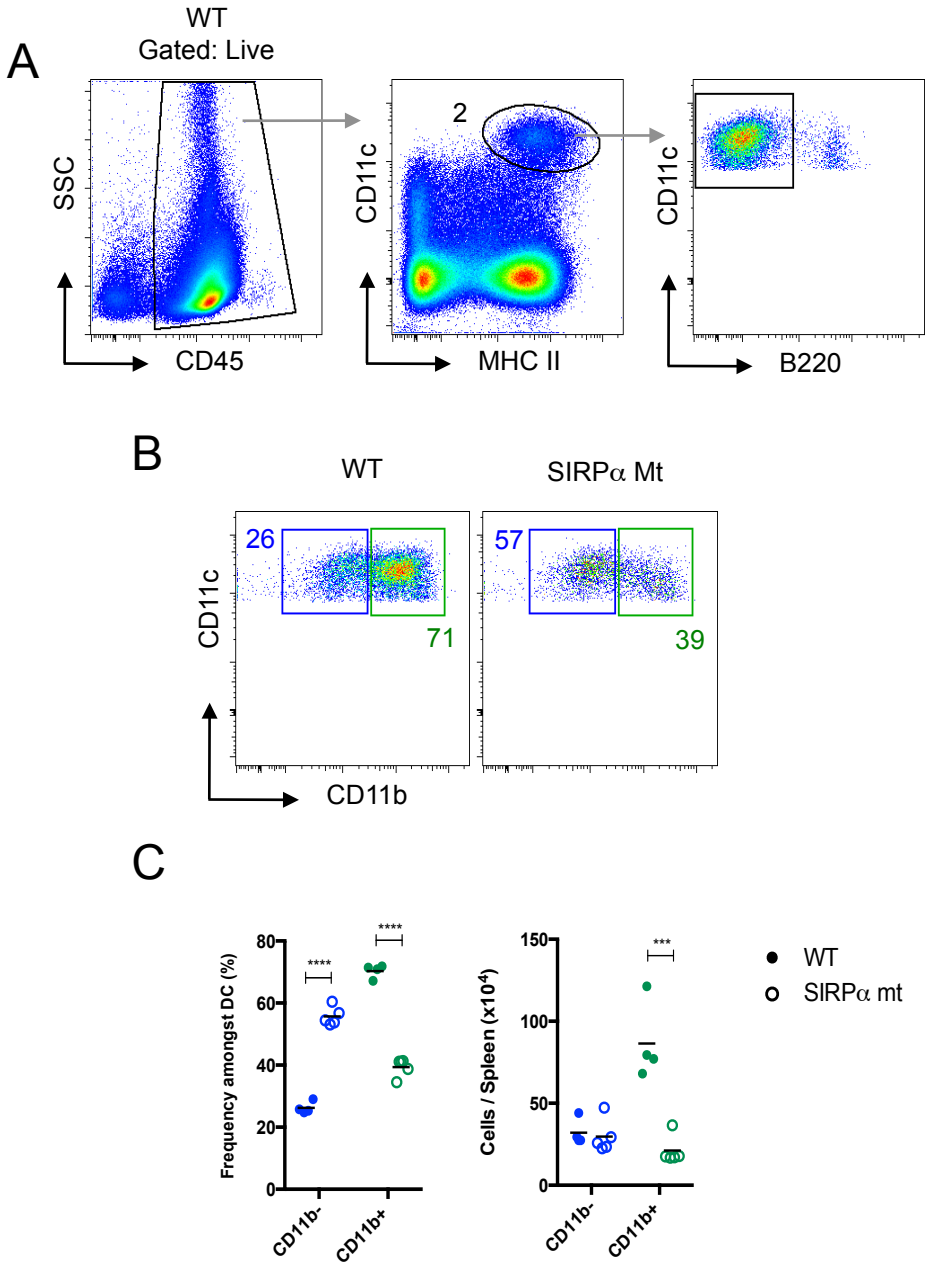

Figure 3.4: Dendritic cells in the spleen of SIRPα mt mice

A Spleen cells were isolated from WT and SIRPα mt mice and conventional DC were identified as live (7-AAD$^-$) CD45$^+$ CD11c$^+$ B220$^-$ leukocytes. **B** CD11b$^+$ and CD11b$^-$ subsets were identified. **C** Frequency of CD11b$^+$ and CD11b$^-$ DC amongst total DC (left) and absolute numbers (right) are shown. Data are from a single experiment with n=4-5. ***p<0.001, ****p<0.0001 Student's t-test.

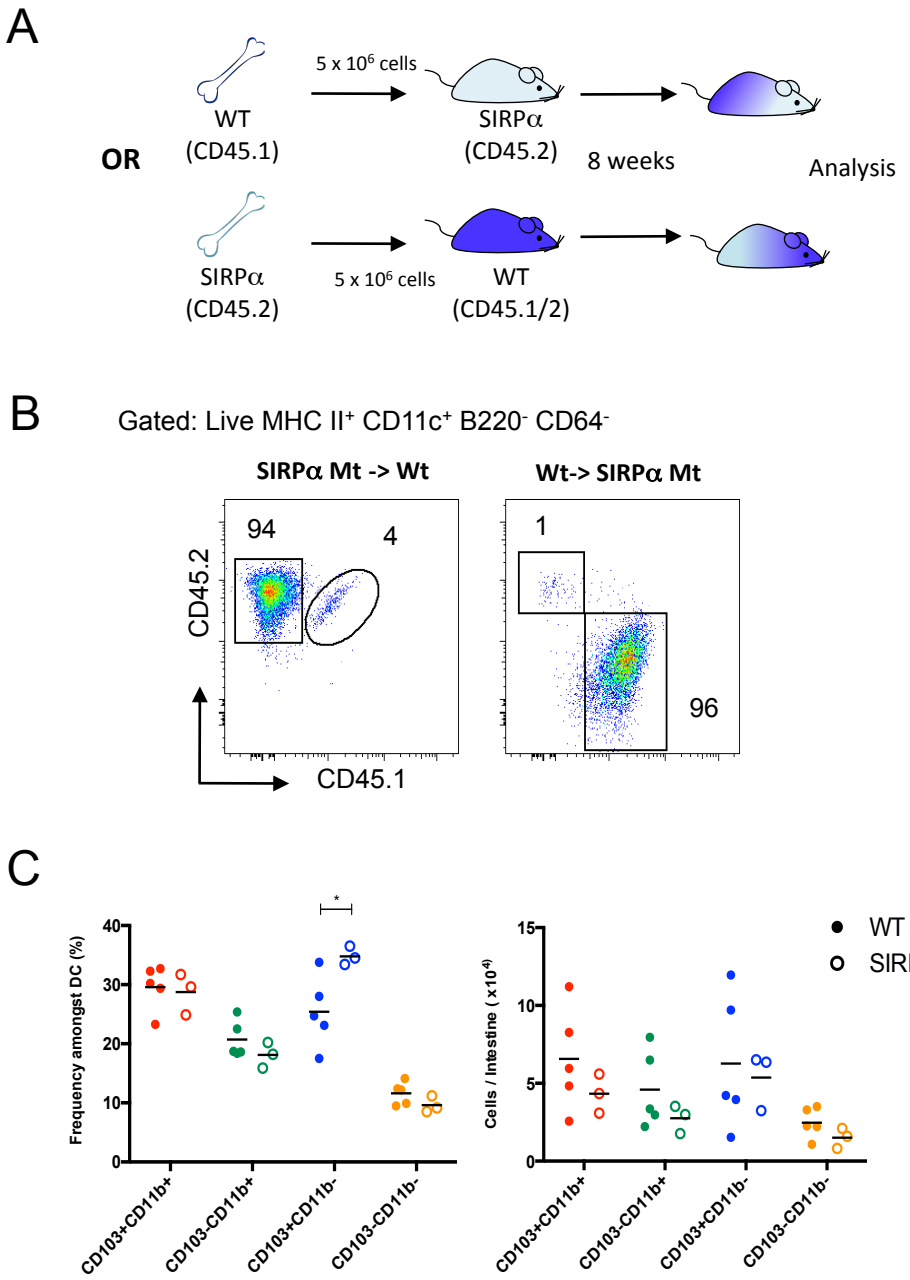

Figure 3.5: Dendritic cells in the small intestinal lamina propria of WT -> SIRPα mt and SIRPα mt -> WT BM chimeras

A Bone marrow chimeras were generated by either transfer of CD45.1⁺ WT BM into irradiated CD45.2⁺ SIRPα mt recipients, or by transfer of CD45.2⁺ SIRPα mt BM into irradiated CD45.1⁺x CD45.2⁺ WT recipients. **B** Engraftment of donor cells was assessed eight weeks later by analysing expression of CD45.2 or CD45.1 on live, MHC II⁺ CD11c⁺ CD64⁻ DC in SI LP. **C** Frequencies amongst total DC (left panel) and absolute numbers (right panel) of DC subsets based on CD11b and CD103 expression. Data are from a single experiment with n=3-5. *p<0.05, Student's t-test.

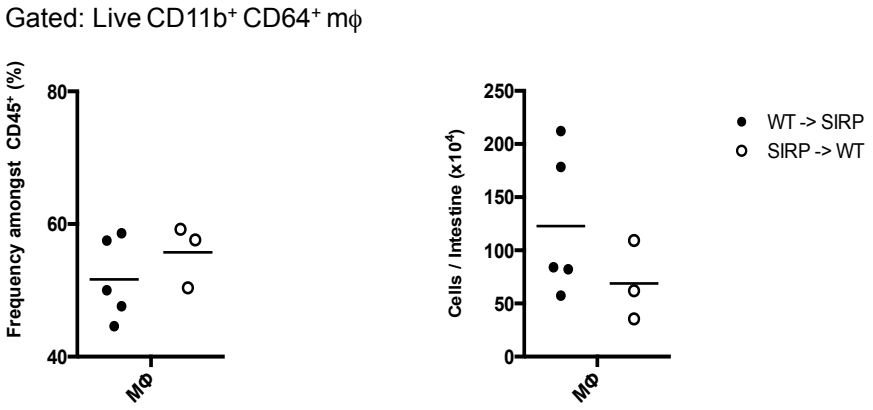

Figure 3.6: Mϕ in the small intestinal lamina propria of WT -> SIRPα mt and SIRPα mt -> WT BM chimeras

Bone marrow chimeras were generated by transfer of CD45.1$^+$ WT BM into irradiated CD45.2$^+$ SIRPα mt recipients, or by transfer of CD45.2$^+$ SIRPα mt BM into irradiated CD45.1$^+$x CD45.2$^+$ WT recipients. Engraftment of donor cells was assessed eight weeks later. Frequency amongst CD45$^+$ leukocytes (left panel) and absolute numbers (right panel) of live CD11b$^+$ CD64$^+$ mϕ. Data are from a single experiment with n=3-5.

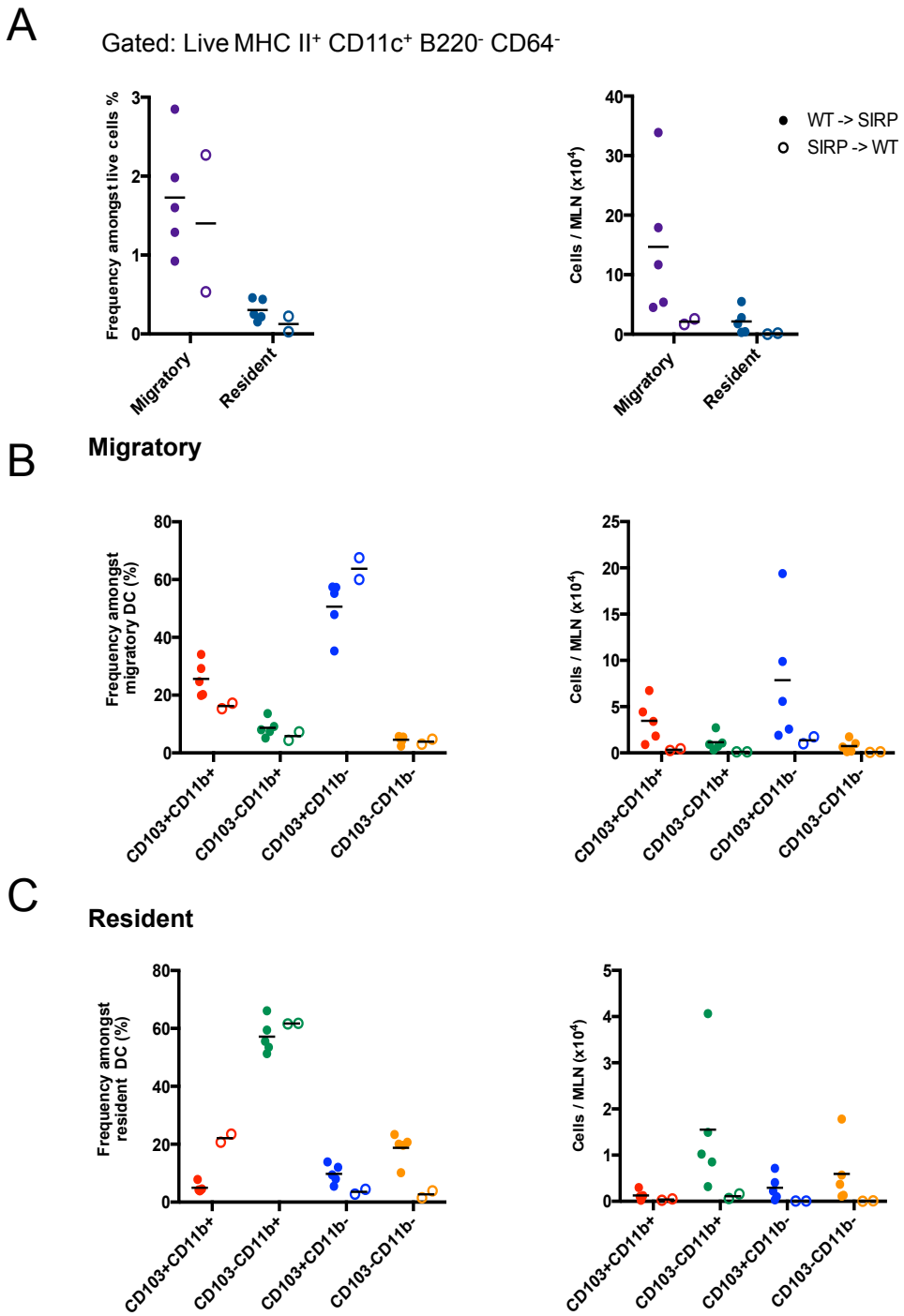

Figure 3.7: Dendritic cells in the MLN of WT -> SIRPα mt and SIRPα mt -> WT BM chimeras

Bone marrow chimeras were generated by transfer of CD45.1+ WT BM into irradiated CD45.2+ SIRPα mt recipients, or by transfer of CD45.2+ SIRPα mt BM into irradiated CD45.1+x CD45.2+ WT recipients. Engraftment of donor cells was assessed eight weeks later. **A** Frequency (left panel) and absolute numbers (right panel) of migratory (MHCII^{hi} CD11c+) and resident (MHCII^{int} CD11c+) DC in the MLN. **B** Frequency (left panel) and absolute numbers (right panel) of DC subsets amongst migratory MLN DC based on expression of CD103 and CD11b. **C** Frequency (left panel) and absolute numbers (right panel) of DC subsets amongst resident MLN DC based on expression of CD103 and CD11b. Data are from a single experiment with n=2-5.

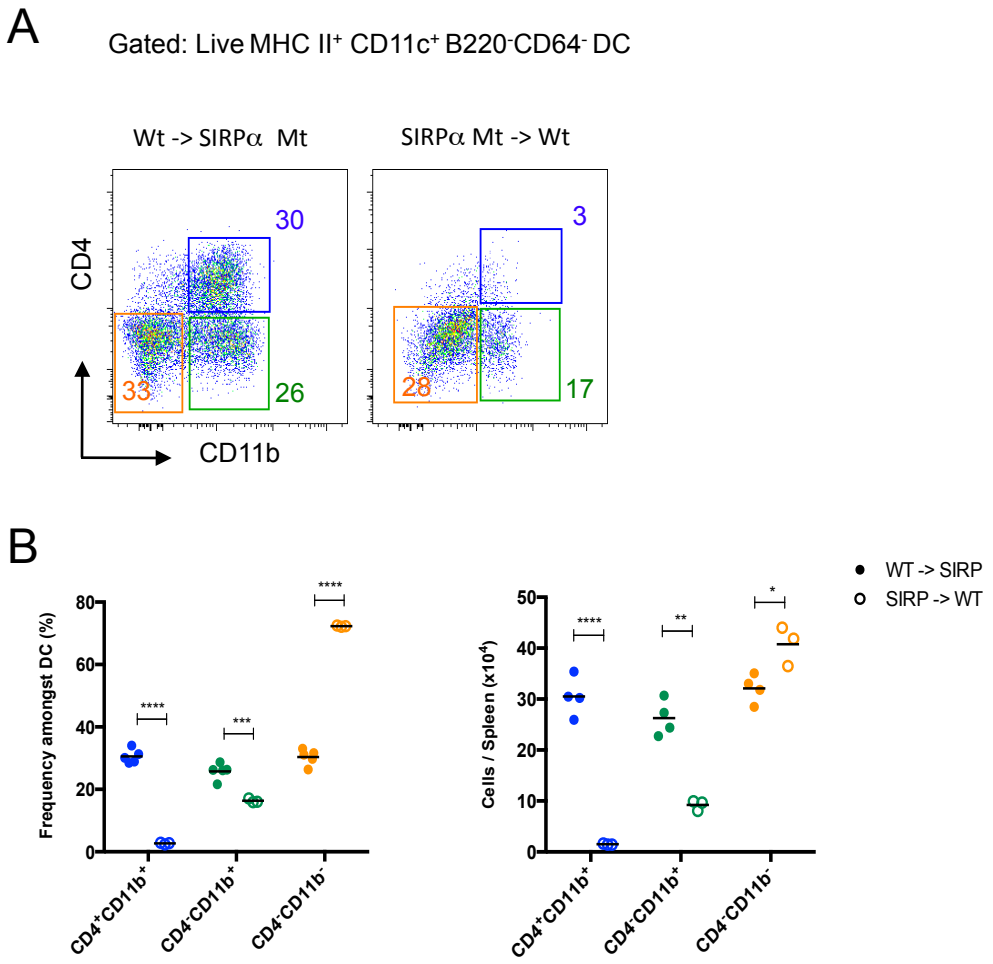

Figure 3.8: Dendritic cells in the spleen of WT -> SIRPα mt and SIRPα mt -> WT BM chimeras

Bone marrow chimeras were generated by either transfer of CD45.1+ WT BM into irradiated CD45.2+ SIRPα mt recipients, or by transfer of CD45.2+ SIRPα mt BM into irradiated CD45.1+x CD45.2+ WT recipients. Engraftment of donor cells was assessed eight weeks later. **A** Representative dot plots showing identification of DC subsets based on CD4 and CD11b expression. **B** Frequency (left panel) and absolute numbers (right panel) of live MHC II+ CD11c+ CD64- DC based on CD4 and CD11b expression. Data are from a single experiment with n=3-5. *p<0.05, **p<0.01, ***p<0.001, ****p<0.0001 Student's t-test.

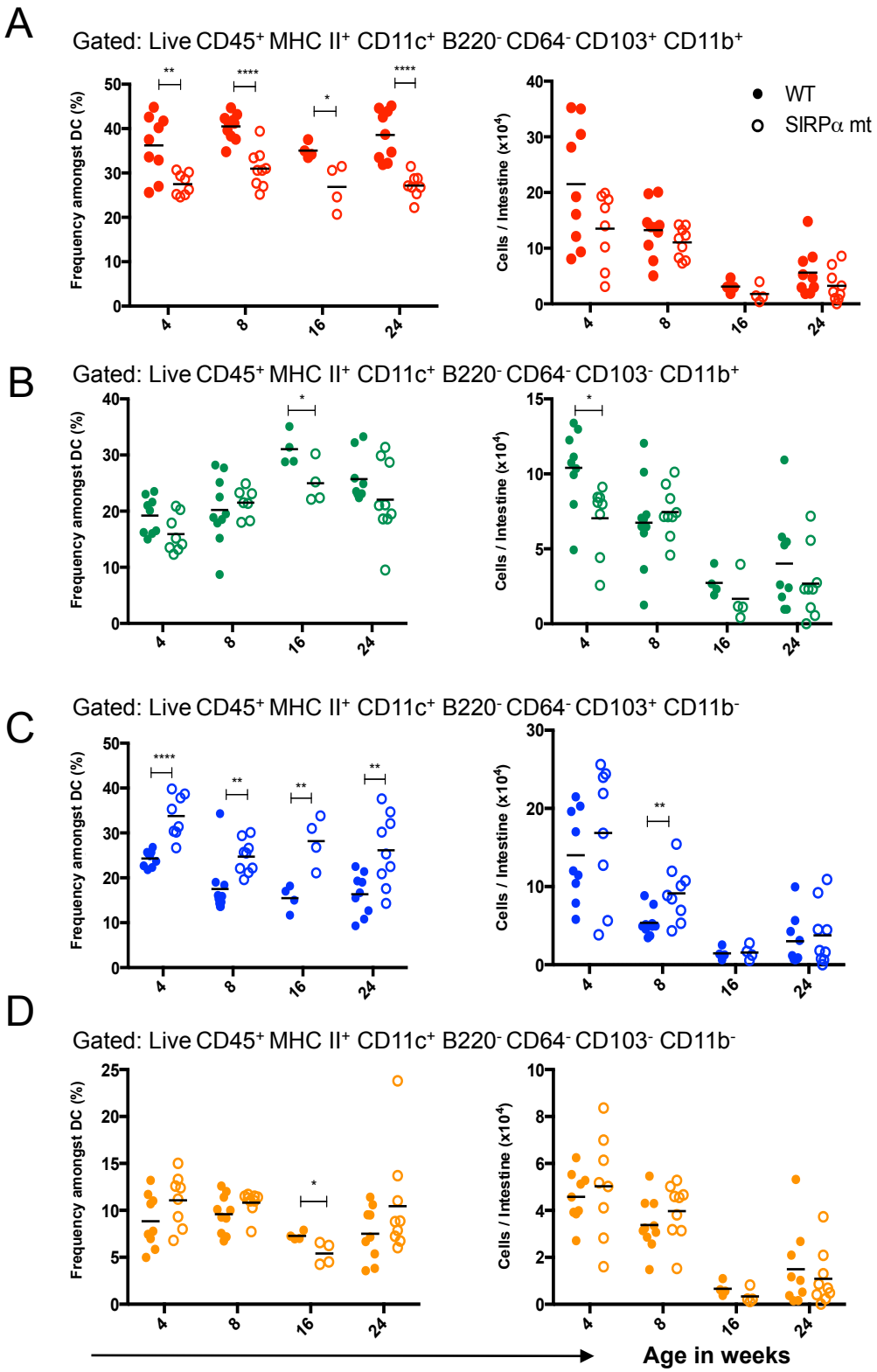

Figure 3.9: Effects of age on DC subsets in the small intestinal lamina propria of SIRPα mt mice

Live CD11c$^+$ MHC II$^+$ B220$^-$ CD64$^-$ leukocytes in SI LP were analysed for the expression of CD103 and CD11b in WT and SIPRα mt mice from four to 24 weeks of age. Frequency amongst total DC (left) and absolute numbers (right) are shown for **A** CD103$^+$CD11b$^+$ **B** CD103$^-$CD11b$^+$ **C** CD103$^+$CD11b$^-$ and **D** CD103$^-$CD11b$^-$ DC. Data are from at least three experiments with a total of 9 mice per group. *p<0.05, **p<0.01, ****p<0.0001 Student's t-test.

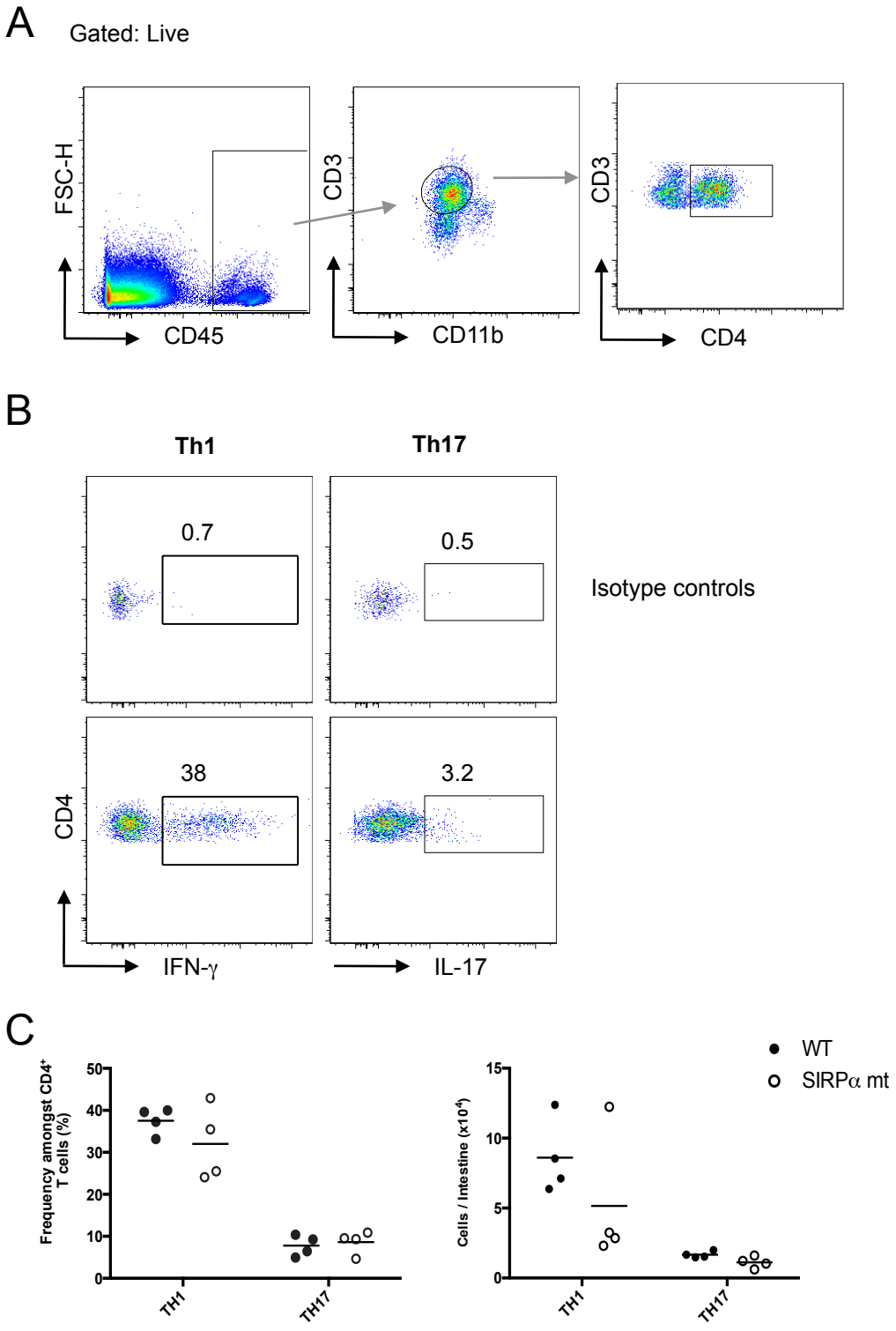

Figure 3.10: Effects of age on CD4⁺ T cell subsets in the small intestinal lamina propria of aged SIRPα mt mice

Total SI LP cells were isolated from 24 week old WT and SIRPα mt mice and incubated for 4.5 hours with PMA, ionomycin, brefeldin and monensin before analysis of CD4⁺ T cells by intracellular staining. **A** Gating strategy for identifying CD4⁺ T cells as live CD11b⁻ CD3⁺ cells. **B** Intracellular expression of INFγ and IL-17 assessed by flow cytometry using appropriate antibodies with gates set on isotype controls. **C** Frequencies and absolute numbers of Th1 and Th17 cells amongst CD4⁺ T cells. Data are from a single experiment with n=4 mice/group.

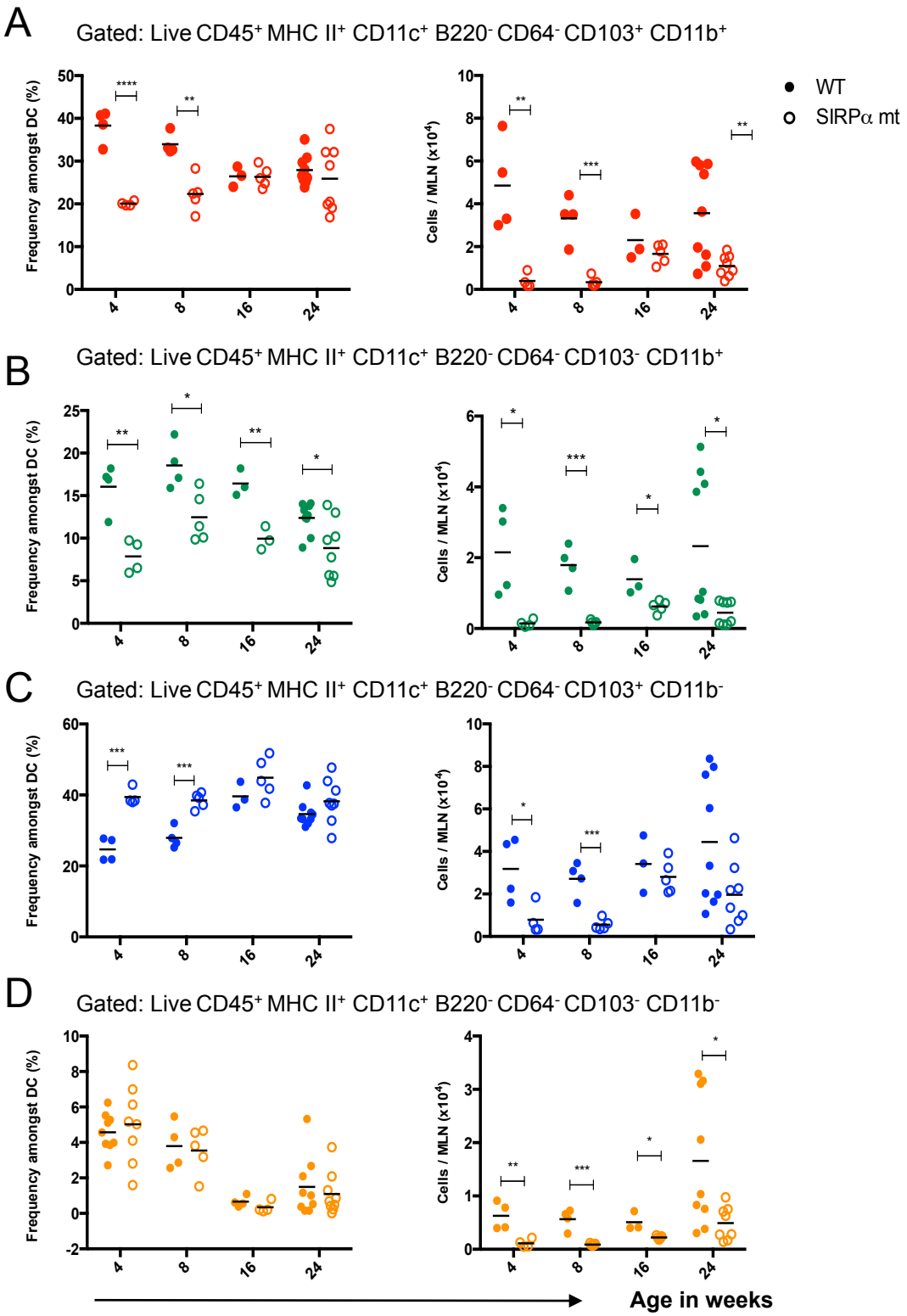

Figure 3.11: Effects of age on migratory DC subsets in the MLN of SIRPα mt mice
Live CD11c$^+$ MHC II^{hi} B220$^-$ CD64$^-$ migratory D Cin MLN were analysed for the expression of CD103 and CD11b in WT and SIPRα mt mice from four to 24 weeks of age. Frequency amongst total DC (left) and absolute numbers (right) are shown for **A** CD103$^+$CD11b$^+$ **B** CD103$^-$CD11b$^+$ **C** CD103$^+$CD11b$^-$ and **D** CD103$^-$CD11b$^-$ DC. Data are from at least three experiments with a total of 9 mice per group. *p<0.05, **p<0.01, ***p<0.001, ****p<0.0001 Student's t-test.

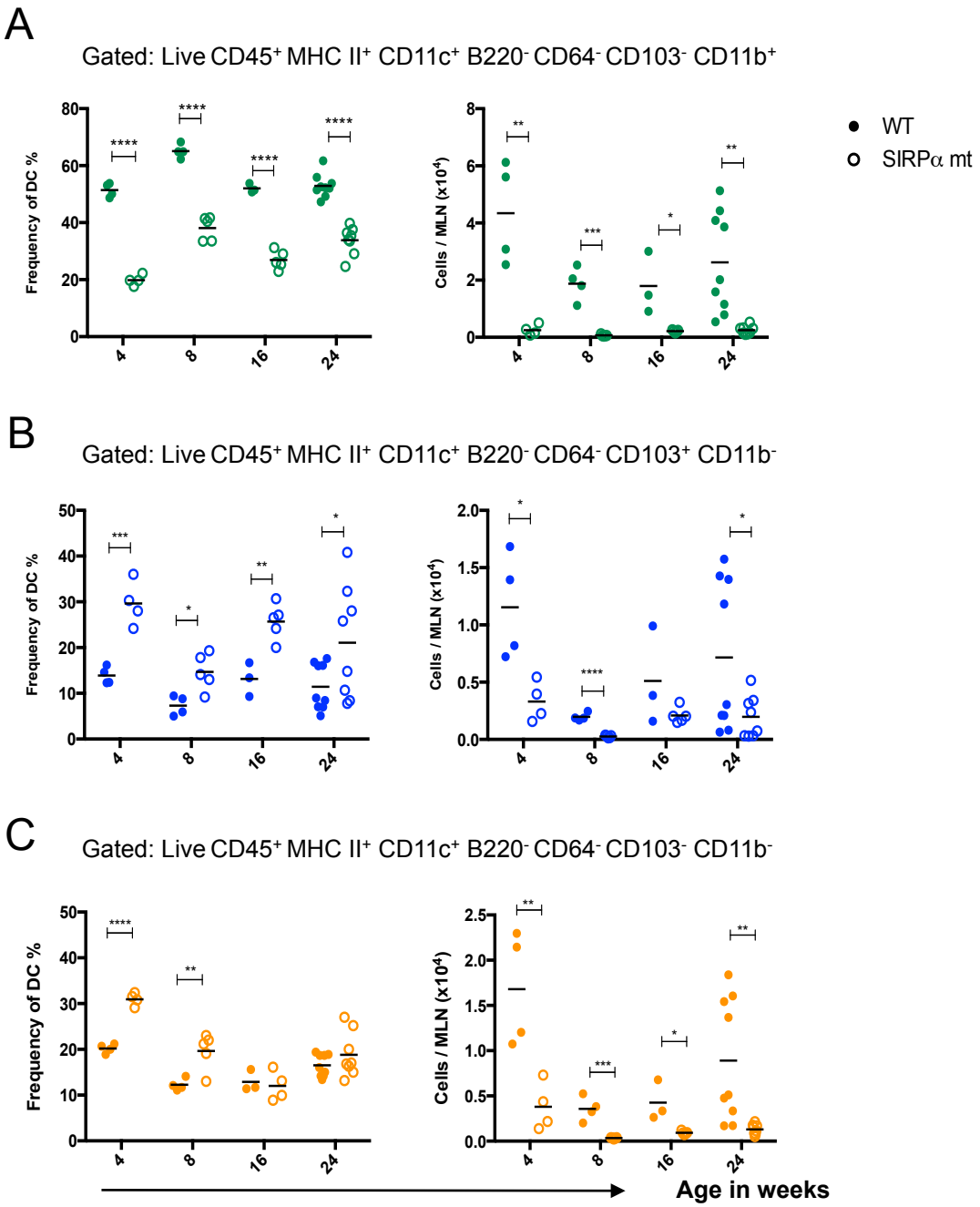

Figure 3.12: Effects of age on resident DC subsets in the MLN of SIRPα mt mice
Live CD11c$^+$ MHC II^{int} B220$^-$ CD64$^-$ resident DC in MLN were analysed for the expression of CD103 and CD11b in WT and SIPRα mt mice from four to 24 weeks of age. Frequency amongst total DC (left) and absolute numbers (right) are shown for **A** CD103$^-$CD11b$^+$ **B** CD103$^+$CD11b$^-$ and **C** CD103$^-$CD11b$^-$ DC. Data are from at least three experiments with a total of 9 mice per group. *p<0.05, **p<0.01, ***p<0.001, ****p<0.0001 Student's t-test.

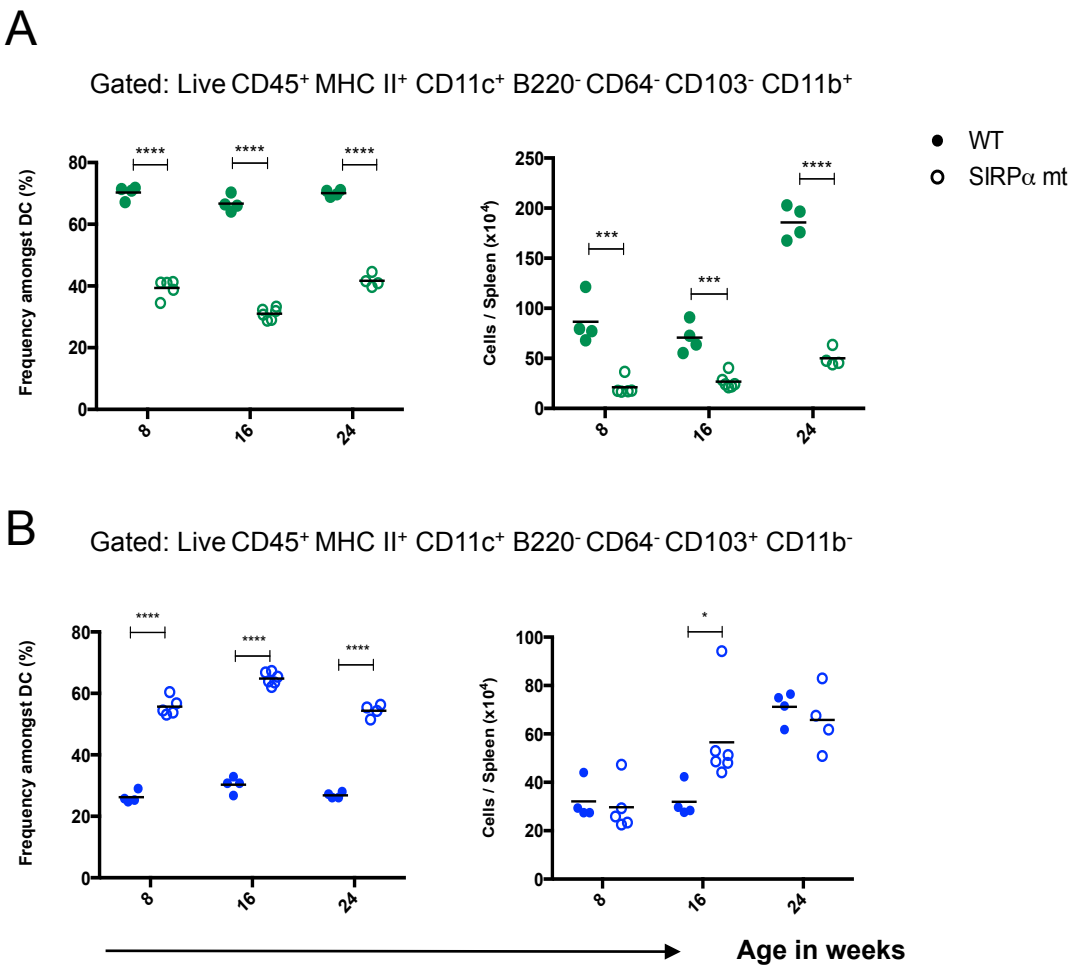

Figure 3.13: Effects of age on DC subsets in the spleen of SIRPα mt mice
Spleen cells were isolated from WT and SIRPα mt mice and live CD11c$^+$ MHC II$^+$ CD64$^-$ leukocytes were analysed for the expression of CD11b from between four weeks to 24 weeks of age. Frequency and absolute numbers are shown for **A** CD11b$^+$ **B** CD11b$^-$. Data are from at least three experiments with n=4-9. *p<0.05, ***p<0.001, ****p<0.0001 Student's t-test.

Chapter 4

Development of dendritic cells in neonatal mice

4.1 Introduction

In Chapter 3, I confirmed previous findings from our laboratory that there was a selective reduction in $CD103^+CD11b^+$ DC in the intestine of SIRPα mt mice. However, when I generated BM chimeras, I observed a resolution of the DC phenotype in both the intestine and MLN of these animals. As this suggested these could be age-related changes in DC development, I went on to assess how populations of DC subsets changed with age in the intestine of SIRPα mt and WT mice.

As a result of these studies, I became interested in when the DC defect first appeared in life and how intestinal DC populations are shaped throughout development from early life onwards. In this chapter I explored DC subset development from late embryogenesis, throughout the neonatal period and into maturity. To extend this work, I also established how two other molecules (CD101 and Trem-1) could be used to define DC differentiation in more depth. Lastly, I examined how DC function and T cell composition changed with age.

4.2 Age dependent effects on intestinal dendritic cell subsets

Having identified a reduction in $CD103^+CD11b^+$ DC in SIRPα mt mice, I decided to investigate at which stage of development this defect first occurs. To do this I first had to establish protocols for characterising intestinal DC early in life. Recent work by Bain *et al.* had shown that this was possible for macrophages (Bain et al., 2014); therefore I adapted these methods to study DC in the SI, colon, MLN and lung of WT mice.

4.2.1 Development of dendritic cell subsets in the small intestinal lamina propria

Firstly, I examined the SI and isolated lamina propria cells from embryonic day 18 (E18) mice (Fig. 4.1A). Using the same digestion protocol as in adults, I was able to retrieve enough cells to analyse individual animals separately, and as in adults, I first identified live, single $CD45^+$ leukocytes before assessing their expression of MHC II and CD11c. cDC were then identified by exclusion of $B220^+$ pDC and B cells; and after

excluding $CD64^+$ Mϕ, I analysed the expression of CD11b and CD103 by the resulting *bona fide* DC. This showed the same four populations that were present in the adult SI LP, although the relative proportions were markedly different, with very few of the $CD103^+CD11b^+$ subset, predominant in adult SI LP (5% vs 40% respectively). $CD103^+CD11b^-$ DC were the most abundant subset at E18 (approx. 53%), followed by $CD103^-CD11b^+$ DC (27%) and lastly $CD103^-CD11b^-$ DC (11%). $CD103^+CD11b^+$ DC were also rare in the intestine at postnatal D1, but there was a large proportion of $CD103^-CD11b^+$ DC (10% and 47% respectively) as well as substantial numbers of $CD103^+CD11b^-$ DC, which were not as abundant as at E18. Some $CD103^-CD11b^-$ DC were also present on D1 (Fig. 4.1B).

I then went on to analyse the different DC populations in the SI LP at different times after birth. This showed that after a significant increase from E18 to D1, the frequency of $CD103^+CD11b^+$ DC then increased only very slowly during the first few weeks of life, only becoming apparent between 14 and 21 days and not attaining adult levels until 42 days, when there was another marked rise in their frequency. By one year of age, the frequency of $CD103^+CD11b^+$ DC had declined somewhat, confirming what I had found in 24 week old mice in the previous chapter. In parallel with the frequency, the absolute number of $CD103^+CD11b^+$ DC was low until D21, after which it rose towards adult levels, with an especially marked increase between D28 and D42 (Fig 4.2A).

The $CD103^-CD11b^+$ DC population showed a different pattern, rising significantly from approximately 20% at E18 to greater than 40% by D3 (Fig 4.2B). This population then fell sharply until D21, remaining at around the same level thereafter into adult life. The absolute numbers of this subset also began to increase more rapidly after birth than the $CD103^+CD11b^+$ DC, although the greatest changes were also seen from D28.

Although $CD103^+CD11b^-$ DC made up the majority of DC at E18, by birth they had halved in proportion and this remained low until D7, after which they increased significantly to reach roughly the proportions that were then maintained into adult life (Fig 4.2C). As with the other populations, the absolute numbers of $CD103^+CD11b^-$

DC remained low until D28, when they expanded drastically, before falling again in mature adults.

The population of $CD103^{-}CD11b^{-}$ DC was the smallest throughout life and their proportion showed few changes over this period (Fig 4.2D). Their absolute numbers were also lower than those of the other subsets, although interestingly, the age related expansion in this subset seemed to occur earlier, being most apparent on D21.

Thus there are marked changes in the number and composition of the DC subsets found in the SI from before birth onwards, with the numbers of all DC showing a dramatic expansion around the fourth week of life. Around the time of birth the predominant population was the $CD103^{+}CD11b^{-}$ subset, whilst the $CD103^{+}CD11b^{+}$ DC appeared to develop most slowly, not attaining adult proportions until around three to four weeks of age: their expansion was preceded by an increased proportion of $CD103^{-}CD11b^{+}$ DC.

4.2.2 Development of dendritic cell subsets in the colonic lamina propria

Next I analysed the development of DC in the colon, where the composition of DC subsets in adults is different to those of the SI LP. Using the same digestion protocol as in adults and a similar gating strategy applied to the SI LP, the same DC populations could be identified in the colon at E18 (Fig 4.3A). However, the relative proportions were different; the $CD103^{+}CD11b^{+}$ subset was smaller than in adult colon (2% vs. 11% respectively) and was even lower in the embryonic colon than in the SI LP at the same stage (Fig 4.3B). $CD103^{+}CD11b^{-}$ DC were the most abundant subset in E18 colon (approx. 48%), followed by $CD103^{-}CD11b^{+}$ DC (27%) and $CD103^{-}CD11b^{-}$ DC (18%). In the colon at D1, there were virtually no $CD103^{+}CD11b^{+}$ DC and an even higher proportion of $CD103^{-}CD11b^{+}$ DC was present (2% and 68% respectively). In turn, the $CD103^{+}CD11b^{-}$ DC were no longer predominant by D1 and only a few $CD103^{-}CD11b^{-}$ DC were present (Fig 4.3B).

Analysis of mice of different ages showed that the frequency of $CD103^{+}CD11b^{+}$ DC increased very slowly throughout development, rising to 20-30% at D14, which was far lower than in the SI LP. The frequency then remained relatively constant until

reducing at D28, before rising again significantly at D42. In parallel, the absolute number of $CD103^+CD11b^+$ DC was low throughout life, although it increased significantly on D21 (Fig 4.4A).

The $CD103^-CD11b^+$ DC population in the colon showed a similar developmental pattern to those in the SI LP, although they appeared to decrease more rapidly in proportion between D3 and D14 in the colon than in the SI LP, before increasing steadily into adult life. The absolute numbers of this subset increased slowly after birth and reached a peak at D21, compared with D42 in the SI LP. Their numbers then fell again around D28 and plateaued from D42 onwards (Fig 4.4B).

Although $CD103^+CD11b^-$ DC made up the majority of colonic DC at E18 there was then a small and non-significant fall in proportion on D1 before they increased gradually again up until D14. After a further small fall towards D28, the proportion of $CD103^+CD11b^-$ DC stabilised around 40%. The absolute numbers of $CD103^+CD11b^-$ DC remained low until increasing significantly at D42, after which they fell again towards adult levels at D28 (Fig 4.4C). The proportions of $CD103^-CD11b^-$ DC were low throughout life, without obvious changes over this time. Their absolute numbers were also lower than those of the other subsets, although these increased somewhat after D21 (Fig 4.4D).

Thus there were changes in the number and composition of the DC subsets found in the colon from before birth onwards, although these were not as marked as in the SI LP and the generalised expansion in colonic DC occurred earlier than in the SI LP. Around the time of birth in the colon, the predominant population was the $CD103^+CD11b^-$ subset, whilst the $CD103^+CD11b^+$ DC appeared to attain adult proportions around D3 and was preceded by an expanded proportion of $CD103^-CD11b^+$ DC, which then reduced in frequency.

4.2.3 Development of dendritic cell subsets in the MLN

I next examined how the populations of DC in the draining MLN developed in comparison with those in the intestinal mucosa, assessing both the $CD11c^+$ MHC II^{hi} 'migratory' DC that had arrived from the gut and the $CD11c^+$ MHC II^{int} subset of

resident DC as a representative source of DC found in secondary lymphoid organs (Fig 4.5A). In these experiments I could not begin the time course before birth, as I could not identify MLN in E18 mice. However, both migratory and resident subsets of DC could be identified in the MLN of D1 mice, where they were as well defined as in adult mice (Fig 4.5A). It was also possible to see the four populations of migratory DC based on CD11b and CD103 expression (Fig 4.5B-C).

The proportion of $CD103^{+}CD11b^{+}$ DC within the migratory DC population remained low from birth until there was a small increase at D14, followed by a further significant increase after D28, when adult levels were attained. This contrasts with the SI LP, where the adult proportion of approximately 40% was already present by D28. Absolute numbers of this subset were low until D14, before increasing significantly on D21 and reaching adult numbers around D45, with a further slight increase at 1 year (Fig 4.6A).

As in the SI LP, the frequency of $CD103^{-}CD11b^{+}$ DC was highest at birth, before decreasing into adulthood at D28. However, the absolute numbers of this subset did not approach adult levels until after D42 (Fig 4.6B). There were very few migratory $CD103^{+}CD11b^{-}$ DC immediately after birth, but this population then increased in proportion and did so more rapidly when compared with the other subsets, reaching adult values from D14 onwards. As with the other subsets however, the absolute numbers of $CD103^{+}CD11b^{-}$ DC did not change until D21 or later, although again adult levels were then attained relatively quickly compared with the other subsets (Fig 4.6C). The proportion of migratory $CD103^{-}CD11b^{-}$ DC remained low from birth until increasing from D7 to D21 and then decreasing subsequently to adult levels. Total numbers of this subset were low until D21, after which they rose to adult values (Fig 4.6D).

As expected, few if any $CD103^{+}CD11b^{+}$ DC could be found amongst the resident DC population at any time and if present, were likely to be contamination from the migratory compartment (Fig 4.7A). At birth, the majority of resident DC belonged to the $CD103^{+}CD11b^{-}$ DC subset, but the proportion of $CD103^{-}CD11b^{+}$ DC expanded rapidly between D1 and D3, which was also reflected in a transient increase in their number at D3. The frequency of these DC then remained similar (40%) until adult life,

apart from a further fleeting increase at D28 to around 70%. The absolute number of these cells began to increase after D21, reaching adult levels after D42 (Fig 4.7B).

The proportion of resident $CD103^+CD11b^-$ DC fell significantly and dramatically to around 20% by D3, before increasing again on D5 and then falling gradually to their adult levels thereafter (Fig 4.7C). As with the other subsets, the absolute numbers of these cells increased towards adult values after D21. In contrast to their behaviour in intestinal mucosa or amongst migratory MLN, the resident $CD103^-CD11b^-$ DC showed a gradual increase in frequency from birth (Fig 4.7D), although their absolute numbers did not approach adult levels until D42.

4.2.4 Overview of intestinal dendritic cell development

By collating the composition of the intestinal DC dynamics in composite bar charts over time, it was possible to compare how the different DC populations developed. A clear feature was the gradual expansion of the $CD103^+CD11b^+$ DC in the SI LP and migratory MLN. In both tissues this was preceded by expansion of the $CD103^-CD11b^+$ population, which then shrank reciprocally as the $CD103^+CD11b^+$ subset increased. It was notable that these changes appeared to occur somewhat earlier in the SI LP than in the MLN, consistent with these populations developing first in the mucosa, before migrating to the MLN (Fig 4.8 A and C). The age-related increase in $CD103^+CD11b^+$ DC and the reciprocal behaviour of the $CD103^-CD11b^+$ subset was also seen in the colon, although there were considerably fewer $CD103^+CD11b^+$ DC here than in the SI LP (Fig 4.8B).

The $CD103^+CD11b^-$ DC population also showed marked changes with age in the SI LP and migratory MLN. These were the largest population in the SI LP before birth, but their proportion then fell in the first week of life, before increasing towards adult levels thereafter. By contrast, this subset was rare in the migratory MLN until D5, paralleling the loss of these DC from SI LP and again consistent with their emigration from the mucosa. This population also decreased at birth in the colon, perhaps suggesting emigration from this tissue too, or reflecting the expansion of $CD103^-CD11b^+$ DC that occurs at this time. However, by D7 and afterwards, $CD103^+CD11b^-$ DC rapidly became the largest population in the colon, in marked contrast to the SI LP.

By comparison, the proportions of $CD103^{-}CD11b^{-}$ DC did not change markedly with time and the pattern showed no clear relationship to any of the other subsets.

I used resident MLN DC to represent the development of lymphoid DC derived directly from the bloodstream, and this showed that the dominance of $CD103^{+}CD11b^{-}$ DC at birth was rapidly replaced by increasing proportions of $CD103^{-}CD11b^{+}$ DC, which were the majority subset from D3 onwards. There was also an age related increase in the proportion of $CD103^{-}CD11b^{-}$ DC (Fig 4.8D).

The results above showed that the absolute numbers of DC increased with age. However, this was unsurprising given that all the organs themselves expand in size from birth onwards (Fig 4.9A). To correct for this, I assessed the density of each population, measured as numbers per gram of tissue. This showed that there appeared to be an intense burst in DC development in both the SI LP and CLP around D14, when the relative dominance of $CD103^{+}CD11b^{+}$ and $CD103^{+}CD11b^{-}$ DC respectively became established. There was then a second, smaller increase in some populations after D42, especially in the colon (Fig 4.9 B-C). As might be anticipated, the density of migratory DC in the MLN also increased transiently between D7 and D14, but then increased markedly throughout adult life (Fig 4.9D). Interestingly, a similar pattern was seen amongst the resident DC in the MLN, suggesting these changes reflect a generalised process in DC development rather than changes driven by the intestinal environment (Fig 4.9E).

4.2.5 Development of dendritic cells in the lung

As a control for my studies of DC development in the intestine, I examined the lung as an additional mucosal tissue. Using a similar gating strategy to that used for the intestinal lamina propria, MP were identified amongst live ($7AAD^{-}$) $CD45^{+}$ cells as $CD11c^{+}$ MHC II^{+} $B220^{-}$ (Fig 4.10A), $CD64^{+}$ mϕ were excluded, and DC analysed for CD103 and CD11b expression (Fig 4.10B).

Unlike the intestine, the majority of DC in the lung were either $CD103^{-}CD11b^{+}$ or $CD103^{+}CD11b^{-}$ DC at all time points except for D5, when approximately 50% were $CD103^{-}CD11b^{-}$ DC. As expected, few if any $CD103^{+}CD11b^{+}$ DC could be seen at any

age, although in D1 ~3.6% had this phenotype, which then decreased to ~0.8% by D3 (Fig 4.11A). The proportion of $CD103^{-}CD11b^{+}$ DC remained fairly constant at 20% until D14, after which it doubled until dropping back to the adult levels of 20% between D28 and D42. The absolute numbers of this subset were low apart from a marked, but transient expansion at D21 (Fig 4.11B). $CD103^{+}CD11b^{-}$ DC formed the majority subset on D1, but fell transiently at D3. The proportion of $CD103^{+}CD11b^{-}$ DC dropped further at D21 and D28, probably reflecting the increased frequency of $CD103^{-}CD11b^{+}$ DC, while the absolute numbers of $CD103^{+}CD11b^{-}$ DC increased until D21, before falling at D28 (Fig 4.11C). Although the proportions and numbers of $CD103^{-}CD11b^{-}$ DC were generally low, their numbers showed a transient expansion at D21, similar to that seen for the other subsets (Fig 4.11D).

The composite bar chart highlighted the absence of $CD103^{+}CD11b^{+}$ DC, as well as the expansion of $CD103^{-}CD11b^{+}$ DC and reciprocal decrease in $CD103^{+}CD11b^{-}$ DC at around D21 (Fig 4.12A). Measuring the density of the DC subsets per gram of tissue showed that lung mass increased steadily to D42 and that there was a transient expansion in DC numbers at D7 (Fig 4.12B). CD103 expression increased in the $CD103^{+}CD11b^{-}$ DC to D7, after which it increased only slightly further to D21.

4.3 Phenotypic dissection of intestinal dendritic cell development

The results above suggested that the maturation of $CD103^{+}CD11b^{+}$ DC in the intestine was delayed in comparison to the other subsets and that this may be preceded by the development of the $CD103^{-}CD11b^{+}$ subset. While performing these experiments, on-going work in the laboratory of Professor Mowat suggested that these subsets might be related to each other in adulthood. Therefore I decided to explore further whether such a connection could explain my results.

4.3.1 CD103 expression on intestinal dendritic cell subsets

To determine if one DC subset was developmentally related to another, I first examined the phenotype of the individual subsets in more detail to study whether this might reveal additional stages in development. To begin with, I assessed the levels of CD103 expression on the DC subsets at different times after birth. This

showed that $CD103^+CD11b^+$ DC consistently expressed lower levels than $CD103^+CD11b^-$ DC in both the SI LP and CLP at all ages. This seemed to reflect that whereas CD103 expression by $CD103^+CD11b^+$ DC increased only modestly to adult levels from D21, there were marked increases in CD103 expression by the $CD103^+CD11b^-$ subset over time. This was seen most dramatically on D14 in the colon but not until D21 in the SI LP (Fig 4.13A-B). The difference in CD103 expression between the subsets was not as marked amongst migratory DC in MLN, except at D14, when there was a large but transient increase in CD103 expression by the $CD103^+CD11b^-$ subset (Fig 4.13C). CD103 expression by $CD103^+CD11b^-$ DC amongst resident MLN DC did not vary much with age, apart from a small increase towards D7 (Fig 4.13D).

4.3.2 Trem-1 and CD101 as markers of tissue specific dendritic cell differentiation

Next I investigated whether the delayed appearance of $CD103^+CD11b^+$ DC was simply due to an isolated defect in expression of the CD103 molecule, or indicated a failure of the entire developmental program. Therefore I decided to try and find other markers that might allow the $CD103^+CD11b^+$ DC lineage to be identified without using CD103. To do this, I exploited microarray data generated by a previous PhD student in the lab, which had identified a number of genes that were significantly over-expressed by $CD103^+CD11b^+$ DC compared with the $CD103^-CD11b^+$ subset. We hypothesised that some of these would act as surrogate markers that would allow $CD103^+CD11b^+$ DC to be identified (Fig 4.14). Antibodies against some of these markers were screened for their ability to discriminate intestinal DC subsets by flow cytometry and amongst these, Trem-1 and CD101 were selected as being particularly useful.

To investigate whether Trem-1 and CD101 could be used to dissect the development of intestinal DC subsets in more depth, I first examined their expression by DC populations in different organs of adult mice, before moving on to the neonatal intestine.

4.3.2.1 Small intestinal lamina propria

Initially, I looked in the SI LP and analysed the four DC subsets based on CD103 and CD11b for their expression of Trem-1 or CD101. This showed that $CD103^{+}CD11b^{+}$ DC expressed the highest levels of CD101, while some $CD103^{-}CD11b^{+}$ DC expressed CD101, and the $CD103^{+}CD11b^{-}$ and $CD103^{-}CD11b^{-}$ DC expressed very little. A similar pattern was seen for Trem-1 expression (Fig 4.15A). An even clearer pattern emerged when CD101 and Trem-1 were examined in combination, showing that most $CD103^{+}CD11b^{+}$ DC expressed both CD101 and Trem-1 (88%), with a few expressing CD101 or Trem-1 alone (4%). ~20% of $CD103^{-}CD11b^{+}$ DC also expressed both CD101 and Trem-1, while ~15% were positive for either marker alone and the remainder expressed neither molecule. By contrast, $CD103^{+}CD11b^{-}$ and $CD103^{-}CD11b^{-}$ DC expressed very little CD101 or Trem-1, with only a few expressing Trem-1 alone and no $CD101^{+}Trem\text{-}1^{+}$ cells being found (Fig 4.15B-C).

4.3.2.2 Small intestine draining mesenteric lymph nodes

Next I analysed adult MLN and took advantage of recent work in Dr. Simon Milling's lab that had distinguished the segments of the MLN chain that drain the SI LP and CLP (sMLN and cMLN respectively) (Houston et al., 2015). This allowed the comparison of migratory DC deriving from the SI or colon specifically. The expression of CD101 and Trem-1 by migratory DC in the sMLN mirrored that of the SI LP, whereby most $CD103^{+}CD11b^{+}$ DC expressed both CD101 and Trem-1, as did some $CD103^{-}CD11b^{+}$ DC. A few $CD103^{-}CD11b^{+}$ DC also expressed CD101 and Trem-1 alone, but again the $CD103^{+}CD11b^{-}$ and $CD103^{-}CD11b^{-}$ DC were mainly negative for CD101, and a few expressed Trem-1 alone (Fig 4.16). Resident DC in the sMLN were quite distinct, as most expressed no CD101 or Trem-1, apart from a small population (~30%) of $CD103^{-}CD11b^{+}$ DC that were $CD101^{+}$ (Fig 4.17).

4.3.2.3 Colonic lamina propria

Somewhat surprisingly, a different pattern was seen in the colon compared with SI LP. Although most $CD103^{+}CD11b^{+}$ DC expressed CD101, the levels of Trem-1 were much lower than in the SI LP and no Trem-1 was found on any other subset. As in the SI LP,

some colonic CD103$^-$CD11b$^+$ DC were CD101$^+$ (Fig 4.18). I considered the possibility that there may have been specific cleaving of the Trem-1 molecule from the colonic DC subsets during the digestion process, which uses different enzymes from those used in isolating SI LP. To rule this out, I examined the migratory DC in the colon specific cMLN that was obtained using the same digestion protocol as the sMLN, where Trem-1$^+$ DC were abundant.

4.3.2.4 Colonic draining mesenteric lymph nodes

The expression of CD101 and Trem-1 by migratory cMLN DC was similar to that in the CLP, with far fewer CD103$^+$CD11b$^+$ DC expressing CD101 and Trem-1 compared with SI LP or MLN. Thus the lack of Trem-1 in the colon does not appear to reflect an effect of enzymatic digestion (Fig 4.19). As in the sMLN, resident cMLN DC had little expression of CD101 or Trem-1 on any of the DC subsets, except for a small amount (~12%) of CD101 expression on CD103$^-$CD11b$^+$ DC (Fig 4.20).

4.3.2.5 Non-intestinal tissues

As these results suggested that CD101 and Trem-1 expression was a particular feature of CD103$^+$CD11b$^+$ DC in SI LP, I interrogated this observation further by examining the expression of Trem-1 and CD101 by DC subpopulations in non-intestinal tissues. First I examined the skin draining peripheral lymph nodes (PLN), where both migratory and resident DC can be identified on the basis of CD11c and MHC II expression (as in the MLN). As expected, there were virtually no CD103$^+$CD11b$^+$ DC amongst either the migratory or resident populations in skin draining PLN, with most being CD103$^-$CD11b$^+$, CD103$^+$CD11b$^-$ or CD103$^-$CD11b$^-$ DC. Apart from a very small subset of CD103$^-$CD11b$^+$ DC that were CD101$^+$, CD101 and Trem-1 were not expressed to any significant extent by any of the DC subsets within either the migratory or resident compartment, nor by the rare CD103$^+$CD11b$^+$ DC (Fig 4.21 and 4.22, respectively).

None of the three subsets of DC found in the spleen expressed Trem-1, but ~40% of CD103$^-$CD11b$^+$ DC expressed CD101, as did a few CD103$^-$CD11b$^-$ DC. CD101 was absent from CD103$^+$CD11b$^-$ DC (Fig 4.23). The liver (Fig 4.24) and kidney (Fig 4.25)

also contained three DC populations based on CD103 and CD11b expression, lacking the $CD103^+CD11b^+$ DC subset. The pattern of CD101 and Trem-1 expression by these subsets was similar to the spleen, with no Trem-1 expressed by any DC and variable proportions of $CD103^-CD11b^+$ DC expressing CD101. I also examined DC in the heart, where $CD103^+CD11b^+$ DC were also absent. Here none of the DC expressed CD101 or Trem-1 (Fig 4.26).

Four DC subsets could be identified in the lung, although as noted earlier, the frequencies of $CD103^+CD11b^+$ DC were variable and generally very low, with the majority of DC being $CD103^-CD11b^+$ or $CD103^+CD11b^-$. As in the PLN, Trem-1 was not expressed by any DC subset in the lung, but some of them did express CD101 to some extent, with this being most apparent in the rare $CD103^+CD11b^+$ DC (~60%), followed by the $CD103^-CD11b^+$ DC (~20%)(Fig 4.27).

Together these data show that CD101 and Trem-1 can further distinguish $CD103^+CD11b^+$ DC and that co-expression of these markers is selective for this subset in the SI LP. I went on to use these markers to analyse in more detail the development of the $CD103^+CD11b^+$ DC lineage in neonatal intestine.

4.4 Trem-1 and CD101 expression by dendritic cells during development

Having established that Trem-1 and CD101 were suitable for identifying the $CD103^+CD11b^+$ subset of intestinal DC (at least in the SI LP), I went on to use these markers to extend my analysis of DC development in the neonatal intestine. To do this I isolated cells from D1, D14 and 8-10 week old adult mice, having chosen these time points because my earlier studies indicated these were times when substantial changes were taking place in the composition of the DC compartment.

As before, $CD103^+CD11b^+$ DC were rare in D1 SI LP, but their proportion increased substantially by D14 and again in adults (Fig 4.28A). Even on D1, the majority (~60%) of these DC expressed CD101 and this was found on virtually all $CD103^+CD11b^+$ DC by D14. Trem-1 expression took longer to become established, with only a few $CD103^+CD11b^+$ DC expressing Trem-1 on D1. The proportion of $Trem\text{-}1^+$ cells had increased markedly by D14 (76%) and increased only a little more

into adults (88%). At all times the Trem-1$^+$ cells also expressed CD101 (Fig 4.28B; Fig 4.29A). As I found previously, the CD103$^-$CD11b$^+$ DC subset appeared to develop more quickly than the CD103$^+$CD11b$^+$ DC subset, being present in substantial proportions by D1 and reducing somewhat thereafter (Fig 4.28A). At D1 around 50% of CD103$^-$CD11b$^+$ DC expressed CD101, with ~15% of these also expressing Trem-1. The proportions of CD103$^-$CD11b$^+$ DC expressing CD101, either alone or together with Trem-1, increased at D14 before returning to the adult values of ~25% and ~15% respectively (Fig 4.28C; Fig 4.29B). The CD11b$^-$ subsets (CD103$^+$CD11b$^-$ and CD103$^-$CD11b$^-$ DC) had virtually no CD101 expression and only small numbers of Trem-1$^+$ cells at any time after birth, consistent with what I found in adult SI LP (Fig 4.28 D-E; Fig 4.29C-D).

I next examined the colon, where there were very few CD103$^+$CD11b$^+$ DC on D1 but where these increased in frequency to adult levels by D14 (Fig 4.30A). Due to their low numbers, it was difficult to assess the expression of CD101 and Trem-1 on these DC at D1, but by D14 virtually all of these expressed CD101, as in adults. Interestingly, unlike adult CLP, significant numbers of CD103$^+$CD11b$^+$ DC expressed both Trem-1 and CD101 on D14 (~27%). As in SI LP, CD103$^-$CD11b$^+$ DC were already well established in the colon on D1 and remained abundant into adulthood (Fig 4.30A). Interestingly, at D1 some of these DC expressed Trem-1 either alone, or together with CD101, similar to what I found in neonatal SI LP (Fig 4.30B; Fig 4.31A). These populations were virtually absent in the adult CLP. CD103$^-$CD11b$^+$ DC also expressed CD101$^+$ alone in substantial numbers on D1 and appeared to expand markedly on D14 before falling again in adulthood. As in the SI LP, more than 90% of the CD103$^+$CD11b$^-$ and CD103$^-$CD11b$^-$ DC were negative for CD101 or Trem-1 at all times (Fig 4.30 D-E; Fig 4.31C-D).

As I had found earlier, very few migratory DC were present in the MLN on D1 and therefore it was difficult to assess the expression of CD101 and Trem-1 at this time point. By D14, the numbers of migratory DC had increased, and at this time most CD103$^+$CD11b$^+$ DC were CD101$^+$, with ~28% expressing both CD101 and Trem-1, which was much lower than in the SI LP at this time. By adulthood, 50% of migratory CD103$^+$CD11b$^+$ DC were CD101$^+$Trem-1$^+$ (Fig 4.32B; Fig 4.33A). Similar proportions (~25%) of CD103$^-$CD11b$^+$ DC expressed CD101 throughout development, and on D14

some expressed Trem-1 alone, but this was reduced by adulthood. Very few cells in this subset expressed both molecules together (Fig 4.32C; Fig 4.33B). As before, $CD103^{+}CD11b^{-}$ and $CD103^{-}CD11b^{-}$ DC had little or no expression of CD101 or Trem-1 at any time (Fig 4.32 D-E; Fig 4.33C-D).

As in my previous experiments, most of the resident DC in the adult MLN expressed neither CD101 nor Trem-1 and this was generally the case throughout development, apart from transient expression of Trem-1 on $CD103^{-}CD11b^{+}$ DC at D14, similar to what I observed amongst migratory and mucosal DC in this subset at this time. Whether this reflects contamination from the migratory gate remains to be determined (Fig 4.34; Fig 4.35).

4.5 Functional consequences of intestinal dendritic cell development

In the final experiments in this chapter, I examined whether the age-related changes in DC subsets had functional consequences.

4.5.1 Retinoic acid production by dendritic cells in neonatal intestine

As described earlier, a characteristic feature of intestinal DC is their ability to produce retinoic acid by the metabolism of vitamin A and therefore I used this property to assess how DC function in the intestine changed during early life. First I analysed RALDH activity in total SI LP DC from D1, D7 or 8-10 week old adult mice using the Aldefluor™ assay (Fig 4.36A). As expected, a large proportion of adult mucosal DC were Aldefluor™$^{+}$. By contrast, very few Aldefluor™$^{+}$ DC were present on D1 and these positive cells expressed only low levels of RALDH. Aldefluor™ activity was somewhat increased on D7, but was still significantly less than that of the adult DC (Fig 4.36B).

I went on to look at the individual DC subsets, all of which expressed Aldefluor™ in the adult (Fig 4.37B). The highest proportion of Aldefluor™$^{+}$ cells was amongst the $CD103^{+}CD11b^{+}$ DC subset in the adult, but the highest level of expression was by the $CD103^{+}CD11b^{-}$ DC. Although Aldefluor™$^{+}$ cells were detectable amongst most of the DC subsets present at D1, the levels were lower than those in the equivalent adult

subsets and $CD103^{-}CD11b^{-}$ DC contained no $Aldefluor^{TM+}$ cells. By D7 the proportion of $Aldefluor^{TM+}$ cells amongst $CD103^{+}CD11b^{-}$ and $CD103^{-}CD11b^{-}$ DC had reached that of the adult, when the levels were also almost equivalent. By contrast the proportion of $Aldefluor^{TM+}$ cells amongst $CD103^{+}CD11b^{+}$ and $CD103^{-}CD11b^{+}$ DC actually fell between D1 and D7 and the levels of RALDH in these subsets remained significantly below the adult levels (Fig 4.37). These data indicate that RA production takes some time to develop after birth, even when the principal RA producing subsets have already begun to accumulate.

4.5.2 Age dependent development of effector T cells in small intestinal lamina propria

I next went on to investigate whether the changes in DC composition and function in neonates correlated with $CD4^{+}$ effector T cell development, as different DC subsets in the intestine are able to polarise naïve $CD4^{+}$ T cells differently (Cerovic et al., 2013; Coombes et al., 2007; Sun et al., 2007). To do this, I isolated SI LP leukocytes, stimulated them with PMA and ionomycin for 4.5 hours and assessed their expression of IL-17, IFNγ and FoxP3 by intracellular staining. In these experiments I identified T cells using CD5 instead of CD3, as CD3 can be internalised from the T cell membrane after activation (Yamane et al., 1991). $CD5^{+}$ B cells were excluded using B220 and the remaining $CD5^{+}$ $CD4^{+}$ T cells analysed (Fig 4.38A). Positive intracellular staining for Treg, Th1 and Th17 cells was determined by comparing with appropriate isotype controls (Fig 4.38B). The time course started at D7, as I was unable to isolate enough SI LP leukocytes for the PMA/ionomycin restimulation from D1 mice.

The frequency of $CD4^{+}$ T cells amongst total $CD45^{+}$ leukocytes decreased significantly between D7 (~30%) and D21 (~20%) and again from D21 to D42 (~10%), before the frequency stabilised in 8-10 week old adults. Although the absolute numbers of $CD4^{+}$ T cells did not change significantly over the time course, there was a slight increase in their number at 8-10 weeks, which was not significant due to the variability between individual results (Fig 4.38A; lower panel).

$FoxP3^{+}$ Treg cells increased significantly in proportion from D7 (~4%) until D42 (~14%), at which point they were similar to those in the 8-10 week old adult (~15%).

There was also a general trend for the frequency of both Th1 and Th17 cells to increase as the mice matured to adulthood, although from D21 onwards Th1 and Th17 cells made up a significantly lower proportion of $CD4^+$ T cells. The numbers of $FoxP3^+$ Tregs also increased significantly from D7 (~0.6 $x10^4$) to ~6 $x10^4$ at D42 and to ~10 $x10^4$ in adults. The Th1 and Th17 cells gradually increased in number with time, but remained significantly less abundant than $FoxP3^+$ Tregs from D21 onwards (Fig 4.38B).

4.6 Summary

The results of this chapter show that DC are present in the intestine from before birth, but the composition of the population changes markedly from then until adult life, particularly in the neonatal period. Thus, although $CD103^+CD11b^+$ DC were the predominant population in the adult SI LP, this pattern did not become established until around 28 days after birth and these DC were rare in the neonatal SI LP until D5. The appearance of $CD103^+CD11b^+$ DC was preceded by the presence of a substantial number of $CD103^-CD11b^+$ DC, which then fell towards adult levels. $CD103^+CD11b^-$ DC were the predominant subset in embryonic SI LP, but their frequency fell markedly after birth, before a second expansion after D7 which meant that they became the second most abundant DC subset in the SI LP thereafter.

The development of $CD103^+CD11b^+$ DC in the CLP was slower than in the SI LP and this subset never reached the same proportions as in the SI LP and did not really become established until D14, a week later than in the SI LP. However, as in the SI LP, the increase in colonic $CD103^+CD11b^+$ DC frequency coincided with a decrease in $CD103^-CD11b^+$ DC.

The development of migratory DC subsets in MLN mirrored that of the lamina propria of the intestine, resembling the SI LP in particular. However the expansion in the proportion of $CD103^+CD11b^+$ DC was more dramatic than in either the SI LP or CLP and it was delayed when compared to the lamina propria. In parallel, the contraction of the $CD103^-CD11b^+$ DC population was also more evident in MLN, whereas $CD103^+CD11b^-$ DC increased relatively gradually as the mice matured.

The resident compartment of MLN DC was used as an example of blood derived DC in secondary lymphoid organs. As expected, $CD103^+CD11b^+$ DC were missing from this population and the much greater proportion of $CD103^-CD11b^+$ DC accumulated progressively from birth until D28. These changes were paralleled by contraction in the proportion of $CD103^+CD11b^-$ DC that predominated at birth. I also used the lung as a non-intestinal mucosal tissue, where again $CD103^+CD11b^+$ DC were almost absent. As with resident MLN DC, there was an increase in $CD103^-CD11b^+$ DC from D3 up until D28 in both proportion and absolute number, whilst the $CD103^+CD11b^-$ DC initially dropped in proportion from D1 to D3, and then increased and stabilised from D5 to D28. Although there were similarities between the resident MLN DC and the lung DC, there were subtle differences in the dynamics of the DC subsets, probably reflecting differences in the local environment.

Because I was concerned that the increasing size of the tissues during development might confound interpretation of the results, I also calculated the number of cells per gram of tissue. This showed that although the absolute numbers of DC populations increased progressively with time, their density in the LP did not change as markedly, apart from a transient expansion at D14. This increase in density at D14 was also seen amongst migratory and resident MLN DC, and a similar pattern was seen in the lung, except that the early transient expansion occurred at D7 as opposed to D14.

An additional feature that changed as DC developed in the SI LP and CLP was that the level of CD103 expression increased progressively on both subsets of $CD103^+$ DC as the mice matured, especially on $CD103^+CD11b^-$ DC. However, this was not seen with $CD103^+CD11b^-$ DC in the MLN or lung, suggesting there may be a local factor in the intestine that influences the expression of CD103.

These changes in CD103 expression and the apparently reciprocal behaviour of $CD103^+CD11b^+$ and $CD103^-CD11b^+$ DC led me to explore the development of the $CD103^+CD11b^+$ lineage in more detail, and specifically to examine how these subsets might be related. To do this I exploited microarray data generated in the lab that had identified CD101 and Trem-1 as markers that were differentially upregulated between $CD103^+CD11b^+$ and $CD103^-CD11b^+$ DC. Flow cytometric analysis of adult tissues confirmed this by showing that $CD103^+CD11b^+$ and $CD103^-CD11b^+$ DC in the

SI LP and migratory sMLN expressed CD101 and Trem-1, whereas no resident MLN DC expressed Trem-1 and only a few $CD103^{-}CD11b^{+}$ DC in the intestine expressed CD101. Interestingly, the expression of both Trem-1 and CD101 was different in the CLP and cMLN, where there was little or no expression of Trem-1 by $CD103^{-}CD11b^{+}$ or $CD103^{-}CD11b^{+}$ DC. This was also true of Trem-1 expression by DC in all other tissues and therefore appeared to be a specific feature of intestinal DC, particularly those in the SI. However, CD101 was expressed by DC in other tissues such as the spleen, liver, kidney and lung where it was confined mostly to the $CD103^{-}CD11b^{+}$ DC, as well as to the rare $CD103^{+}CD11b^{+}$ DC found in the lung. PLN and heart DC did not express CD101.

These results indicated that Trem-1 and CD101 were selective markers of $CD103^{+}CD11b^{+}$ DC developing from $CD103^{-}CD11b^{+}$ DC. Therefore I went on to look at the effects of ageing on CD101 and Trem-1 expression by intestinal DC. These experiments showed that CD101 and Trem-1 expression by $CD103^{+}CD11b^{+}$ or $CD103^{-}CD11b^{+}$ DC in SI LP and migratory MLN generally increased with age. However, despite the absence of Trem-1 expression in the adult CLP, a transient population of $CD101^{+}$Trem-1^{+} cells was present amongst $CD103^{+}CD11b^{+}$ DC in the CLP at D14. The lack of expression of CD101 and Trem-1 by $CD103^{+}CD11b^{-}$ and $CD103^{-}CD11b^{-}$ DC in SI LP, CLP and MLN did not change with age.

Taken together, these results suggest that development of $CD103^{+}CD11b^{+}$ DC could be related to the $CD103^{+}CD11b^{-}$ DC, evidenced by their reciprocal increase and decrease, respectively. Furthermore, increasing levels in the co-expression of CD101 and Trem-1 amongst $CD103^{+}CD11b^{+}$ DC, compared to the more dynamic expression in $CD103^{-}CD11b^{+}$ DC could indicate a shared maturation pathway in these DC subsets.

Lastly, I investigated if these phenotypic changes with age in intestinal DC were associated with any functional differences. To address this, I first assessed RA production by the various subsets from the SI LP at different ages, and found that although RALDH activity was present in most DC subsets at birth, the frequency of positive DC and the levels of expression increased thereafter. This took longest for $CD103^{+}CD11b^{+}$ and $CD103^{-}CD11b^{+}$ DC, which only acquired adult levels after D7,

whereas the $CD103^{+}CD11b^{-}$ and $CD103^{-}CD11b^{-}$ DC subsets had already reached adult levels by D7.

Next I examined for the presence of differentiated $CD4^{+}$ T in the mucosa, as this is known to reflect the activity of different intestinal DC subsets. These results showed that the proportion of total $CD4^{+}$ T cells amongst $CD45^{+}$ leukocytes reduced with age, while the absolute numbers of T cells did not vary greatly from D7 until adulthood. $FoxP3^{+}$ Tregs were always the most abundant $CD4^{+}$ T cell population, while Th1 and Th17 cells were fairly similar in frequency and number, both to each other and throughout development.

Overall the results in this chapter show that the distinctive composition of the intestinal DC compartment takes some time to develop after birth and that this occurs differently in the different parts of the gut. In addition, these dynamic changes particularly affected the development of the intestine specific $CD103^{+}CD11b^{+}$ DC. These changes reflect the complex maturation process involving a number of different phenotypic changes, rather than just the acquisition of CD103, and are associated with functional maturation as shown by the production of RA. Following on from these results in the next chapter I went on to look at how age effected DC transcriptional and growth factor receptors along with CD101 and Trem-1 expression in SIRPα mt and $CCR2^{-/-}$ mice. I also looked at the role of Trem-1 in DC development.

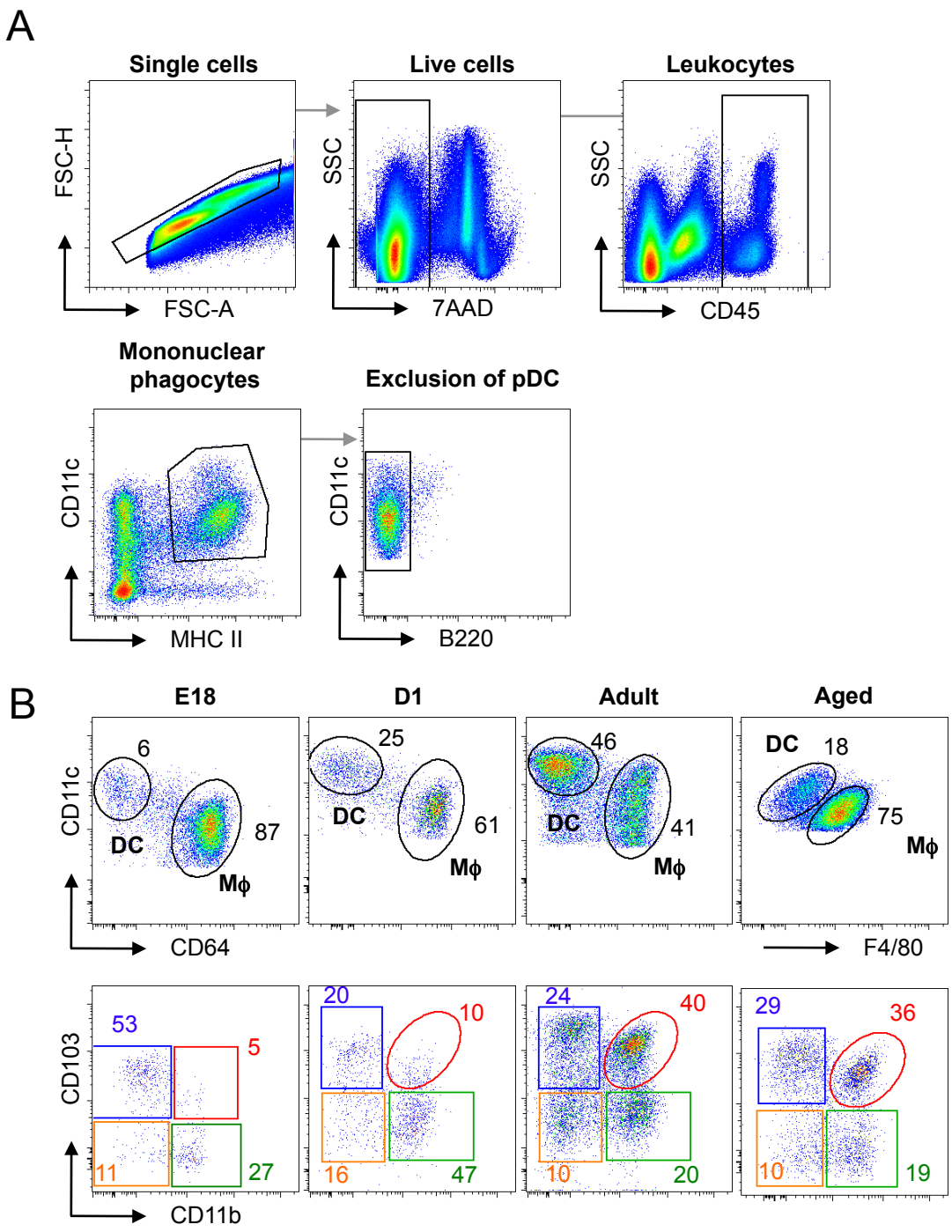

Figure 4.1: Identification of dendritic cells in small intestinal lamina propria at different ages

A SI LP cells were isolated from embryonic D18 (E18) WT mice by enzymatic digestion, and after identifying single cells based on FSC-A and FSC-H, mononuclear phagocytes (MP) were identified amongst live 7AAD$^-$ CD45$^+$ leukocytes as MHC II$^+$ CD11c$^+$. **B** After exclusion of B220$^+$ CD11c$^+$ plasmacytoid DC (pDC), conventional DC were identified as CD11c$^+$ CD64$^-$ (or F4/80$^-$), while Mϕ were CD11c$^+$ CD64$^+$ (top panels). The DC were then subdivided into four populations based on expression of CD103 and CD11b (bottom panels). The graphs show representative data from mice aged E18, D1 after birth, 8-10 week old adults and one-year old aged mice.

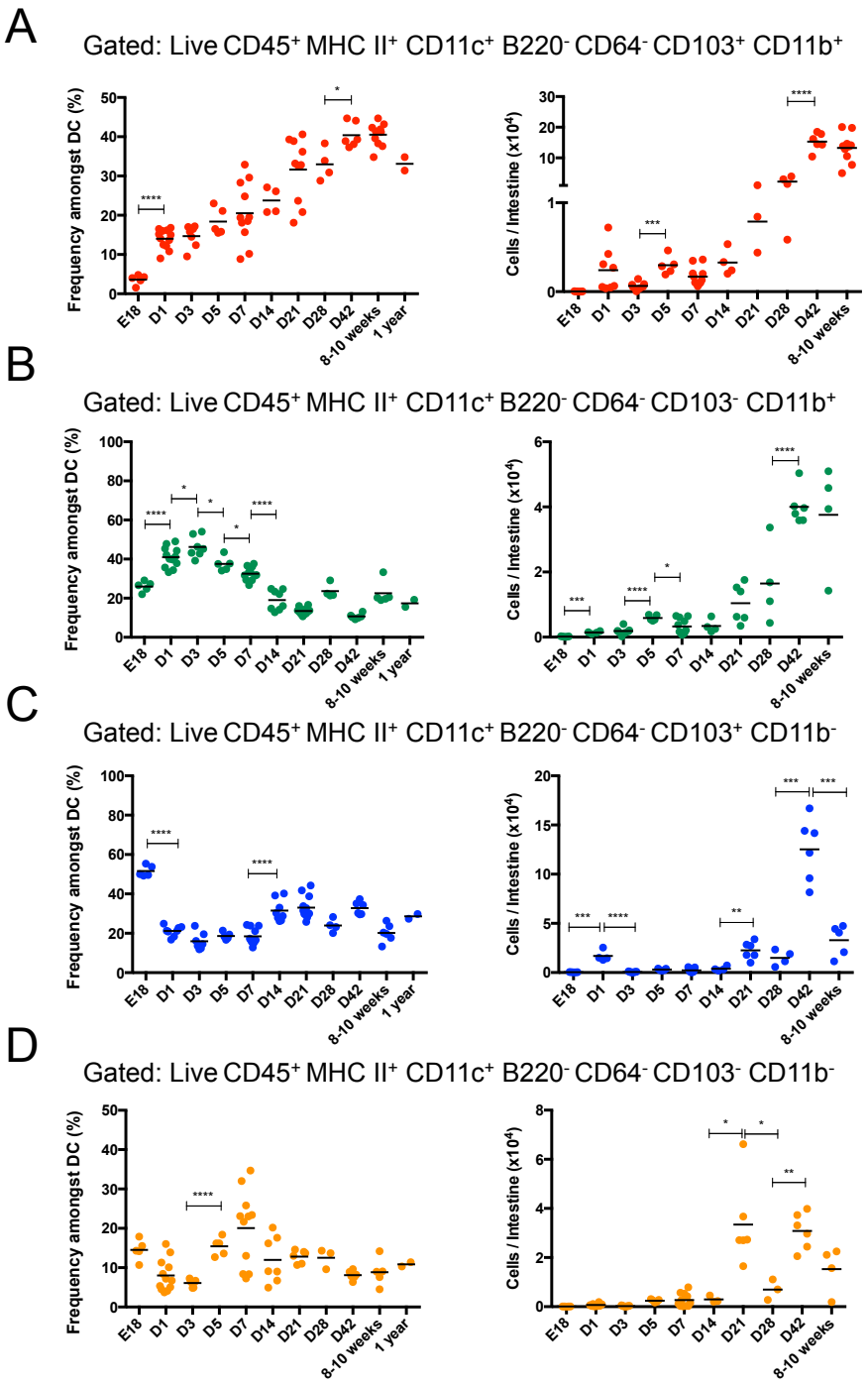

Figure 4.2: Effects of age on dendritic cells in small intestinal lamina propria
SI LP cells were isolated from WT mice, and live MHC II$^+$ CD11c$^+$ B220$^-$ CD64$^-$ leukocytes were analysed for the expression of CD103 and CD11b from E18 to one year of age. Frequency (left panels) and absolute numbers (right panels) of **A** CD103$^+$CD11b$^+$ **B** CD103$^-$CD11b$^+$ **C** CD103$^+$CD11b$^-$ and **D** CD103$^-$CD11b$^-$ DC. Each dot represents an individual mouse and the results are derived from at least 10 different litters. *p<0.05, **p<0.01, ***p<0.001, ****p<0.0001 Student's t-test.

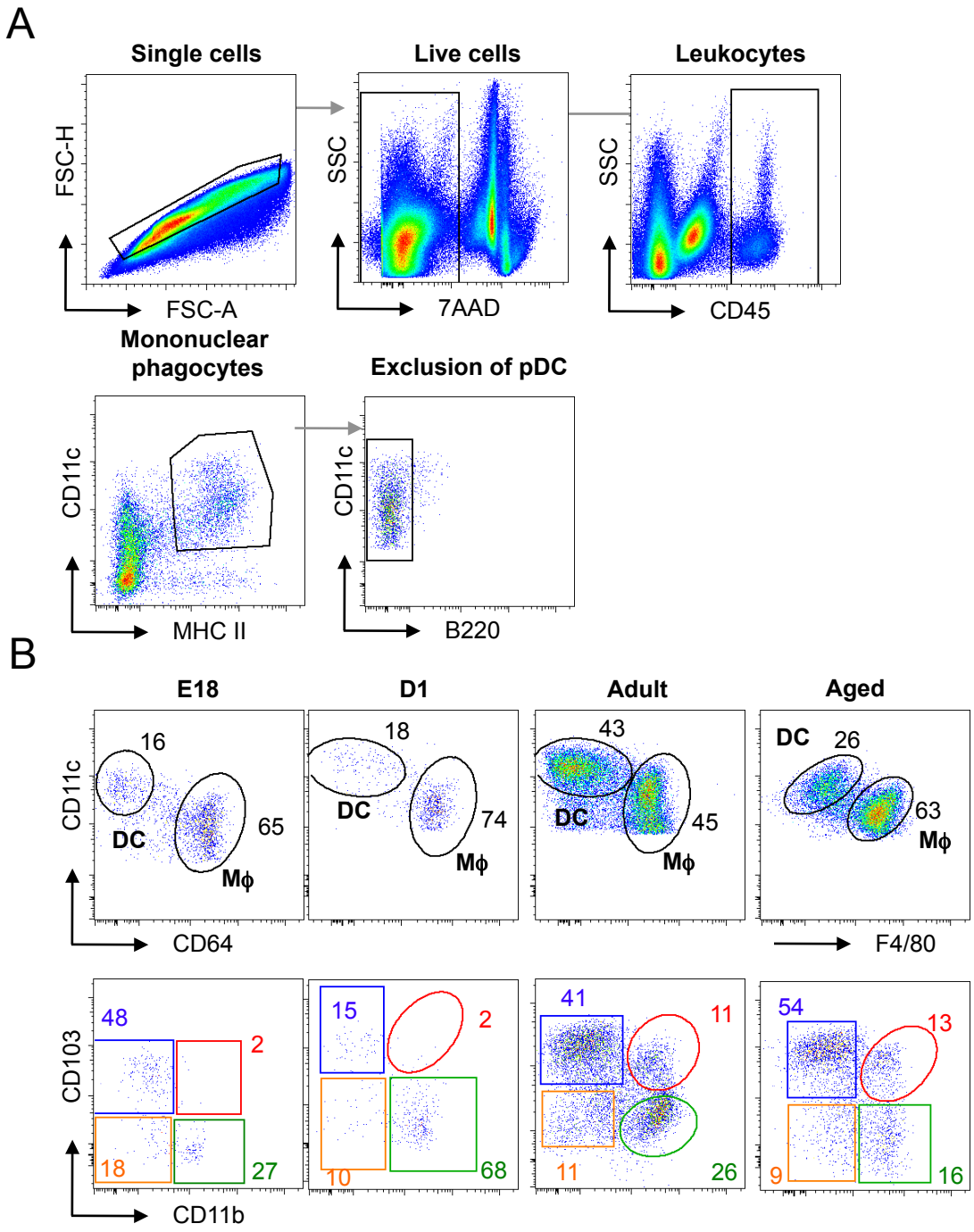

Figure 4.3: Identification of dendritic cells in colonic lamina propria at different ages

A CLP cells were isolated from embryonic D18 (E18) WT mice by enzymatic digestion and after identifying single cells based on FSC-A and FSC-H, mononuclear phagocytes (MP) were identified amongst live 7AAD$^-$ CD45$^+$ leukocytes as MHC II$^+$ CD11c$^+$. **B** After exclusion of B220$^+$ CD11c$^+$ plasmacytoid DC (pDC), conventional DC were identified as CD11c$^+$ CD64$^-$ (or F4/80$^-$), while Mϕ were CD11c$^+$ CD64$^+$ (top panels). The DC were then subdivided into four populations based on expression of CD103 and CD11b (bottom panels). The graphs show representative data from mice aged E18, D1 after birth, 8-10 week old adults and one-year old aged mice.

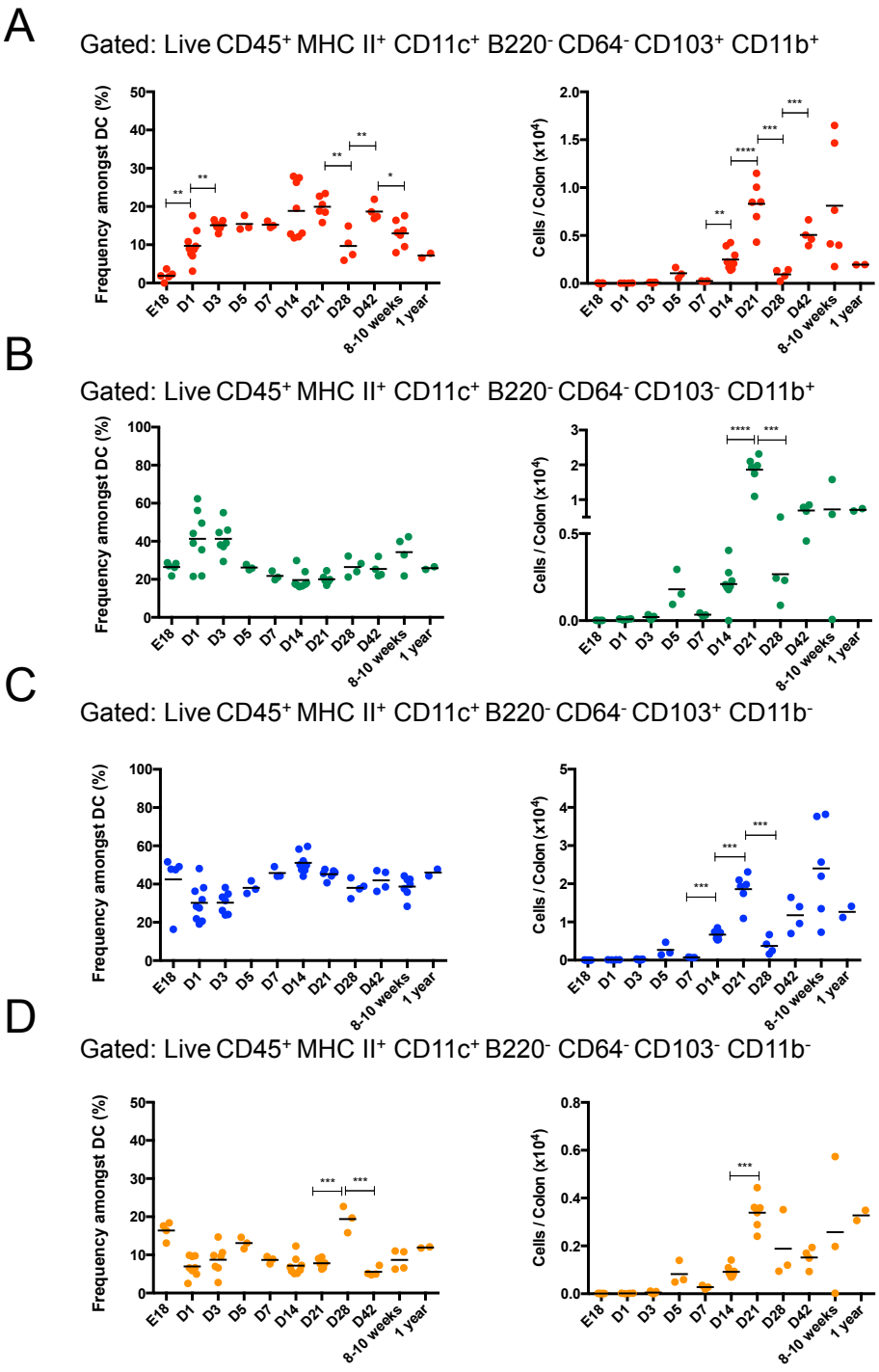

Figure 4.4: Effects of age on dendritic cells in colonic lamina propria

CLP cells were isolated from WT mice, and live MHC II$^+$ CD11c$^+$ B220$^-$ CD64$^-$ leukocytes were analysed for the expression of CD103 and CD11b from E18 to one year of age. Frequency (left panels) and absolute numbers (right panels) of **A** CD103$^+$CD11b$^+$ **B** CD103$^-$CD11b$^+$ **C** CD103$^+$CD11b$^-$ and **D** CD103$^-$CD11b$^-$ DC. Each dot represents an individual mouse and the results are derived from at least 10 different litters. *p<0.05, **p<0.01, ***p<0.001, ****p<0.0001 Student's t-test.

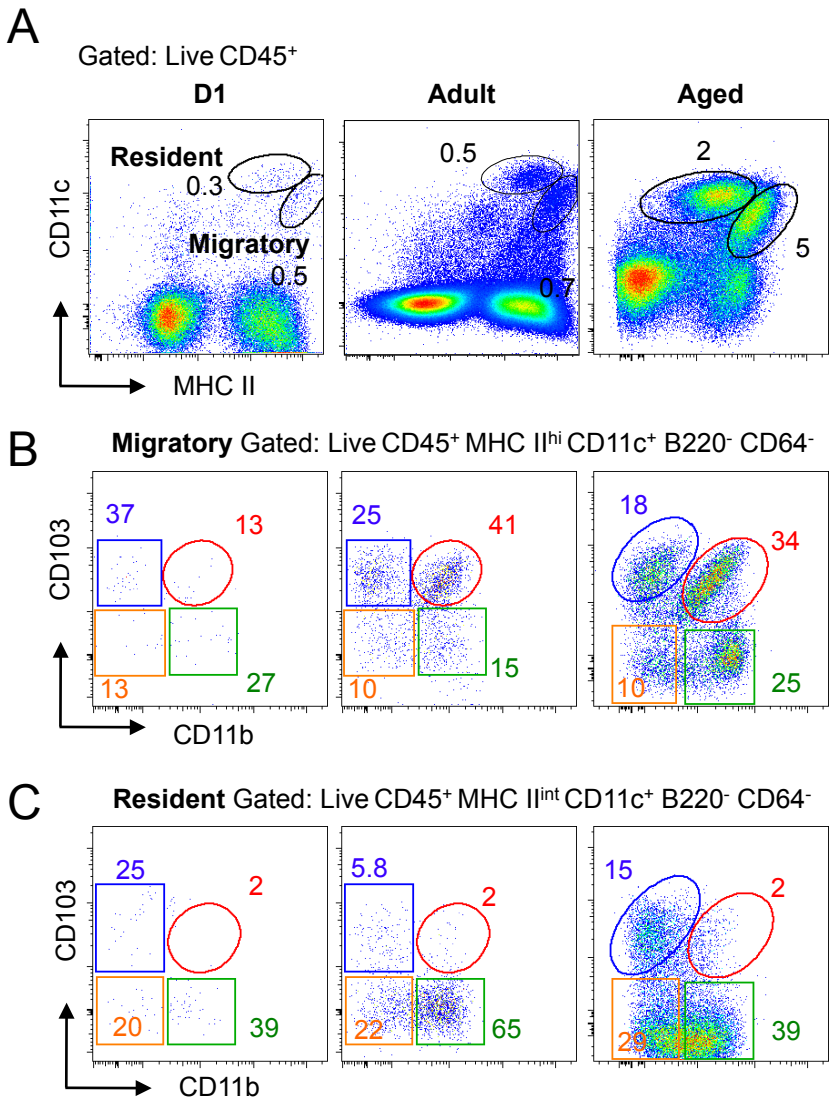

Figure 4.5: Identification of dendritic cells in MLN at different ages

A MLN cells were isolated from WT MLN by enzymatic digestion, and after identifying single cells based on FSC-A and FSC-H, migratory DC were identified amongst live 7AAD$^-$ CD45$^+$ leukocytes as MHC II^{hi} CD11c$^+$ and resident DC were identified as MHC II^{int} CD11c$^+$. **B** Migratory conventional DC or **C** Resident conventional DC were identified as CD11c$^+$ B220$^-$ CD64$^-$ and assessed for the expression CD103 and CD11b. The DC were then subdivided into four populations based on expression of CD103 and CD11b. The graphs show representative data from mice aged D1 after birth, 8-10 week old adults and one-year old aged mice.

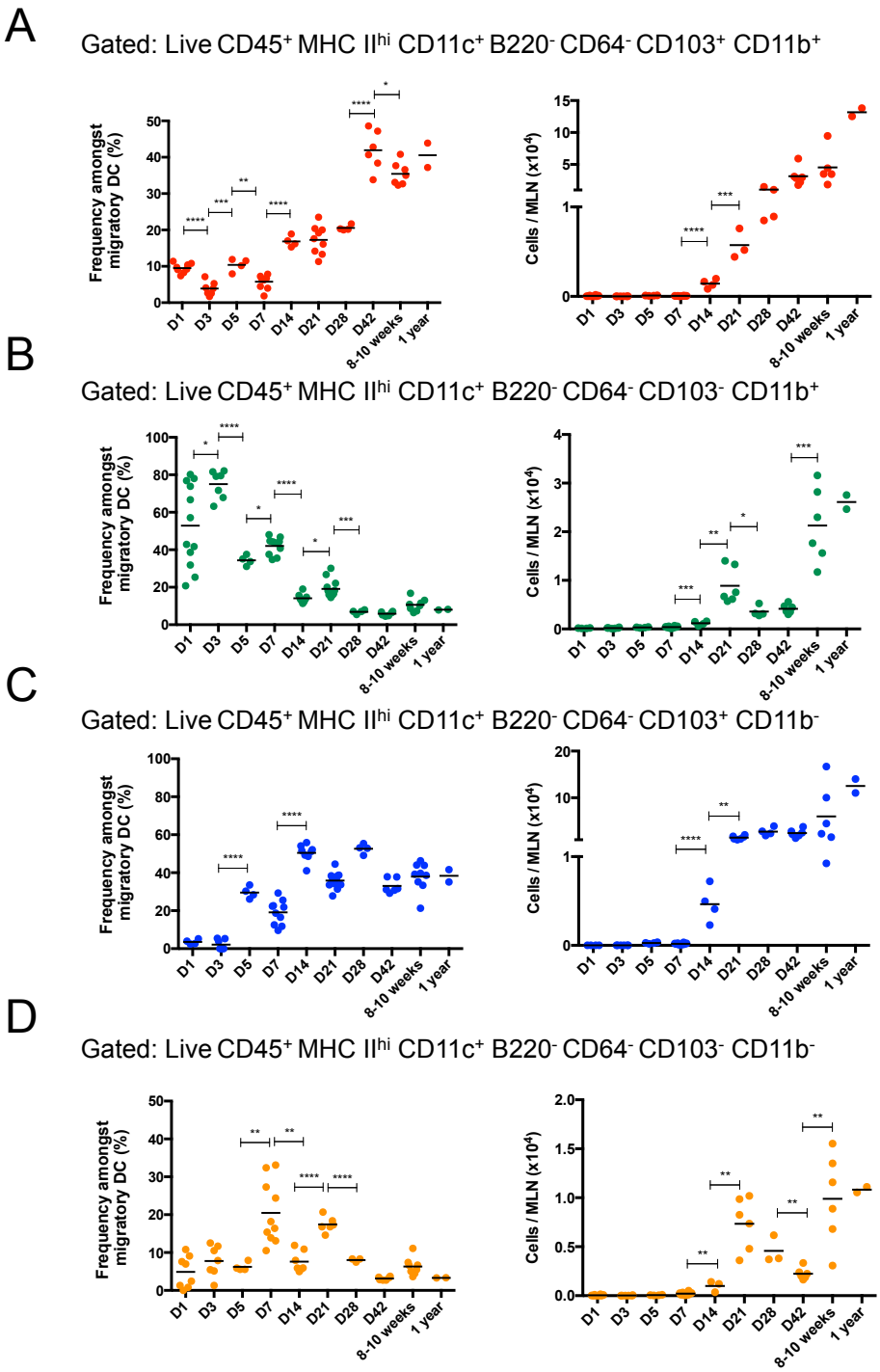

Figure 4.6: Effects of age on migratory dendritic cells in MLN

MLN cells were isolated from WT mice and live MHC II^{hi} CD11c^{+} B220^{-} CD64^{-} leukocytes were analysed for the expression of CD103 and CD11b from D1 to one year of age. Frequency (left panels) and absolute numbers (right panels) of **A** CD103^{+}CD11b^{+} **B** CD103^{-}CD11b^{+} **C** CD103^{+}CD11b^{-} and **D** CD103^{-}CD11b^{-} DC. Each dot represents an individual mouse and the results are derived from at least 10 different litters. *p<0.05, **p<0.01, ***p<0.001, ****p<0.0001 Student's t-test.

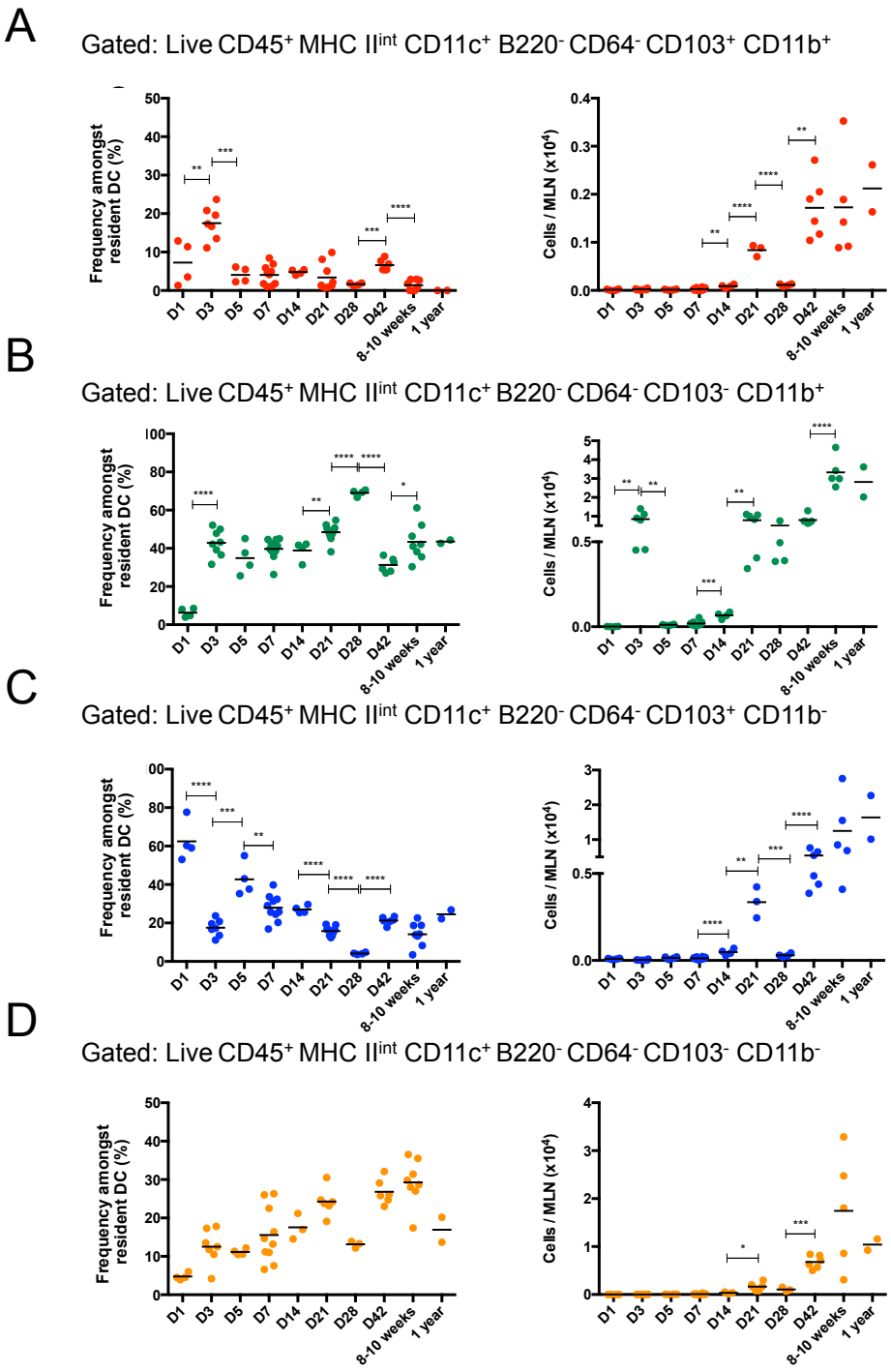

Figure 4.7: Effects of age on resident dendritic cells in MLN

MLN cells were isolated from WT mice and live MHC II^{int} CD11c^{+} B220^{-} CD64^{-} leukocytes were analysed for the expression of CD103 and CD11b from D1 to one year of age. Frequency (left panels) and absolute numbers (right panels) of **A** CD103^{+}CD11b^{+} **B** CD103^{-}CD11b^{+} **C** CD103^{+}CD11b^{-} and **D** CD103^{-}CD11b^{-} DC. Each dot represents an individual mouse and the results are derived from at least 10 different litters. *p<0.05, **p<0.01, ***p<0.001, ****p<0.0001 Student's t-test.

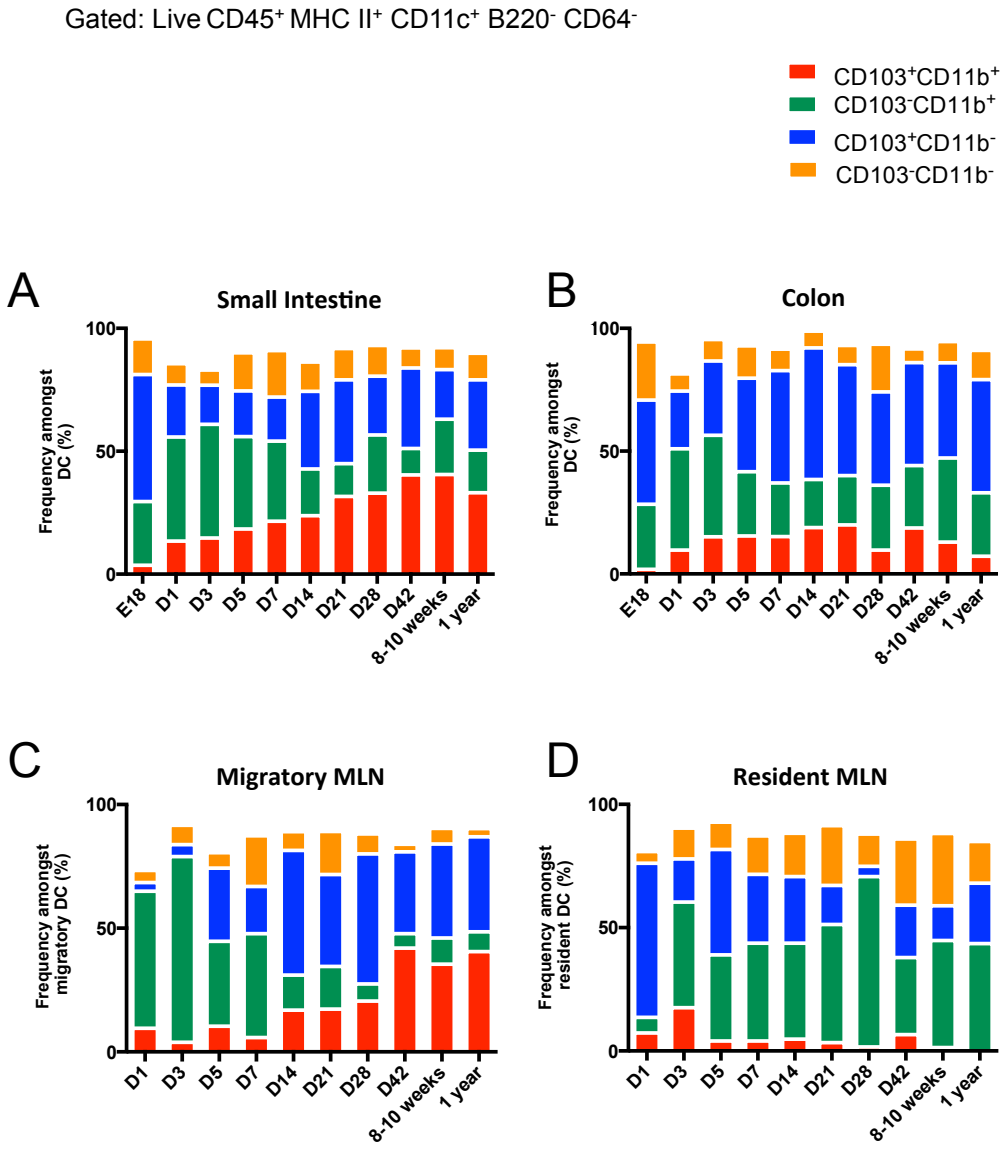

Figure 4.8: Effects of age on the composition of intestinal dendritic cell populations

Frequencies of CD103 and CD11b based DC subsets in **A** SI LP, **B** CLP, **C** migratory MLN compartment and **D** resident MLN compartment from E18 until adulthood. The data are pooled from at least ten experiments with at least n=3 animals per group of mice per time point.

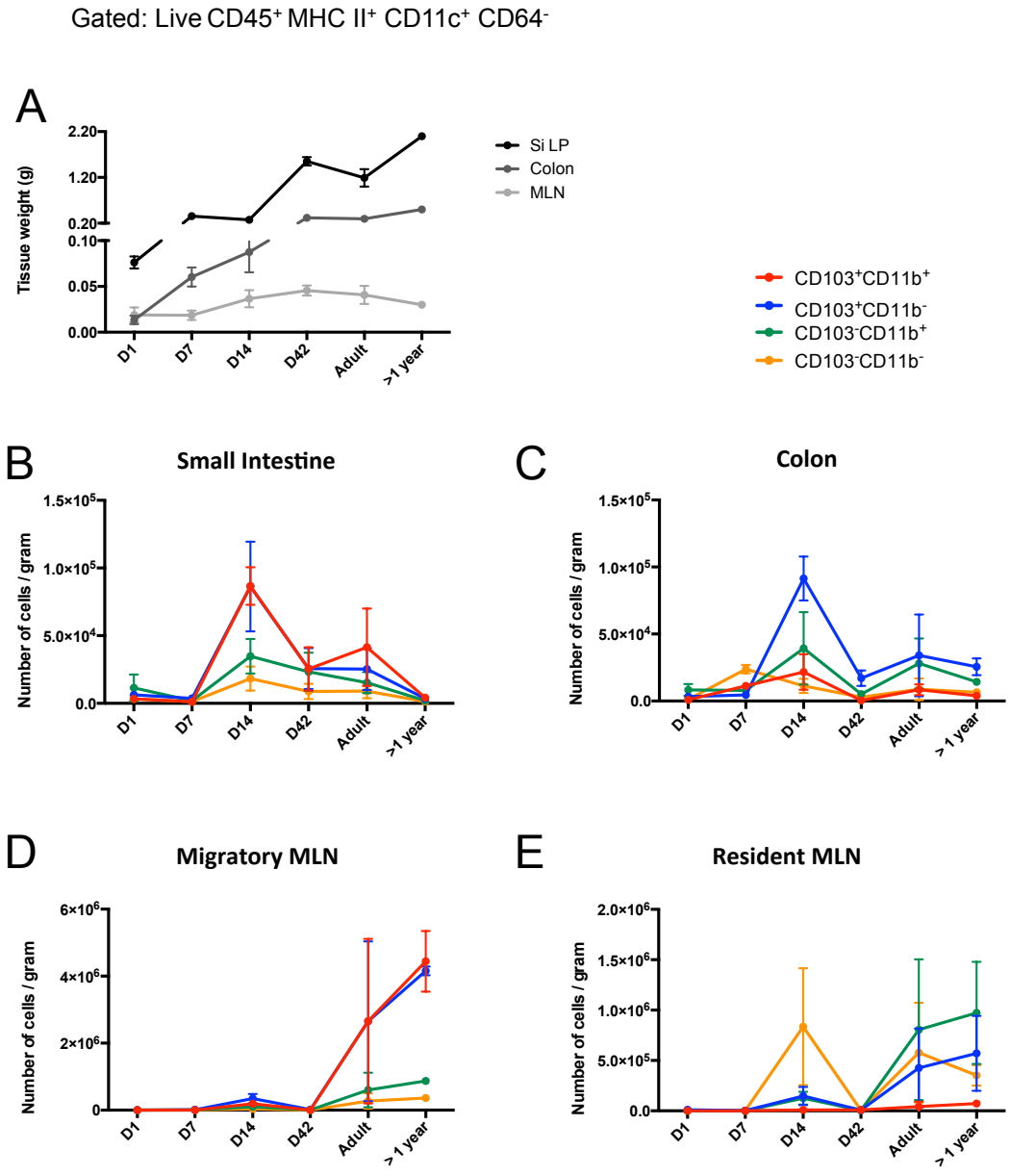

Figure 4.9: Effects of age on the density of intestinal dendritic cell populations
A Weights of SI, colon and MLN from D1 until adulthood. The frequencies of CD103 and CD11b based DC subsets expressed per gram of tissue were then assessed in **B** SI LP, **C** CLP, **D** migratory MLN compartment and **E** resident MLN compartment. The data are pooled from at least five experiments in total with at least n=3 animals per group of mice per time point.

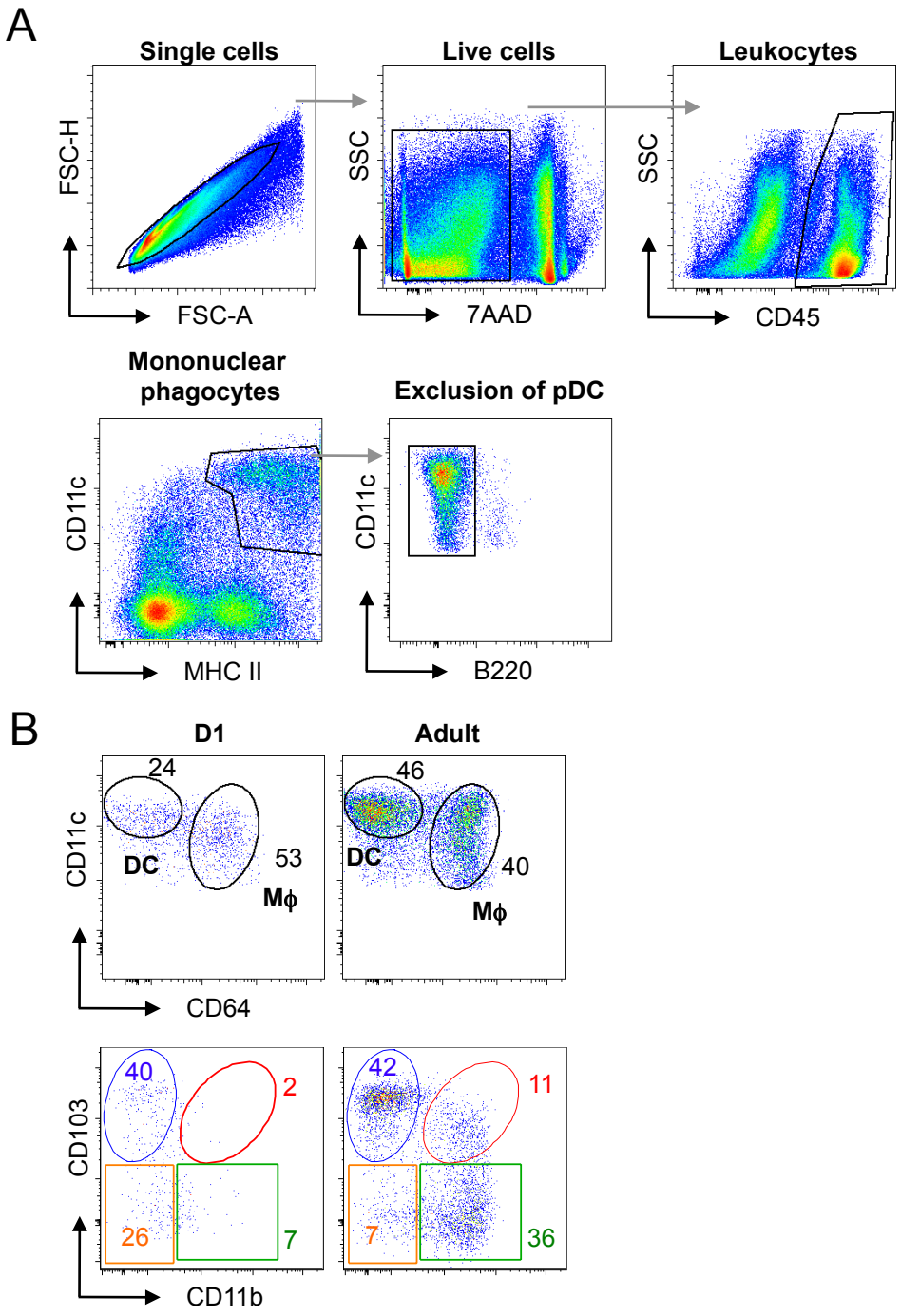

Figure 4.10: Identification of dendritic cells in the lung at different ages

A Lung cells were isolated from D1 WT mice by enzymatic digestion, and after identifying single cells based on FSC-A and FSC-H, mononuclear phagocytes (MP) were identified amongst live 7AAD$^-$ CD45$^+$ leukocytes as MHC II$^+$ CD11c$^+$. **B** After exclusion of B220$^+$ CD11c$^+$ plasmacytoid DC (pDC), conventional DC were identified as CD11c$^+$ CD64$^-$, while Mϕ were CD11c$^+$ CD64$^+$ (top panels). The DC were then subdivided into four populations based on expression of CD103 and CD11b (bottom panels). The graphs show representative data from mice aged E18, D1 after birth, 8-10 week old adults and one-year old aged mice.

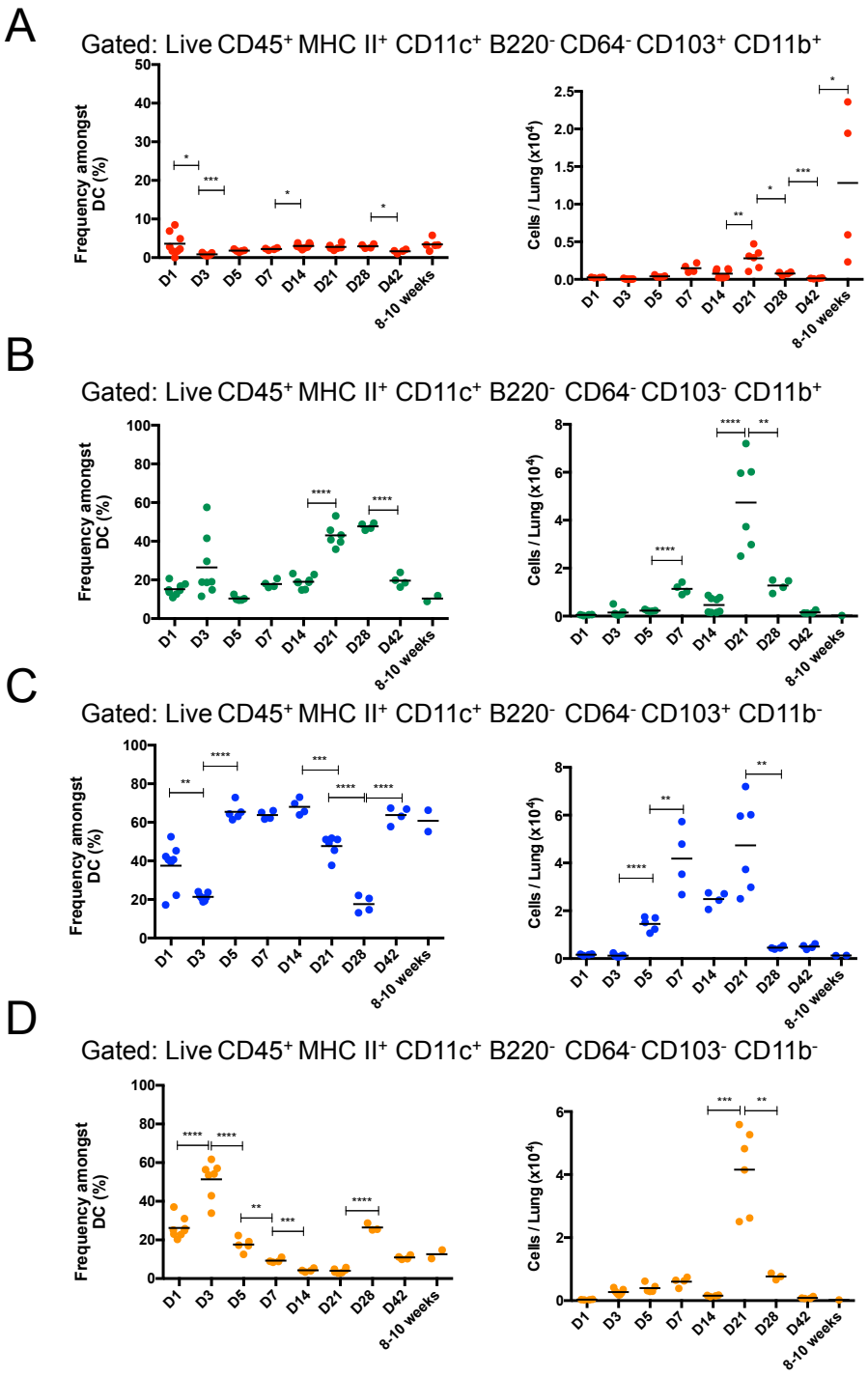

Figure 4.11: Effects of age on dendritic cells in the lung

Lung cells were isolated from WT mice and live MHC II$^+$ CD11c$^+$ B220$^-$ CD64$^-$ leukocytes were analysed for the expression of CD103 and CD11b from D1 to 8-10 week old adults. Frequency (left panels) and absolute numbers (right panels) of **A** CD103$^+$CD11b$^+$ **B** CD103$^-$CD11b$^+$ **C** CD103$^+$CD11b$^-$ and **D** CD103$^-$CD11b$^-$ DC. Each dot represents an individual mouse and the results are derived from at least 10 different litters. *p<0.05, **p<0.01, ***p<0.001, ****p<0.0001 Student's t-test.

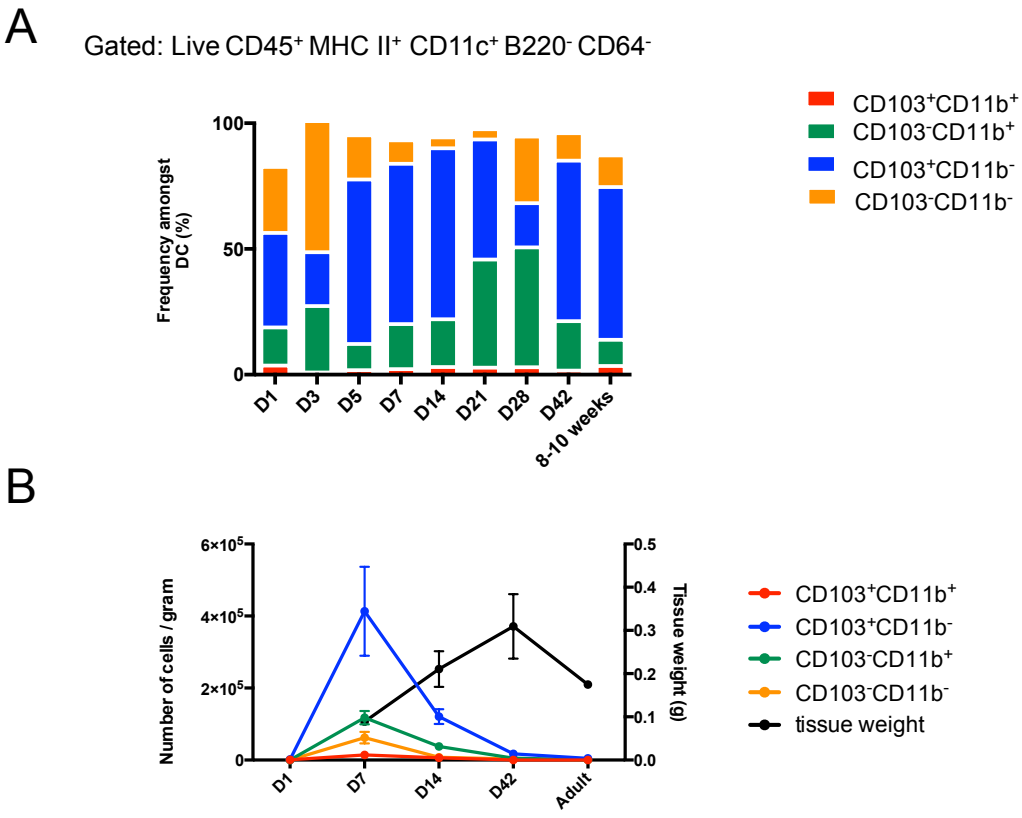

Figure 4.12: Effects of age on composition of lung dendritic cells
A Frequencies of CD103 and CD11b based DC subsets in the lung. **B** Weights of lungs and frequencies of CD103 and CD11b based DC subsets expressed per gram of tissue. The data are pooled from at least ten experiments with at least n=3 animals per group of mice per time point.

Gated: Live CD45$^+$ MHC II$^+$ CD11c$^+$ B220$^-$ CD64$^-$

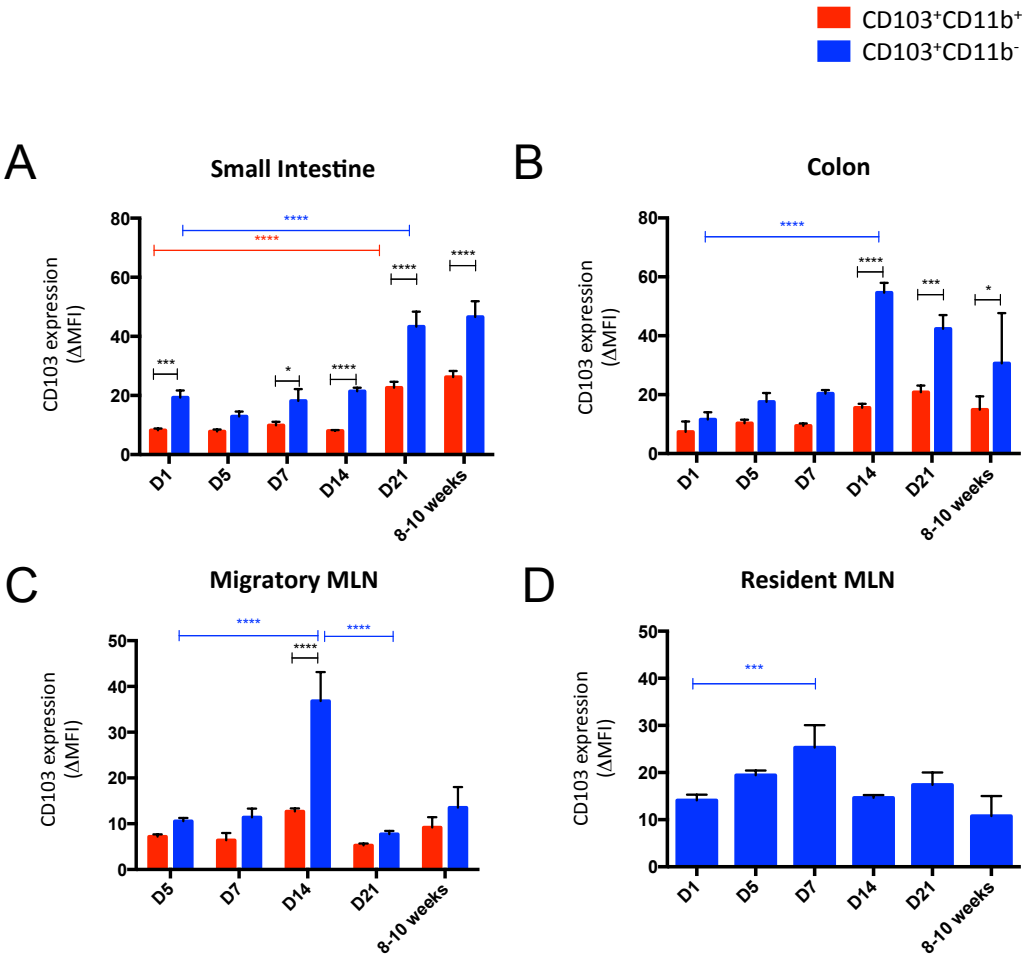

Figure 4.13: Effects of age on CD103 expression by intestinal dendritic cell subsets

Levels of CD103 on CD103$^+$CD11b$^+$ and CD103$^+$CD11b$^-$ DC from **A** SI LP, **B** CLP, **C** migratory MLN compartment and **D** resident MLN compartment. The results shown are the differences in mean fluorescence intensity (ΔMFI) between the CD103$^-$CD11b$^-$ DC and the CD103 expressing DC subset. The data are pooled from at least ten experiments with at least n=3 animals per group of mice per time point. *p<0.05, ***p<0.001, ****p<0.0001, Student's t-test.

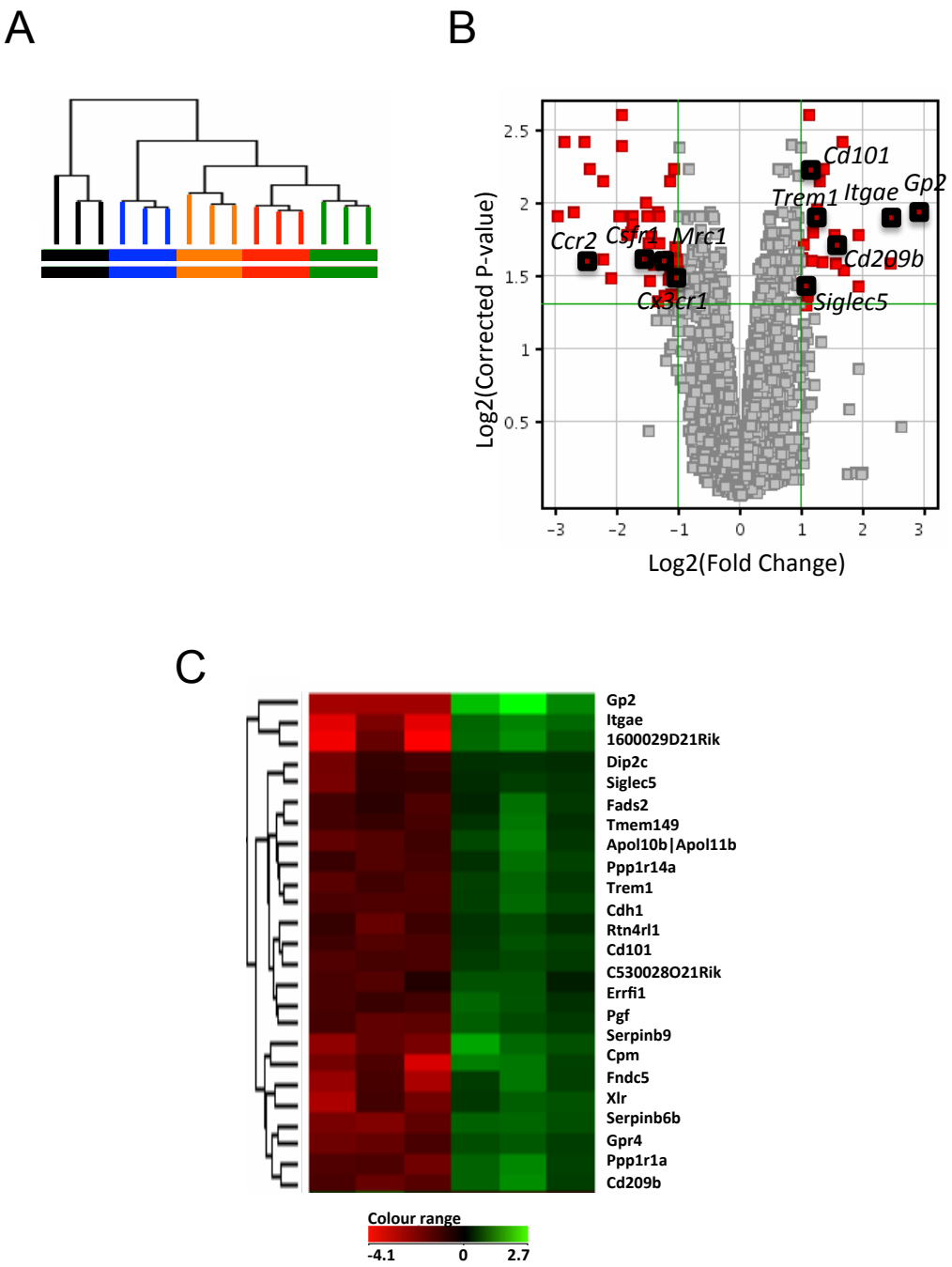

Figure 4.14: Gene expression profiles of mononuclear phagocyte subsets
Expression profiles were established using Mouse GeneChip 1.0 ST arrays (Affymetrix). Array data was analysed using Genespring 13.0 GX software, normalised using RMA16. **A** MP subsets were clustered according to expression levels of all genes/entities ■mϕ, ■CD103^{+}CD11b^{-}, ■CD103^{-}CD11b^{-}, ■CD103^{+}CD11b^{+}, ■CD103^{-}CD11b^{+}. **B** Volcano plot showing expression levels of all entities in CD103^{+}CD11b^{+} compared to CD103^{-}CD11b^{+} DC. Genes satisfying a FC cut off of 2 and a corrected p value cut off of 0.05 shown in red, annotated genes outlined in black. **C** Annotated heatmap displaying the relative signalling intensities of the 25 entities more highly expressed in CD103^{+}CD11b^{+} compared to CD103^{-}CD11b^{+} DC. Data was kindly generated by Charlotte Scott and analysed by Carolyn Thomson, University of Glasgow.

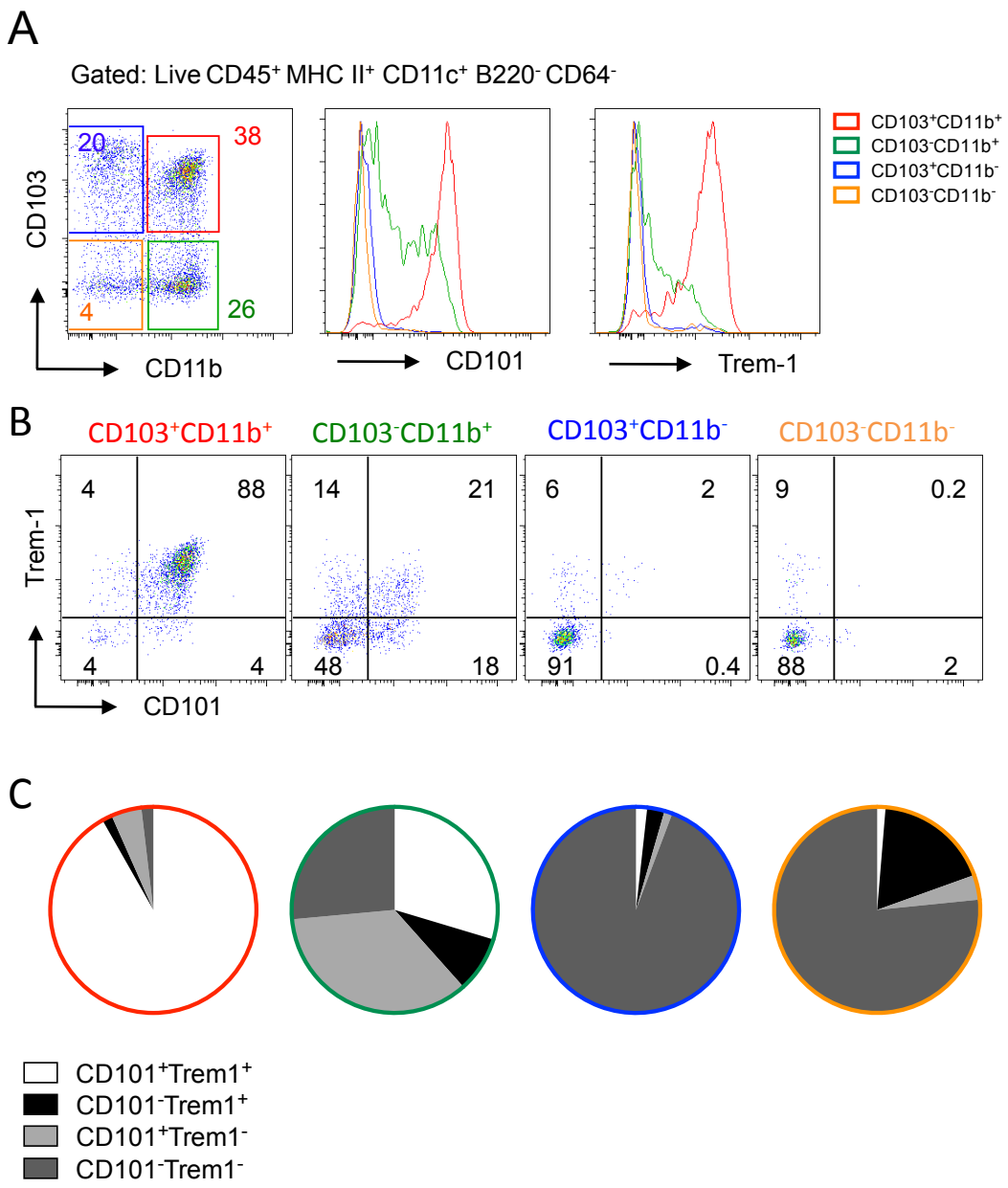

Figure 4.15: Expression of Trem-1 and CD101 by small intestinal dendritic cells

Cells were isolated from the SI LP of adult mice and conventional DC identified as single, live, CD45$^+$ MHC II$^+$ CD11c$^+$ CD64$^-$ B220$^-$ cells. **A** Representative analysis shows the four DC populations based on CD11b and CD103 expression, together with the levels of CD101 and Trem-1 on each of the DC subsets. **B** Co-expression of CD101 and Trem-1 by each subset with gates set based on appropriate isotype controls. **C** Frequencies of each subset expressing CD101 and/ or Trem-1, with the data representing the mean of 4 - 6 mice/group. Results are pooled from two experiments.

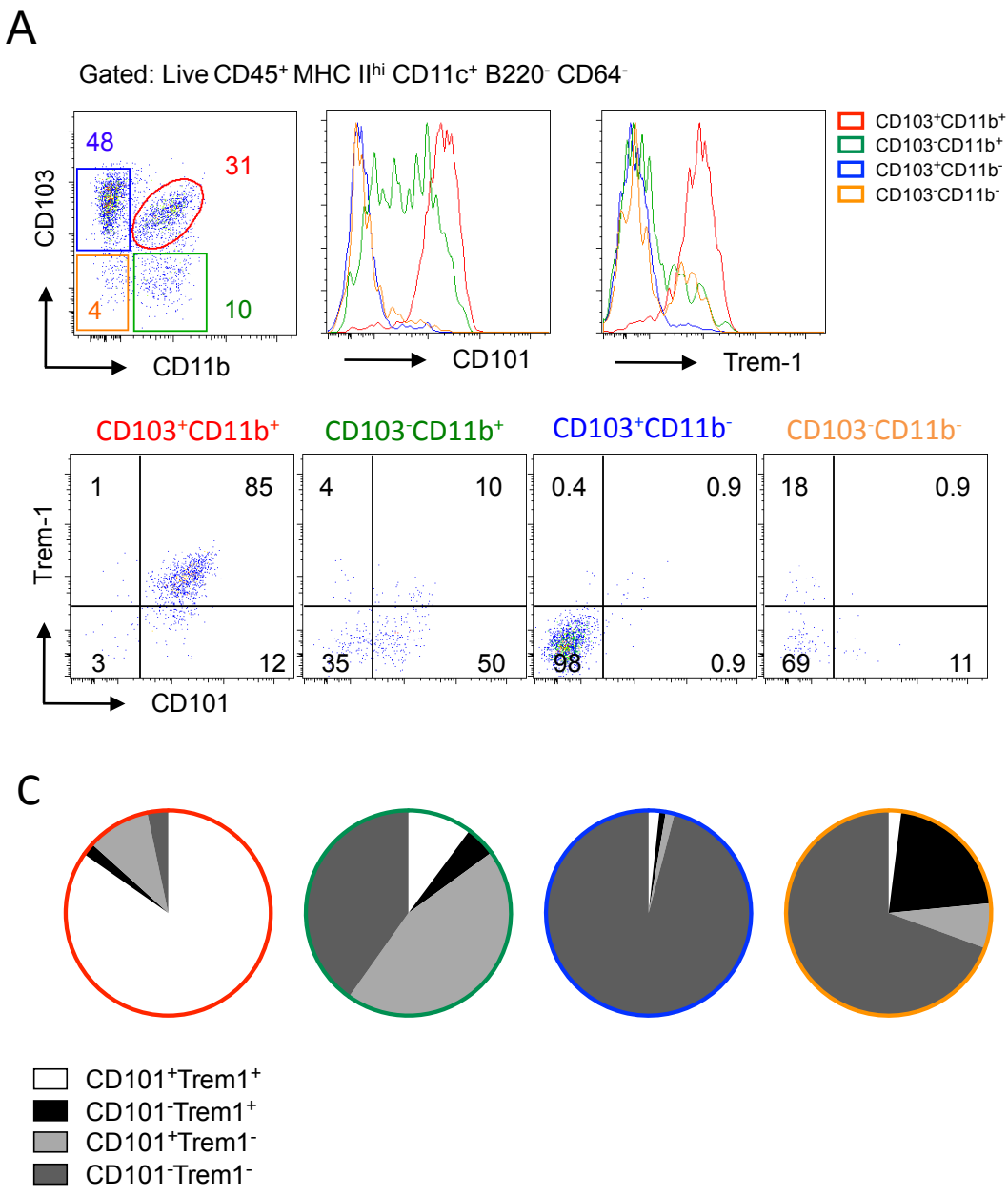

Figure 4.16: Expression of Trem-1 and CD101 by migratory small intestinal MLN dendritic cells

Cells were isolated from the sMLN of adult mice and migratory conventional DC identified as single, live, CD45$^+$ MHC II^{hi} CD11c$^+$ CD64$^-$ B220$^-$ cells. **A** Representative analysis shows the four DC populations based on CD11b and CD103 expression, together with the levels of CD101 and Trem-1 amongst each of the DC subsets. **B** Co-expression of CD101 and Trem-1 by each subset with gates set based on appropriate isotype controls. **C** Frequencies of each subset expressing CD101 and/ or Trem-1, with the data representing the mean of 4 mice/group. Results are from one experiment.

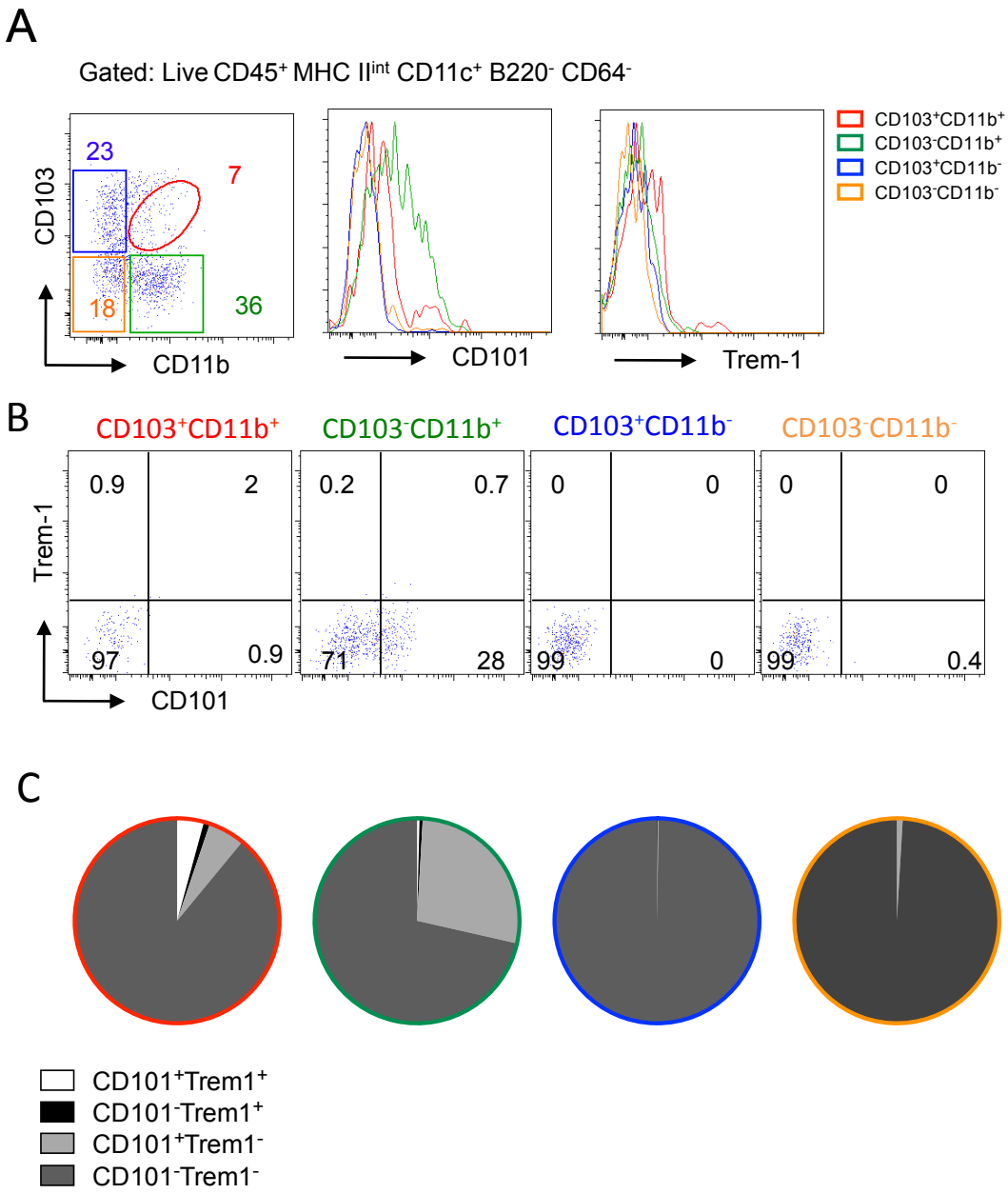

Figure 4.17: Expression of Trem-1 and CD101 by resident small intestinal MLN dendritic cells

Cells were isolated from the sMLN of adult mice and resident conventional DC identified as single, live, CD45$^+$ MHC II^{int} CD11c$^+$ CD64$^-$ B220$^-$ cells. **A** Representative analysis shows the four DC populations based on CD11b and CD103 expression, and the levels of CD101 and Trem-1 amongst each of the DC subsets. **B** Co-expression of CD101 and Trem-1 by each subset with gates set based on isotype controls. **C** Frequencies of each subset expressing CD101 and Trem-1 with the data representing the mean of 4 mice/ group.

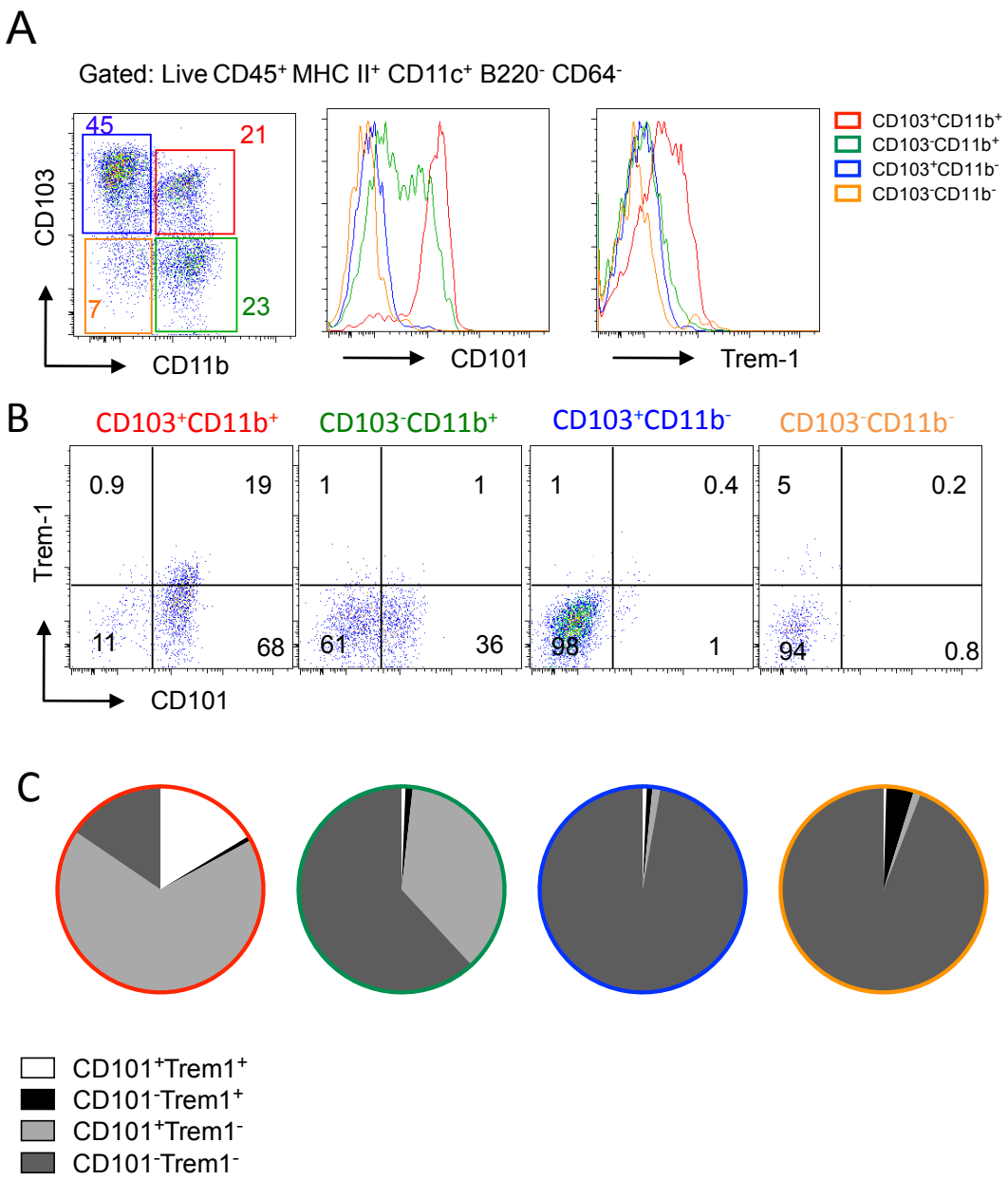

Figure 4.18: Expression of Trem-1 and CD101 by colonic dendritic cells
Cells were isolated from the CLP of adult mice and conventional DC identified as single, live, CD45$^+$ MHC II$^+$ CD11c$^+$ CD64$^-$ B220$^-$ cells. **A** Representative analysis shows the four DC populations based on CD11b and CD103 expression, together with the levels of CD101 and Trem-1 on each of the DC subsets. **B** Co-expression of CD101 and Trem-1 by each subset with gates set based on appropriate isotype controls. **C** Frequencies of each subset expressing CD101 and/ or Trem-1, with the data representing the mean of 4 - 6 mice/group. Results are pooled from two experiments.

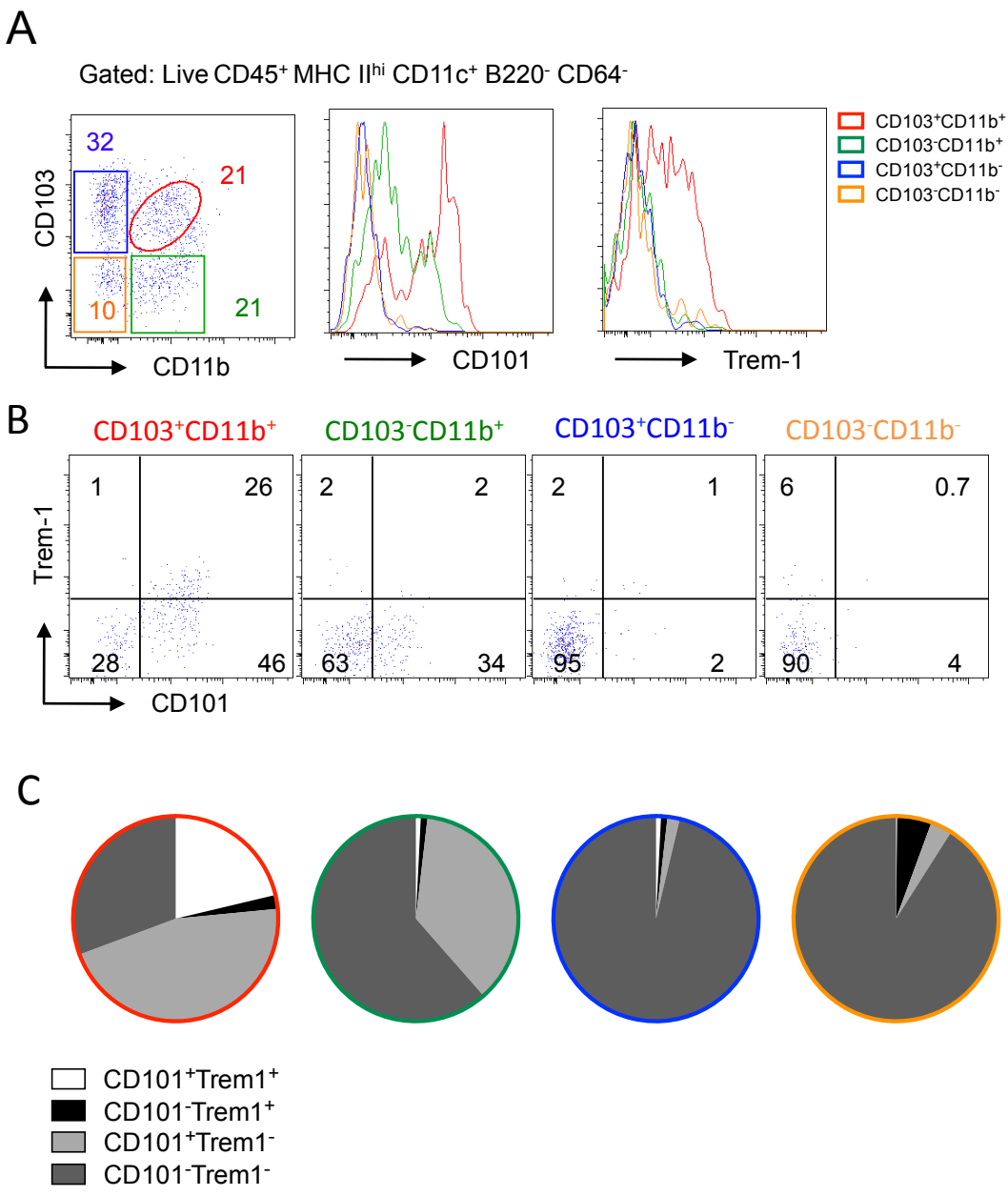

Figure 4.19: Expression of Trem-1 and CD101 by migratory colonic MLN dendritic cells

Cells were isolated from the cMLN of adult mice and migratory DC identified as single, live, CD45$^+$ MHC II^{hi} CD11c$^+$ CD64$^-$ B220$^-$ cells. **A** Representative analysis shows the four DC populations based on CD11b and CD103 expression, together with the levels of CD101 and Trem-1 on each of the DC subsets. **B** Co-expression of CD101 and Trem-1 by each subset with gates set based on appropriate isotype controls. **C** Frequencies of each subset expressing CD101 and/ or Trem-1, with the data representing the mean of 4 - 6 mice/group. Results are pooled from two experiments.

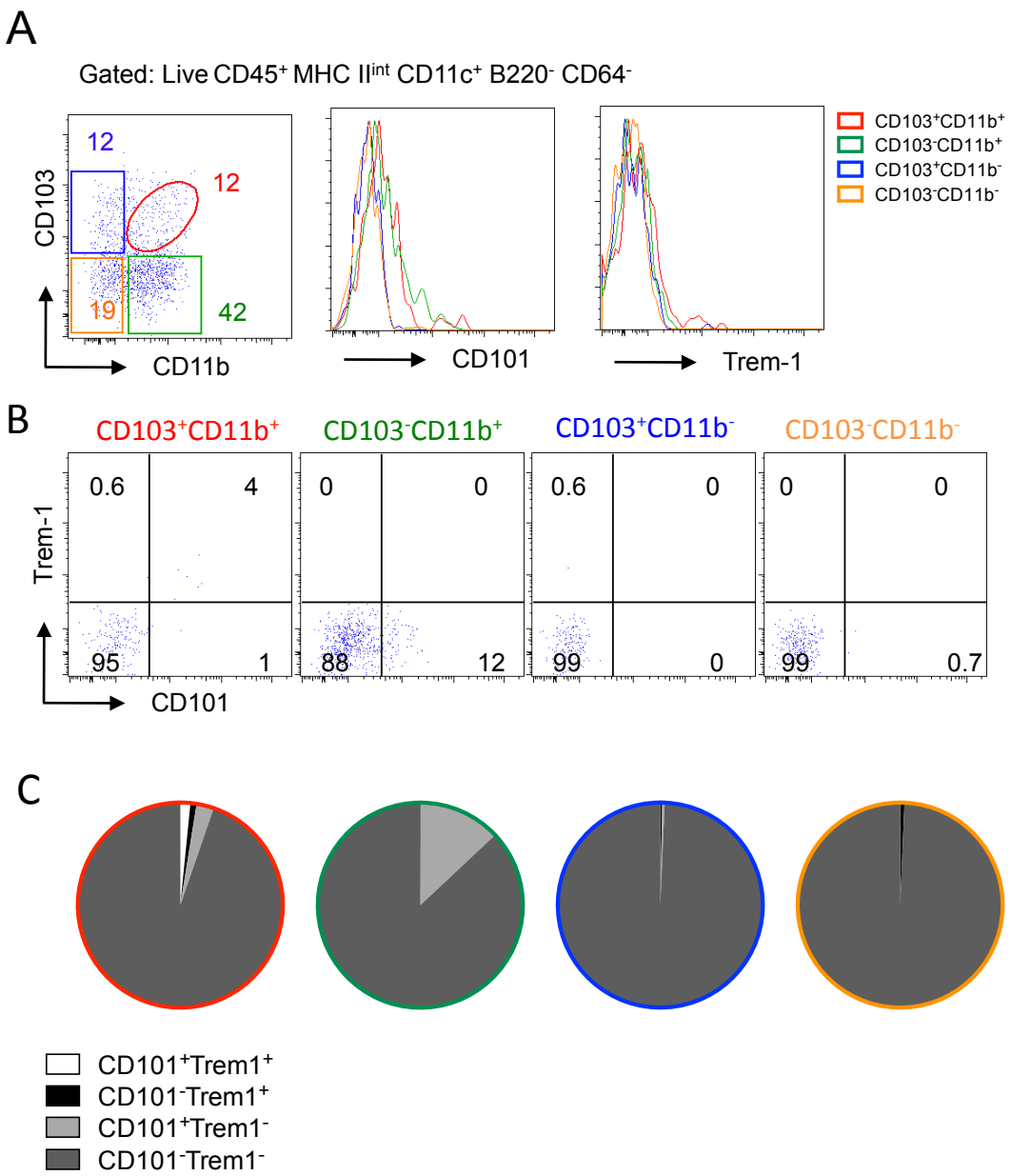

Figure 4.20: Expression of Trem-1 and CD101 by resident colonic MLN dendritic cells

Cells were isolated from the cMLN of adult mice and resident DC identified as single, live, CD45$^+$ MHC II^{int} CD11c$^+$ CD64$^-$ B220$^-$ cells. **A** Representative analysis shows the four DC populations based on CD11b and CD103 expression, together with the levels of CD101 and Trem-1 on each of the DC subsets. **B** Co-expression of CD101 and Trem-1 by each subset with gates set based on appropriate isotype controls. **C** Frequencies of each subset expressing CD101 and/ or Trem-1, with the data representing the mean of 4 - 6 mice/group. Results are pooled from two experiments.

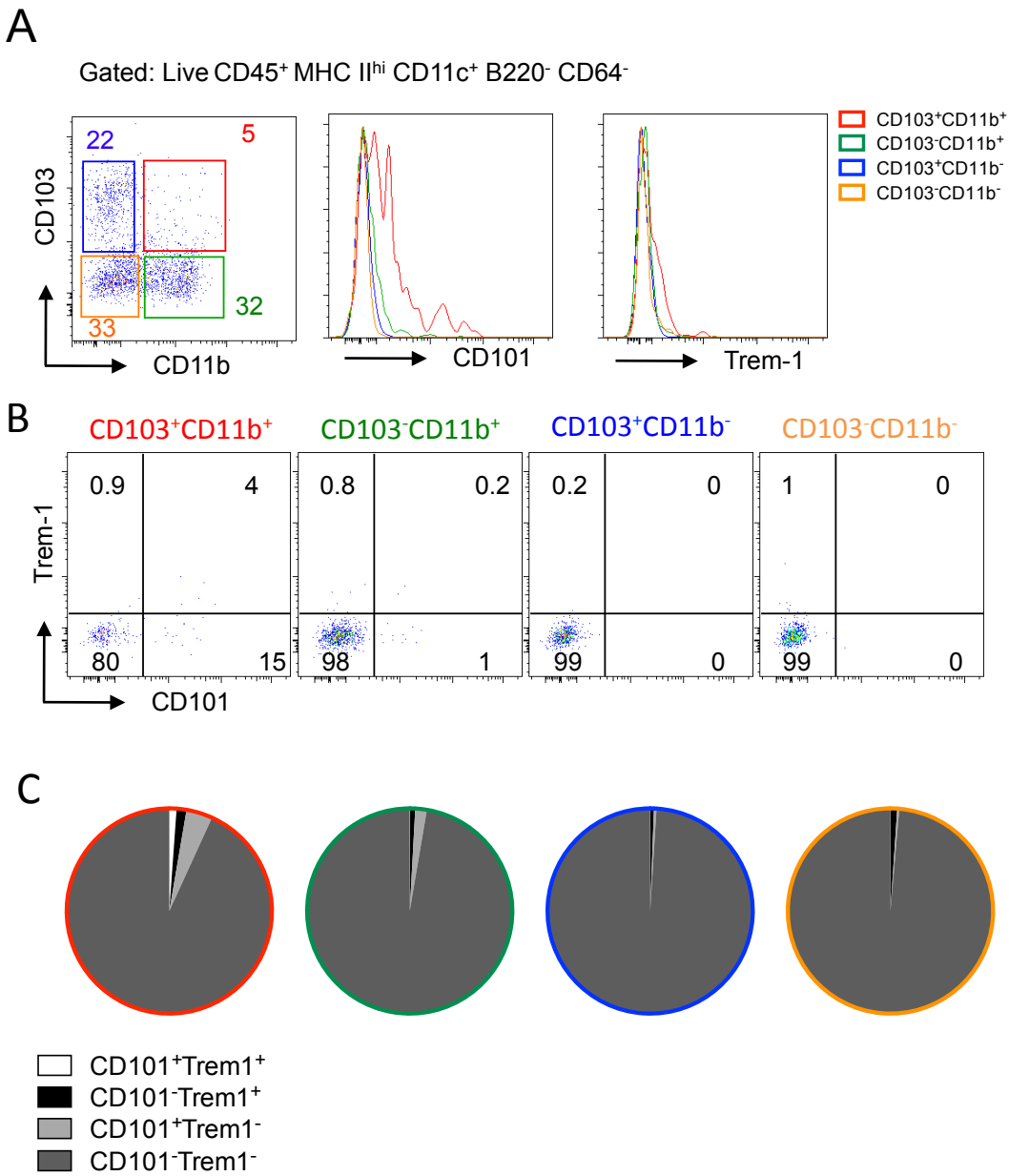

Figure 4.21: Expression of Trem-1 and CD101 by migratory peripheral LN dendritic cells

Cells were isolated from the PLN of adult mice and migratory DC identified as single, live, CD45$^+$ MHC II^{hi} CD11c$^+$ CD64$^-$ B220$^-$ cells. **A** Representative analysis shows the four DC populations based on CD11b and CD103 expression, together with the levels of CD101 and Trem-1 on each of the DC subsets. **B** Co-expression of CD101 and Trem-1 by each subset with gates set based on appropriate isotype controls. **C** Frequencies of each subset expressing CD101 and/ or Trem-1, with the data representing the mean of 4 - 6 mice/group. Results are pooled from two experiments.

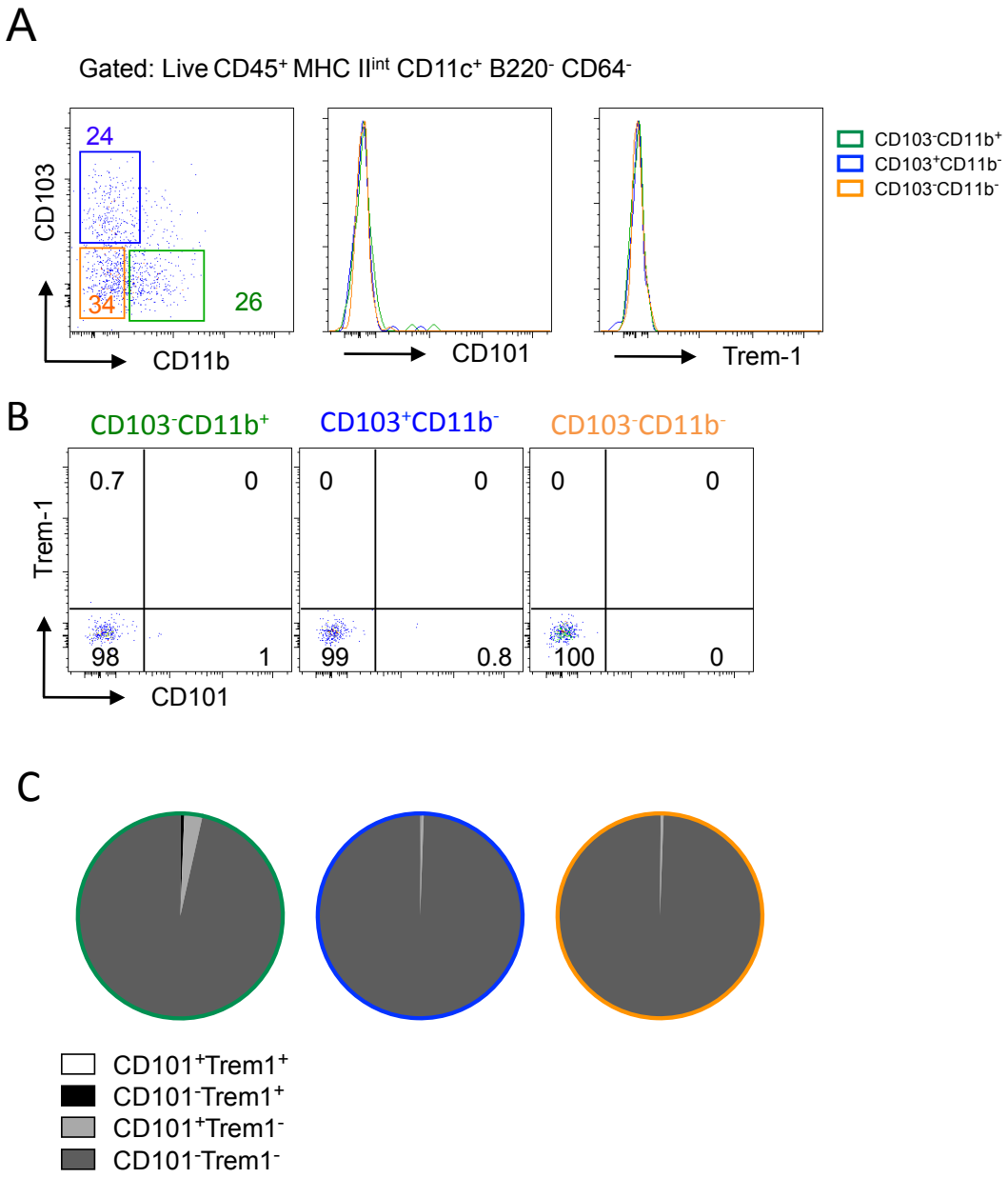

Figure 4.22: Expression of Trem-1 and CD101 by resident peripheral LN dendritic cells

Cells were isolated from the PLN of adult mice and resident DC identified as single, live, $CD45^+$ MHC II^{int} $CD11c^+$ $CD64^-$ $B220^-$ cells. **A** Representative analysis shows the DC populations based on CD11b and CD103 expression, together with the levels of CD101 and Trem-1 on each of the DC subsets. **B** Co-expression of CD101 and Trem-1 by each subset with gates set based on appropriate isotype controls. **C** Frequencies of each subset expressing CD101 and/ or Trem-1, with the data representing the mean of 4 - 6 mice/group. Results are pooled from two experiments.

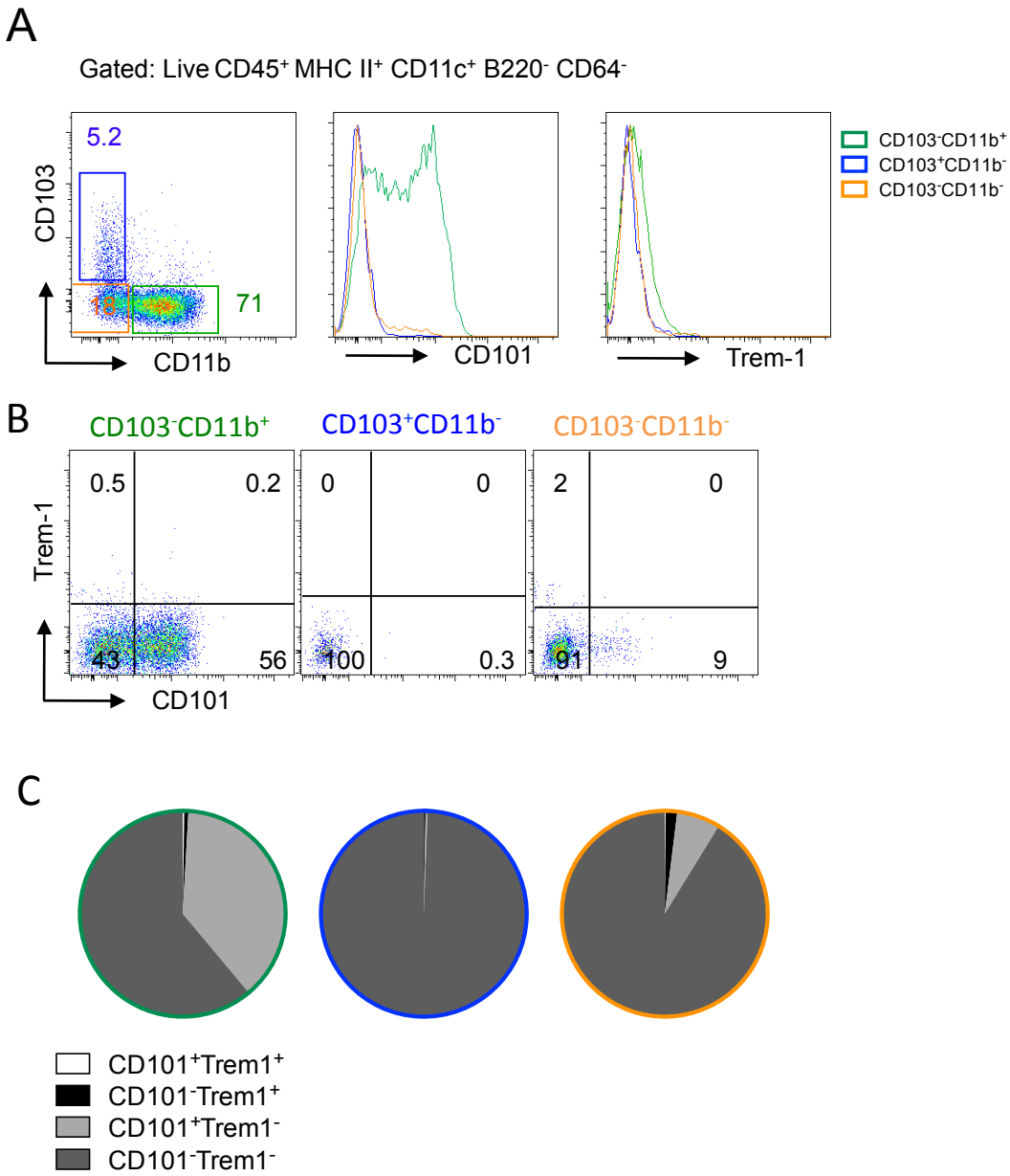

Figure 4.23: Expression of Trem-1 and CD101 by spleen dendritic cells
Cells were isolated from the spleen of adult mice and DC identified as single, live, $CD45^+$ $MHC\ II^+$ $CD11c^+$ $CD64^-$ $B220^-$ cells. **A** Representative analysis shows the DC populations based on CD11b and CD103 expression, together with the levels of CD101 and Trem-1 on each of the DC subsets. **B** Co-expression of CD101 and Trem-1 by each subset with gates set based on appropriate isotype controls. **C** Frequencies of each subset expressing CD101 and/ or Trem-1, with the data representing the mean of 4 - 6 mice/ group. Results are pooled from two experiments.

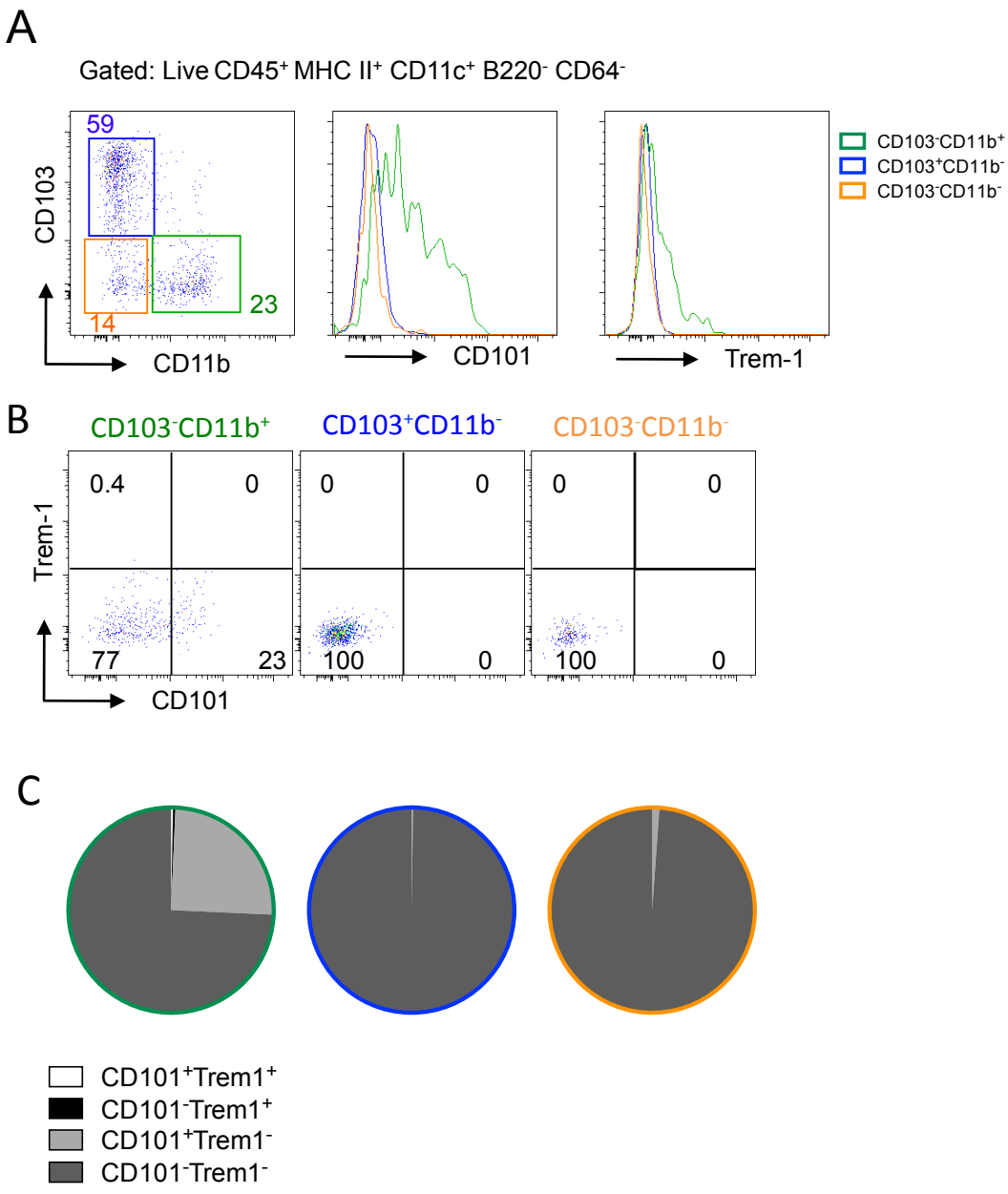

Figure 4.24: Expression of Trem-1 and CD101 by liver dendritic cells
Cells were isolated from the liver of adult mice and DC identified as single, live, $CD45^+$ $MHC\ II^+$ $CD11c^+$ $CD64^-$ $B220^-$ cells. **A** Representative analysis shows the DC populations based on CD11b and CD103 expression, together with the levels of CD101 and Trem-1 on each of the DC subsets. **B** Co-expression of CD101 and Trem-1 by each subset with gates set based on appropriate isotype controls. **C** Frequencies of each subset expressing CD101 and/ or Trem-1, with the data representing the mean of 4 - 6 mice/ group. Results are pooled from two experiments.

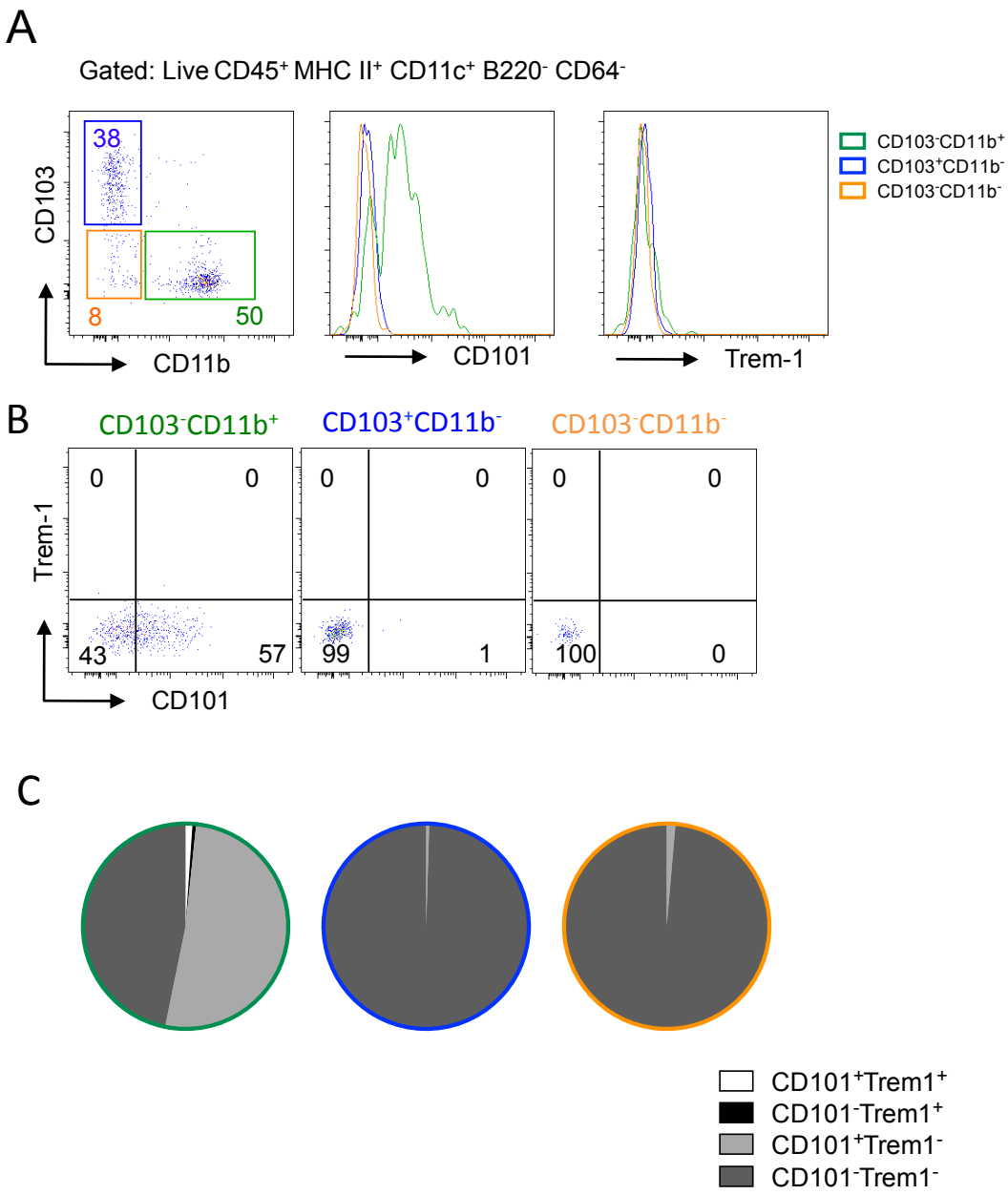

Figure 4.25: Expression of Trem-1 and CD101 by kidney dendritic cells
Cells were isolated from the kidney of adult mice and DC identified as single, live, $CD45^+$ $MHC\ II^+$ $CD11c^+$ $CD64^-$ $B220^-$ cells. **A** Representative analysis shows the DC populations based on CD11b and CD103 expression, together with the levels of CD101 and Trem-1 on each of the DC subsets. **B** Co-expression of CD101 and Trem-1 by each subset with gates set based on appropriate isotype controls. **C** Frequencies of each subset expressing CD101 and/ or Trem-1, with the data representing the mean of 4 - 6 mice/ group. Results are pooled from two experiments.

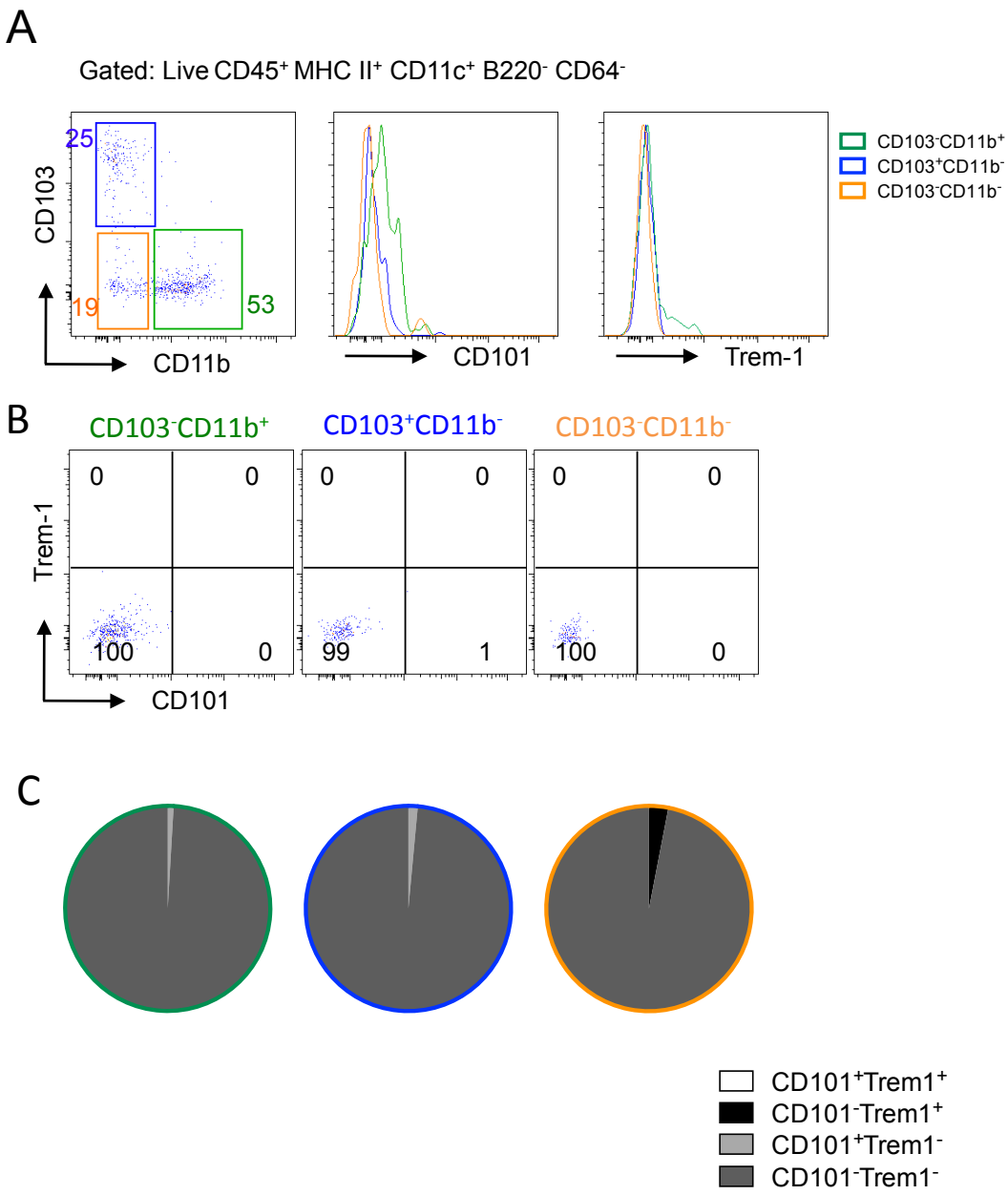

Figure 4.26: Expression of Trem-1 and CD101 by heart dendritic cells
Cells were isolated from the heart of adult mice and DC identified as single, live, $CD45^+$ $MHC\ II^+$ $CD11c^+$ $CD64^-$ $B220^-$ cells. **A** Representative analysis shows the DC populations based on CD11b and CD103 expression, together with the levels of CD101 and Trem-1 on each of the DC subsets. **B** Co-expression of CD101 and Trem-1 by each subset with gates set based on appropriate isotype controls. **C** Frequencies of each subset expressing CD101 and/ or Trem-1, with the data representing the mean of 4 - 6 mice/ group. Results are pooled from two experiments.

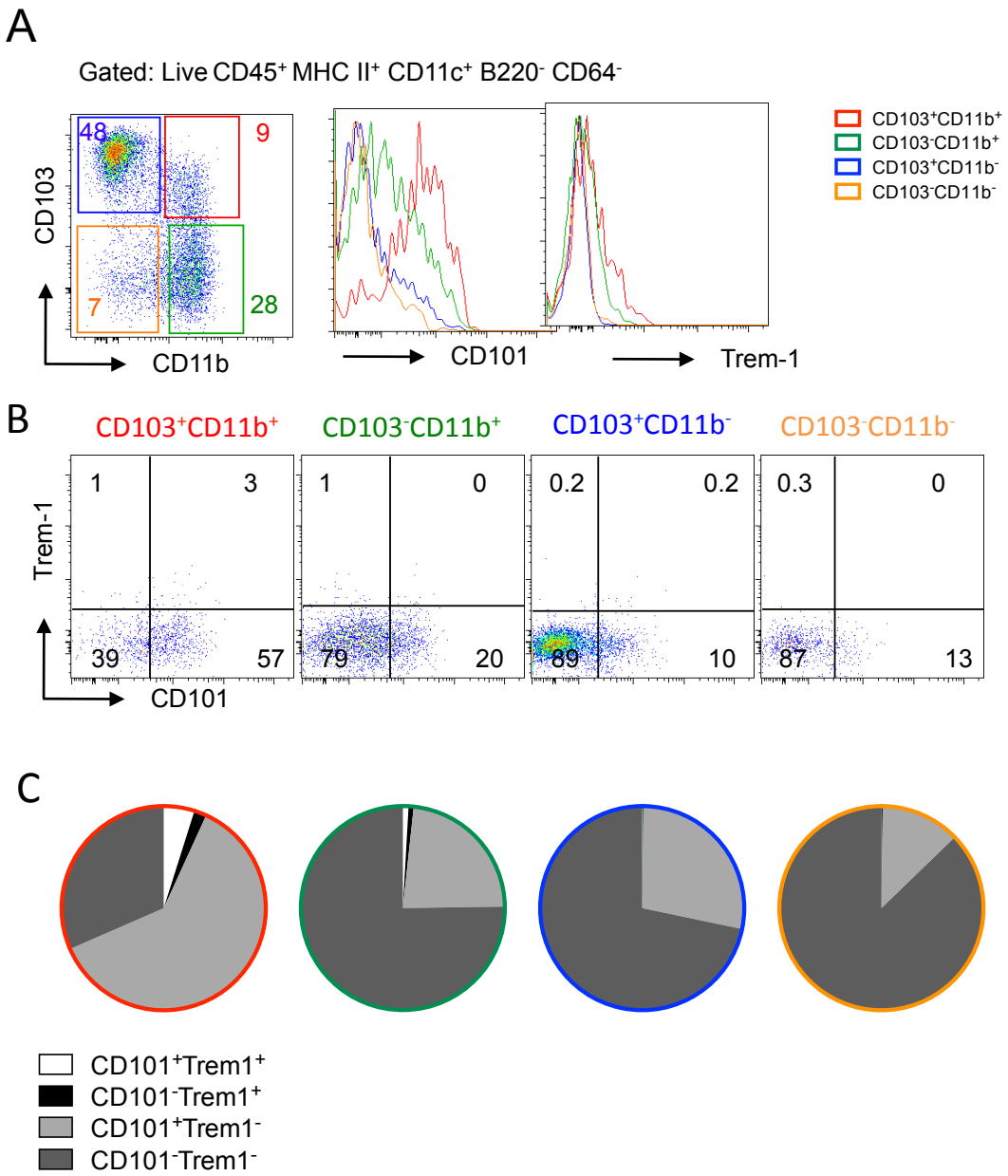

Figure 4.27: Expression of Trem-1 and CD101 by lung dendritic cells
Cells were isolated from the lung of adult mice and DC identified as single, live, $CD45^+$ MHC II^+ $CD11c^+$ $CD64^-$ $B220^-$ cells. **A** Representative analysis shows the four DC populations based on CD11b and CD103 expression, together with the levels of CD101 and Trem-1 on each of the DC subsets. **B** Co-expression of CD101 and Trem-1 by each subset with gates set based on appropriate isotype controls. **C** Frequencies of each subset expressing CD101 and/ or Trem-1, with the data representing the mean of 4 - 6 mice/group. Results are pooled from two experiments.

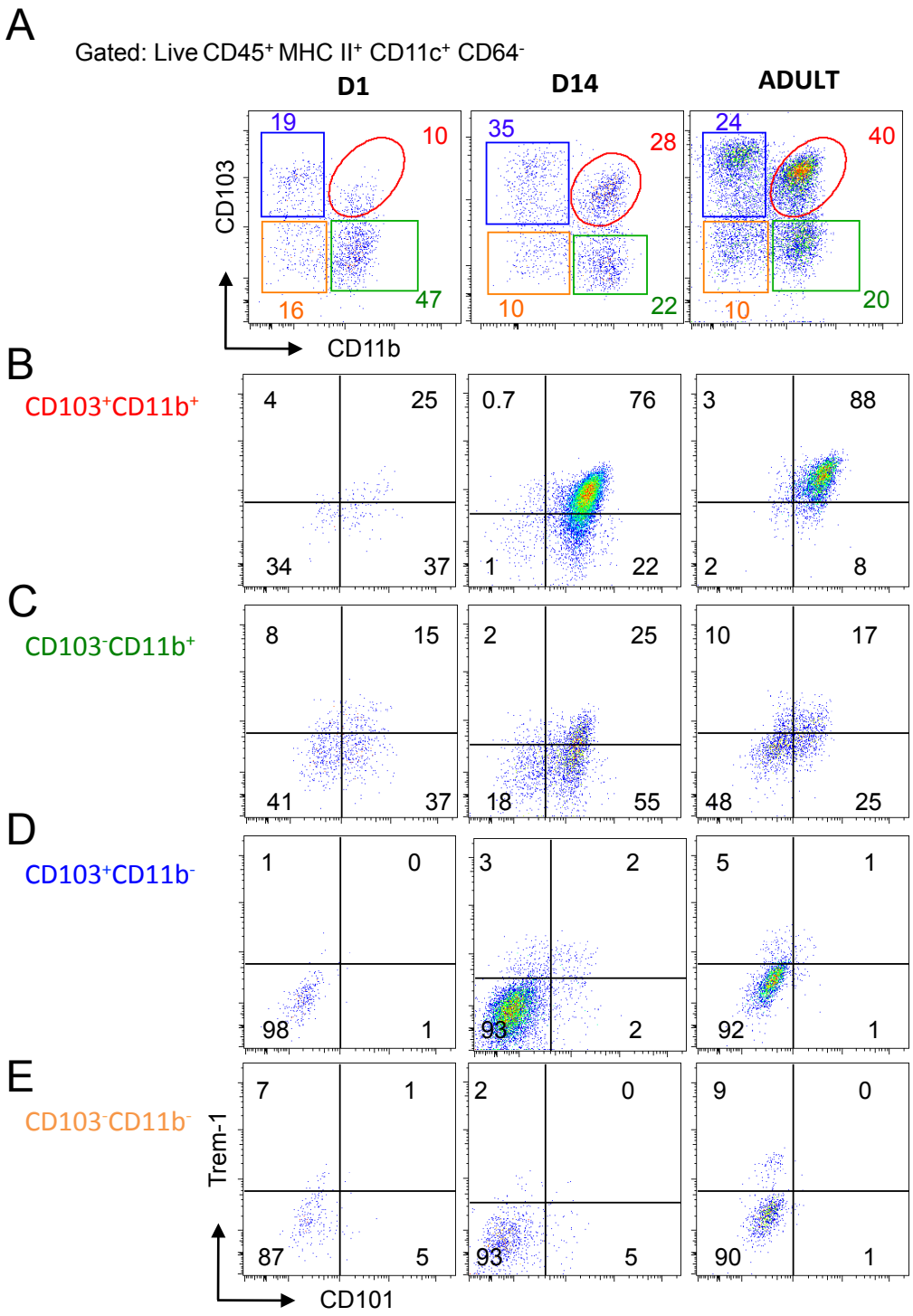

Figure 4.28: CD101 and Trem-1 expression by small intestinal dendritic cells during development

Cells were isolated from SI LP. Live CD11c$^+$ MHC II$^+$ CD64$^-$ leukocytes were analysed for the expression of CD103 and CD11b from D1 to adulthood (8-10 weeks). **A** Representative analysis shows the four DC populations based on CD11b and CD103 expression at D1, D14 and on adults. Co-expression of CD101 and Trem-1 at each time point, with gates set based on isotype controls by **B** CD103$^+$CD11b$^+$, **C** CD103$^-$CD11b$^+$, **D** CD103$^+$CD11b$^-$ and **E** CD103$^-$CD11b$^-$. Data are representative of one experiment at each time point with n=4-8 mice/group.

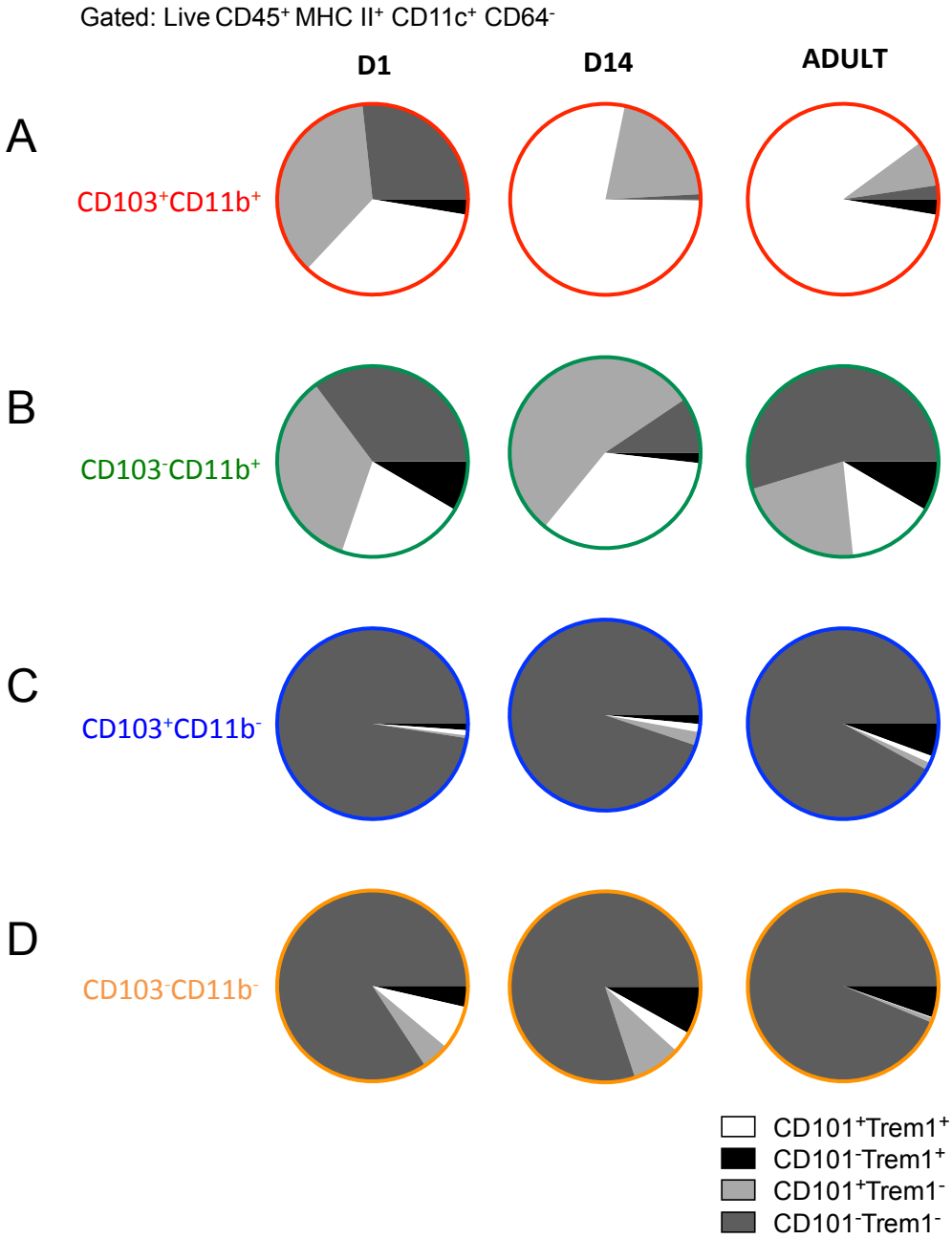

Figure 4.29: Expression of Trem-1 and CD101 by small intestinal dendritic cells during development

Schematic depiction of the distribution of CD101$^+$Trem-1$^+$ (white), CD101$^-$Trem-1$^+$ (black), CD101$^+$Trem-1$^-$ (light grey) and CD101$^-$Trem-1$^-$ (dark grey) cells amongst each DC subset in the SI LP from mice at D1, D14 and in adults. **A** CD103$^+$CD11b$^+$, **B** CD103$^-$CD11b$^+$, **C** CD103$^+$CD11b$^-$ and **D** CD103$^-$CD11b$^-$ DC. Data are means of one experiment at each time point with n=4-8 mice/group.

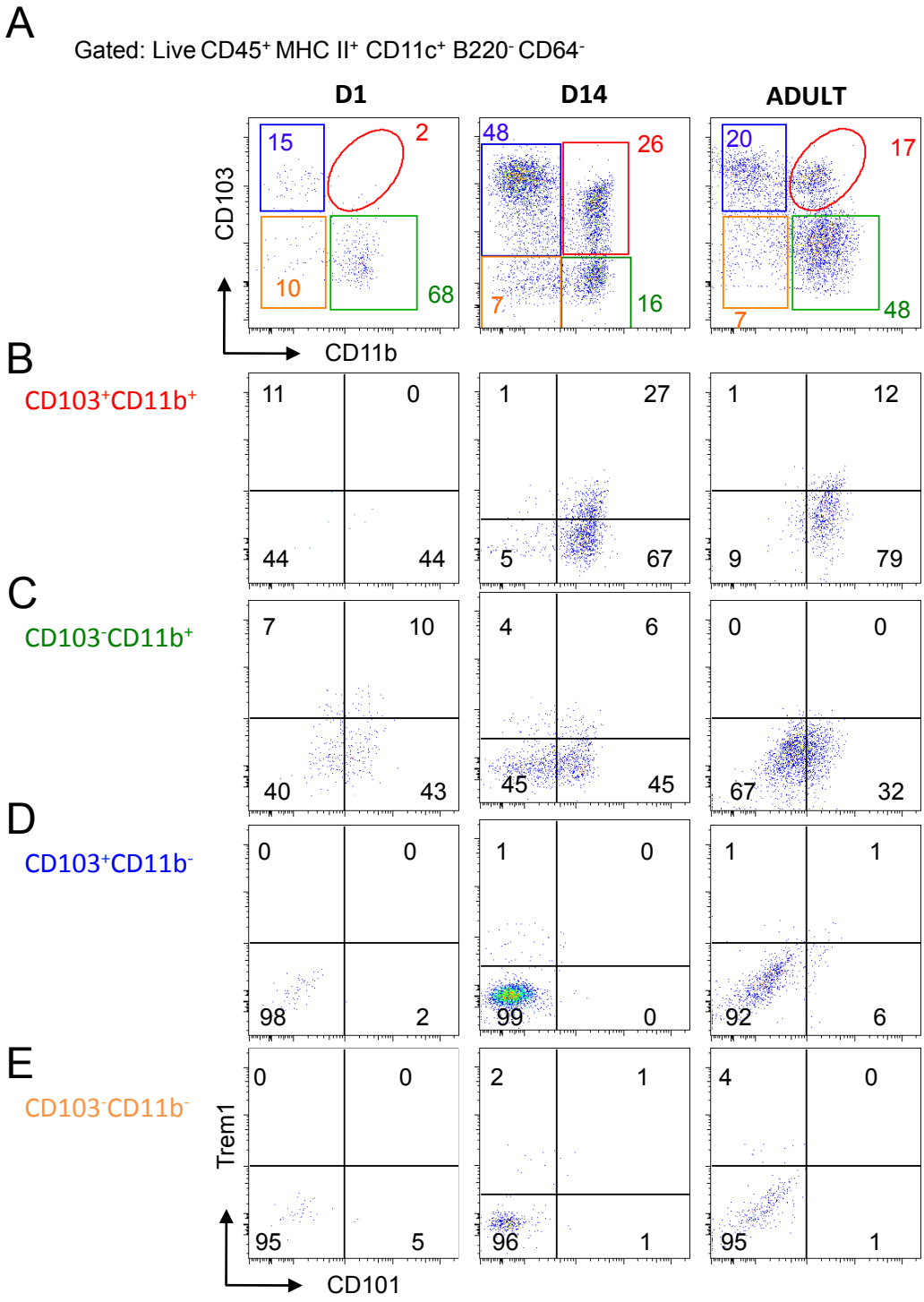

Figure 4.30: Expression of Trem-1 and CD101 by colonic dendritic cells during development

Cells were isolated from CLP. Live CD11c+ MHC II+ CD64- leukocytes were analysed for the expression of CD103 and CD11b from D1 to adulthood (8-10 weeks). **A** Representative analysis shows the four DC populations based on CD11b and CD103 expression at D1, D14 and on adults. Co-expression of CD101 and Trem-1 at each time point, with gates set based on isotype controls by **B** CD103+CD11b+, **C** CD103-CD11b+, **D** CD103+CD11b- and **E** CD103-CD11b-. Data are representative of one experiment at each time point with n=4-8 mice/group.

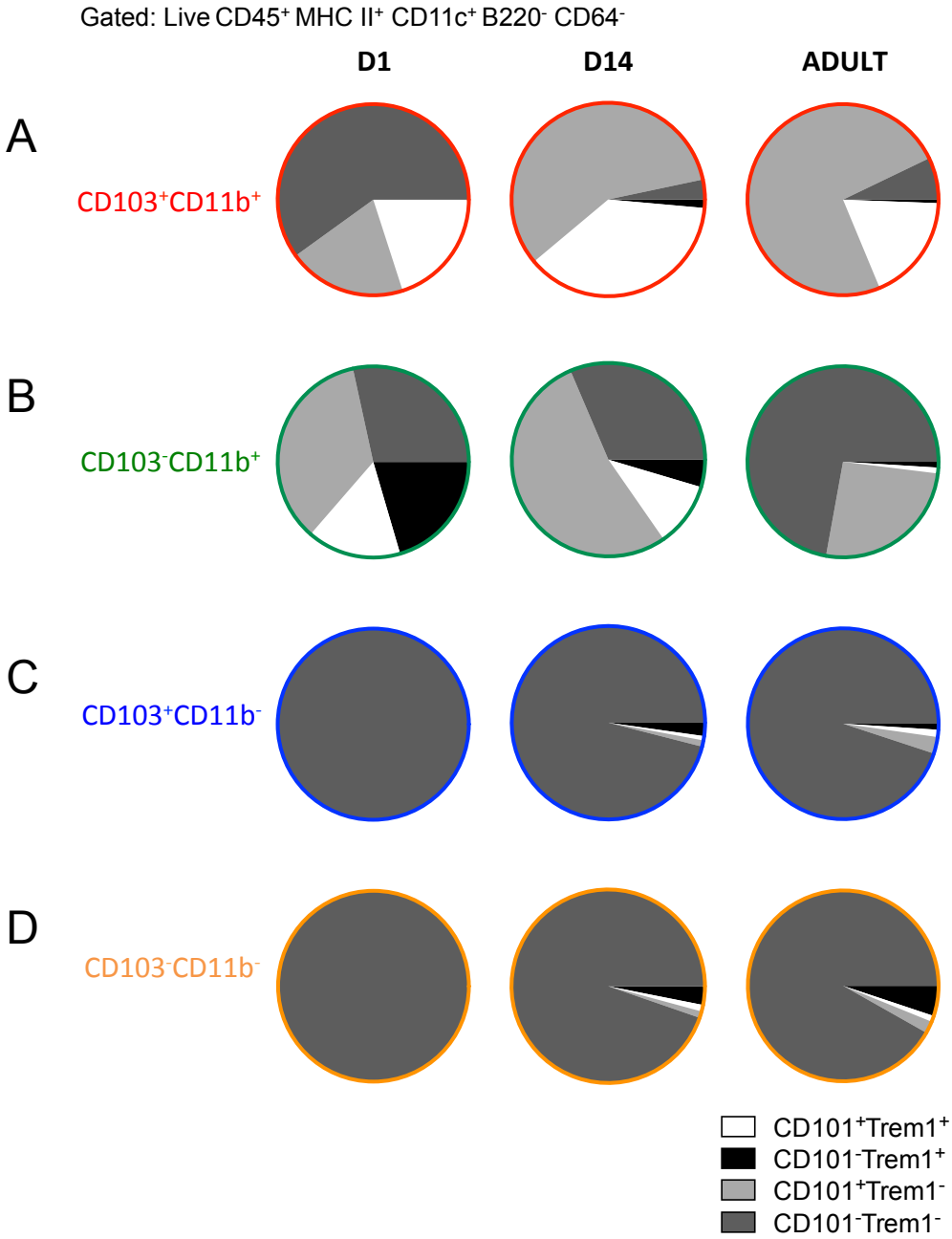

Figure 4.31: Expression of Trem-1 and CD101 by colonic dendritic cells during development

Schematic depiction of the distribution of CD101$^+$Trem-1$^+$ (white), CD101$^-$Trem-1$^+$ (black), CD101$^+$Trem-1$^-$ (light grey) and CD101$^-$Trem-1$^-$ (dark grey) cells amongst each DC subset in the CLP from mice at D1, D14 and in adults. **A** CD103$^+$CD11b$^+$, **B** CD103$^-$CD11b$^+$, **C** CD103$^+$CD11b$^-$ and **D** CD103$^-$CD11b$^-$ DC. Data are means of one experiment at each time point with n=4-8 mice/group.

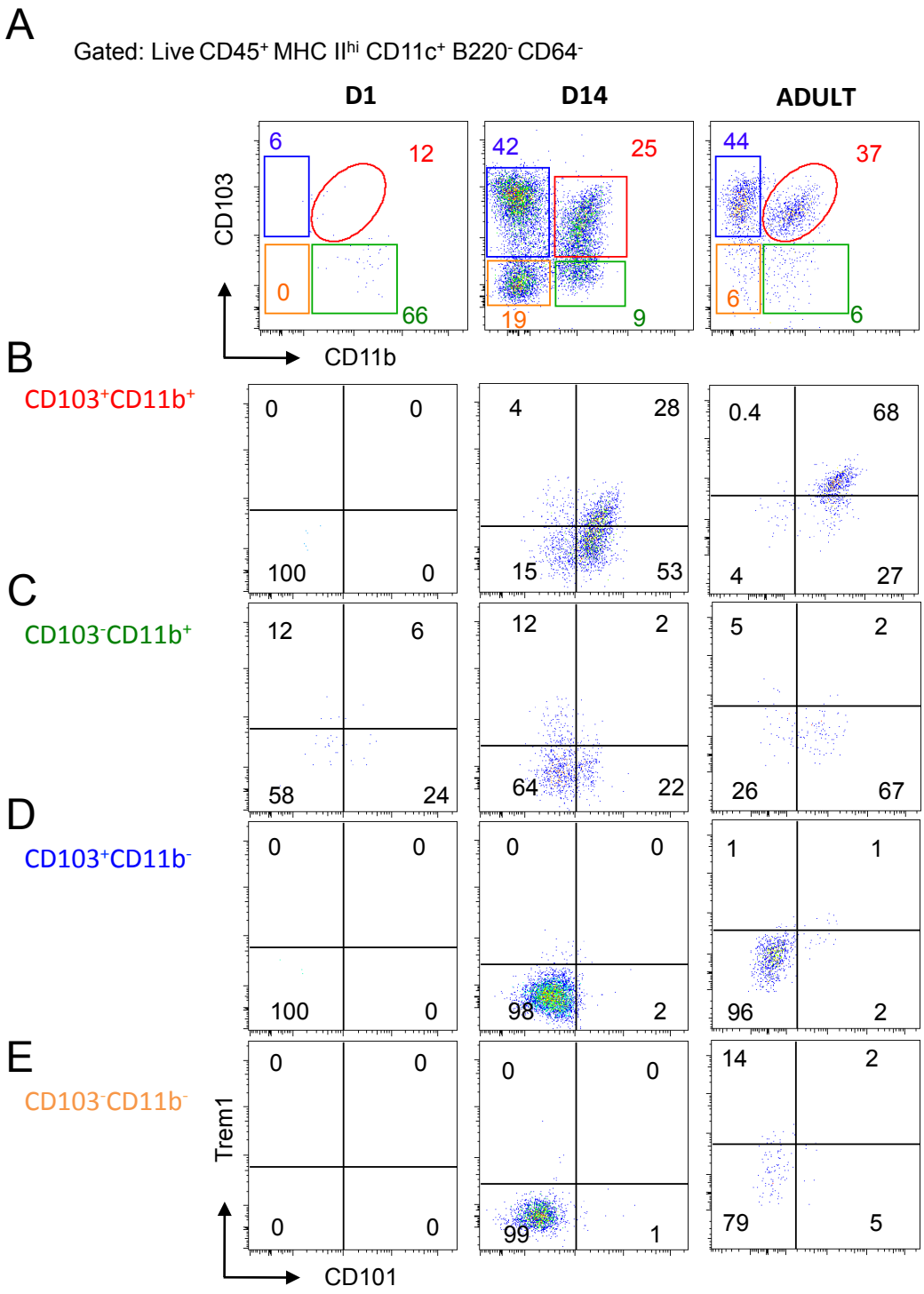

Figure 4.32: Expression of Trem-1 and CD101 by migratory MLN dendritic cells during development

Cells were isolated from MLN and live CD11c$^+$ MHC Ii^{hi} B220$^-$ CD64$^-$ migratory DC were were analysed for the expression of CD103 and CD11b from D1 to adulthood (8-10 weeks). **A** Representative analysis shows the four DC populations based on CD11b and CD103 expression at D1, D14 and on adults. Co-expression of CD101 and Trem-1 at each time point, with gates set based on isotype controls by **B** CD103$^+$CD11b$^+$, **C** CD103$^-$CD11b$^+$, **D** CD103$^+$CD11b$^-$ and **E** CD103$^-$CD11b$^-$. Data are representative of one experiment at each time point with n=4-8 mice/group.

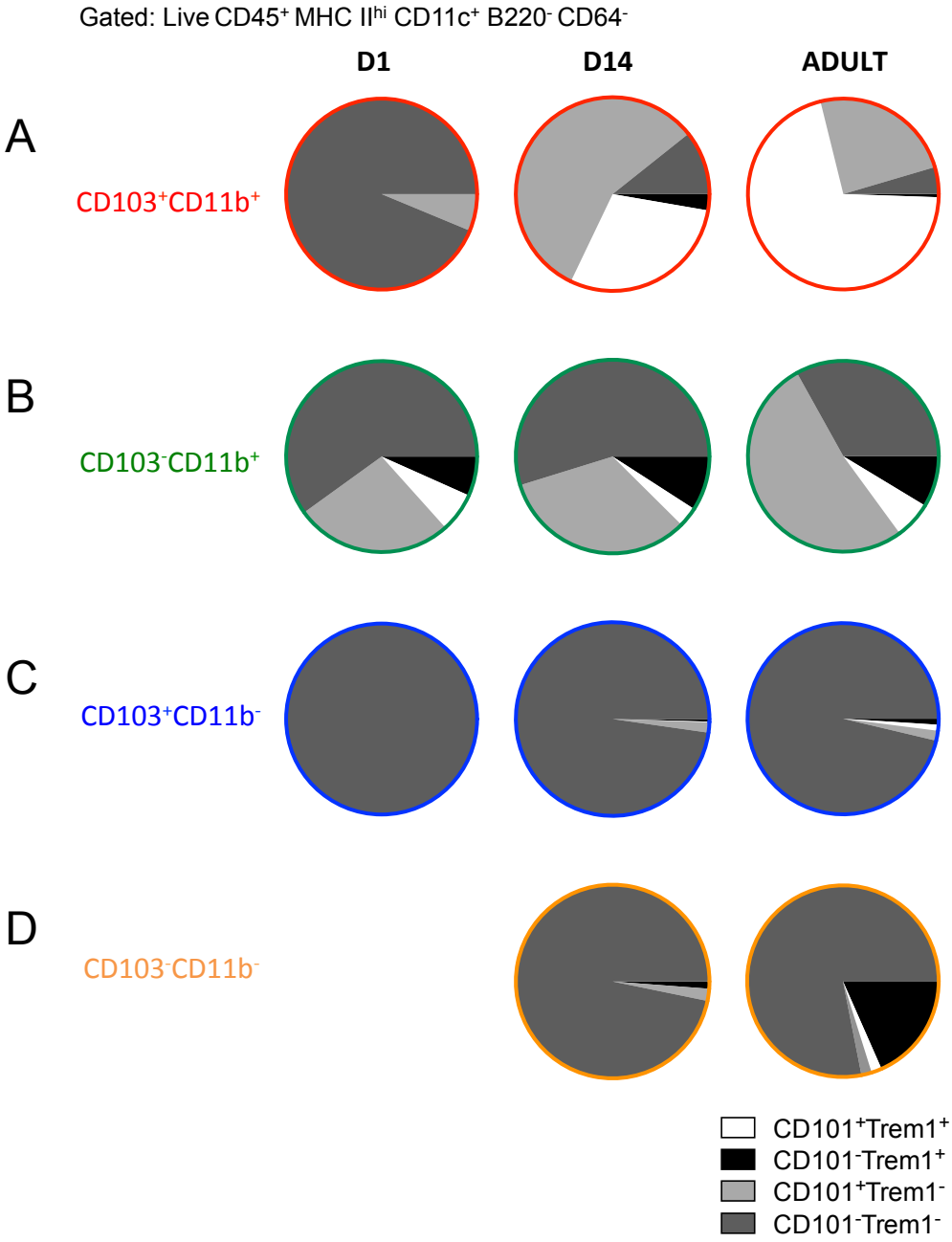

Figure 4.33: Expression of Trem-1 and CD101 by migratory MLN dendritic cells during development

Schematic depiction of the distribution of CD101$^+$Trem-1$^+$ (white), CD101$^-$Trem-1$^+$ (black), CD101$^+$Trem-1$^-$ (light grey) and CD101$^-$Trem-1$^-$ (dark grey) cells amongst each DC subset in the migratory MLN compartment from mice at D1, D14 and in adults. **A** CD103$^+$CD11b$^+$, **B** CD103$^-$CD11b$^+$, **C** CD103$^+$CD11b$^-$ and **D** CD103$^-$CD11b$^-$ DC. Data are means of one experiment at each time point with n=4-8 mice/group.

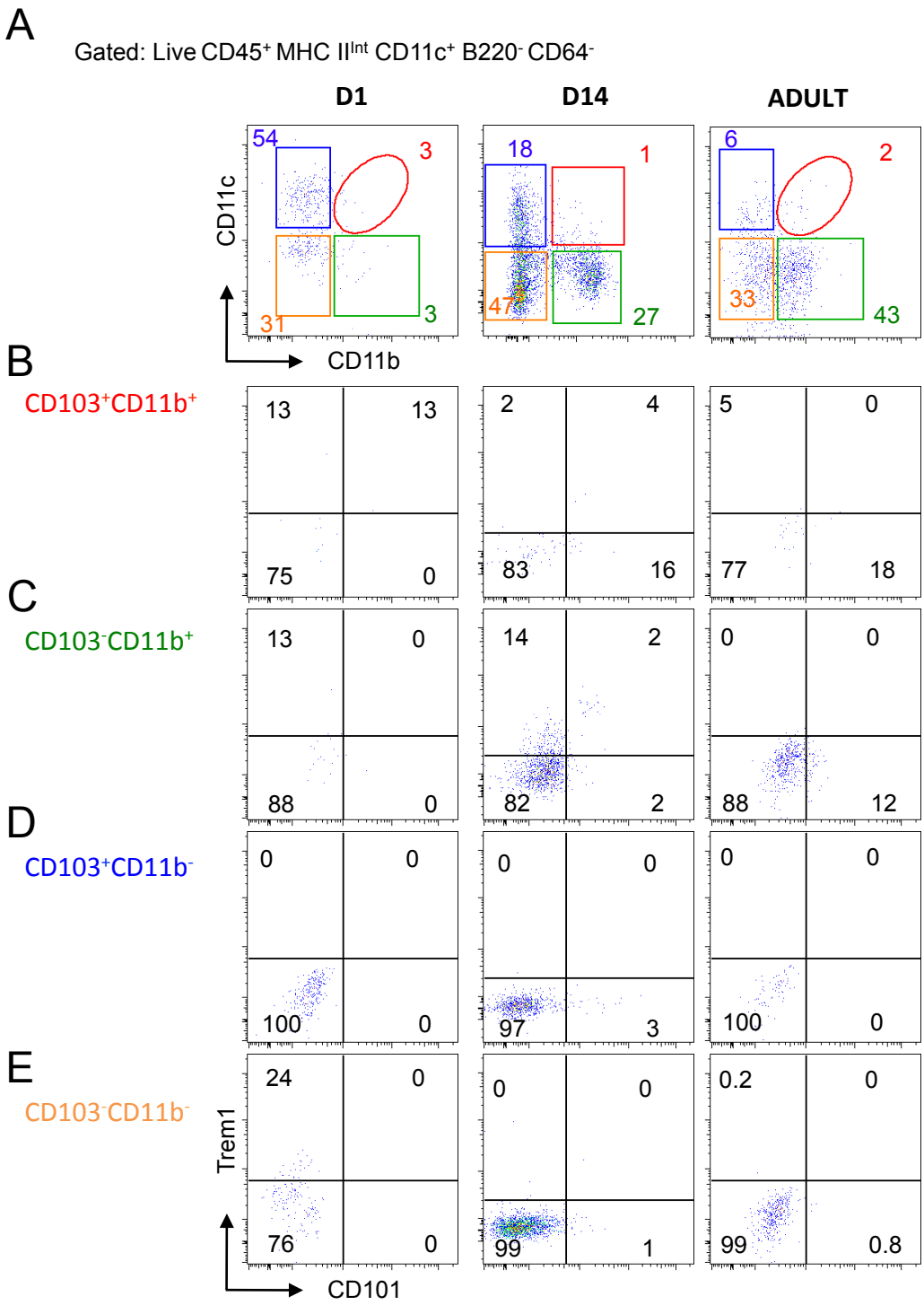

Figure 4.34: Expression of Trem-1 and CD101 by resident MLN dendritic cells during development

Cells were isolated from MLN. Live CD11c+ MHC IIInt CD64- resident DC were were analysed for the expression of CD103 and CD11b from D1 to adulthood (8-10 weeks). **A** Representative analysis shows the four DC populations based on CD11b and CD103 expression at D1, D14 and on adults. Co-expression of CD101 and Trem-1 at each time point, with gates set based on isotype controls by **B** CD103+CD11b+, **C** CD103-CD11b+, **D** CD103+CD11b- and **E** CD103-CD11b-. Data are representative of one experiment at each time point with n=4-8 mice/group.

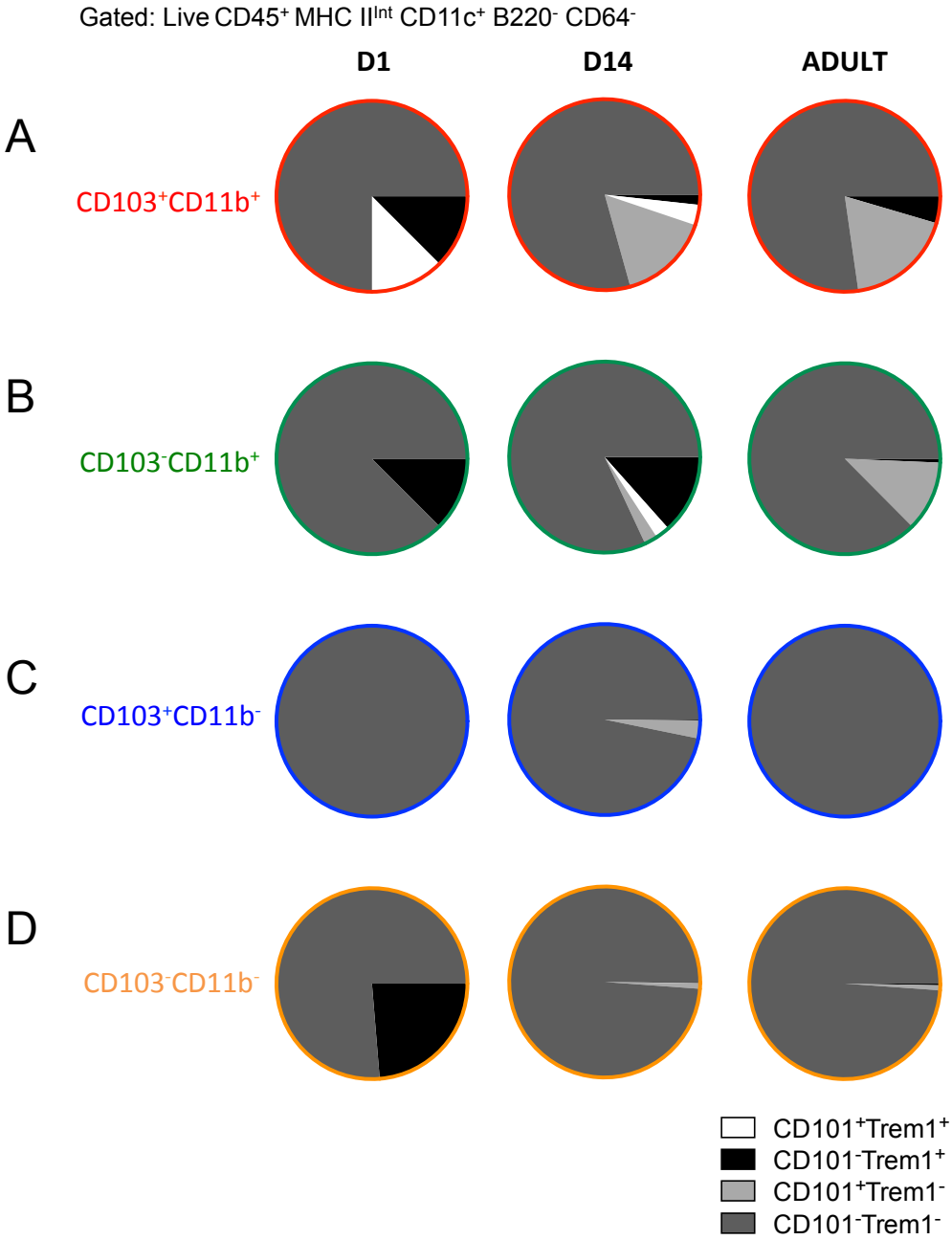

Figure 4.35: Expression of Trem-1 and CD101 by resident MLN dendritic cells during development

Schematic depiction of the distribution of CD101$^+$Trem-1$^+$ (white), CD101$^-$Trem-1$^+$ (black), CD101$^+$Trem-1$^-$ (light grey) and CD101$^-$Trem-1$^-$ (dark grey) cells amongst each DC subset in the resident MLN compartment from mice at D1, D14 and in adults. **A** CD103$^+$CD11b$^+$, **B** CD103$^-$CD11b$^+$, **C** CD103$^+$CD11b$^-$ and **D** CD103$^-$CD11b$^-$ DC. Data are means of one experiment at each time point with n=4-8 mice/group.

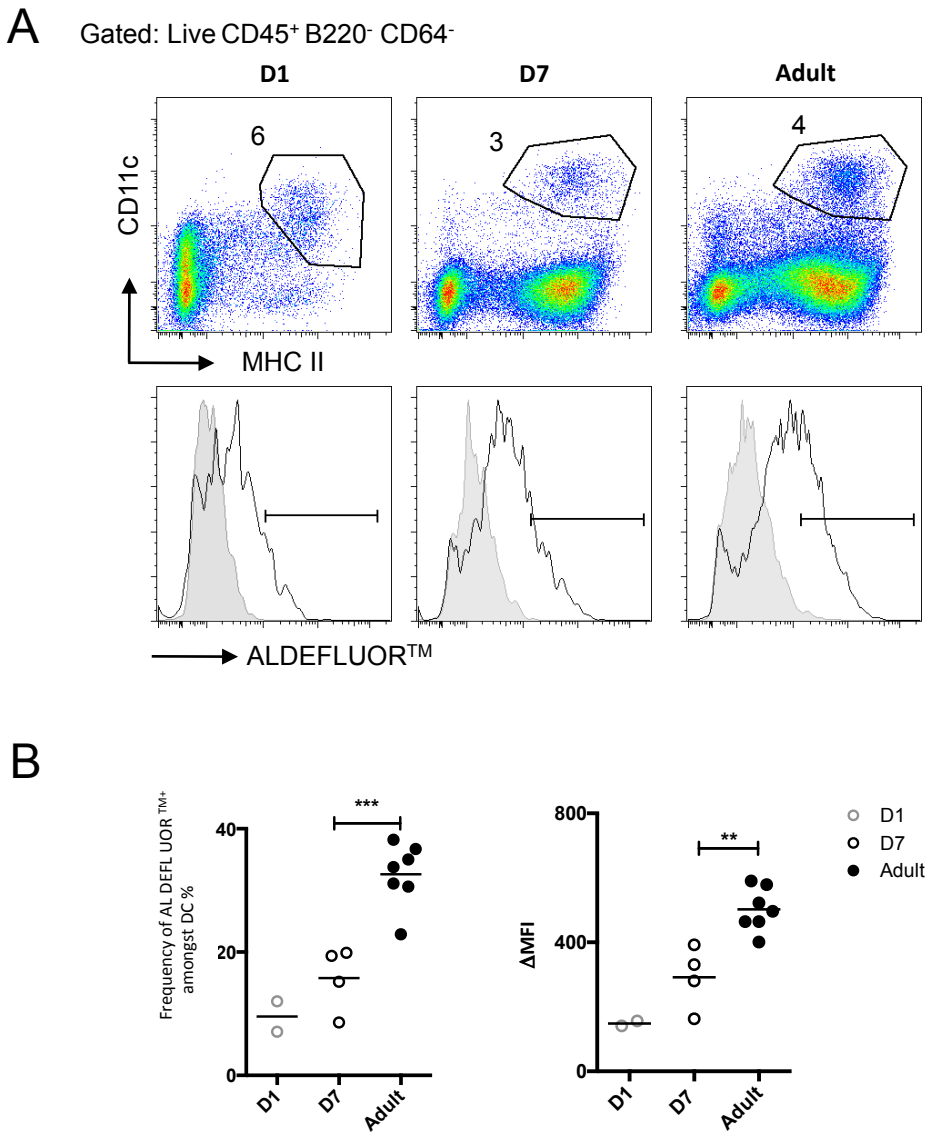

Figure 4.36: Effects of age on retinoic acid production by dendritic cells from small intestinal lamina propria

Total SI LP cells were incubated with the fluorescent ALDH substrate ALDEFLUOR™ in the presence or absence of the ALDH inhibitor diethylaminobenzoaldehyde (DEAB) and stained for flow cytometry. **A** Representative FACS plots showing total MHC II$^+$ CD11c$^+$ CD64$^-$ B220$^-$ DC at D1, D7 and 8-10 week old adults (top panels), together with histograms showing ALDEFLUOR™ fluorescence in the presence (grey line) or absence (black line) of DEAB (bottom panels). **B** Frequency of ALDEFLUOR™$^+$ DC amongst total DC or Δ Mean fluorescence intensity (MFI) for ALDEFLUOR™ activity (MFI in absence of DEAB – MFI in presence of DEAB) for total DC. Data are representative of one experiment for each time point with n=2-3 (D7) or n=4 (D14). **p<0.01, ***p<0.001. Student's t-test.

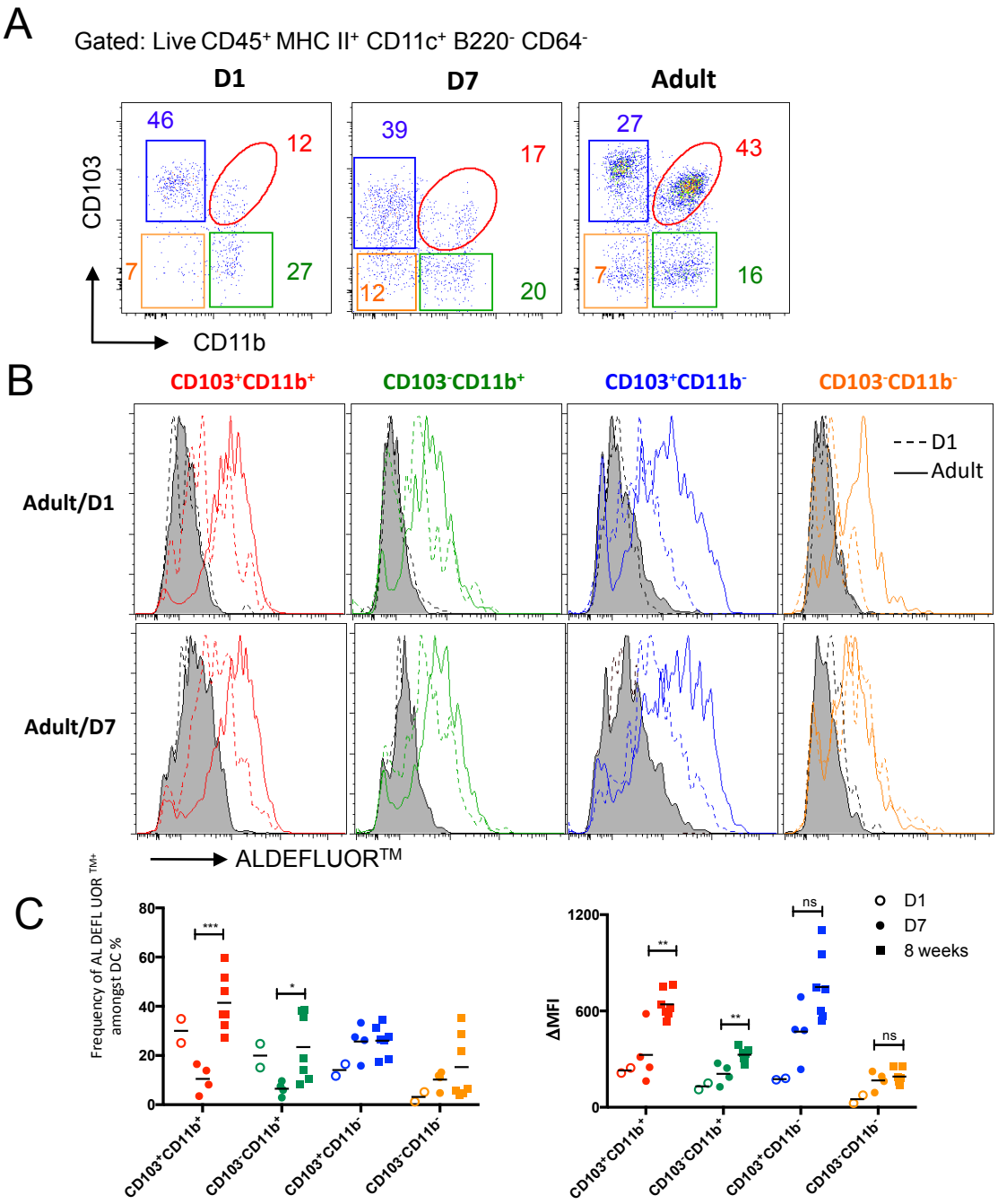

Figure 4.37: Effects of age on retinoic acid production by dendritic cells subsets from small intestinal lamina propria

Total SI LP cells were incubated with the fluorescent ALDH substrate ALDEFLUOR™ in the presence or absence of the ALDH inhibitor diethylaminobenzoaldehyde (DEAB) and subsequently stained for flow cytometry. **A** Representative FACS plots showing DC subsets at D1, D7 and 8-10 week old adults. **B** Histograms of results from D1 (top panels) or D7 (bottom panels), each compared with adults, showing ALDEFLUOR™ fluorescence by DC subsets in the presence (grey line) or absence (coloured) of DEAB. **C** Frequency of ALDEFLUOR™+ amongst total DC or Δ Mean fluorescence intensity (MFI) for ALDEFLUOR™ activity (MFI in absence of DEAB – MFI in presence of DEAB) for DC subsets. Data are representative of one experiment for each time point with n=2-3 (D7) or n=4 (D14). *p<0.05, **p<0.01, ***p<0.001. Student's t-test.

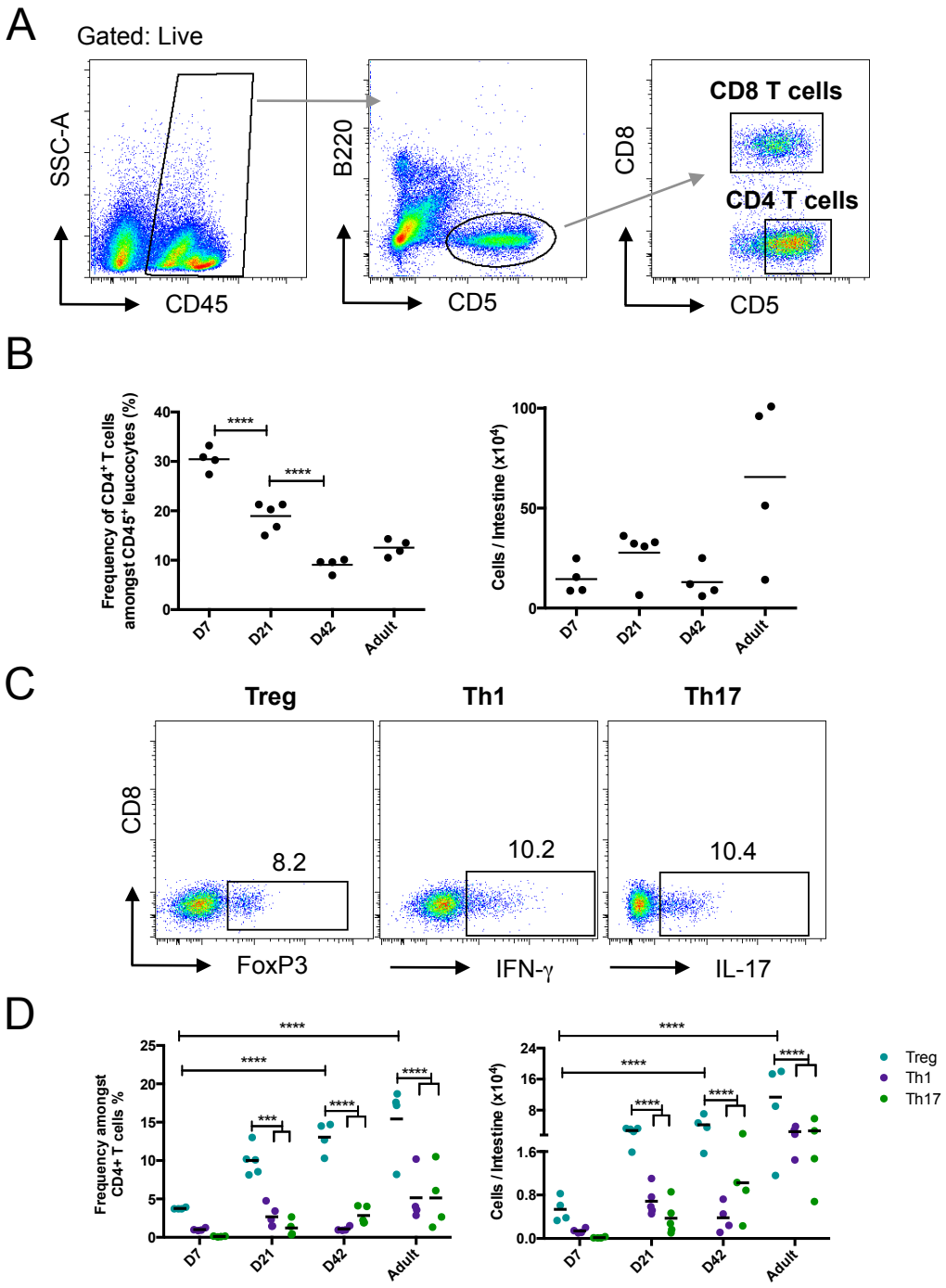

Figure 4.38: Effects of age on CD4⁺ T cells in small intestinal lamina propria
Total SI LP cells were incubated for 4.5 hours with PMA, ionomycin, brefeldin and monensin before analysis of CD4⁺ T cells by intracellular staining. **A** Gating strategy for identifying CD4⁺ T cells as live B220⁻ CD5⁺ CD8⁻ cells in SI LP of 8-10 week adult mice. **B** Frequencies amongst total CD45⁺ leukocytes (left) and absolute numbers (right) of CD4⁺ T cells. **C** Intracellular expression of FoxP3, INFγ and IL-17 assessed by flow cytometry using appropriate antibodies with gates set on isotype controls. **D** Frequencies and absolute numbers of Treg, Th1 and Th17 cells amongst CD4⁺ T cells isolated from mice at D7, D21, D42 or 8-10 week adults. Data are from a single experiment with n=4-5 mice/group. ***p<0.001, ****p<0.0001 Student's t-test.

Chapter 5

Characterisation of intestinal factors involved in DC development from neonates to adults

5.1 Introduction

Having shown in previous chapters that the defect in $CD103^+CD11b^+$ DC in the intestine of SIRPα mt mice resolved with age, I then went on to investigate how DC subsets developed in WT mice from embryonic life until one year of age. This showed that unlike the other DC subsets, $CD103^+CD11b^+$ DC were not present at birth, and that they took some time to reach normal numbers. I also discovered that CD101 and Trem-1 expression could be used to dissect DC development in more detail, with Trem-1 being largely restricted to $CD103^+CD11b^+$ DC and some $CD103^-CD11b^+$ DC. Using these markers confirmed that the slow appearance of $CD103^+CD11b^+$ DC reflected a delayed developmental programme rather than simply a lack of upregulation of CD103.

In this chapter, I used CD101 and Trem-1 to explore the ontogeny of intestinal DC subsets in $CCR2^{-/-}$ and SIRPα mt mice, both of which have selective defects in one particular group of DC (Persson et al., 2013b; Scott et al., 2014b; 2014a). To extend these studies, I also examined the expression of different DC growth factor receptors on DC subsets from mice of different ages, and I investigated whether Trem-1 played any role in DC development. Lastly, I examined the role of the microbiota in driving the differentiation of intestinal DC subsets.

5.2 Effects of age on expression of DC growth factor receptors

Having established the pattern of development of the DC subsets in the intestine, I wanted to try and understand some of the factors that might regulate these age related processes. GM-CSFR (CSF-2R), IRF-4 and TGFβR (our unpublished findings) are all required for the development of $CD103^+CD11b^+$ DC in the intestine, as is retinoic acid receptor α (RARα) (Agace and Persson, 2012; Bogunovic et al., 2009; Persson et al., 2013b). Therefore I thought it would be of interest to determine whether the expression of these receptors might correlate with the development of the DC subsets in the neonatal period. To do this I performed qPCR analysis of FACS purified DC subsets from D4, D14, D21 and 8 week old SI LP (Fig 5.1).

There were no significant differences in *Csfra1* between any of the DC subsets at any time point, although overall the levels were usually lower in the $CD103^-CD11b^+$ subset compared with the others. These patterns also did not change with age (Fig 5.2A). *Irf4* expression also showed few significant effects on subsets or time, although *Irf4* mRNA was higher in $CD103^-CD11b^-$ DC at D4 than in any other subset, when it was also significantly increased compared with the same subset at older ages. Additionally, at D14 there was a transient but significant increase in *Irf4* mRNA expression amongst $CD103^+CD11b^-$ DC compared with $CD103^-CD11b^+$ DC (Fig 5.2B). Analysis of *Tgfbr1* mRNA expression also showed few consistent differences between the subsets at different times, except on D14 of age, when there were significantly greater levels of mRNA in $CD103^+CD11b^-$ and $CD103^-CD11b^-$ DC compared with $CD103^-CD11b^+$ DC. D14 $CD103^+CD11b^+$ DC also expressed more *Tgfbr1* mRNA than $CD103^+CD11b^-$ DC on D4 and D21, as well as in adults. In general, the levels of *Tgfbr1* were highest in all subsets on D14 (Fig 5.2C). Expression of *Rara* mRNA showed considerable variability between samples and the levels were generally low. However, $CD103^+CD11b^-$ DC expressed significantly more *Rara* on D4 compared with the other three subsets and this remained the general trend throughout development until adulthood, when $CD103^+CD11b^+$ DC expressed similar amounts to $CD103^+CD11b^-$ DC in the adult intestine (Fig 5.2D).

Overall, these data showed few consistent differences between the transcript levels of key receptors and transcription factors during the development of the different DC subsets and did not provide clear evidence for individual pathways in this process.

5.3 Postnatal development of intestinal DC in SIRPα mt mice

Due to the defect in individual DC subsets that has been described in adulthood, I next went on to examine DC development in SIRPα mt mice. As I showed in Chapter 3, adult mice that lack SIRPα signalling have a selective defect in $CD103^+CD11b^+$ DC. I was therefore interested in examining whether this defect was present from early on in life. Furthermore, since carrying out that initial work, I had validated the use of CD101 and Trem-1 as tools for dissecting the lineage of $CD103^+CD11b^+$ DC in WT

neonatal mice. This enabled me to examine further and in greater depth the natural defect in $CD103^+CD11b^+$ DC that occurs in SIRPα mt mice.

5.3.1 CD103 and CD11b expression

The selective defect in the proportion and absolute number of $CD103^+CD11b^+$ DC in SIRPα mt SI was already clear by D7 of age, and indeed, it was relatively greater at this stage than I had found in adults. As a result there were negligible numbers of these DC in SIRPα mt mice at this age (Fig 5.3A). As I had found in WT mice, the frequency and numbers of $CD103^+CD11b^+$ DC were rising towards the levels observed in adult SI LP by D14, but the significant deficit in SIRPα mt mice was still present (Fig 5.3B).

Interestingly the proportion of $CD103^-CD11b^+$ DC was higher in SIRPα mt SI LP compared with WT (~24% vs ~18%) on D7, unlike what I had found in adults. However, the absolute numbers of $CD103^-CD11b^+$ DC were reduced in the SIRPα mt compared with the WT at this early time point (Fig 5.3A), and by D14 both the frequency and number of this subset were similar in SIRPα mt and WT SI LP. The frequency of $CD103^+CD11b^-$ DC was not significantly different between WT and SIRPα mt mice on D7 of age, although the absolute numbers were reduced amongst SIRPα mt mice. As I had found in adults, by D14 the proportion of $CD103^+CD11b^-$ DC was increased in SIRPα mt mice compared with WT mice, although the absolute numbers were not different (Fig 5.3B). The proportion $CD103^-CD11b^-$ DC was increased significantly in D7 SIRPα mt mice compared with WT mice, but the absolute numbers were significantly lower (Fig 5.3A) and these differences had disappeared by D14 (Fig 5.3B).

There were no differences between migratory DC subsets in the MLN of SIRPα mt and WT mice at D7, perhaps reflecting the very low number of these cells at this time (Fig 5.4A). However, by D14 the proportions of all subsets resembled the pattern seen in their adult counterparts, with reduced $CD103^+CD11b^+$ and increased $CD103^+CD11b^-$ DC in the SIRPα mt mice; there was also now a marked reduction in the absolute numbers of all migratory DC subsets present in the MLN of SIRPα mt mice compared

with WT at D14 (Fig 5.4B). There were no differences in the frequency or number of the different resident DC subsets present in the MLN at D7. However, as I had observed in adult mice, the frequencies of $CD103^{-}CD11b^{+}$ and of $CD103^{+}CD11b^{-}$ DC showed trends toward being decreased and increased respectively in SIRPα mt neonatal mice (Fig 5.5A; Fig 3.3B). By D14, there were reduced proportions of $CD103^{-}CD11b^{+}$ DC and increased proportions of $CD103^{+}CD11b^{-}$ DC amongst resident MLN DC, but again the numbers of all resident DC subsets were now markedly reduced in SIRPα mt MLN, as was the case in adults (Fig 5.5B; Fig 3.3C).

5.3.2 CD101 and Trem-1 expression

I next used CD101 and Trem-1 to ascertain whether the reduction in $CD103^{+}CD11b^{+}$ DC in the SIRPα mt intestine was simply due to the lack of CD103 up-regulation. I first analysed CD101 and Trem-1 expression by total $CD11b^{+}$ DC in D7 neonate and 8 week old adult SI LP, as this could be where those DC might be (Fig. 5.6A). As expected, the frequency of total $CD11b^{+}$ DC was reduced significantly in SIRPα mt mice at both time points, reflecting the usual predominance of $CD103^{+}CD11b^{+}$ DC in the intestine of WT mice. The proportion of total $CD11b^{+}$ DC also did not increase as much from D7 into adulthood in the SIRPα mt SI LP, as it did in WT mice (Fig 5.6B). In parallel, SIRPα mt SI LP had a significantly lower proportion of $CD11b^{+}$ DC expressing CD101 compared with WT intestines at both D7 and in adults, although interestingly, in both strains there were greater proportions of $CD11b^{+}$ DC expressing CD101 in D7 mice than in adults. A similar pattern was seen with Trem-1 expression amongst total $CD11b^{+}$ DC, where a significantly fewer proportion of these cells expressed Trem-1 in both neonatal and adult SIRPα mt SI LP compared with WT controls. However unlike CD101, the proportion of $CD11b^{+}$ DC expressing Trem-1 increased with age in both WT and SIRPα mt mice (Fig 5.6C).

I went on to investigate the expression of CD101 and Trem-1 by the individual subsets of $CD11b^{+}$ DC in WT and SIRPα mt mice. As both subsets predominantly lacked CD101 and TREM1 expression in adult mice, the expression of these markers on $CD103^{+}CD11b^{-}$ and $CD103^{-}CD11b^{-}$ DC was not assessed in this experiment (Fig. 4.33). As I had found in these previous experiments, the majority of $CD103^{+}CD11b^{+}$

DC in WT adult SI LP expressed both CD101 and Trem-1, whereas WT CD103^{-}CD11b^{+} DC were more heterogeneous, with ~22% and ~14% expressing CD101 and Trem-1 respectively. There was a small but significant decrease in the proportion of CD103^{+}CD11b^{+} DC that co-expressed CD101 and Trem-1 in adult SIRPα mt mice compared with the WT subset, although most of the remainder expressed CD101 or Trem-1 alone (Fig 5.7B). As in WT mice, CD103^{-}CD11b^{+} DC in SIRPα mt mice were heterogeneous for the expression of CD101 and Trem-1, although again there were significantly fewer in proportion expressing both CD101 and Trem-1 compared with controls (~14% vs ~4%). There were no differences in the proportion of CD103^{-}CD11b^{+} DC expressing CD101 or Trem-1 alone, but the proportion of CD101^{-}Trem-1^{-} DC was significantly higher in SIRPα mt mice compared with controls (Fig 5.7B). The differences between WT and SIRPα mt SI LP DC were even more striking on D7 than in adults, with much greater differences in the frequency of CD101^{+}Trem-1^{+} DC amongst both CD103^{+}CD11b^{+} (~35%) and CD103^{-}CD11b^{+} (~4%) DC compared with ~69% and 14% in WT mice of the same age (Fig. 5.7A).

Thus lack of signalling through SIRPα appears to have an even more profound effect on DC development early in life than it does in adults, and this is not simply due to the lack of acquisition of CD103 on CD103^{+}CD11b^{+} DC. Rather it affects a wide ranging developmental pathway, as indicated by reduced acquisition of CD101 and Trem-1.

5.4 Role of CCR2 in the development of CD11b^{+} DC

I next examined intestinal DC in CCR2$^{-/-}$ mice, which are known to have reduced frequency and numbers of CD103^{-}CD11b^{+} DC in the intestine (Scott et al., 2014a). I did not have access to neonatal CCR2$^{-\backslash-}$ mice, as they were bred at a different facility. I was therefore only able to analyse adults of this strain. In contrast to what had been shown previously in the lab, there were no significant differences in the frequency of total CD11b^{+} DC or of the individual DC subsets in CCR2$^{-/-}$ mice compared with age matched WT controls, although there was a trend towards a reduction in CD103^{-}CD11b^{+} DC in the SI LP (Fig 5.8A-B). There were also no significant differences between CCR2$^{-/-}$ and WT mice in the proportion of total CD11b^{+} DC expressing CD101.

However a significantly greater proportion of CD11b^{+} DC expressed Trem-1 in CCR2$^{-/-}$ mice compared with WT controls (Fig 5.8C).

When the CD103^{+}CD11b^{+} and CD103^{-}CD11b^{+} DC subsets were analysed individually, I found that the large majority of CD103^{+}CD11b^{+} DC were CD101^{+}Trem-1^{+} in both CCR2$^{-/-}$ and WT SI LP, although there was a small but significant increase in the proportion of these DC expressing both CD101 and Trem-1 in CCR2$^{-/-}$ mice compared with WT mice. CD103^{-}CD11b^{+} DC were heterogeneous for CD101 and Trem-1 in both strains, and there were no significant differences between them in the expression of these markers (Fig 5.9A). As was shown previously in the laboratory, a small subset of CD103^{-}CD11b^{+} DC in WT SI LP expressed CCR2, and interestingly, these did not express either CD101 or Trem-1 (Fig 5.9B).

5.5 Effects of Trem-1 on intestinal DC development

So far, I have shown that intestinal DC subsets develop gradually over time, particularly the CD103^{+}CD11b^{+} DC (Chapter 4). Moreover, this development is not simply due to the upregulation of CD103, commonly used to define the four intestinal DC subsets, but reflects a more complex programme involving the acquisition of other molecules including CD101 and Trem-1.

As Trem-1 seemed to be particularly associated with the CD103^{+}CD11b^{+} lineage, I decided to investigate whether Trem-1 itself played any role in the development of DC in the SI LP. To do this I collaborated with Professor Christoph Mueller's group at the University of Bern, where they had generated Trem-1$^{-/-}$ mice. As a preliminary step, I was sent flow cytometry data from SI LP digests they had carried out on Trem-1$^{-/-}$ and Trem-1$^{+/+}$ (WT) littermate mice, and I analysed the results using the strategies I had applied to my own animals. Unfortunately, there was a significant amount of cell death in all of the samples, and I thought it sensible only to analyse those that had greater than 50% viability, which was one WT and two Trem-1$^{-/-}$ mice.

In these samples I was able to identify the four subsets of cDC based on CD11b and CD103 expression in both WT and Trem-1$^{-/-}$ SI LP. However, the relative frequencies of the subsets present in the WT SI LP were different from those that I, and others,

had observed in the SI LP of Glasgow mice, with only ~20% of the total DC being $CD103^+CD11b^+$, compared with the ~40% that I reported previously (Fig 5.10A). In parallel, the proportion of $CD103^+CD11b^-$ DC was much higher than what myself, and others, have reported. Although the low number of mice makes it impossible to come to any precise conclusion, the frequency of $CD103^+CD11b^+$ DC appeared to be increased in Trem-$1^{-/-}$ mice compared with their WT control, with a reciprocal decrease in $CD103^+CD11b^-$ DC. The proportions of $CD103^-CD11b^+$ and $CD103^-CD11^-$ DC were identical in the two strains (Fig 5.10B). I was not able to generate any absolute numbers in this experiment, as no total cell counts had been carried out when the tissues were harvested. In addition, the host group had not stained for CD101 or Trem-1, or taken other tissues for more detailed comparison.

Although this analysis was inconclusive, there appeared to be some evidence that the absence of Trem-1 might influence DC development in the intestine. Therefore, I decided to investigate further by obtaining BM from the Mueller group and generating competitive BM chimeras. CD45.2/CD45.1 WT recipients were reconstituted with a 90:10 mix of $CD45.2^+$ WT and $CD45.1^+$ WT (WT:WT) BM cells or with a 85:15 mix of $CD45.2^+$ Trem-$1^{-/-}$ and $CD45.1^+$ WT (Trem-$1^{-/-}$:WT) BM cells (Fig. 5.11). In each case, my intention had been to set up 50:50 chimeras, but the $CD45.1^+$ WT BM cells appeared to have undergone selective death during the preparation process. This was only highlighted when I assessed the levels of chimerism eight weeks after reconstitution. To standardise the analysis of chimerism, I used $CD19^+$ blood B cells as these do not express Trem-1 and therefore should not be affected by its absence (Fig 5.12A). Consistent with the ratio I had used to reconstitute, the level of chimerism in WT:WT chimeras was ~90:10. However, despite reconstituting with a 85:15 ratio, by 8 weeks the level of chimerism in Trem-$1^{-/-}$:WT chimeras was ~94:6 (Fig 5.12B). These ratios were then used to normalise the values obtained from the other cell types. In comparison to B cells, $Ly6C^{hi}$ monocytes and neutrophils from CD45.2 WT BM appeared to reconstitute recipients more efficiently than their CD45.1 WT counterparts, with normalised ratios of ~4 and ~2.5 respectively, perhaps reflecting the viability of the original inoculum as mentioned above (Fig 5.12B). However, CD45.2 Trem-$1^{-/-}$ BM was markedly less efficient than its CD45.1 WT counterpart in reconstituting these myeloid cells (especially neutrophils, which are

uniformly Trem-1^{+} in WT mice), while only a small proportion of Ly6C^{hi} monocytes are normally Trem-1^{+} (Fig 5.12A).

DC in the SI LP behaved more like blood neutrophils than B cells, showing a CD45.2:CD45.1 ratio of ~2 in WT:WT chimeras. Interestingly, CD45.2 Trem-1$^{-/-}$ BM was less capable of generating all DC subsets than the WT BM, giving ratios even lower than those of blood B cells under the same conditions. However, this affected all DC subsets equally in both types of chimera, indicating that the effects were not related to the levels of Trem-1 expressed by the different DC subsets. Unfortunately, problems with the digestion process meant I only had two WT:WT chimeras to analyse in this experiment, and therefore it was not possible to assess statistical significance between the cell populations present in the SI LP of the WT:WT and Trem-1$^{-/-}$:WT chimeras (Fig 5.13B). I was also unable to obtain more Trem-1$^{-/-}$ BM to repeat these studies in the time remaining to me.

Monocytes entering the LP also express Trem-1 (Bouchon et al., 2000). Therefore, to extend these findings, I also examined the monocyte/mϕ continuum in the SI LP. These cells were identified as live, side scatter^{lo}, CD11b^{+} B220^{-} and CD64^{int-hi}. They were then subsetted based on the expression of MHC II and Ly6C (Fig 5.14A; (Bain et al., 2013)). According to this strategy, P1 is made up of Ly6C^{hi} MHC II^{-} monocytes that are newly arrived from the blood, whilst P2 are Ly6C^{hi} MHC II^{+} cells transitioning into mϕ. The Ly6C^{-} MHC II^{+} mature mϕ can then be further differentiated into P3 and P4 based on the level of CX3CR1 expression (Bain et al., 2013; Tamoutounour et al., 2013). Consistent with recent results from the laboratory, showing that intestinal mϕ are derived by continuous replenishment from circulating monocytes, all the mϕ lineage populations behaved more like blood Ly6C^{hi} monocytes than B cells in WT:WT chimeras, showing a CD45.2:CD45.1 ratio of ~2.5 for Ly6C^{hi} P1 monocytes and slightly lower levels as the cells progressed through P2 to P3/P4 (Fig 5.14B&C). Again as I found with blood monocytes, the ratios for reconstitution of intestinal mϕ were reduced in Trem-1$^{-/-}$:WT chimeras.

I also examined the colon of these competitive chimeras, where again the DC subsets in WT:WT chimeras were reconstituted preferentially by CD45.2^{+} BM (Fig 5.15A&B). Ranging from ~3-5, the CD45.2:CD45.1 ratios were higher than those in the SI LP (Fig

5.15B). In the Trem-1$^{-/-}$:WT chimeras, the DC subsets again showed an even greater defect in reconstitution by Trem-1$^{-/-}$ BM and, like the SI LP, this was less efficient than blood B cells (Fig 5.15B). Although there were too few samples to perform statistical analysis, it appeared that in WT:WT chimeras there was a trend towards CD45.2^{+} BM being better able to generate CD103^{-}CD11b^{+} DC than CD103^{+}CD11b^{+} DC. As in the SI LP, there were no observable differences between the DC subsets in any of the chimeras (Fig 5.15A-B). Analysis of monocytes and mϕ in the colon showed the same patterns of reconstitution as in the SI LP where the ratios for reconstitution were lower in Trem-1$^{-/-}$:WT chimeras compared to WT:WT chimeras (Fig 5.16A-B).

Next I analysed the reconstitution of DC subsets in both the resident and migratory compartments of the MLN of the chimeric mice. As in the SI LP and CLP, CD45.2^{+} WT BM contributed to migratory DC populations to a greater extent than in blood B cells, while CD45.2^{+} Trem-1$^{-/-}$ BM was less efficient than the equivalent WT BM (Fig 5.17A-B). Although there were insufficient samples to carry out statistical analysis, it appeared that CD45.2^{+} WT BM was better able to generate migratory CD103^{-}CD11b^{+} DC than CD103^{+}CD11b^{+} DC, with CD45.2:CD45.1 ratios of ~4 and ~2 respectively (Fig 5.17B). This pattern was more similar to that seen in the CLP than in the SI LP. The resident compartment of MLN DC behaved differently to other DC populations, as reconstitution by CD45.2^{+} BM appeared better than that of B cells, regardless of whether it was of WT or Trem-1$^{-/-}$ origin (Fig 5.18A-B). However, the relative defect in reconstitution by Trem-1$^{-/-}$ BM remained apparent, with the most striking difference being in the CD103^{-}CD11b^{+} DC subset, where the CD45.2:CD45.1 ratio was ~34 (Fig 5.18B). However, it should be pointed out that this result is from just one animal and therefore could be an anomaly. Overall, these data show that the lack of Trem-1 expression on haematopoietic cells causes a reduction in the ability of leukocytes to reconstitute irradiated chimeras, regardless of whether or not that cell type expresses Trem-1 or not. However this applies equally to all DC subsets in the mucosa and migratory DC in the MLN, and there was no evidence that Trem-1 played a selective role in the development of individual subsets.

5.6 The influence of microbiota on intestinal DC

The results of preceding experiments showed that intestinal DC populations changed markedly during the neonatal period, and in some cases also with ageing. One hypothesis I considered to explain these effects was that the acquisition of the microbiota may be responsible. To test this, I looked at intestinal DC in antibiotic treated and germ-free adult mice.

5.6.1 The effects of antibiotic treatment on intestinal DC

Eight-week old WT mice were treated with an antibiotic cocktail containing 1 mg/ml Cefoxitin, Gentamicin, Metronidazol, and Vancomycin, previously reported to deplete the microbiota sufficiently to impair DC function within 1-2 weeks (Diefenbach et al., 2012). Mice were administered antibiotics orally in drinking water containing artificial sweetener, or maintained on normal drinking water containing sweetener for two weeks. Although I did not have access to facilities that would have allowed me to confirm directly that the antibiotic protocol had reduced the microbiota, this appeared to be the case, as the treated mice had markedly enlarged caeca compared with controls (data not shown). However, neither the frequency nor the numbers of any of the DC subsets in the SI LP were affected by treatment with antibiotics (Fig. 5.19A-B). Similar results were found when I examined the CLP, apart from a small but significant reduction in the frequency of $CD103^{+}CD11b^{-}$ DC in the antibiotic treated mice (Fig. 5.20). In contrast to these findings on DC, there was a significant reduction in the proportion of $FoxP3^{+}$ Tregs in the SI LP of antibiotic treated mice, although the populations of Th17 and Th1 cells were unaffected (Fig. 5.19C).

Consistent with the findings in the SI LP and CLP, antibiotic treatment had little effect on migratory DC in MLN, where the only significant change was a reduced frequency $CD103^{-}CD11b^{-}$ DC (Fig 5.21). By contrast, although the relative frequencies of the various subsets of resident DC in the MLN were not affected by antibiotic treatment, the absolute numbers of $CD103^{+}CD11b^{-}$ and $CD103^{-}CD11b^{-}$ DC were significantly reduced in these mice, and there was also a trend toward reduced numbers of $CD103^{-}CD11b^{+}$ DC (Fig. 5.22).

5.6.2 The effects of a germ free environment on DC development

As the administration of antibiotics to mice with an intact microbiota had very few significant effects on intestinal DC, I decided to examine whether longer term or complete absence of microbiota might have more influence. To do this, I exploited a collaboration with the Institute of Food Research in Norwich where there was a germ-free colony. Unfortunately, at the time of my visit it was found that the 'facility barrier' had recently been breached, meaning the germ-free status of the mice was unclear. Despite this, I decided to proceed with the experiment, and subsequent analysis revealed that the animals had a greater diversity of bacterial species at both the family and genus level, but fewer copy numbers of those bacteria when compared with SPF controls (Fig 5.23). In the SPF mice, it appeared there was a predominance of Lachnospiraceae, which was not present in the GF mice (Fig 5.23A). As in antibiotic treated mice, there were no differences in the relative frequencies of the DC subsets in the SI LP between GF and conventional mice, although there was a slight reduction in the number of $CD103^{-}CD11b^{-}$ DC in GF animals (Fig 5.24A). In the CLP, the only significant changes in germ-free mice was an increased proportion of $CD103^{-}CD11b^{+}$ DC and a reduced frequency of $CD103^{+}CD11b^{-}$ DC, together with a slight increase in the $CD103^{-}CD11b^{-}$ DC (Fig. 5.24B). There were no differences in the proportions or numbers of DC subsets amongst the migratory or resident compartments of MLN between germ-free and conventional mice (Fig 5.25).

5.7 Summary

In this chapter I attempted to investigate the factors that might drive the differentiation of intestinal DC subsets during development, with particular regard to the $CD103^{+}CD11b^{+}$ DC subset. First I examined the expression of factors known to influence DC development, but found few consistent differences in the levels of mRNA for the genes encoding CSF2-Rα1, IRF4, TGFβR and RARα amongst the DC subsets at different times. Although these results could suggest that responsiveness to these factors may already be imprinted from birth, the data were highly variable and this needs to be repeated. Next I investigated whether the selective effects of the SIRPα mutation on $CD103^{+}CD11b^{+}$ DC were already manifest during the first and second

weeks of life. This appeared to be the case and indeed, the defect was more pronounced in the SI LP at D7 of age than at D14 or in adults. Furthermore, there was a defect in the numbers of all DC subsets at D7, perhaps suggesting that there is a generalised delay in DC development in these mice. None of these features were seen amongst migratory DC MLN at D7, perhaps due to the very low number of these cells at this age, but the selective defect in $CD103^+CD11b^+$ DC and concomitant increase in $CD103^+CD11b^-$ DC frequency were present by D14. The generalised reduction of DC numbers seen in adults was also now present at this time. The frequency of $CD103^-CD11b^+$ DC was decreased amongst resident MLN DC by D14, when there was a reciprocal increase in $CD103^+CD11b^-$ DC. At this time, there were also fewer resident DC of all subsets. The expression of both CD101 and Trem-1 was reduced amongst total $CD11b^+$ DC from SI LP of SIRPα mt mice at both D7 and D14, as was the co-expression of CD101 and Trem-1 by $CD103^+CD11b^+$ and $CD103^-CD11b^+$ DC. These changes did not resolve with age.

I next extended previous findings in the laboratory, which had revealed that a subset of $CD103^-CD11b^+$ DC was absent in $CCR2^{-/-}$ mice, by showing that the absence of these cells did not affect the proportion of $CD11b^+$ DC that expressed CD101. By contrast Trem-1 expression was increased on $CD103^-CD11b^-$ DC in $CCR2^{-/-}$ mice, as was the co-expression of CD101 and Trem-1 amongst $CD103^+CD11b^+$ DC in these animals. This may reflect the absence of a $CCR2^+$ subset of these DC, which I found to lack either marker. Thus the CCR2-dependent DC population does not appear to overlap with those that go on to express CD101 or Trem-1.

In the previous chapter, I demonstrated that Trem-1 expression was a selective feature of $CD103^+CD11b^+$ DC and I therefore examined whether Trem-1 had a direct role in the development of these cells. The limited experiments that were possible from analysis of cells isolated by collaborators in Bern revealed few if any effects on intestinal DC. Nor were there selective effects on any DC subset when $Trem\text{-}1^{-/-}$ BM was used to generate competitive chimeras. However, $Trem\text{-}1^{-/-}$ BM showed a generalised defect in the ability to generate all leukocytes in the mucosa and migratory MLN, but not in resident MLN DC. Lastly, I tested the hypothesis that the microbiota might be involved in shaping the intestinal DC subsets, but analysis of

both antibiotic treated animals and germ-free mice showed that the microbiota had little effect on the DC populations present in the intestine.

Together, these results show that the specific acquisition of $CD103^+CD11b^+$ DC appears not to be dependent on the specific upregulation of genes encoding CSF2-Rα1, IRF4, TGFβR and RARα, nor on the expression of Trem-1. Furthermore, bacterial load in the intestinal mucosa does not seem to be the sole reason for the presence of $CD103^+CD11b^+$ DC. These data show that $CD103^+CD11b^+$ DC lineage is complicated and is likely to be a combination of different factors including age and environment.

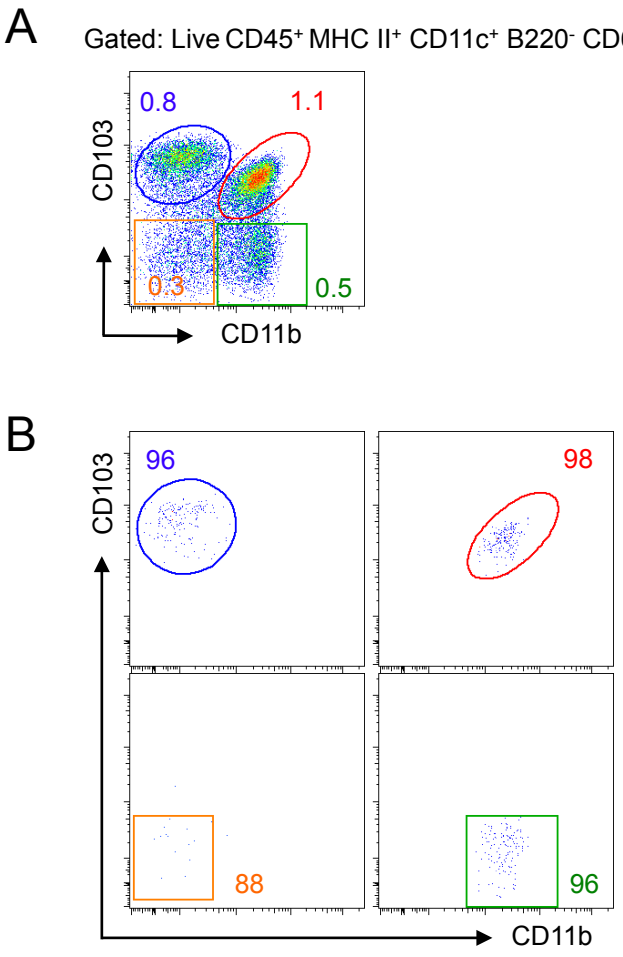

Figure 5.1: Purification of small intestinal DC subsets by FACS
SI LP cells were isolated from WT mice at 8 weeks of age and DC identified as live (7-AAD$^-$) CD11c$^+$ MHC II$^+$ B220$^-$ CD64$^-$ cells. **A** Representative dot plot showing the expression of CD11b and CD103 by DC from adult mice and the frequency of each subset as a proportion of total cells. **B** Representative plots showing the proportion of each cell type as a percentage after sorting. Data are representative of at least 10 independent experiments with 2-7 mice pooled per experiment.

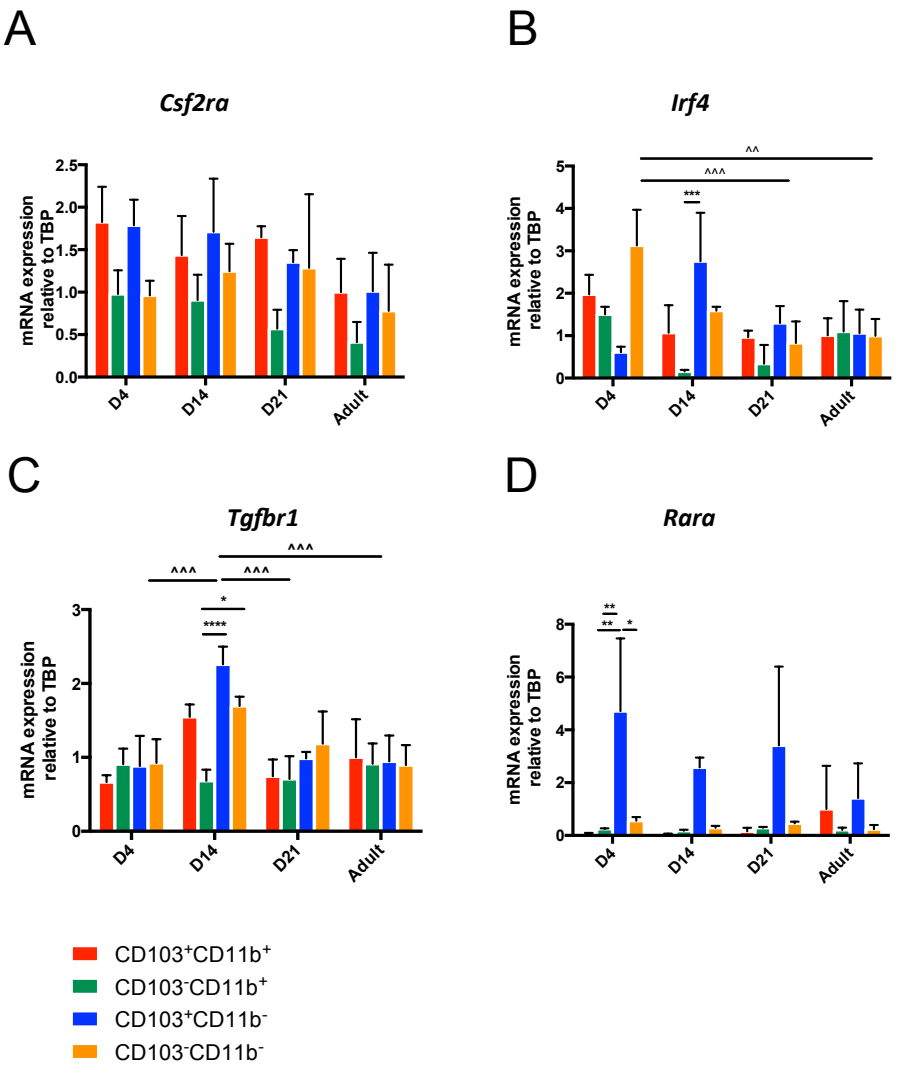

Figure 5.2: Expression of transcriptional and growth factor receptors by small intestinal DC subsets at different ages

A-D. SI LP DC were FACS-purified from wild type mice aged D4, D14, D21 or 8 week old adult as described in Fig. 5.1 and analysed by qRT-PCR for the expression of mRNA for (A) *Csf2ra1,* (B) *Irf4,* (C) *Tgfbr1* and (D) *Rara*. Results shown are relative to TATA binding protein (*TBP*) using the 2-ΔΔct method with adult $CD103^+CD11b^+$ DC set to 1. Data are from a single experiment with cells pooled from 2-7 mice per time point with n=3 biological replicates per group. * $p<0.05$, ** $p<0.01$, *** $p<0.001$, **** $p<0.0001$ within a time point. ^^ $p<0.01$, ^^^ $p<0.001$ across different time points, Two-way ANOVA with Bonferroni post-test.

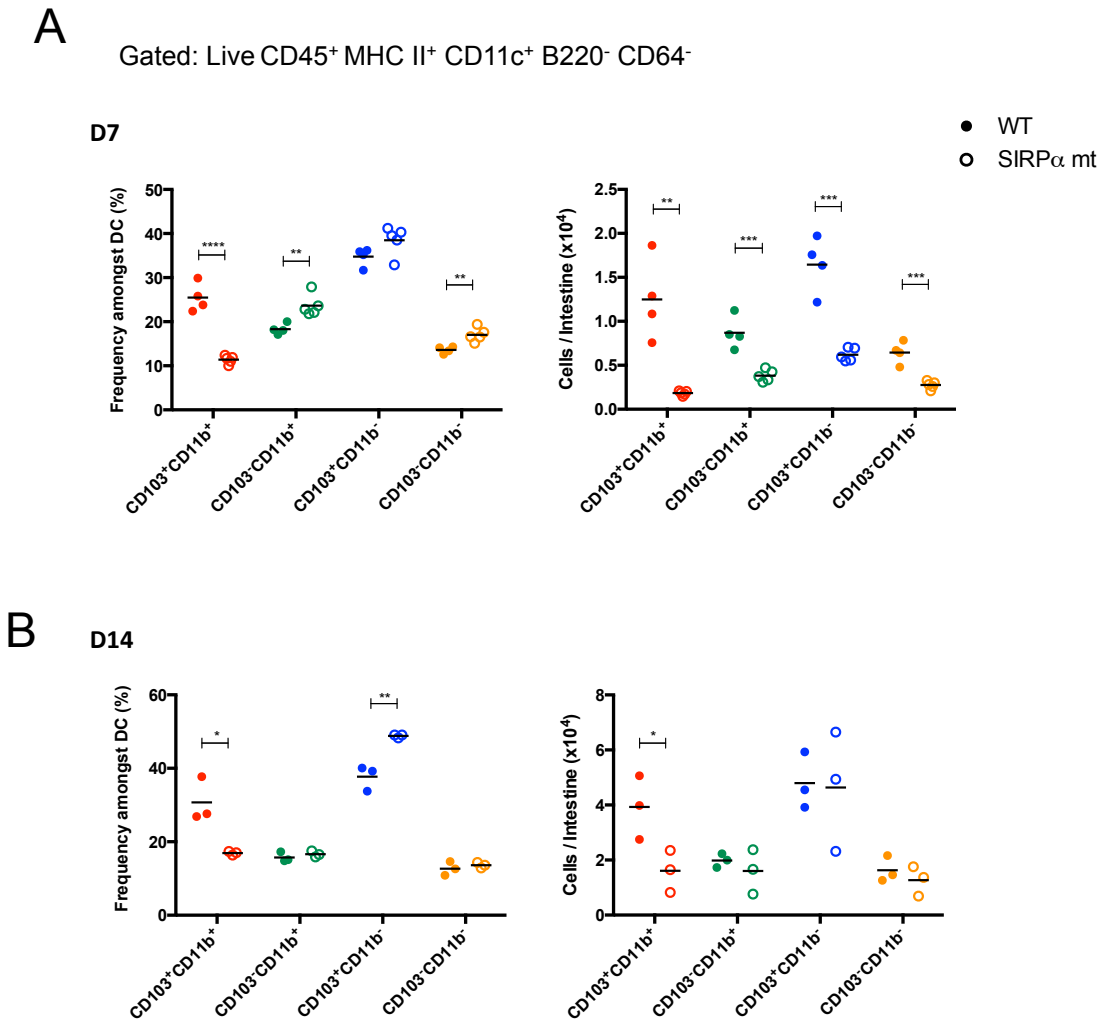

Figure 5.3: Development of small intestinal DC subsets in SIRPα mt mice

SI LP cells were isolated from WT and SIRPα mt mice and live MHC II$^+$ CD11c$^+$ B220$^-$ CD64$^-$ DC were analysed for the expression of CD103 and CD11b. Frequencies amongst total DC (left panels) and absolute numbers (right panels) were analysed at **A** D7 and **B** D14. Data are from one experiment with 3-5 animals per group. *p<0.05, **p<0.01, ***p<0.001, ****p<0.0001 Student's t test.

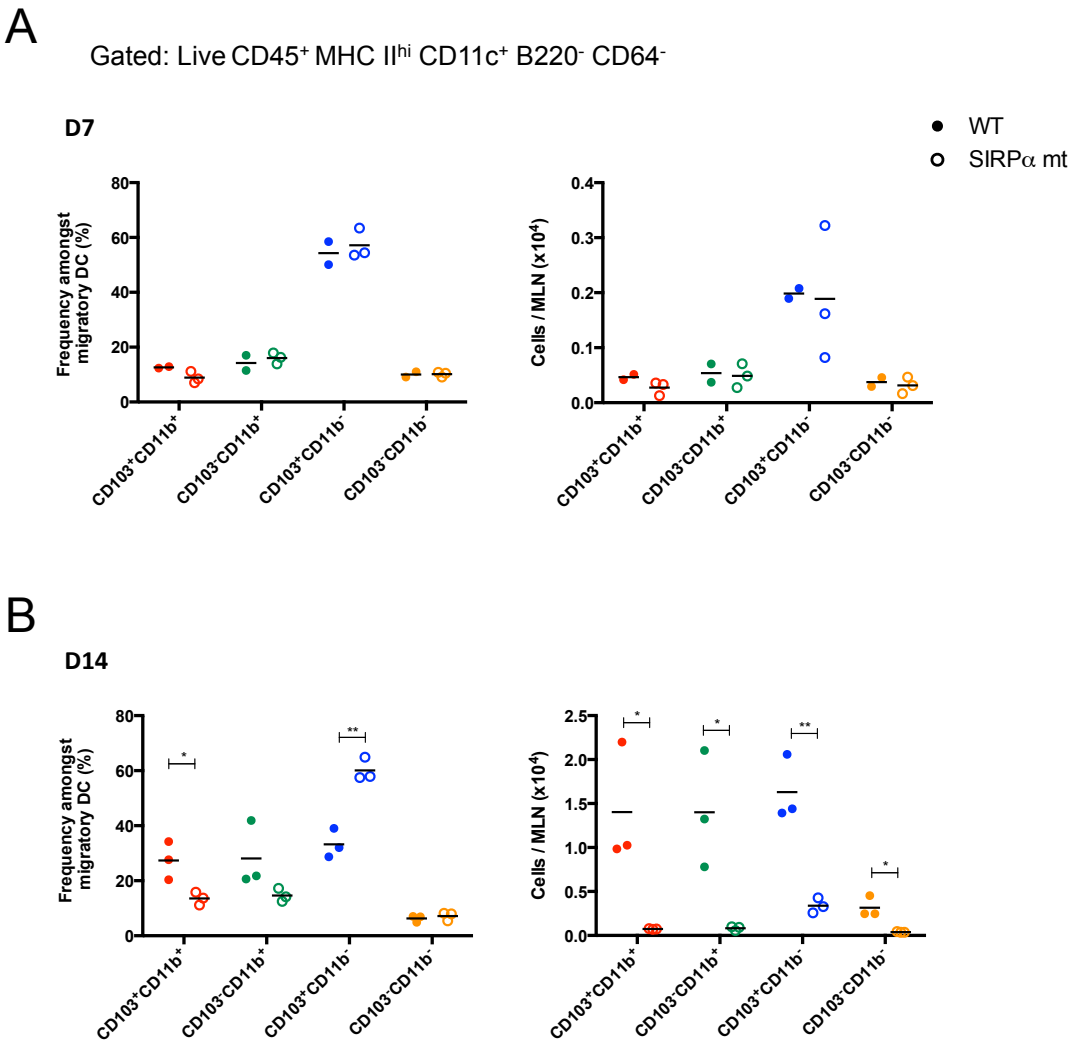

Figure 5.4: Development of migratory DC subsets in the MLN of SIRPα mt mice

MLN cells were isolated from WT and SIRPα mt mice and live MHC II^{hi} CD11c^{+} B220^{-} CD64^{-} migratory DC were analysed for the expression of CD103 and CD11b. Frequencies amongst total migratory DC (left panels) and absolute numbers (right panels) were analysed at **A** D7 and **B** D14. Data are from one experiment with 3-5 animals per group. *p<0.05, **p<0.01, Student's t test.

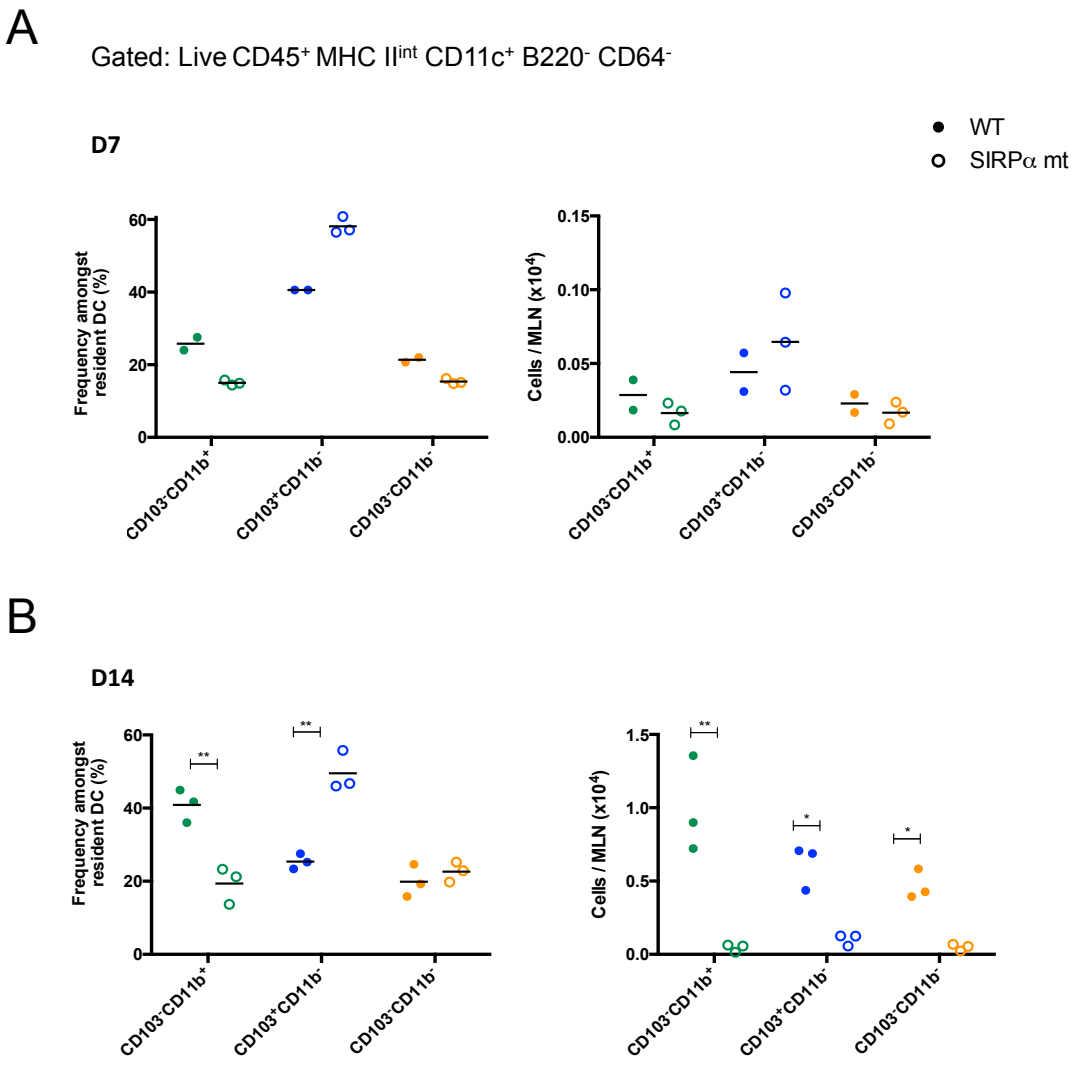

Figure 5.5: Development of resident DC subsets in the MLN of SIRPα mt mice

MLN cells were isolated from WT and SIRPα mt mice and live MHC II^{int} CD11c^{+} B220^{-} CD64^{-} resident DC were analysed for the expression of CD103 and CD11b. Frequencies amongst resident DC (left panels) and absolute numbers (right panels) were analysed at **A** D7 and **B** D14. Data are from one experiment with 3-5 animals per group. *p<0.05, **p<0.01, Student's t test.

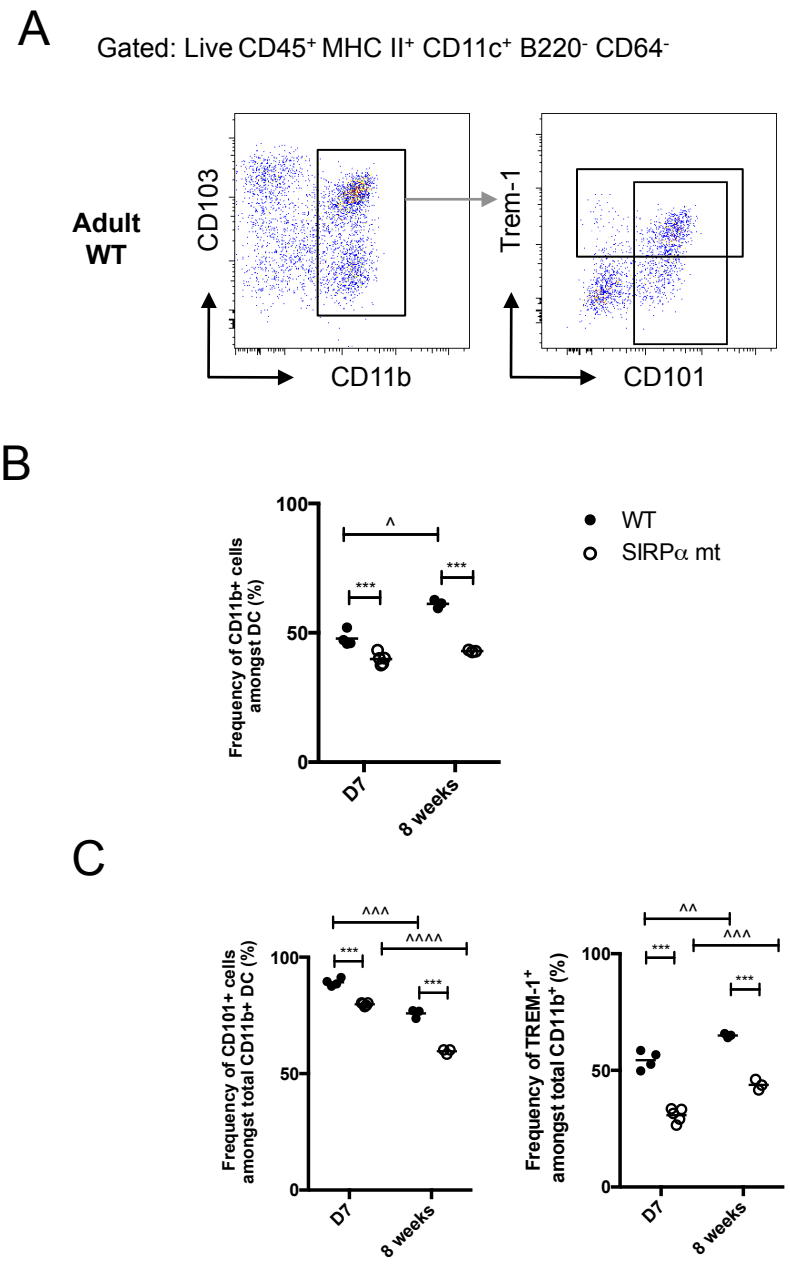

Figure 5.6: Expression of CD101 and Trem-1 by small intestinal DC from SIRPα mt mice at different ages

SI LP cells were isolated from D7 or 8 week old adult WT and SIRPα mt mice and DC identified as single, live CD45$^+$ CD11c$^+$ MHC II$^+$ CD64$^-$ leukocytes. **A** Representative dot plots showing the expression of CD11b and CD103 on DC in adult WT mice (left panel), together with the expression of CD101 and Trem-1 by total CD11b$^+$ DC (right panel). **B** Frequency and absolute numbers of total CD11b$^+$ DC amongst total DC. **C** Frequency of CD101$^+$ (left panel) or Trem-1$^+$ (right panel) cells amongst total CD11b$^+$ DC. Data are from a single experiment with n=4-5. ***p<0.001, ^p<0.05, ^^p<0.01, ^^^p<0.001, ^^^^p<0.000,1 Student's t test.

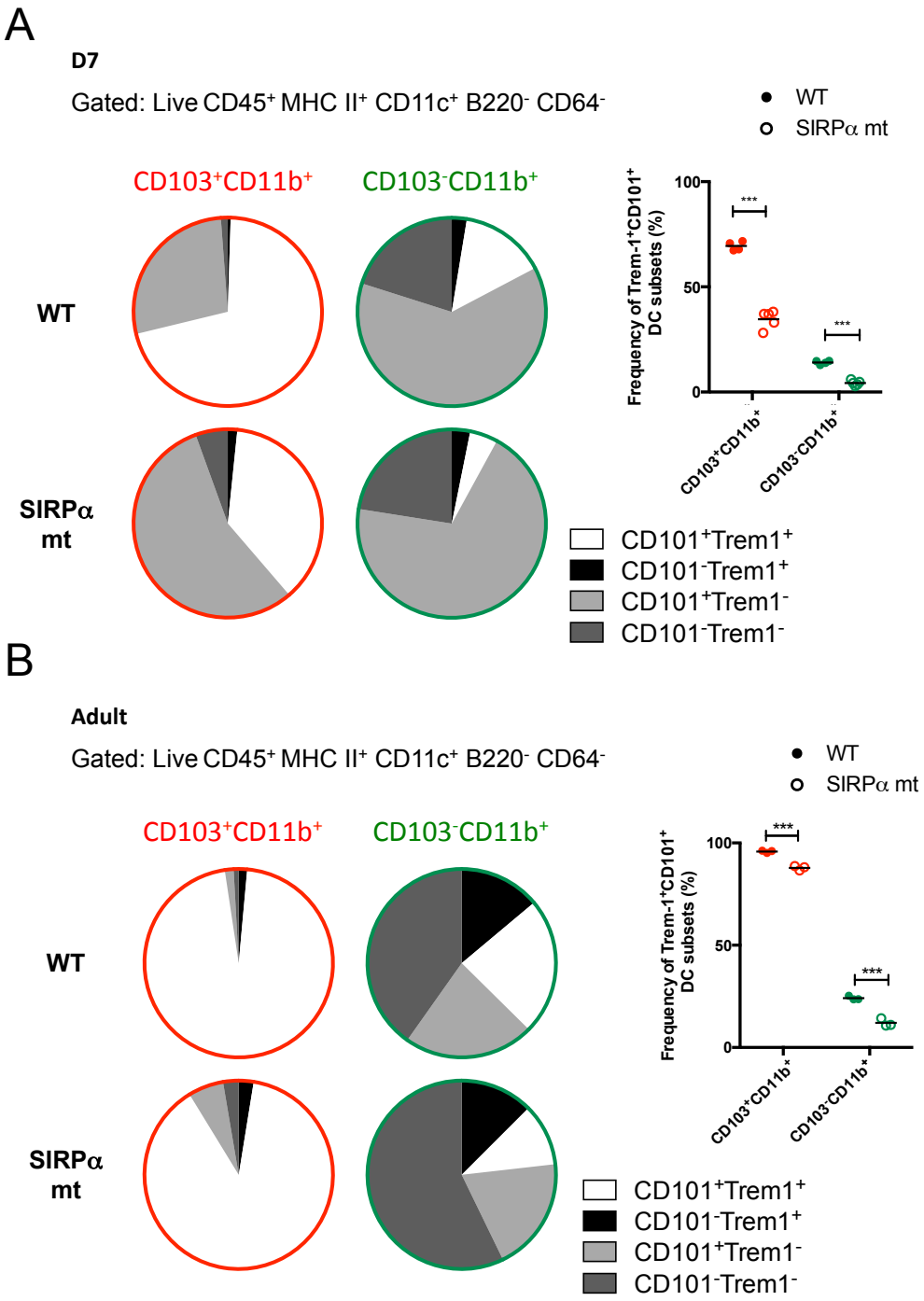

Figure 5.7: Expression of CD101 and Trem-1 by small intestinal DC from SIRPα mt mice at different ages

SI LP cells were isolated from D7 or 8 week old adult WT and SIRPα mt mice and DC identified as single, live CD45+ CD11c+ MHC II+ CD64- leukocytes. The pie-charts represent the proportions of cells expressing CD101 and Trem-1 amongst CD103+CD11b+ (red) or CD103-CD11b+(green) DC and the frequencies of those that are CD101+Trem-1+ (far right panel) for **A** adults and **B** D7 mice. Data are from a single experiment with n=4-5. ***p<0.001, Student's t test.

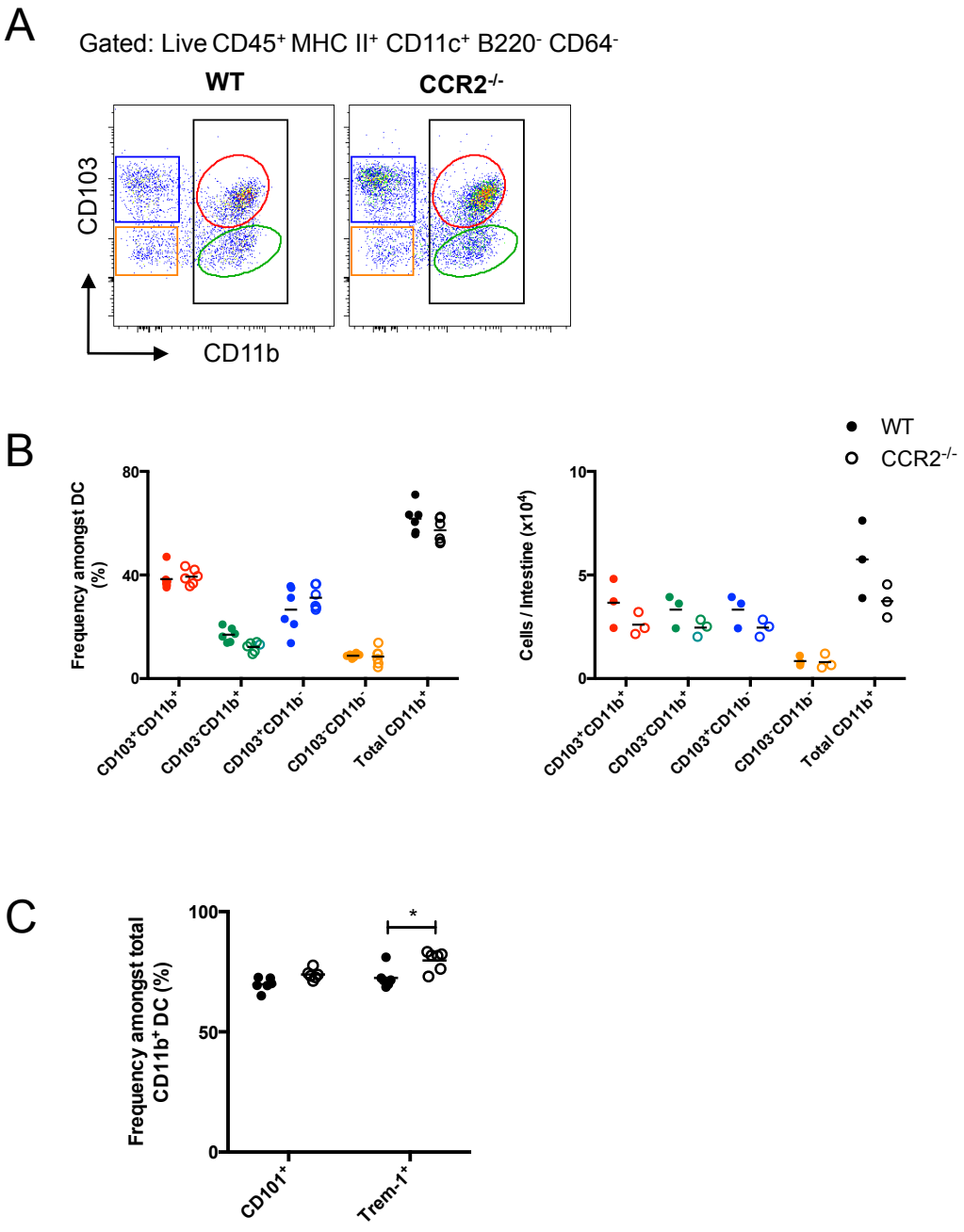

Figure 5.8: CD101 and Trem-1 expression by small intestinal DC from CCR2$^{-/-}$ mice

SI LP cells were isolated from 8 week old adult WT and CCR2$^{-/-}$ mice and DC identified as single, live CD45^{+} CD11c^{+} MHC II^{+} B220^{-} CD64^{-} leukocytes. **A** Representative dot plots showing the expression of CD11b and CD103 on total DC (left panel). **B** Frequencies amongst total DC and absolute numbers of DC subsets or total CD11b^{+} DC amongst total DC. **C** Frequency of CD101^{+} or Trem-1^{+} DC amongst total CD11b^{+} DC. Data are from a single experiment with n=4-5. *p<0.05, Student's t test.

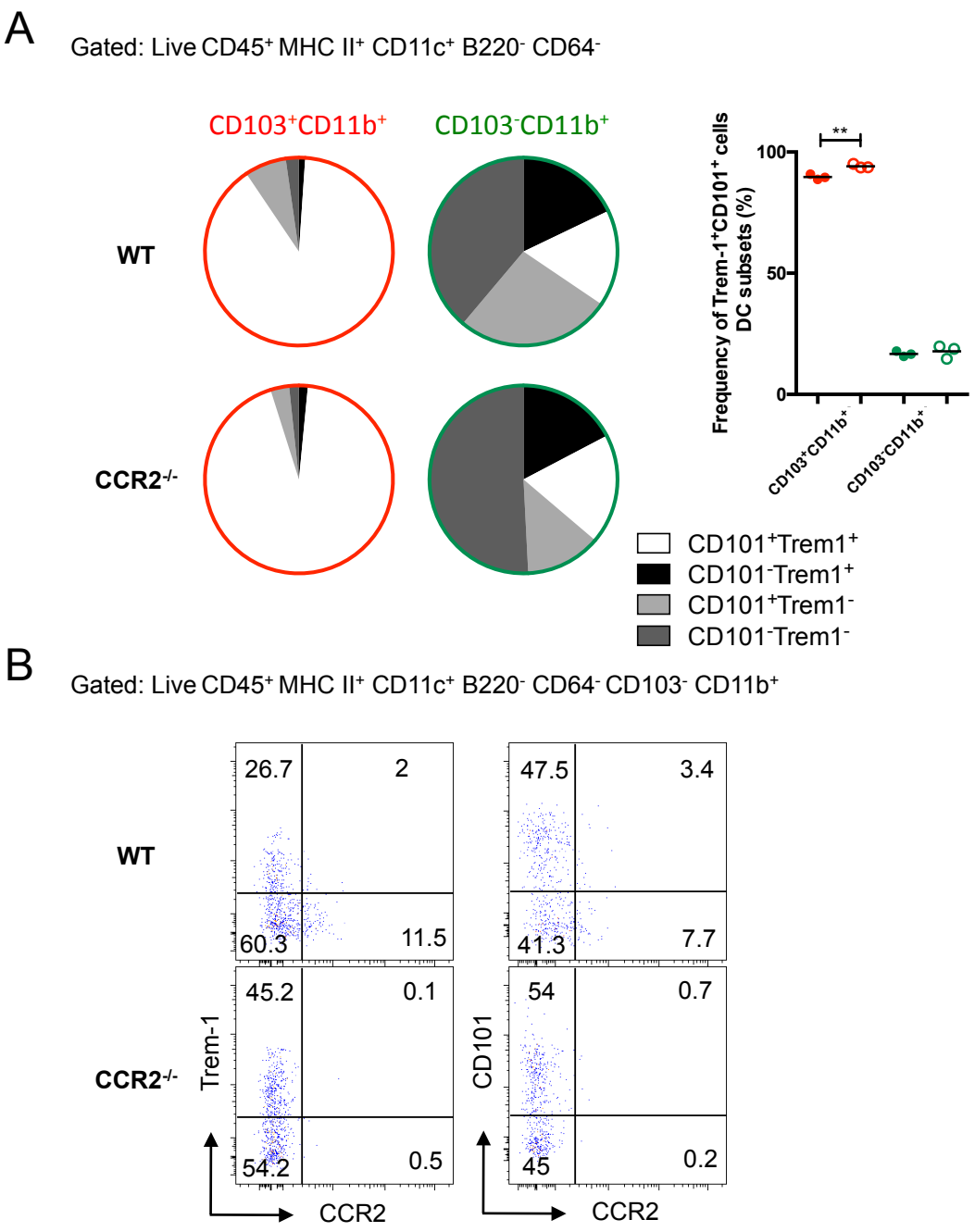

Figure 5.9: CD101 and Trem-1 expression by small intestinal DC from CCR2$^{-/-}$ mice

SI LP cells were isolated from 8-10 week old adult WT and CCR2$^{-/-}$ mice and DC identified as live CD45^{+} CD11c^{+} MHC II^{+} B220^{-} CD64^{-} leukocytes. **A** Pie-charts representing the proportions of cells expressing CD101 and Trem-1 amongst CD103^{+}CD11b^{+} (red) or CD103^{-}CD11b^{+} (green) DC and the frequencies of those that are CD101^{+}Trem-1^{+} (far right panel). **B** Representative dot plots of WT (top panels) or CCR2$^{-/-}$ (bottom panels) CD103^{-}CD11b^{+} DC showing expression of CCR2 vs. Trem-1 or CD101. Data are from a single experiment with n=4-5. **p<0.01, Student's t test.

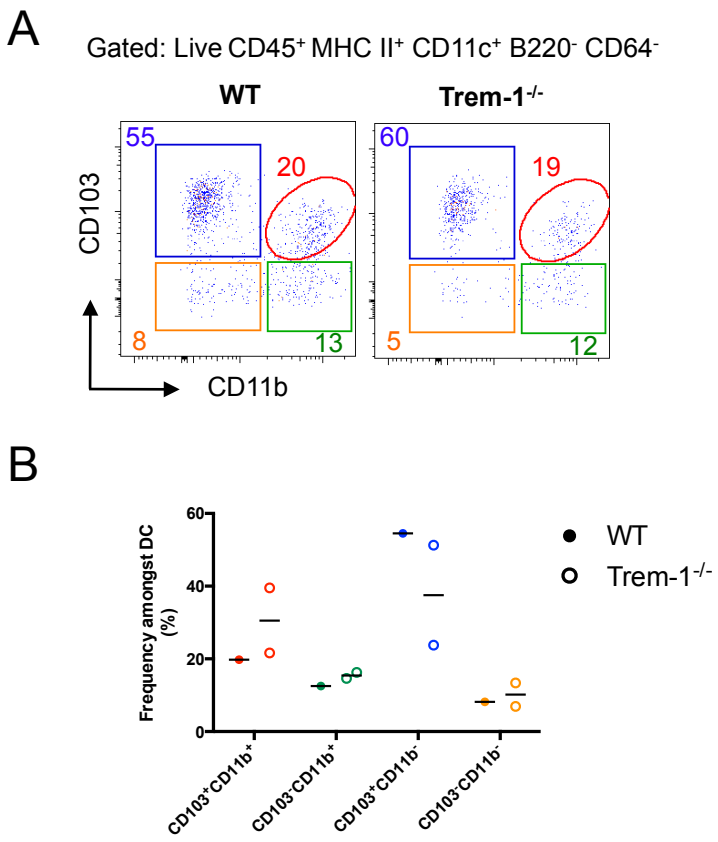

Figure 5.10: CD11b and CD103 expression by small intestinal DC from Trem-1$^{-/-}$ mice

SI LP cells were isolated from 8-10 week old adult WT and Trem-1$^{-/-}$ mice and DC identified as live CD45^{+} CD11c^{+} MHC II^{+} B220^{-} CD64^{-} leukocytes. **A** Representative dot plots showing expression of CD11b and CD103 on DC. **B** Replicate data showing frequency of the four DC subsets amongst total DC. Data are from a single experiment with n=1-2.

A

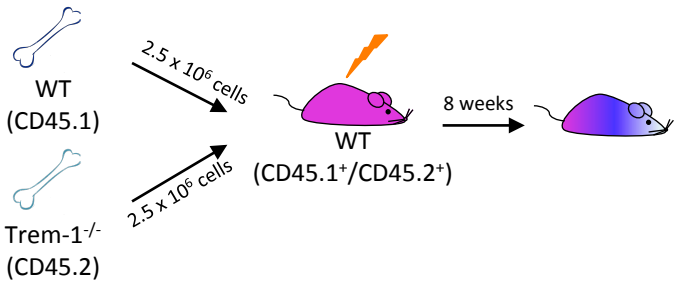

B

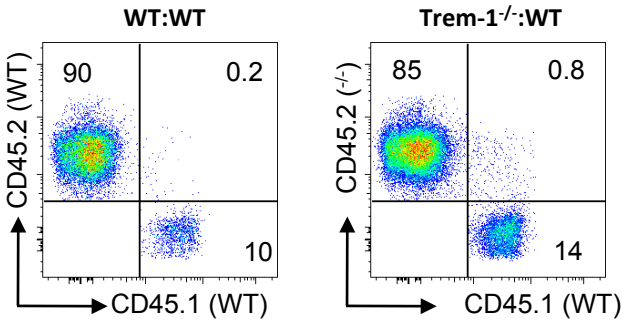

Figure 5.11: Generation of WT:WT or Trem-1$^{-/-}$:WT competitive BM chimeras
A Mixed WT:WT or Trem-1$^{-/-}$:WT BM chimeras were generated by lethally irradiating CD45.1^{+}CD45.2^{+} WT recipient mice and reconstituting with an approximately 90:10 mix of CD45.2^{+} WT and CD45.1^{+} WT or CD45.2^{+} Trem-1$^{-/-}$and CD45.1^{+} WT BM respectively. **B** CD45.1 and CD45.2 expression by the BM precursors used to reconstitute irradiated recipients.

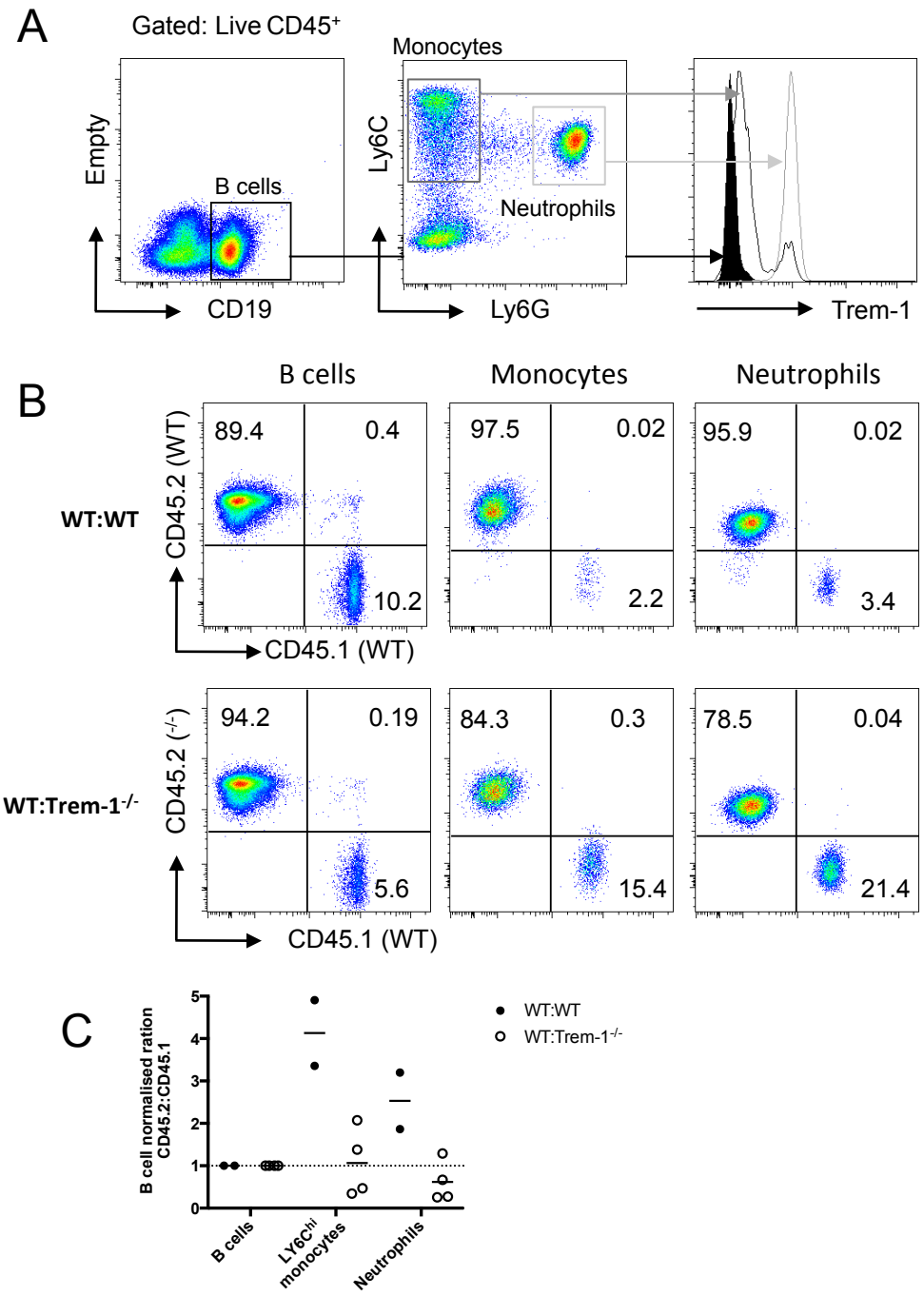

Figure 5.12: Chimerism of leukocyte populations in the blood of WT:WT or WT:Trem-1$^{-/-}$ competitive BM chimeras

Mixed WT:WT or WT:Trem-1$^{-/-}$ BM chimeras were generated as described in Figure 5.11 and chimerism assessed in blood 8 weeks after reconstitution. **A** Trem-1 expression and **B** proportion of CD45.1^{+} cells (WT) and CD45.2^{+} cells (WT or Trem-1$^{-/-}$) amongst B cells, Ly6C^{hi} monocytes and neutrophils from WT:WT chimeras (top panels) or WT:Trem-1$^{-/-}$ chimeras (bottom panels). **C** Ratio of CD45.2:CD45.1 derived cells in WT:WT and WT:Trem-1$^{-/-}$ chimeras normalised to peripheral blood B cells in the same mice. Data are from a single experiment with n=2-4 mice/group.

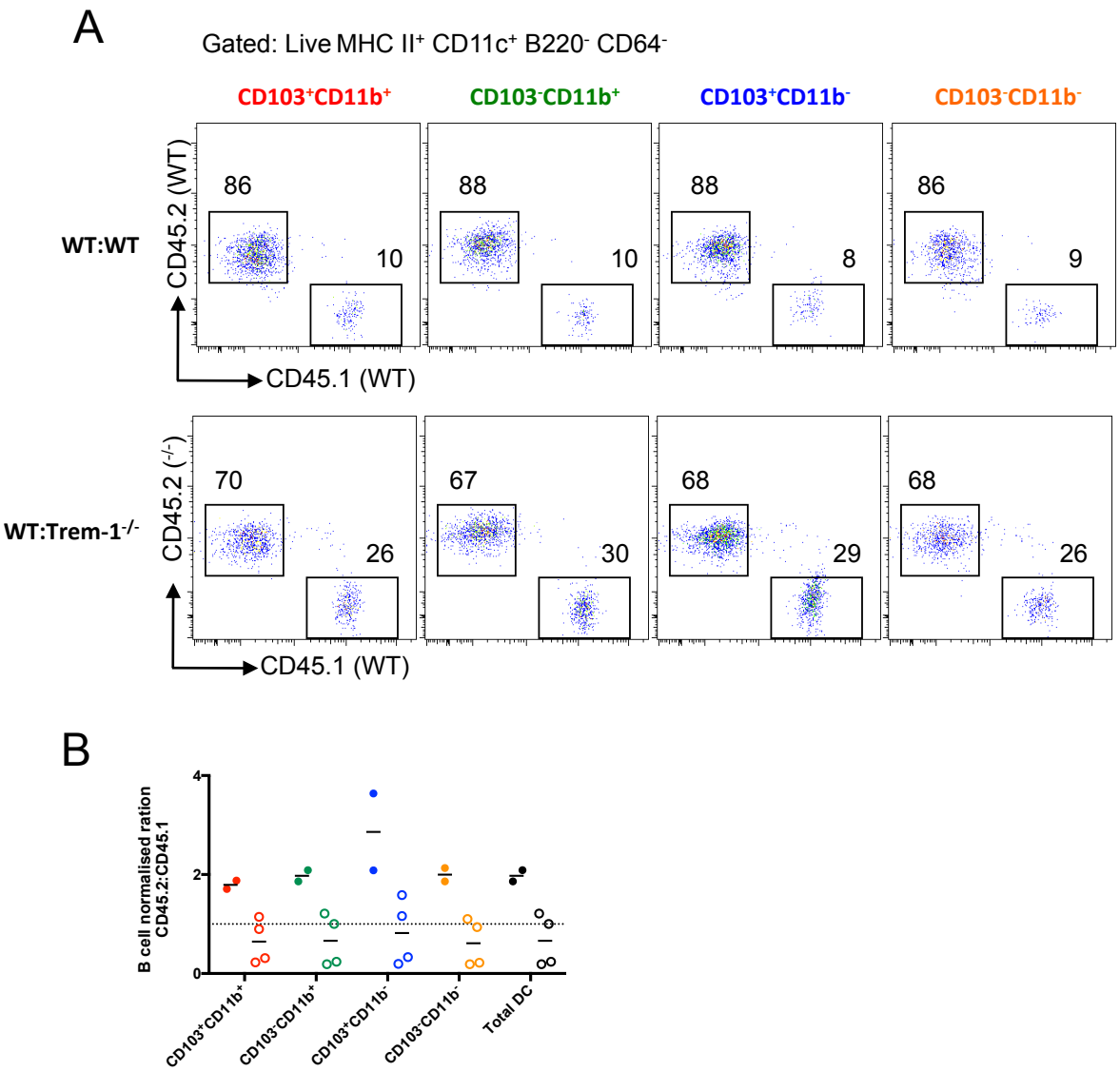

Figure 5.13: DC in the small intestine lamina propria of WT:WT or WT:Trem-1$^{-/-}$ competitive BM chimeras

Mixed WT:WT or WT:Trem-1$^{-/-}$ BM chimeras were generated as described in Figure 5.11 and chimerism assessed 8 weeks after reconstitution. CD11b and CD103 defined subsets amongst live MHC II^{+} CD11c^{+} CD64^{-} DC in SI LP were analysed for CD45.1 and CD45.2 expression and **A** the proportion of CD45.1^{+} cells (WT) and CD45.2^{+} cells (WT or Trem-1$^{-/-}$) amongst DC subsets from WT:WT chimeras (top panels) or WT:Trem-1$^{-/-}$ chimeras (bottom panels) are shown. **B** Ratio of CD45.2:CD45.1 derived cells in WT:WT and WT:Trem-1$^{-/-}$ chimeras normalised to peripheral blood B cells in the same mice. Data are from a single experiment with n=2-4 mice/group.

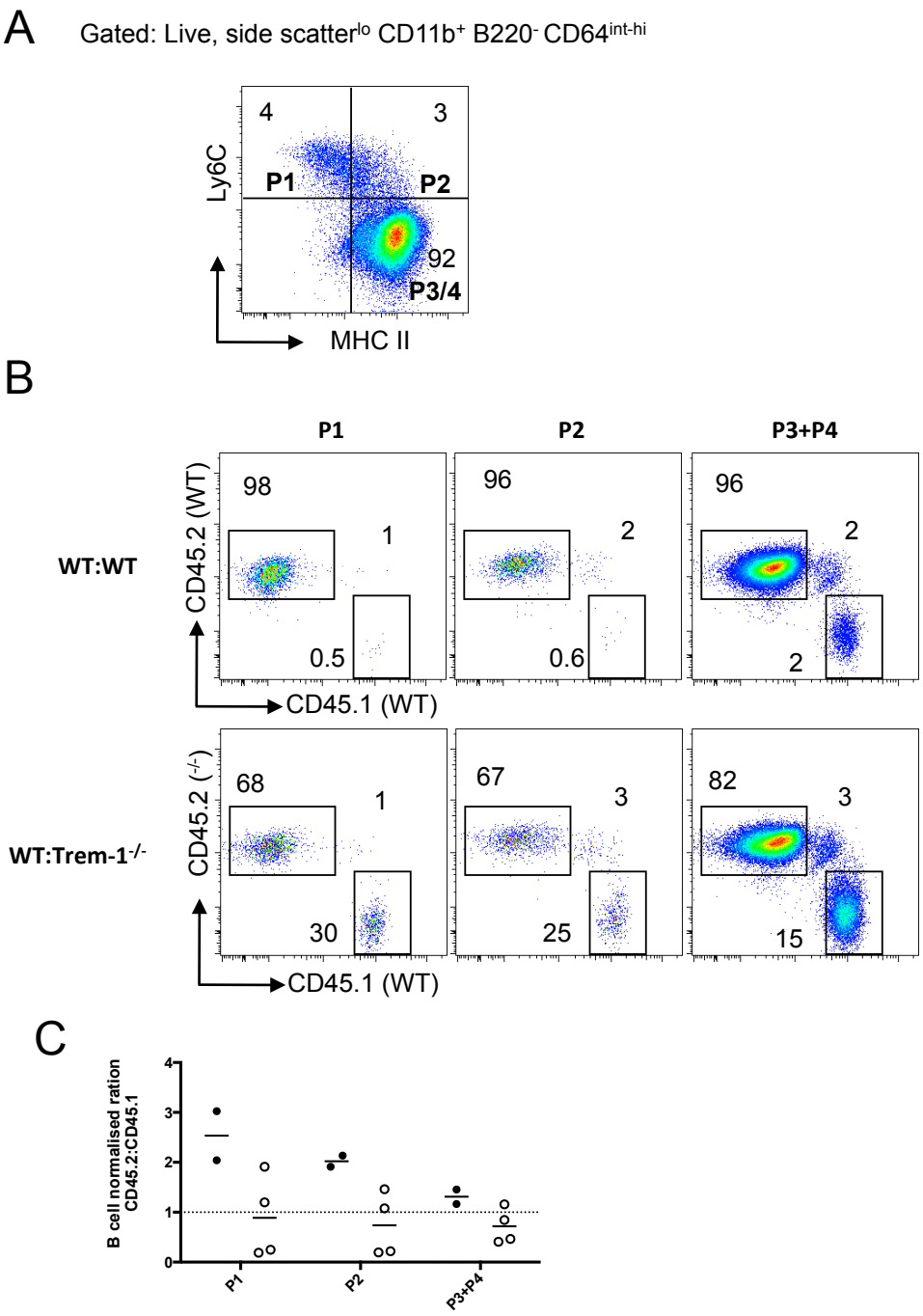

Figure 5.14: Monocytes and macrophages in the small intestinal lamina proporia of WT:WT or WT:Trem-1$^{-/-}$ competitive BM chimeras

Mixed WT:WT or WT:Trem-1$^{-/-}$ BM chimeras were generated as described in Figure 5.11 and chimerism assessed 8 weeks after reconstitution. **A** Monocyte/mϕ subsets amongst live MHC II^{+} CD11c^{+} MP in SI LP were analysed for CD45.1 and CD45.2 expression and **B** the proportion of CD45.1^{+} cells (WT) and CD45.2^{+} cells (WT or Trem-1$^{-/-}$) amongst MP subsets from WT:WT chimeras (top panels) or WT:Trem-1$^{-/-}$ chimeras (bottom panels) are shown. **C** Ratio of CD45.2:CD45.1 derived cells in WT:WT and WT:Trem-1$^{-/-}$ chimeras normalised to peripheral blood B cells in the same mice. Data are from a single experiment with n=2-4 mice/group.

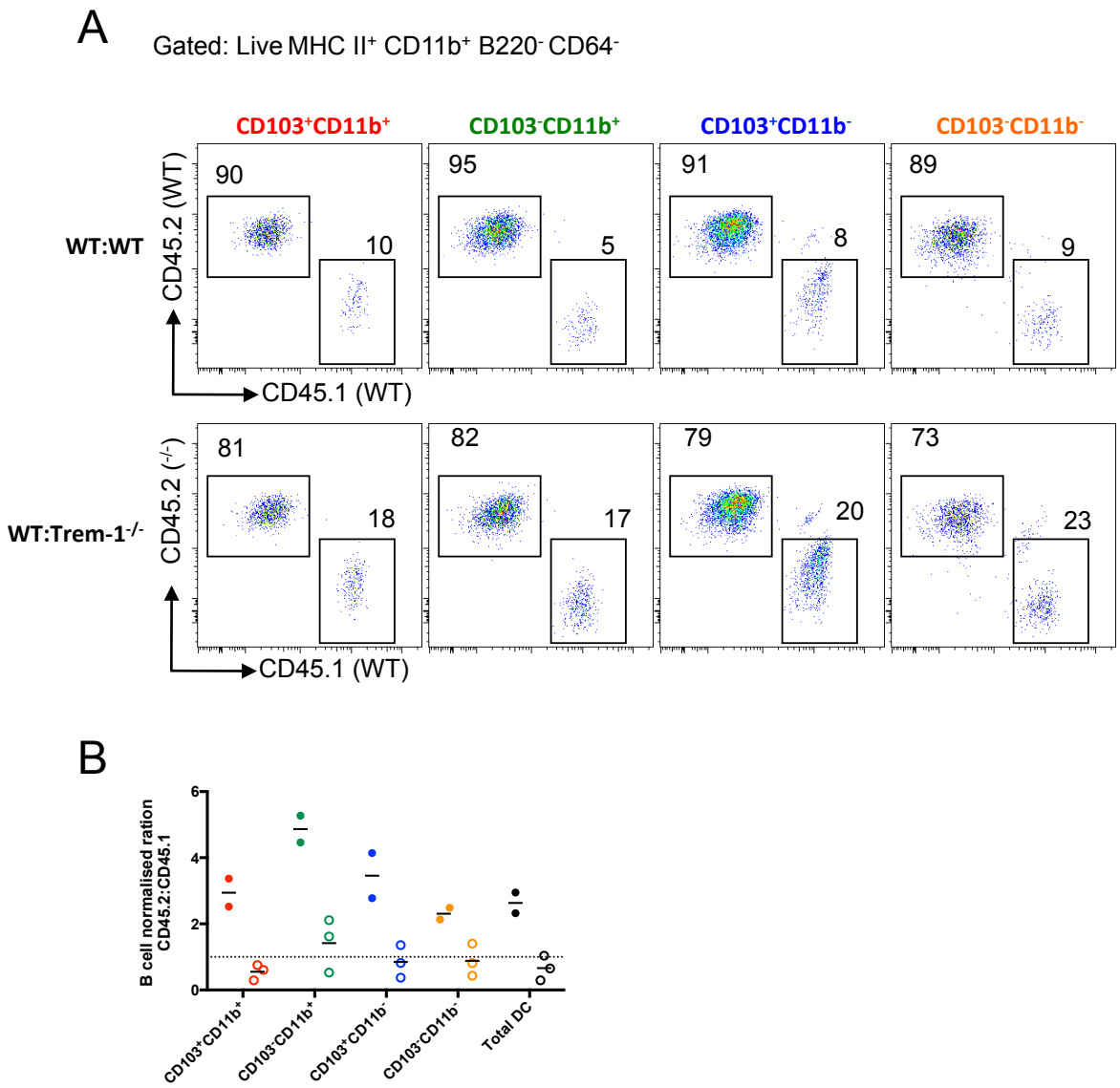

Figure 5.15: DC in the colonic lamina propria of WT:WT or WT:Trem-1$^{-/-}$ competitive BM chimeras

Mixed WT:WT or WT:Trem-1$^{-/-}$ BM chimeras were generated as described in Figure 5.11 and chimerism assessed 8 weeks after reconstitution. CD11b and CD103 defined subsets amongst live MHC II^{+} CD11c^{+} CD64^{-} DC in CLP were analysed for CD45.1 and CD45.2 expression and **A** proportion of CD45.1^{+} cells (WT) and CD45.2^{+} cells (WT or Trem-1$^{-/-}$) amongst DC subsets from WT:WT chimeras (top panels) or WT:Trem-1$^{-/-}$ chimeras (bottom panels) are shown. **B** Ratio of CD45.2:CD45.1 derived cells in WT:WT and WT:Trem-1$^{-/-}$ chimeras normalised to peripheral blood B cells in the same mice. Data are from a single experiment with n=2-4 mice/group.

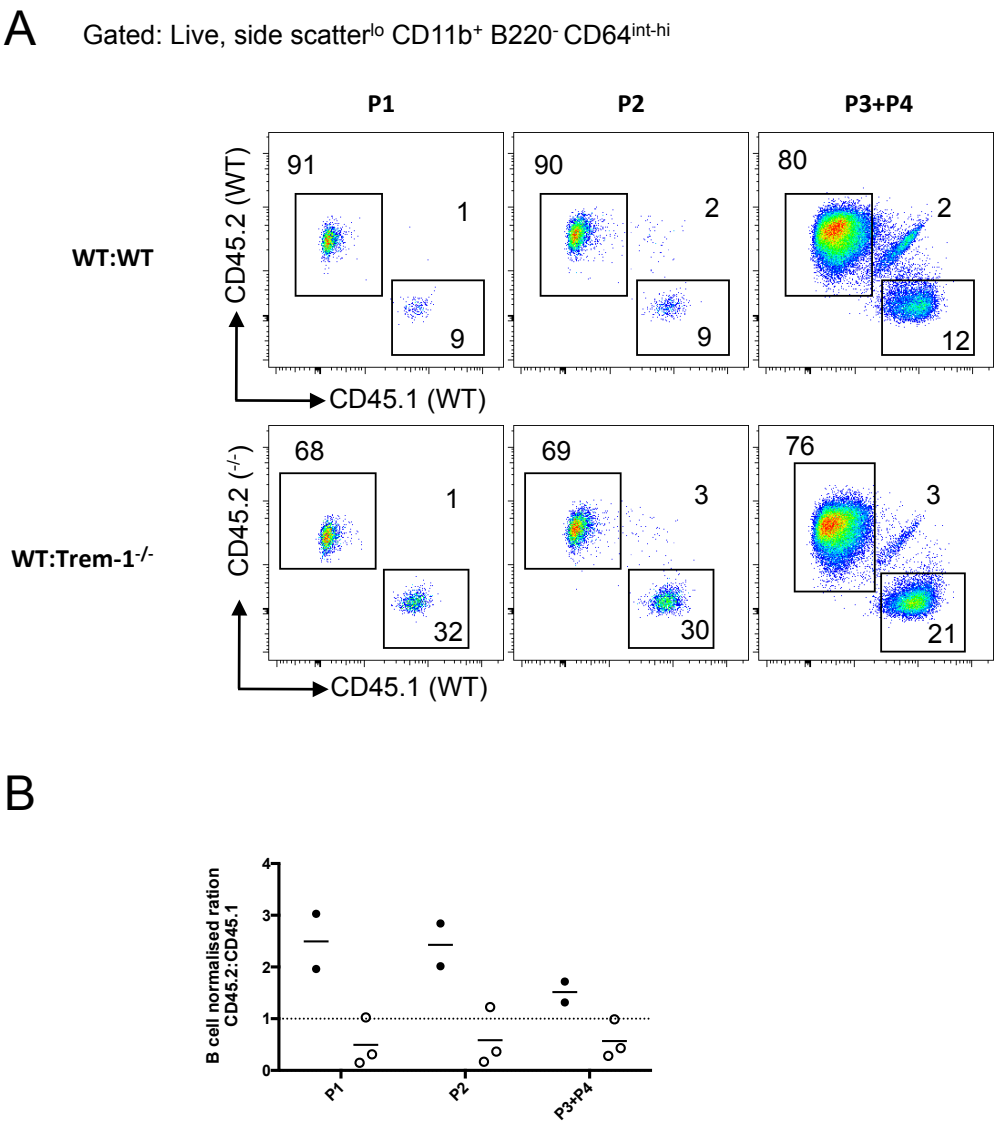

Figure 5.16: Monocytes and macrophages in the colonic lamina propria of WT:WT or WT:Trem-1$^{-/-}$ competitive BM chimeras

Mixed WT:WT or WT:Trem-1$^{-/-}$ BM chimeras were generated as described in Figure 5.11 and chimerism assessed 8 weeks after reconstitution. **A** Monocyte/mϕ subsets amongst live MHC II$^+$ CD11c$^+$ MP in CLP were analysed for CD45.1 and CD45.2 expression and **B** the proportion of CD45.1$^+$ cells (WT) and CD45.2$^+$ cells (WT or Trem-1$^{-/-}$) amongst MP subsets from WT:WT chimeras (top panels) or WT:Trem-1$^{-/-}$ chimeras (bottom panels) are shown. **C** Ratio of CD45.2:CD45.1 derived cells in WT:WT and WT:Trem-1$^{-/-}$ chimeras normalised to peripheral blood B cells in the same mice. Data are from a single experiment with n=2-4 mice/group.

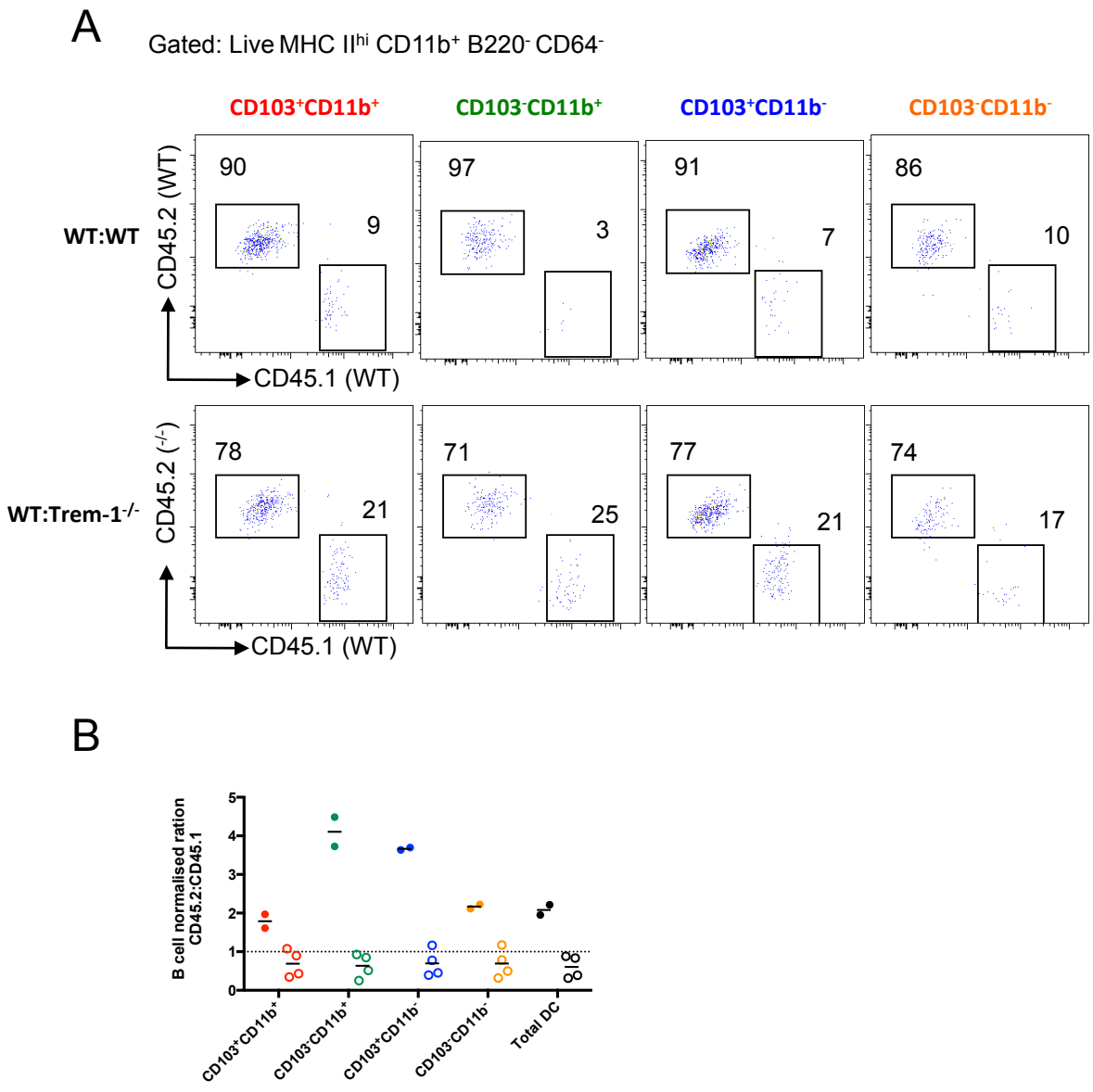

Figure 5.17: Migratory DC in the mesenteric lymph node of WT:WT or WT:Trem-1$^{-/-}$ competitive BM chimeras

Mixed WT:WT or WT:Trem-1$^{-/-}$ BM chimeras were generated as described in Figure 5.11 and chimerism assessed 8 weeks after reconstitution. CD11b and CD103 defined subsets amongst migratory live MHC II^{hi} CD11c^{+} CD64^{-} DC in MLN were analysed for CD45.1 and CD45.2 expression and **A** the proportion of CD45.1^{+} cells (WT) and CD45.2^{+} cells (WT or Trem-1$^{-/-}$) amongst DC subsets from WT:WT chimeras (top panels) or WT:Trem-1$^{-/-}$ chimeras (bottom panels) are shown. **B** Ratio of CD45.2:CD45.1 derived cells in WT:WT and WT:Trem-1$^{-/-}$ chimeras normalised to peripheral blood B cells in the same mice. Data are from a single experiment with n=2-4 mice/group.

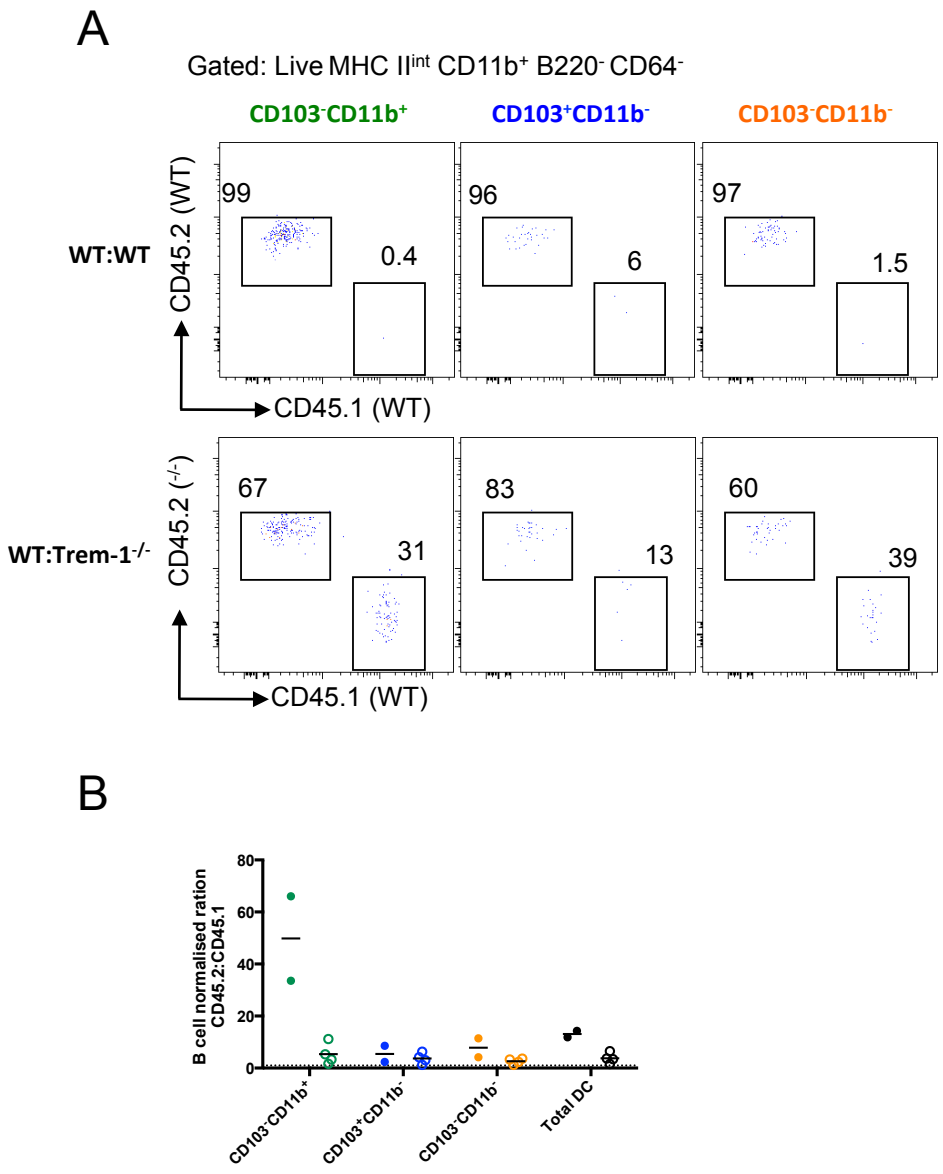

Figure 5.18: Resident DC in the MLN of WT:WT or WT:Trem-1$^{-/-}$ competitive BM chimeras

Mixed WT:WT or WT:Trem-1$^{-/-}$ BM chimeras were generated as described in Figure 5.11 and chimerism assessed 8 weeks after reconstitution. CD11b and CD103 defined subsets amongst resident live MHC II^{int} CD11c^{+} CD64^{-} DC in MLN were analysed for CD45.1 and CD45.2 expression and **A** the proportion of CD45.1^{+} cells (WT) and CD45.2^{+} cells (WT or Trem-1$^{-/-}$) amongst DC subsets from WT:WT chimeras (top panels) or WT:Trem-1$^{-/-}$ chimeras (bottom panels) are shown. **B** Ratio of CD45.2:CD45.1 derived cells in WT:WT and WT:Trem-1$^{-/-}$ chimeras normalised to peripheral blood B cells in the same mice. Data are from a single experiment with n=2-4 mice/group.

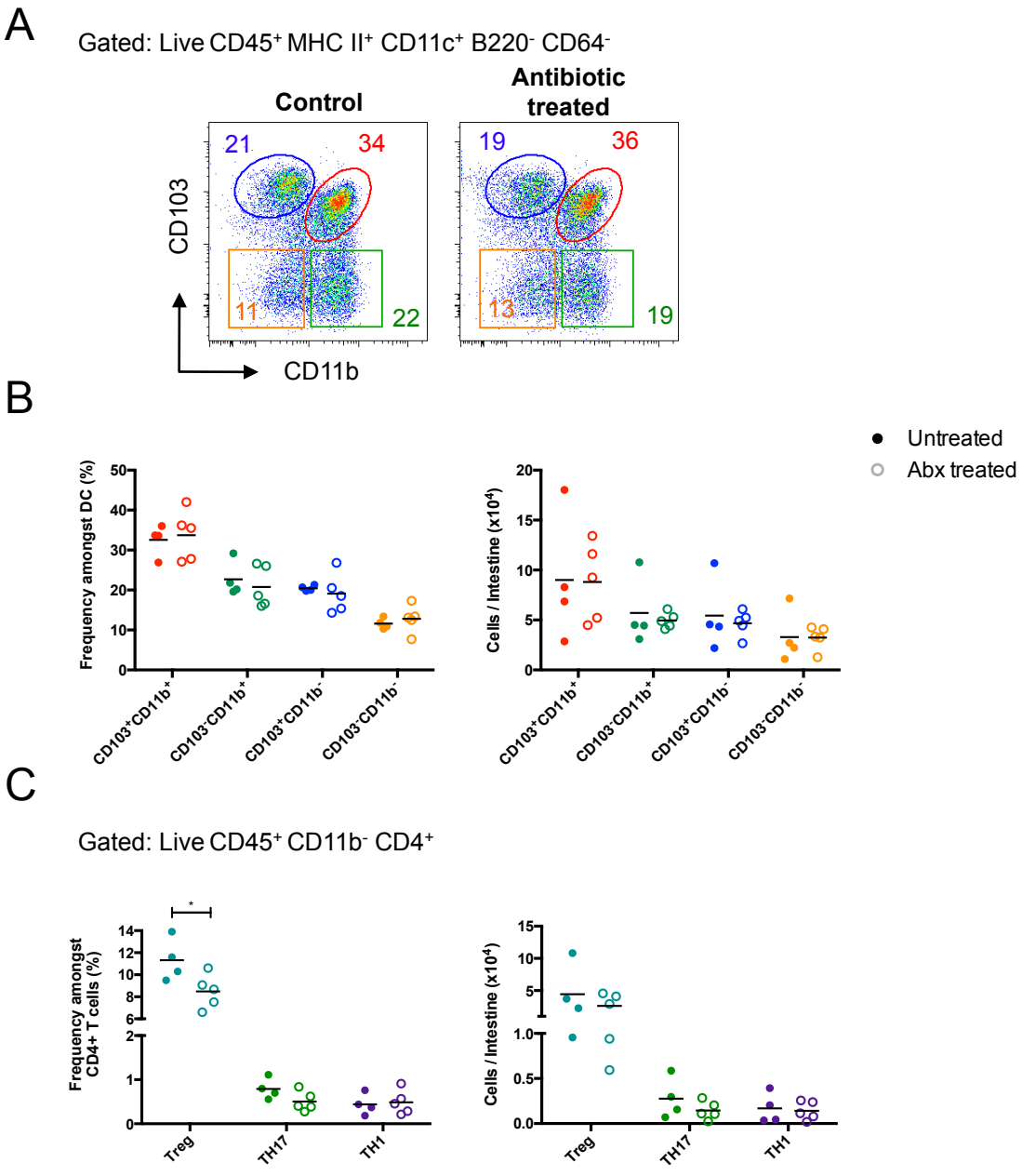

Figure 5.19: Effects of antibiotics on DC and T cells in the small intestinal lamina propria

SI LP cells were isolated from adult WT mice treated with 1 mg/ml Cefoxitin, 1 mg/ml Gentamicin, 1 mg/ml Metronidazol, and 1 mg/ml Vancomycin in the drinking water for two weeks (Abx) or from controls given plain water with sweetener, and DC identified as single live (7-AAD$^-$) CD45$^+$ CD11c$^+$ MHC II$^+$ B220$^-$ CD64$^-$ cells. **A** Representative dot plots showing the expression of CD11b and CD103 by DC from control and antibiotic treated mice. **B** Frequencies amongst total DC (left) and absolute number (right) of DC subsets. **C** Expression of FoxP3, Il-17 and IFNγ by B220$^-$CD3$^+$CD4$^+$ T cells assessed by intracellular cytokine staining. The results shown are frequencies (left) and absolute numbers (right) of Treg, Th17 and Th1 cells. Data are from a single experiment with n=4-5. *p<0.05 Student's t test.

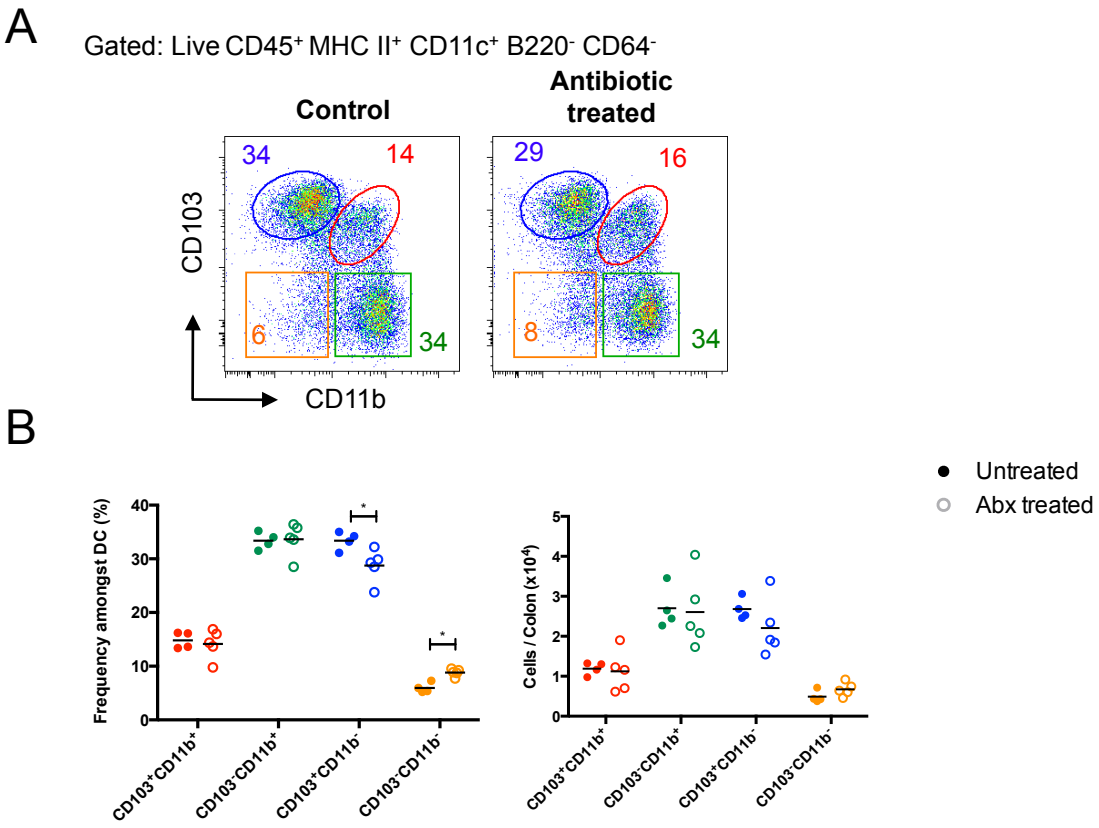

Figure 5.20: Effects of antibiotics on DC in colonic lamina propria

CLP cells were isolated from adult WT mice treated with 1 mg/ml Cefoxitin, 1 mg/ml Gentamicin, 1 mg/ml Metronidazol, and 1 mg/ml Vancomycin in the drinking water for two weeks (Abx) or from controls given plain water with sweetener, and DC identified as single live (7-AAD$^-$) CD45$^+$ CD11c$^+$ MHC II$^+$ B220$^-$ CD64$^-$ cells. **A** Representative dot plots showing the expression of CD11b and CD103 by DC from control and antibiotic treated mice. **B** Frequencies amongst total DC (left) and absolute number (right) of DC subsets. Data are from a single experiment with n=4-5. *p<0.05, Student's t test.

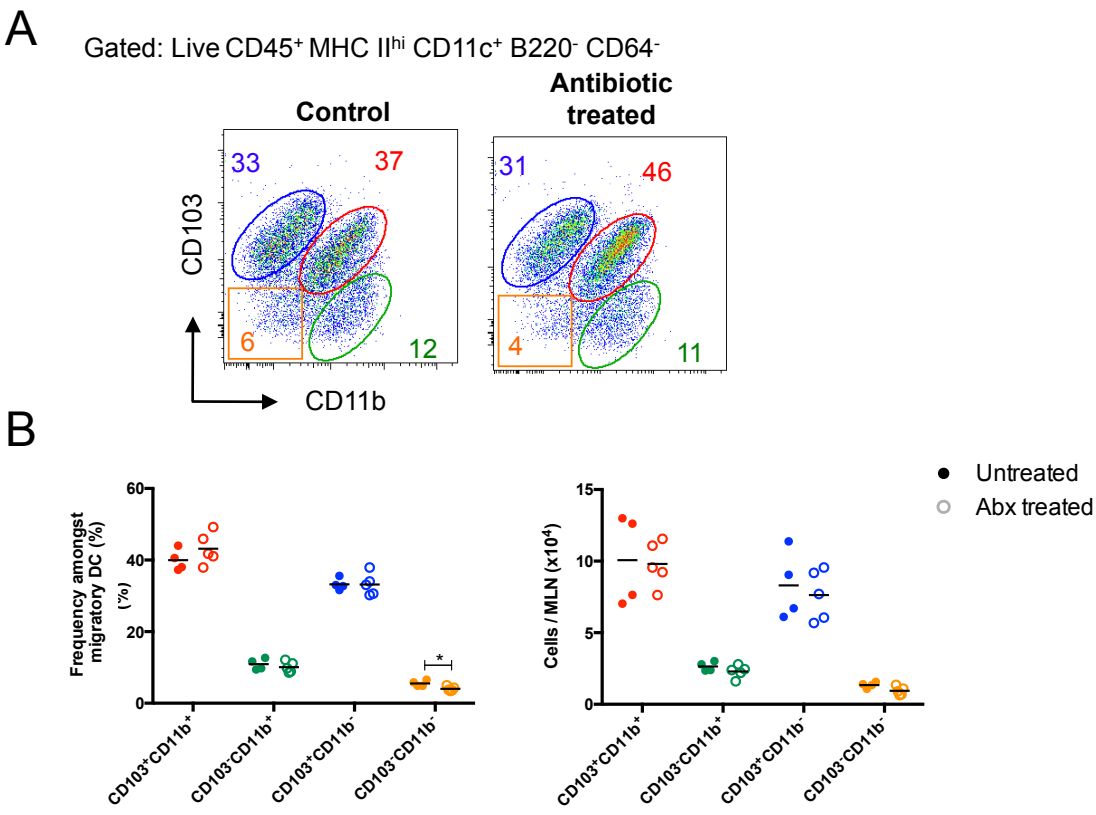

Figure 5.21: Effects of antibiotics on migratory DC in MLN

MLN cells were isolated from adult WT mice treated with 1 mg/ml Cefoxitin, 1 mg/ml Gentamicin, 1 mg/ml Metronidazol, and 1 mg/ml Vancomycin in the drinking water for two weeks (Abx) or from controls given plain water with sweetener, and migratory DC identified as single live (7-AAD$^-$) CD45$^+$ CD11c$^+$ MHC II^{hi} B220$^-$ CD64$^-$ cells. **A** Representative dot plots showing the expression of CD11b and CD103 by migratory DC from control and antibiotic treated mice. **B** Frequencies amongst total migratory DC (left) and absolute number (right) of DC subsets. Data are from a single experiment with n=4-5. *p<0.05, Student's t test.

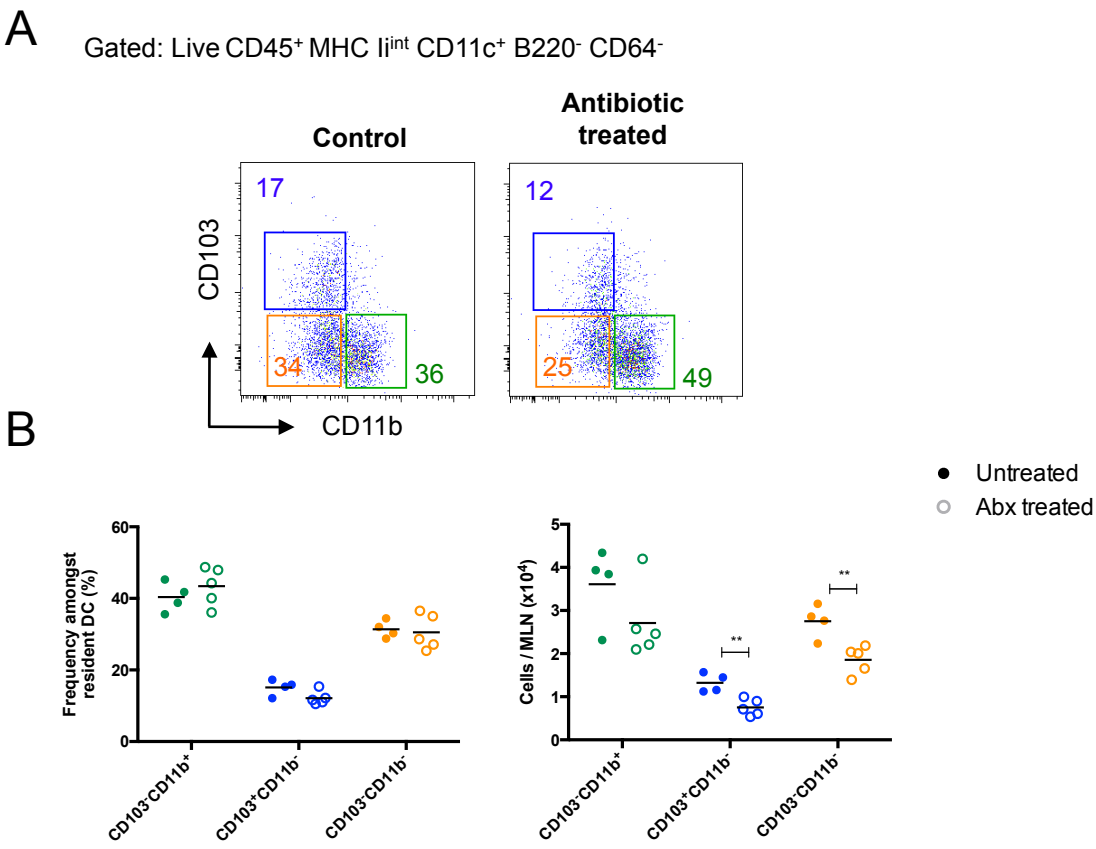

Figure 5.22: Effects of antibiotics on resident DC in MLN

MLN cells were isolated from adult WT mice treated with 1 mg/ml Cefoxitin, 1 mg/ml Gentamicin, 1 mg/ml Metronidazol, and 1 mg/ml Vancomycin in the drinking water for two weeks (Abx) or from controls given plain water with sweetener, and resident DC identified as single live (7-AAD$^-$) CD11c$^+$ MHC II^{int} B220$^-$ CD64$^-$ cells. **A** Representative dot plots showing the expression of CD11b and CD103 by resident DC from control and antibiotic treated mice. **B** Frequencies amongst total resident DC (left) and absolute number (right) of DC subsets. Data are from a single experiment with n=4-5. **p<0.01, Student's t test.

A

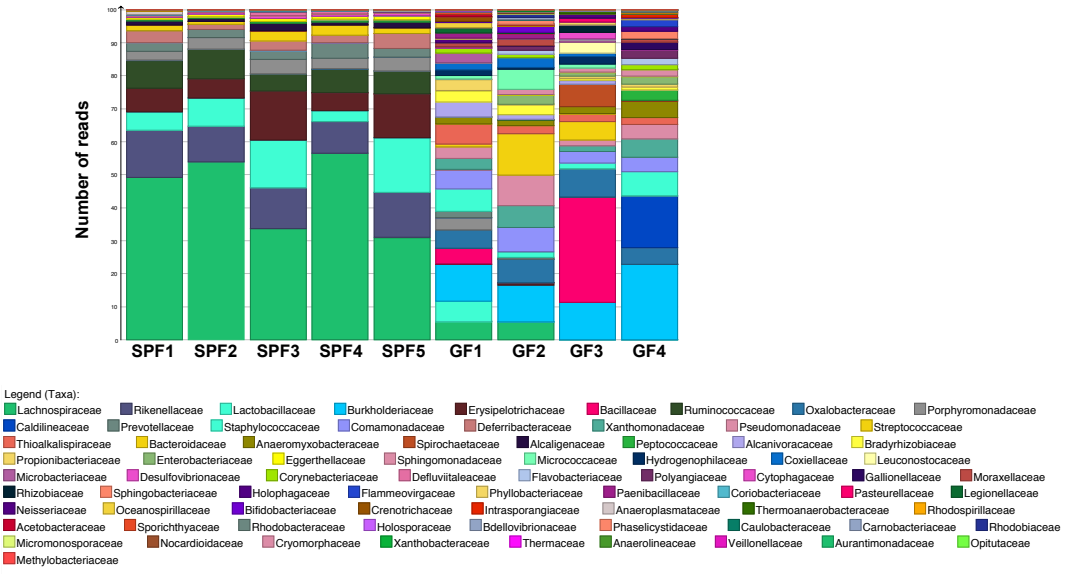

B

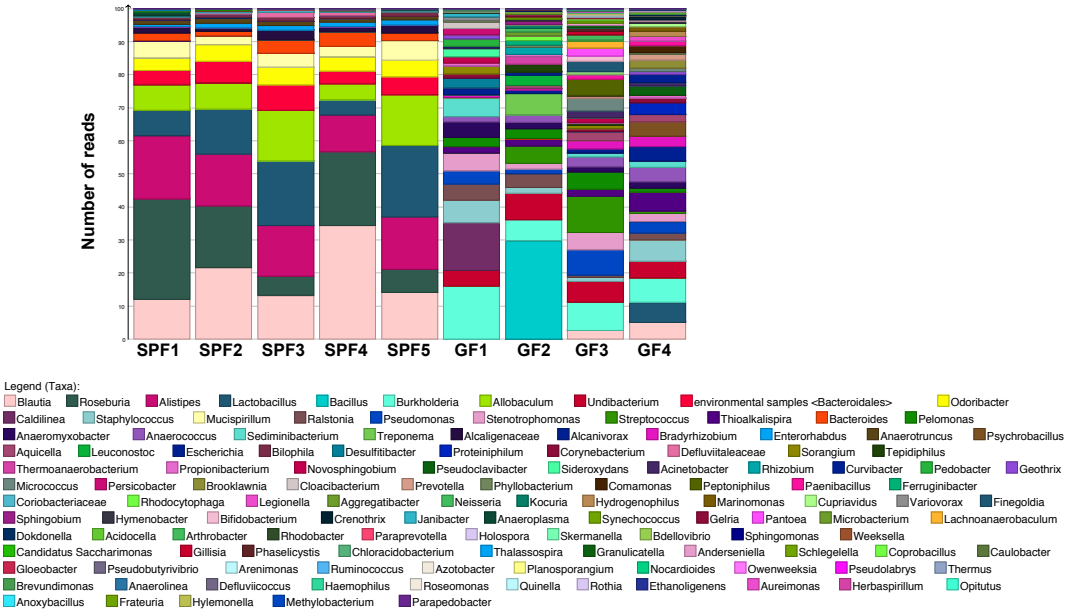

Figure 5.23: 16s analysis of Germ Free and SPF caeca

Caecal contents were taken for 16s analysis from GF animals used in experiments alongside SPF mice housed at the facility in Norwich. The taxonomy profile is shown as the number of reads for the specific bacterial sequence at **A** family and **B** genus level. With thanks to Lindsay Hall and Suparna Mitra at IFR, Norwich for providing me with these data.

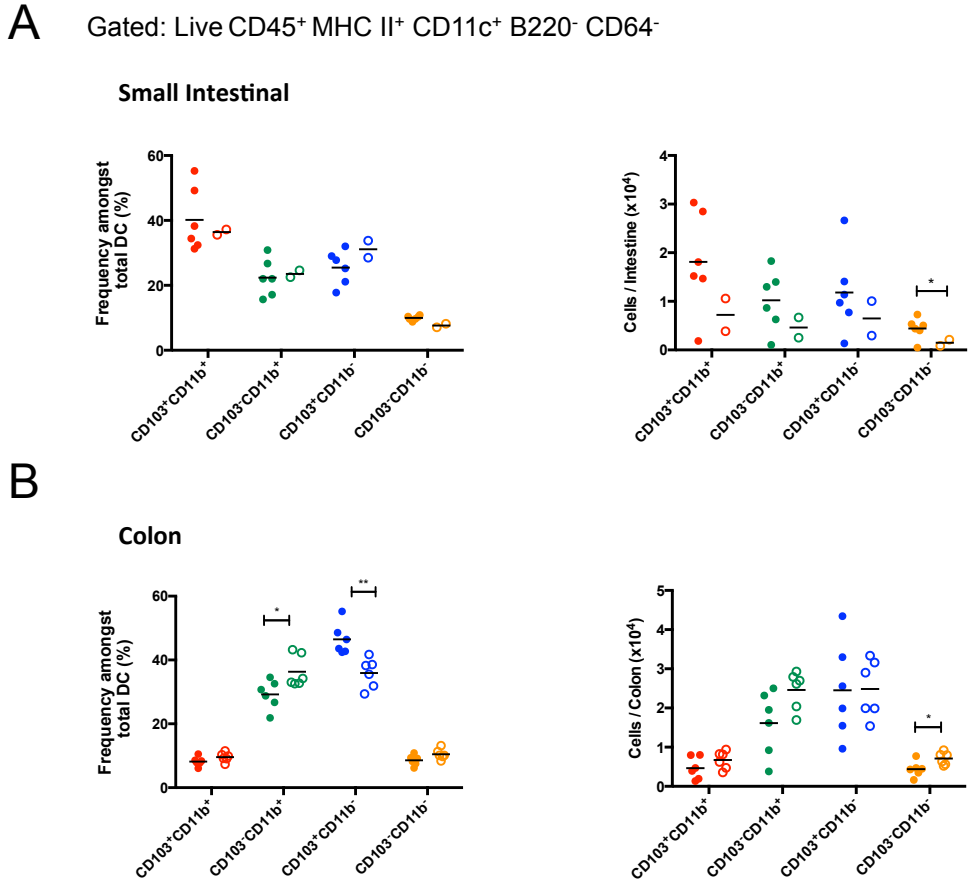

Figure 5.24: Intestinal DC subsets in germ free mice

Cells were isolated from adult conventional or germ free mice and DC identified as live (7-AAD$^-$) CD45$^+$ CD11c$^+$ MHC II$^+$ B220$^-$ CD64$^-$ cells. Frequencies amongst total DC (left) and absolute number (right) of DC subsets from **A** SI LP or **B** CLP. Data are from a single experiment with n=2-6. *p<0.05, **p<0.01, Student's t test.

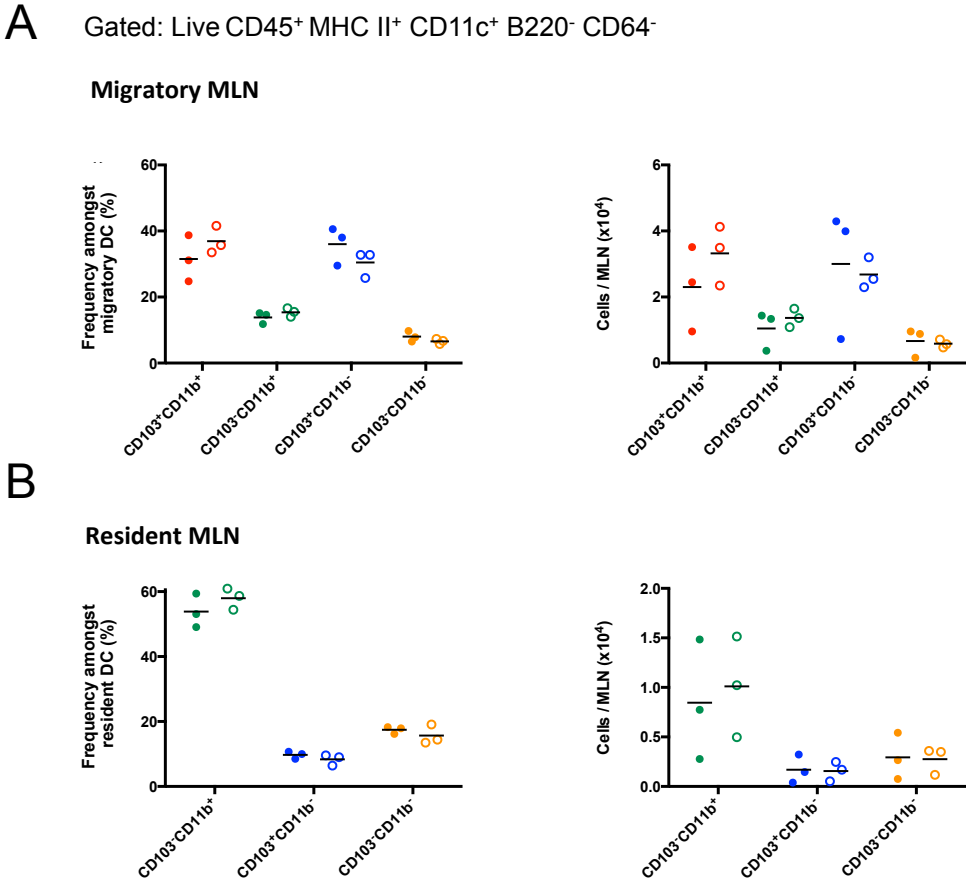

Figure 5.25: Intestinal DC subsets in the mesenteric lymph nodes of germ free mice

Cells were isolated from adult WT or germ free mice, and DC identified as live (7-AAD$^-$) CD11c$^+$ MHC II$^+$ B220$^-$ CD64$^-$ cells. Frequencies amongst total migratory or resident DC (left) and absolute number (right) of DC subsets from **A** MHC II^{hi} migratory or **B** MHC II^{int} resident DC. Data are from a single experiment with n=3.

Chapter 6

General Discussion

6.1 Introduction

The constant pressure on the intestinal immune system to induce tolerance to harmless antigens from commensal bacteria and dietary constituents, or to mount an active immune response against harmful pathogens leads to great complexity. DC are the link between the 'outside' luminal world and the 'inside' adaptive immune response. Until recently, the distinctions between DC and mϕ, the other main antigen presenting cell in the intestine, have been largely ignored, leading to misunderstanding of their exact roles in the intestinal immune system. The main differences between the two cell types is that DC migrate to the MLN and can induce an adaptive immune response by presenting antigen to naïve T cells, whereas mϕ remain sessile in the LP, scavenging pathogens and damaged cells as well as maintaining epithelial barrier integrity (Cerovic et al., 2014a). With the increasing clarity of the differences between these two cell types, the main aim of my thesis was to analyse the different subsets of DC in the intestine, paying particular attention to how the populations changed from birth into adulthood and trying to understand some of the pathways involved in their development.

When I began my PhD, it had recently been shown that MHC II and CD11c were insufficient to distinguish between DC and mϕ in the intestinal LP, with additional markers such as CD64 being required (Bain et al., 2013; Tamoutounour et al., 2012). Work by a number of groups, including a previous PhD student in the laboratory, Charlotte Scott, exploited these insights to develop rigorous gating strategies that showed there were four genuine subsets of DC in the intestine based on the expression of CD11b and CD103. This had revealed that the $CD103^+$ population previously thought to be homogeneous, contained both $CD11b^+$ and $CD11b^-$ subsets. In addition, presence of genuine $CD103^-$ subsets, previously included with mϕ, was established (Cerovic et al., 2014a; Denning et al., 2011; Schlitzer et al., 2013; Scott et al., 2011).

6.2 The DC landscape changes with age

In chapter 4, I showed how the intestinal DC subsets changed relative to one another from birth into adulthood, something that had not previously been explored. The most interesting finding was that although DC were present in the SI LP before birth, $CD103^+CD11b^+$ DC were rare at birth, and their numbers only slowly increased with age until they became the most dominant population by D28. Interestingly, although ~10% of $CD103^+CD11b^+$ DC were seen among the migratory DC at D1, their proportions did not increase further until D14, around the time that mice begin to ingest solid food to supplement their main milk diet. In contrast, the proportion of $CD103^-CD11b^+$ DC increased earlier and then fell as the proportion of $CD103^+CD11b^+$ DC increased, suggesting a reciprocal relationship between the subsets. These changes were mirrored amongst the migratory DC in the MLN although were delayed in this tissue, consistent with the need for DC to enter from afferent lymph. The same pattern was observed in the CLP, though $CD103^+CD11b^+$ DC are less frequent in this site. In contrast to this pattern amongst $CD11b^+$ subsets, $CD103^+CD11b^-$ DC were already abundant in both the SI LP and CLP before birth and although their absolute numbers increased, their proportions behaved independently of other subsets.

There have been few studies applying modern methodology to investigate how the immune system develops in the neonatal intestine at the cellular level. A recent detailed report showed that there was defective activation of $CD4^+$ T cells in the intestine early in life, partially as a result of an active suppression mechanism. Although these authors speculated that these features might be related to defects in antigen presentation, they showed that the numbers of DC and mϕ did not seem to change after birth. Although this contrasts with my own work, Torow *et al.* measured cell numbers as a proportion of total $CD45^+$ cells, of which DC and mϕ make up a very small proportion. Thus they had failed to observe subtle changes in these populations, especially in DC subsets (Torow et al., 2015).

The processes responsible for driving the appearance of DC in the neonatal intestine remain to be defined, as do the mechanisms involved in the development of the different subsets. Many factors change in the immune system and intestine early in

life, including the colonisation of the microbiota, presence of breast milk, changes in the diet at weaning, structural maturation of the mucosa, hormones etc. Perhaps the most obvious one is the rapid exposure to microbes which occurs at birth due to the maternal vaginal and faecal microbiotas (Francino, 2014). The subsequent establishment and diversification of the microbiota may be one way in which DC differentiation can be influenced in the intestine during this time, although my experiment with antibiotics in adults might argue against this (see below). The question then arises of how DC are already present in the LP and migratory compartment in the MLN at birth or just after. The likelihood that bacteria are present *in utero* (Francino, 2014) is one possibility, alternatively is that constitutive migration of DC carrying self antigen from the embryonic intestine leads to their presence in the MLN from early in life (Huang et al., 2000).

Another hypothesis for the differential appearance of DC subsets in the intestine is that each may have a distinct precursor whose development and or emigration from the BM occurs at different times. Although all cDC originate from a common precursor, recent evidence suggests there may be specific precursors already committed to the cDC1 or cDC2 lineage (Schlitzer et al., 2015; Zeng et al., 2012). This could explain the differential appearance of DC subsets as they would likely be under the control of different external factors promoting their differentiation at different times. To test this, single cell analysis of individual DC subsets and precursors could be performed to assess if there are common transcriptional clusters between the different gut DC susbets.

As I wasn't able to analyse pre-DC in this way, I examined whether the expression of genes involved in DC development might correlate with the appearance of the different subsets after birth. CSF-2 is required for the development of $CD103^{+}CD11b^{-}$ DC in tissues apart from the intestine, and for the development of intestinal $CD103^{+}CD11b^{+}$ DC (Greter et al., 2012). Although my results suggested there might be a trend towards a decrease in *Csf2ra* expression by all DC subsets as the mice aged, these differences were not significant, and in general, there was no obvious pattern of change in *Csf2ra* expression between the DC subsets over time.

$CD103^+CD11b^+$ DC have a selective requirement for IRF4 signalling in development, with both $CD11b^+$ DC subsets expressing high levels of IRF4 protein in adults (Persson et al., 2013b). However, the only significant difference I found was that $CD103^+CD11b^-$ DC expressed significantly more *Irf4* than $CD103^-CD11b^+$ DC on D14. The reasons for this discrepancy are not clear. *Tgfbr1* expression was studied as recent work in our laboratory has shown that CD11c-Cre.*Tgfbr1*$^{fl/fl}$ mice lacked $CD103^+CD11b^+$ DC selectively, but had an increased proportion of $CD103^-CD11b^+$ DC, suggesting that TGFβ might control the transition between these subsets. TGFβ has previously been shown to be important on splenic cDC function, but not required for their development (Laouar et al., 2005; Strobl and Knapp, 1999). On the other hand, Langerhans cells, (which, although not strictly DC, share some of their functional properties) do require TGFβ for their development (Zahner et al., 2011). I hypothesised that increased levels of *Tgfbr1* in $CD103^-CD11b^+$ DC might accompany the expansion of $CD103^+CD11b^+$ DC around D14. There was indeed an increase in transcription of *Tgfbr1* at D14, but this was only significant for $CD103^-CD11b^+$ DC, with a small increase in $CD103^+CD11b^+$ DC.

Lastly, I examined the expression of *Rara*. Intestinal $CD103^+$ DC not only produce RA, but RA can promote the development of $CD103^+CD11b^+$ DC (Agace and Persson, 2012). Unexpectedly however, the only population I found to express significant levels of *Rara* were $CD103^+CD11b^-$ DC and this was seen at all time points. Although it is possible that one of the other receptors for RA might have allowed discrimination between the subsets, it has been reported that RARα is the most highly expressed in intestinal $CD103^+$ DC, followed by RARγ while RARβ is barely detectable (Jaensson-Gyllenbäck et al., 2011). Therefore it seems likely that RARα should have been a useful marker. Together, these analyses of gene expression on the different DC subsets at different ages are largely inconclusive and were subject to considerable variability. This may reflect the difficulties I had in sorting suitable numbers of the DC subsets from neonatal intestine and unfortunately, for this reason I was also unable to repeat these experiments, though it would be worth pursuing.

These molecules were measured at the mRNA level due to low cell numbers and lack of robust antibodies to some of these molecules, though it would be interesting to

understand how these genes are regulated in the production of protein at the different ages. To extend these findings further, other genes such as *Irf8* (involved in $CD103^+CD11b^-$DC differentiation (Luda et al., 2016)) as well as CCR9 and $\alpha4\beta7$, reported to be present on the intestine specific pre-DC (Zeng et al., 2012) should be analysed. Other receptors that could also change with age are the TLRs, differentially expressed amongst the DC subsets and thought to provide the DC subsets with their specific ability to prime naïve T cells with different effector responses. Co-stimulatory molecules as well would help to determine the functional capacity of the DC in neonates and how these might change with age. To complement these findings, I would measure vitamin A, retinol, RA and CSF-2 in the mucosa itself as it might be that in lieu of changes in the receptors on DC subsets, the developmental patterns of the DC subsets arise from the availability of the factors themselves.

There were also changes in the relative numbers of DC subsets amongst blood derived resident MLN DC, although the populations are less complex than in the LP, with $CD103^+CD11b^+$ DC essentially being almost absent, apart from a few contaminants from the migratory compartment. As in the LP, $CD103^+CD11b^-$ DC were the most prevalent subset amongst resident MLN DC at birth, although from D3 onwards the $CD103^-CD11b^+$ subset took over. Together these results could suggest that $CD103^+CD11b^-$ DC are the first to develop from blood derived precursors, or that these are the first to seed secondary lymphoid organs, where they account for the majority of DC in T cell areas (Houston et al., 2015). Indeed, I was unable to remove ILF from the colon in any mice or PP in the neonatal mice. I also analysed DC in the lung as an example of a mucosal tissue other than the intestine. My results confirmed that there were very few $CD103^+CD11b^+$ DC in the lungs at any time, though on D1 there made up ~3.6%. However, this may simply reflect the very low numbers of total DC in the neonatal lung and equating to one cell in a gate making up a significant frequency. In contrast to the intestine and MLN, $CD103^+CD11b^-$ DC made up the greatest proportion of DC at most time points in the lung, confirming a previous report (Ruckwardt et al., 2014), while $CD103^-CD11b^+$ DC proportions increased also increased with age. The differences between the lung and LP could be due to the different functions the organs perform and/or to their distinct microbiota (Barfod et al., 2013; Segal and Blaser, 2014). $CD103^+CD11b^-$ DC cross-present antigen to $CD8^+$ T

cells, and are therefore well adapted in responding to viral pathogens. They also have a unique capacity to transport apoptotic cells to the draining LN (del Rio et al., 2007; Desch et al., 2011; Ginhoux et al., 2009a). It is possible that due to the lungs' constant exposure to viral antigen there is a requirement for $CD103^{+}CD11b^{-}$ DC to be the dominant population here, while in the intestine there is a strong pressure on generating Th1 and Th17 responses towards the various antigen, performed more by $CD103^{-}CD11b^{+}$ DC (Cerovic et al., 2013; Scott et al., 2014a).

6.2.1 The role of the microbiota in DC development

As noted above, the expansion of DC in neonatal intestine occurred at the time when the microbiota is becoming established, and given the marked effects that bacteria and their products have on DC (Francino, 2014; Ivanov et al., 2009; Janelsins et al., 2014; Ng et al., 2010), it seemed feasible that these might influence the differentiation of the DC subsets. In parallel, the developing DC populations would be important for ensuring that the neonatal immune system begins to make appropriate responses to these new arrivals. Although I was not able to explore the relationship between the microbiota and DC in the neonatal intestine, I did attempt to address the issue by investigating the effects of antibiotic treatment in adult mice. It was evident that the antibiotics had been effective, as shown by the enlarged caeca of treated mice, however all DC subsets were unaffected in SI LP, CLP and MLN, apart from a decrease in the proportion of $CD103^{+}CD11b^{-}$ DC in the CLP. However, this was not reflected in a difference in cell number on this population, and as this experiment was only carried out in one cohort of mice, it would be important to repeat it. If repeated, it would also be important to address how effective this antibiotic regime was, by performing 16s RNA sequencing of the microbiome in faecal and intestinal samples as this might also highlight a role for individual species as well as relative abundance.

As I was somewhat surprised by the apparent lack of effect of the antibiotic regime and I could not be sure of how effective the depletion of the microbiota had been, I went on to plan experiments in adult GF mice. Unfortunately, due to the recent and unintended recolonisation of these mice, it was difficult to draw any confident conclusions from these experiments. However, sequencing of the microbiome did indicate the 'GF' animals had a greater diversity of bacterial species at both the family

and genus level, but fewer copy numbers of those bacteria when compared with SPF controls. This was consistent recent colonisation where many bacterial species were competing for a niche in the intestine. The results did corroborate my findings in antibiotic treated mice, as there were no consistent differences amongst the DC subsets in the SI LP and MLN, compared with conventional mice, although the proportion of $CD103^{+}CD11b^{-}$ DC was decreased in the CLP of GF mice. Together these experiments indicate that although the microbiota might play some role in the differentiation of individual DC subsets in the intestine its presence is not an absolute requirement. Indeed other studies in GF animals have also shown DC do not show altered activation markers (Walton et al., 2006), nor does their migration to the MLN change after treatment with broad spectrum antibiotics or in GF animals, although it is dependent on MyD88 signalling (Hagerbrand et al., 2015). It would be important to repeat these experiments to extend these findings while analysis of neonatal GF intestines would provide evidence as to whether DC are impacted by the microbiota during development. Although previous GF studies have highlighted that absence of the intestinal microbiota has little impact on DC subsets proportions and their migration, there is evidence that intestinal organisms can influence DC. In particular, SFB have been shown to promote $CD103^{+}CD11b^{+}$ DC to produce Il-23 and generate Th17 cells (Goto et al., 2014; Ivanov et al., 2009). This kind of relationship between individual bacterial species and DC subsets might regulate how DC subsets develop in the LP. Re-colonisation of specific bacterial species might allow this to be tested.

As my experiments suggested there might be little effect of the microbiota on DC subsets, another local factor might be involved in their development in the neonatal period. The diet is the other major factor that changes around the time I found the biggest shifts in DC populations. Mice consume their mother's milk only for the first two weeks of life, after which they supplement milk by nibbling solid food that falls from the feeders. In our animal facility, mice are fully weaned and separated from their mothers at 21 days of age, though in the future, to test the impact of weaning on DC populations, it could be delayed and compared with those weaned at D21. Although my data showed a mostly gradual increase in the proportions and numbers of DC subsets after birth, as assessed per intestine, calculating the density of cells per gram of tissue indicated that the peak increases in cellularity, occurred in the SI LP

and CLP at D14. This could suggest that the expansion of DC numbers may be driven by the introduction of new materials into the diet. Again this would seem a sensible strategy to allow the immune system to deal with novel food proteins.

The $CD103^+CD11b^+$ DC subset was the one whose numbers were particularly age dependent, and one component of the diet which could influence the development of these cells is vitamin A. A number of studies have shown that retinoic acid promotes the differentiation of $CD103^+CD11b^+$ DC, and the only source of RA in mammals is metabolism of vitamin A from the diet (Klebanoff et al., 2013; Zeng et al., 2016). However, vitamin A is known to cross the placenta and plays a crucial role in embryonic development and is also present in maternal milk (Davila et al., 1985; Green et al., 2001). Therefore, the newborn mouse clearly already has a source of RA that could drive the development of $CD103^+CD11b^+$ DC, yet these DC are absent before birth, suggesting that additional factors may be involved, either alone or together with RA and that these do not become available until after birth and especially at the time of weaning.

Other factors that infants receive from maternal milk are IgG (Israel et al., 1995) and IgA (Tourneur and Chassin, 2013). The role of maternally derived IgG is in the prevention of perinatal infection, but also modulates the developing immune system by inducing tolerance towards dietary and commensal proteins. IgA has a similar role, but is specific to mucosal sites and is thought to act as immunological 'fly paper' by promoting and stabilising the biofilm produced by bacteria (Macpherson et al., 2001; 2008). As there are no recent studies describing how the levels of these immunoglobulins directly affect DC in the neonate it would be interesting to see if any of the changes correlate with the changes in DC populations I have described.

6.2.2 Functional maturation of intestinal DC

The low numbers of DC obtained from neonatal intestine meant that it was difficult to carry out functional assessments of the developing populations directly. Furthermore, previous work in our laboratory has shown that flow cytometric analysis of conventional activation markers such as CD80, CD86 and CCR7 is unreliable. However, one marker that did appear to change with age was CD103,

whose expression increased over time, especially amongst the $CD103^+CD11b^+$ population. Although the function of CD103 remains unclear its ligand E-cadherin is expressed on epithelial cells in the intestine, and this interaction has been suggested to maintain the survival and positioning of CD103 expressing DC and $CD8^+$ T cells (Strauch et al., 2001). Interestingly, $CD103^+CD11b^+$ DC always express lower levels of CD103 than $CD103^+CD11b^-$ DC and it is tempting to speculate that this could mean $CD103^+CD11b^-$ DC reside closer to the epithelium than $CD103^+CD11b^+$ DC. By extrapolation the lower expression of CD103 on neonatal DC could therefore indicate that DC in infant mucosa do not interact as closely with the epithelium as their adult counterparts. Immunofluorescence staining of intestinal tissue sections would be required to test these ideas directly and to my knowledge this has not been studied, perhaps because of the number of parameters that would be required to identify different DC subsets precisely.

The one functional parameter that I did assess was the ability of DC to produce RA, using the Aldefluor™ assay. These studies showed that fewer of all the neonatal DC subsets produced RA compared with adults and the levels of ALDH activity were also lower. However, both parameters increased with age, with adult levels matched by $CD103^+CD11b^-$ and $CD103^-CD11b^-$ DC by D7, whilst both $CD103^+CD11b^+$ and $CD103^+CD11b^+$ DC were significantly lower than their adult counterparts. Together with the expression of CD103, these results suggest that not only do the populations take some time to establish after birth, but their functional capacity also takes time to mature. The low production of RA by neonatal DC would suggest that there might be deficiencies in the induction of the gut homing molecules CCR9 and $\alpha4\beta7$ on T cells (Jaensson-Gyllenbäck et al., 2011). Furthermore, work carried out while I was writing my thesis also showed that neonatal intestinal $CD103^+$ DC were less able to produce RA and went on to show that this restricted oral tolerance in neonates (Turfkruyer et al., 2015). Until about three weeks of age there are few T cells present in the intestine, as they have not yet exited the thymus, thus this defect on D1 and D7 may not be of practical significance. However, it clearly would be important for the RA generating capacity of the DC to keep up with the increasing amount of antigen in the developing intestine so that appropriate T cell responses can be generated in the mucosa. The acquisition of RA production could reflect intrinsic changes in DC as

they mature or the levels of vitamin A in the diet. An additional factor could be the presence of ligands for peroxisome proliferator-activated receptor (PPAR)γ, which induce vitamin A metabolising activity in human monocyte-derived DC (Szatmari et al., 2006) and expression of *Aldh1a2* in murine splenic DC (Housley et al., 2009). Natural PPARγ ligands, such as polyunsaturated fatty acids are present in the gut, however are only reported at low levels, with weak binding affinities. Another PPARγ ligand is linoleic acid found in the diet or synthesised by commensal bacteria (Dubuquoy et al., 2006; Kelly et al., 2003) therefore it would be interesting to see if these ligands are available in neonatal intestine to begin imprinting of RA metabolism in DC. Additional studies to investigate whether neonatal DC have the same capacity to present antigen to T cells and how the T cells become polarised would further our understanding as to how functional neonatal DC are. I did attempt to carry out DC-T cell co-cultures using DC isolated from neonatal SI LP, but the small number of cells and the lack of viability from these cultures did not allow me to obtain any results from these experiments. In the absence of these co-cultures working, I did take whole SI LP digests from D7, D21, D42 and adults to look at the cytokine production by the T cells present. I would have predicted a significant increase in Th17 cells, in line with the published data describing them as being most abundant in the SI LP compared to Tregs (Denning et al., 2011) and to be reliant on the presence of functional $CD103^+CD11b^+$ DC (Persson et al., 2013b; Scott et al., 2014b; Welty et al., 2013) which increase with age. However, my findings would suggest that although there was a trend in the increase of Th17 cells, these were never greater than the frequency or numbers of Tregs. This would lead me to conclude that in these experiments, IL-17 and IFNγ cytokine staining may have not worked properly, and the transcription factor staining for $FoxP3^+$ Tregs was favoured. These experiments would need to be repeated and perhaps staining for the transcription factors, RORγt and GATA3 would help to distinguish Th17 and Th1 cells respectively.

6.3 Trem-1 and CD101 as markers of DC differentiation

CD101 and Trem-1 were markers identified in a microarray performed on SI LP DC subsets by a previous PhD student, as being highly upregulated in $CD103^+CD11b^+$ DC compared with $CD103^-CD11b^+$ DC. They have been subsequently proved useful in

dissecting the relationship between these subsets in mice lacking TGFβR signalling on DC and therefore I studied their expression by DC at different ages to try and explore the delayed differentiation of $CD103^+CD11b^+$ DC in more detail. I first investigated their expression by DC subsets in different tissues from adult mice. This showed that most $CD103^+CD11b^+$ DC in the SI LP expressed both molecules, as did this subset in the migratory compartment of the SI draining MLN (sMLN). No DC population in any other adult tissue showed this pattern of co-expression, even in the CLP or its draining cMLN, where only small numbers of the rarer $CD103^+CD11b^+$ DC subset were $CD101^+$Trem-1^+. Trem-1 expression in particular was highly restricted to intestinal DC, being found mostly on the SI LP $CD103^+CD11b^+$ DC. CD101 expression was found more widely on a proportion of $CD11b^+$ DC in many tissues including $CD103^-CD11b^+$ DC in SI LP and CLP.

While I was finishing my PhD, other workers also reported that CD101 expression was a marker of intestinal cDC2 and that this is dependent on vitamin A (Zeng et al., 2016). However, in contrast to my studies, Zeng *et al*. did not observe CD101 expression on $CD103^-CD11b^+$ DC, although their gating strategy did not distinguish mϕ from DC and as mϕ comprise the majority of this population and are $CD101^-$, they could have missed the small subset of *bona fide* DC that were $CD101^+$. Interestingly, the proportion of $CD11b^+$ DC that expressed CD101 varied considerably between tissues, being high in resident intestinal DC, spleen, lung and kidney but low or absent in skin draining LN and heart. The reasons for these differences are unknown, although it would be interesting to examine how this correlates with the levels of RA in each tissue, or if it is dependent on vitamin A.

The role of CD101 on intestinal DC is also unclear, although it has been shown to inhibit T cell activation when ligated on human DC (Bouloc et al., 2000; Soares et al., 1998). However, as it appeared to define particular stages in the differentiation of the $CD11b^+$ lineage in the intestine, I went on to assess the levels of Trem-1 and CD101 on intestinal and MLN DC subsets during neonatal life. These data generally confirmed that the subset-restricted patterns of expression were consistent throughout life. However, co-expression of Trem-1 and CD101 increased with age amongst $CD103^+CD11b^+$ DC, and was variable on $CD103^-CD11b^+$ DC in SI LP and migratory MLN DC, but not in the CLP, where the relative expression actually

decreased on both CD103^{+}CD11b^{+} and CD103^{-}CD11b^{+} DC with age. The expression of CD101 alone reduced amongst CD103^{+}CD11b^{+} DC with age in the SI LP but increased in the CLP most likely due to the absence of Trem-1 expression in the latter. However, in both DC compartments of the MLN there were no distinct expression patterns of these molecules alone. This suggests that the difference between SI and colon in expression of CD101 and Trem-1 may be due to a local factor that inhibits their expression by CD103^{+}CD11b^{+} and CD103^{-}CD11b^{+} DC in the CLP. Whether these markers are expressed on pre-DC and why they are not expressed on all intestinal DC subsets has yet to be determined.

Trem-1 expression by cDC has not been reported previously and it was believed that it was restricted to blood monocytes and neutrophils, where it appeared to amplify inflammatory responses by modulating TLR signalling (Bouchon et al., 2001; 2000; Gibot et al., 2004). Via its ability to recognise multimerised PGLYRP1 on neutrophils, it has recently been shown that cytokine production by human neutrophils and mϕ is enhanced (Read et al., 2015). In the intestine, Trem-1 expression has been studied mostly in the context of inflammation where it is expressed on monocytes and inflammatory mϕ, but is absent on steady state mϕ, possibly in response to the microbiota (Schenk et al., 2005). Its role in inflammation is supported by the findings that Trem-1$^{-/-}$ mice are less susceptible to experimental colitis and produce lower amounts of cytokines in response to Leishmania infection (Weber et al., 2014). According to the Immgenn database, other myeloid cells express Trem-1 in resting mice, although it has been reported to be expressed by Langerhans cells and BM DC under hypoxic conditions (Bosco et al., 2010; Pierobon et al., 2016). As the intestine is likely to be a hypoxic environment compared with other organs, this could perhaps explain the presence of Trem-1 in the gut. However, this does not explain why expression is absent from the colon, which may be more hypoxic than the SI, nor why it is so restricted to a single subset of DC. Similarly, its function on CD103^{+}CD11b^{+} DC is unknown. This suggests again, that a local factor specific to the SI such as RA or TGFβ may be involved in the imprinting of Trem-1 on CD103^{+}CD11b^{+} DC. Interestingly however, the absence of CD103^{+}CD11b^{+} DC *in vivo* leads to defective Th17 responses (Denning et al., 2007; Persson et al., 2013b; Scott et al., 2014b; Welty et al., 2013) and could suggest that Trem-1 might be involved in the recognition of

specific microbes. This could be explored by challenging Trem-1$^{-/-}$ mice with known Th17 driving bacteria such as *Citrobacter rodentium* or SFB to see if there is a defect in Th17 production in the absence of Trem-1 signalling.

6.4 Role of SIRPα and CCR2 on intestinal DC

SIRPα is expressed by all CD11b^{+} DC in mice and is now considered to be a definitive marker of the cDC2 lineage in all species (Guilliams et al., 2014; Persson et al., 2013a). Although its exact function on DC is unknown, the cytoplasmic domain of SIRPα contains an ITIM motif and it has been shown to have inhibitory effects on mϕ when triggered by its ubiquitously expressed ligand CD47 (Barclay, 2009; Matozaki et al., 2009; Tsai et al., 2010). When I began my PhD, the previous PhD student in the laboratory had found that mice with a mutation in the signalling domain of SIRPα had a selective reduction in intestinal CD103^{+}CD11b^{+} DC. This was associated with a defect in the generation of local Th17 cells, leading to increased susceptibility to infection by *Citrobacter rodentium*, whereas oral tolerance could be induced normally by feeding protein antigen (Scott et al., 2014b). Importantly the defect in DC reflected lack of signalling via SIRPα, as it was replicated in CD47KO mice and the initial aim of my PhD was to study SIRPα signalling in intestinal DC. However I was unable to obtain sufficient numbers of DC to identify signalling molecules by Western blotting and I therefore decided to try and explore the phenotype of SIPRα mt mice in more detail *in vivo*. After confirming the reduced frequency and number of intestinal CD103^{+}CD11b^{+} DC, I went on to show that this defect was already present from D7 of life.

How age affects DC development in SIRPα mt mice has not been examined previously. Rather than the continuum of ages analysed in WT animals previously, I examined what I had determined as key ages from the WT mice; D7 when CD103^{+}CD11b^{+} DC were beginning to establish, D14 when weaning begins, 4 weeks- just after mice have been separated from their mother, 8 week old adults, as well as 16 and 24 week old adults to monitor ageing. In the SI LP, I found a generalised defect amongst all DC subsets in SIRPα mt mice at D7, which was absent at other time points. By D14 there was a significant reduction in CD103^{+}CD11b^{+} DC frequency that remained at all time

points studied, in line with published findings in adults (Scott et al., 2014b). However in contrast to the published data, cell numbers were not reduced in SIRPα mt mice after D14, and it appeared that the numbers of Th17 cells in SIRPα mt intestine were comparable to those in the WT intestine of 24 week old mice, contradictory to the reduction previously shown in 8-10 week old mice (Scott et al., 2014b).

To better interpret the $CD103^+CD11b^+$ DC defect in SIRPα mt mice, I looked at the expression of CD101 and Trem-1 in D7 and adult SI LP amongst total $CD11b^+$ DC, $CD103^-CD11b^+$ DC and $CD103^+CD11b^+$ DC. At both time points, I found that CD101 and Trem-1 expression was reduced amongst these subsets in SIRPα mt mice, albeit to a lesser extent in the adult. Therefore it seems that SIRPα signalling is required not only for the generation of $CD103^+CD11b^+$ DC, but also for specific developmental processes within both $CD103^-CD11b^+$ and $CD103^+CD11b^+$ DC. My experiments in SIRPα mt -> WT and WT -> SIRPα mt BM chimeras did not help discern whether the defects I saw were as a result of hematopoietic cell SIRPα signalling, as the frequency of $CD103^+CD11b^+$ DC was reduced in both sets of chimeras compared to what I saw in the intact WT mice. The only significant difference was a greater frequency of $CD103^+CD11b^-$ DC in SIRPα mt -> WT chimeras compared with WT -> SIRPα mt chimeras, similar to what I had seen in the intact SIRPα mt mice. Unfortunately due to lack of mice and time, the BM chimera experiment did not include WT -> WT or SIRPα mt -> SIRPα mt chimeras as controls, meaning it was not possible to determine if this reflected a genuine absence of the selective defect, or if irradiation had had a generalised effect on the dynamics of DC reconstitution in the intestine.

Amongst migratory MLN DC, there were no significant differences in the DC subsets at D7, however by D14 there was a significant reduction in the frequency of $CD103^+CD11b^+$ DC as in the SI LP, and general lymphopaenia observed in adult MLN. By 4 weeks there was also a reduction in the proportion of $CD103^-CD11b^+$ DC that remained until 24 weeks but was not seen in the SI LP. There were no significant differences amongst any of the migratory MLN DC in BM chimeras. Together with what I reported in SI LP DC subsets, it appears that in the neonate there is a defect in the ability for all DC subsets to fill the intestinal niche, while after D14, this becomes apparent only in $CD103^+CD11b^+$ DC. Furthermore, the $CD103^+CD11b^+$ DC defect is

less robust as the mice exceed eight weeks. It also indicates a potential for defective migration of SIRPα$^+$ DC from the SI LP to the MLN, which has previously been reported in the skin and lung (Hagnerud et al., 2006; Raymond et al., 2010; 2009; Van Vu Quang et al., 2006). This had been investigated by collection of pseudo-afferent lymph of the MLN, by a previous PhD student, however there were no conclusive results, in part due to the age of the canulated mice and variability in results (Charlotte Scott; unpublished data) and would therefore need repeating to confirm if migration is affected in intestinal homeostasis of SIRPα mt mice.

Amongst resident MLN DC and spleen DC there was a consistent reduction in CD11b$^+$ DC with a reciprocal increase in CD103$^+$ DC frequency in SIPRα mt mice, which was unaffected by the age of the mice. In the BM chimeras the same defect was seen in the spleen only, consistent with what has previously been reported (Saito et al., 2010; Washio et al., 2015), while amongst resident MLN DC, all defects in SIRPα mt DC reconstitution were lost. Together with the defect amongst all intestinal DC subsets at D7 and in the MLN throughout life, these data suggest that there may be a generalised defect in the homeostasis of DC generated from SIRPα mt mice, and that this is more profound in younger animals. In mice that lack IRF4 signalling in CD11c$^+$ cells, there too were reduced numbers of total MLN DC, although this was a result of a selective defect in CD103$^+$CD11b$^+$ DC and CD103$^-$CD11b$^+$ DC (Persson et al., 2013b) rather than all the DC subsets as I saw. In SIRPα mt mice, it would appear that there is a defect in pre-DC development, however previous work has shown that there are normal numbers of pre-DC in the BM and blood in SIRPα mt mice (Saito et al., 2010; Scott et al., 2014b). It could also be that recruitment and extravasation into the intestine is impaired in these precursors by lack of SIRPα signalling through CD47 expressed on vascular endothelial cells. Indeed, there have been reports showing that SIRPα – CD47 signaling is required for monocytes to transmigrate across cerebral endothelium (de Vries et al., 2002; Myers et al., 2011). However competitive adoptive transfer of SIRPα mt pre-DC into WT hosts generated all DC subsets in the intestine, with even a selective advantage to having the SIRPα mutation when generating CD103$^+$CD11b$^+$ DC (Scott et al., 2014b), although this indication that SIRPα may normally function as a checkpoint in the development of a specific subset of intestinal DC is contradictory to previous findings in the spleen. Here, pre-DC from

SIRPα mt mice were found to have a reduced ability to generate CD11b$^+$ DC compared with WT pre-DC (Saito et al., 2010). However the latter looked at a later time point after transfer, meaning that the homeostatic levels of SIRPα mt DC might have been reached, but would suggest that further clarification on this matter is required with perhaps analysis of both lymphoid and non-lymphoid tissues at different times post transfer. The accelerated CD103$^+$CD11b$^+$ DC development in the SI LP of SIRPα mt mice correlated with increased apoptosis in the migratory CD103$^+$CD11b$^+$ DC in the MLN, and by proxy was a reflection of the LP, as it was impossible to assess whether this also occurred in the SI LP due to cell death in these preparations (Scott et al., 2014b). It would be interesting to see if Annexin V staining in neonate SI LP is possible as this undergoes a shorter digestion protocol and lead to more viable DC. Analysis of Annexin V staining would allow cell death to be measured during murine development to see if neonatal DC are more susceptible to death than their adult counterparts. This might help to explain the generalised defect seen in SIRPα mt MLN throughout life, and the defect seen in D7 SI LP.

The reduction in mϕ that I observed in adult SIRPα mt SI LP would not be wholly surprising, as mϕ express constitutively high levels of SIRPα, although this is contradictory to the current literature, that shows mϕ are unaffected by the lack of SIRPα signalling (Scott et al., 2014b; Washio et al., 2015). As the defect I observed was subtle, it may have been missed in previous experiments using less stringent gating protocols, or because of differences in microbiota. If confirmed, it would be interesting to determine if the reduced population of intestinal macrophages reflected defective generation, recruitment or local differentiation of the monocytes that are the precursors of resident macrophages in this tissue (Bain et al., 2014). Alternatively, there may be decreased survival of the mature macrophages, as has been suggested for DC.

To see how these data might fit in to homeostatic DC development, I looked at other reports that showed a defect in CD103$^+$CD11b$^+$ DC and reduction in Th17 cells. In the absence of Notch2 or its receptor, the selective loss of CD103$^-$CD11b$^+$ DC in the intestine and CD11b$^+$ DC in the spleen was due to a defect in development and not migration (Lewis et al., 2011; Satpathy et al., 2013). In the skin of IRF4$^{-/-}$ mice there

were similar numbers of $CD11b^+$ DC but these were reduced in the draining LN, which was accounted for by decreased DC migration (Bajana et al., 2012), while when IRF4 is absent on $CD11c^+$ cells, there were reduced $CD103^+CD11b^+$ DC in the intestine and MLN, as well as reduced $CD103^-CD11b^+$ DC in the MLN. These DC had reduced survival compared to WT counterparts (Persson et al., 2013b). In the context of my findings and those already published for SIRPα mt (Scott et al., 2014b) it would seem that development of $CD103^+CD11b^+$ DC is not affected in SIRPα mt mice, though it does seem plausible that migration might be affected along with a fundamental defect in generation of $CD11b^+$ DC in lymphoid tissues. When $CD103^+CD11b^+$ DC are diminished, Th17 cells are reduced in all these models, however this does not explain why I apparently observed a resolution in this phenotype. It might be that certain strains of commensals might change with age in the intestine and that these changes could impact the production of Th17. SFB are one such family of bacteria that have been shown to modulate Th17 responses in the intestine, via $CD103^+CD11b^+$ DC (Ivanov et al., 2009; Schlitzer et al., 2013). Given the variability in some of the results and the known influence of the microbiota on local immune cells, it would be important to take faecal or caecal samples to perform 16S RNA sequencing in future experiments. This would allow direct correlation of differences in the microbiota of SIRPα mt and WT mice with their DC phenotypes and could also reveal whether the selective reduction in $CD103^+CD11b^+$ DC might shape the microbial populations. However it is important to emphasise that all these data need to be confirmed, preferably using cohorts of age matched littermates housed together to eliminate potential confounding factors caused by such subtle differences in microbiota. This is particularly important, as the age-related resolution of the SIRPα mt defect seemed to occur only in the intestine and not in the spleen, suggesting that a local intestinal factor such as the microbiota might be involved.

I was unable to reproduce the statistically significant defect in a subset of intestinal $CD103^-CD11b^+$ DC in $CCR2^{-/-}$ mice that had been reported previously in the laboratory (Scott et al., 2014a). This could be due to a number of reasons, including the fact that I may not have used enough mice to observe what was shown to be a subtle change in DC numbers. However, I did find a trend towards reduced numbers of $CD103^-CD11b^+$ DC in $CCR2^{-/-}$ mice and also confirmed the earlier finding that a subset of this

population expressed CCR2 (Scott et al., 2014a). I went on to use the expression of CD101 and Trem-1 to explore the suggestion made in previous experiments that the $CCR2^{+}$ $CD103^{-}CD11b^{+}$ DC could be an intermediary subset that downregulates CCR2 before becoming $CD103^{+}CD11b^{+}$ DC. However there was no difference in CD101 and Trem-1 expression between the $CCR2^{+}$ and $CCR2^{-}$ subsets of $CD103^{-}CD11b^{+}$ DC, while there was actually a small increase in the proportion of $CD103^{+}CD11b^{+}$ DC that co-expressed CD101 and Trem-1 in $CCR2^{-/-}$ mice, indicating that $CCR2^{+}$ $CD103^{-}CD11b^{+}$ DC were not the cells expressing CD101 and Trem-1 that are predicted to be the direct precursors of $CD103^{+}CD11b^{+}$ DC.

6.5 The role of Trem-1 in DC development

A remarkable finding from my project was that Trem-1 expression by DC was highly restricted to the SI LP, where it was found on most $CD103^{+}CD11b^{+}$ DC, together with some $CD103^{-}CD11b^{+}$ DC. Even more surprising was that this pattern was not replicated in the colon, apart from a very small proportion of these subsets showing transient expression of Trem-1 in the neonatal period. Having identified this selective expression, I decided to investigate whether Trem-1 was involved in the development of $CD103^{+}CD11b^{+}$ DC. Initially I analysed data from an experiment carried out on $Trem\text{-}1^{-/-}$ mice in Christoph Mueller's group at the University of Bern, but only a few of the data points were useable due to cell death and gating problems. This made interpretation very difficult, but those results I did obtain were consistent with information I obtained from the Bern laboratory suggesting that there were no effects of Trem-1 deficiency on any of the DC subsets in the SI LP. However an additional complication to this experiment was that the frequency of $CD103^{+}CD11b^{+}$ DC in the WT controls from Bern appeared to be far lower (~20%) than I had usually seen in Glasgow (~40%). This might have been due to the different digestion protocol used in Bern, potentially leading to enhanced death of $CD103^{+}CD11b^{+}$ DC, a subset I had found to be particularly susceptible to dying when samples had been over-digested. It could also be that PP may not have been removed by the Bern group and as PP contain a large proportion of $CD103^{+}CD11b^{-}$ DC, this could have skewed the DC proportions obtained.

After having seen that the pattern of Trem-1 expression by SI LP CD103^{-}CD11b^{+} and CD103^{+}CD11b^{+} DC was established from birth onwards, I hypothesised that Trem-1 could be involved in DC maturation. As it was not feasible to establish a colony of Trem-1$^{-/-}$ mice in Glasgow and I was unsure of the protocols used by the Bern group to isolate and characterise LP DC, I decided to generate competitive chimeras in Glasgow using BM obtained from Bern. The plan was to reconstitute irradiated WT mice with a 50:50 mixture of CD45.2^{+} Trem-1$^{-/-}$ or CD45.2^{+} Trem-1$^{+/+}$ and CD45.1^{+} WT BM, but when I analysed the cell populations 8 weeks after transfer, I found that there were fewer CD45.1^{+} derived BM cells than I had calculated at the time of transfer. The most likely explanation for this is that there had been selective cell death amongst the CD45.1^{+} WT BM cells which I had stored in a fridge door for 48 hours to mimic the time and movement which CD45.2^{+} Trem-1$^{-/-}$ and Trem-1$^{+/+}$ bones would have experienced during their transport from Bern. It appeared that the conditions of storage in Glasgow may have compromised viability more than those involved in the international transfer. Despite the BM mixtures not achieving the anticipated 50:50 level, the mice did still represent competitive chimeras, as 10-15% of the reconstituted BM was derived from the CD45.1 WT source in each case. However in the blood, monocytes and neutrophils reconstituted less readily from Trem-1$^{-/-}$ BM than WT BM, perhaps consistent with these cells expressing Trem-1 (Bouchon et al., 2000; Zangi et al., 2012). The generation of monocytes and mϕ in the intestine of chimeric mice showed a similar dependence on Trem-1, which could be explained by these cells being derived from blood monocytes (Bain et al., 2014; 2012). More surprisingly, Trem-1$^{-/-}$ BM was also less efficient at generating all DC subsets in the tissues analysed, except for the resident CD103^{-}CD11b^{+} DC in the MLN. This included DC from the SI LP of these animals, although the data from the intestine were again difficult to interpret due to a low number of viable samples. The reasons for all DC subsets to be affected are not wholly clear, as there was no correlation with the expression of Trem-1 by the different subsets, and no defects had been observed in the intact Trem-1$^{-/-}$ mice from Bern. If confirmed, these results would suggest that the defective generation of DC by Trem-1$^{-/-}$ BM in the chimeras is not due to an intrinsic loss of Trem-1, but may reflect the loss of Trem-1 on other cells. As mentioned before, it has not been determined if Trem-1 is expressed on BM precursors cells such as monocytes, HSC, CMP or pre-DC and thus there could be a

role for Trem-1 in the generation of the correct niche required to generate DC. I did not analyse other tissues in these chimeras, so it is possible that a DC defect might be present at other sites as a result of defective generation upstream in their development.

6.6 Concluding remarks

These data have shown how intestinal DC subsets develop with age. More specifically, that $CD103^+CD11b^+$ DC are not present at birth and their appearance is preceded by that of the $CD103^-CD11b^+$ subset. Other evidence suggests these subsets are related to each other and that the $CD103^-CD11b^+$ DC is the intermediate precursor of the $CD103^+CD11b^+$ DC, with this differentiation step occurring only in the intestine. The expression of CD101 and Trem-1 on only a proportion of $CD103^-CD11b^+$ DC, while absent on the other DC subsets, might indicate those $CD103^-CD11b^+$ DC that are about to become $CD103^+CD11b^+$ DC. Furthermore, the microarray analysis which shows only a limited number of genes different between these two $CD11b^+$ subsets and the close clustering of these two subsets when compared to the other subsets all indicate a relationship between them. Due to the specific nature of Trem-1 on intestinal $CD11b^+$ DC, it could be used as a fate-mapping gene to observe how the DC develop from one subset to another, although it would be important to determine exactly when Trem-1 was switched on during DC development. Recent work in our own laboratory further supports a developmental relationship between the two subsets of $CD11b^+$ DC in the intestine, as CD11c-cre-$TGF\beta R1^{fl/fl}$ mice lack $CD103^+CD11b^+$ DC in the intestine but have a reciprocal increase in $CD103^-CD11b^+$ DC and normal numbers of $CD11b^+$ DC expressing CD101 (Drs Jennifer Montgomery and Calum Bain, Personal Communication). To test whether it is indeed $CD101^+$ DC from the $CD103^-CD11b^+$ DC, this population of cells could be sorted and cultured *in vitro* with factors such as retinoic acid and accessed if $CD103^+CD11b^+$ DC are generated. However, these sorts of experiments are not without limitation as they involve isolations of very rare populations of cells, but also *in vitro* cultures can never fully recapitulate *in vivo* conditions due to the lack of local intestinal factors that may all be involved in the maintenance of specific cell types.

The highly restricted distribution of $CD103^+CD11b^+$ DC in the SI LP and, to a lesser extent, in the colon could mean that this population is derived from a specific precursor that is recruited selectively to the mucosa, or that a common precursor develops preferentially due to signals within the local environment. Recently a population of gut-tropic DC progenitors has been described, suggesting that distinct precursors may be involved in the generation of intestinal DC (Zeng et al., 2016; 2012). However, these pre-mucosal DCs (pre- μDCs) were also capable of generating splenic DC and appeared to generate $CD103^+CD11b^-$ DC, even in the SI. These pre-μDC expressed the β7 integrin and B220 and thus exactly how they relate classical pre-DCs, which are $B220^-$ is unclear. On balance, it is likely that local imprinting is the mechanism responsible and as I have discussed above, this could include factors such as the microbiota, diet or indeed host-derived signals generated by local hematopoietic, epithelial, stromal or neural cells. My own, and other results would suggest that the microbiota does not influence the development of the phenotypic subsets of DC in the intestine (Hagerbrand et al., 2015; Walton et al., 2006), although whether their function is altered has not been addressed. Dietary vitamin A has been shown to be important for the development of $CD103^+CD11b^+$ DC and for their ability to generate RA (Agace and Persson, 2012; Coombes et al., 2007). This may reflect a defect in the relevant pre-cDC (Zeng et al., 2012), but it would also be important to use markers such as CD101 and Trem-1 to analyse whether vitamin A also controls the local differentiation of this lineage. Interactions with a number of local stromal and haematopoietic cells have been reported to regulate the development of $CD103^+CD11b^+$ and other intestinal DC, including ILC3, eosinophils and macrophages (Cedric Auffray et al., 2009). These pathways may involve mediators such as Il-1, GM-CSF or RA. The role of such cells and the stage at which they operate could be assessed by co-culturing them or their soluble products with pre-cDC or more mature DC and using CD101, Trem-1 and other markers to determine the nature of the DC that appear. It will also be important to explore if these local factors change during neonatal life in parallel with the dynamic maturation of the DC subsets and the findings presented here should provide the basis for more detailed studies of this kind. Finally it would be important now to extend these experiments in the mouse by exploring whether there are similar processes taking place in the human DC network early in life, and if differences in this might predict later susceptibility to disease.

References

Adkins, B., Leclerc, C., Marshall-Clarke, S., 2004. Neonatal adaptive immunity comes of age. Nature Reviews Immunology 4, 553–564.

Agace, W.W., Persson, E.K., 2012. How vitamin A metabolizing dendritic cells are generated in the gut mucosa. Trends in Immunology 33, 42–48.

Agarwal, S., Rao, A., 1998. Modulation of Chromatin Structure Regulates Cytokine Gene Expression during T Cell Differentiation. Immunity 9, 765–775.

Aggarwal, S., Ghilardi, N., Xie, M.-H., de Sauvage, F.J., Gurney, A.L., 2003. Interleukin-23 Promotes a Distinct CD4 T Cell Activation State Characterized by the Production of Interleukin-17. Journal of Biological Chemistry 278, 1910–1914.

Ajami, B., Bennett, J.L., Krieger, C., Tetzlaff, W., Rossi, F.M.V., 2007. Local self-renewal can sustain CNS microglia maintenance and function throughout adult life. Nature Neuroscience 10, 1538–1543.

Allakhverdi, Z., Comeau, M.R., Jessup, H.K., Yoon, B.-R.P., Brewer, A., Chartier, S., Paquette, N., Ziegler, S.F., Sarfati, M., Delespesse, G., 2007. Thymic stromal lymphopoietin is released by human epithelial cells in response to microbes, trauma, or inflammation and potently activates mast cells. The Journal of experimental medicine 204, 253–258.

Alpan, O., Rudomen, G., Matzinger, P., 2001. The Role of Dendritic Cells, B Cells, and M Cells in Gut-Oriented Immune Responses. J Immunol 166, 4843–4852.

Alvarez, D., Vollmann, E.H., Andrian, von, U.H., 2008. Mechanisms and Consequences of Dendritic Cell Migration. Immunity 29, 325–342.

Annacker, O., Coombes, J.L., Malmstrom, V., Uhlig, H.H., Bourne, T., Johansson-Lindbom, B., Agace, W.W., Parker, C.M., Powrie, F., 2005. Essential role for CD103 in the T cell–mediated regulation of experimental colitis. The Journal of experimental medicine 202, 1051–1061.

Annes, J.P., Munger, J.S., Rifkin, D.B., 2003. Making sense of latent TGFβ activation. J Cell Sci 116, 217–224.

Asseman, C., Read, S., Powrie, F., 2003. Colitogenic Th1 Cells Are Present in the Antigen-Experienced T Cell Pool in Normal Mice: Control by CD4+ Regulatory T Cells and IL-10. J Immunol 171, 971–978.

Auffray, C., Sieweke, M., Geissmann, F., 2009. Blood Monocytes: Development, Heterogeneity, and Relationship with Dendritic Cells. Annu Rev Immunol 27, 669-692.

Baba, N., Samson, S., Bourdet-Sicard, R., Rubio, M., Sarfati, M., 2008. Commensal bacteria trigger a full dendritic cell maturation program that promotes the expansion of non-Tr1 suppressor T cells. Journal of Leukocyte Biology 84, 468–476.

Bachem, A., Güttler, S., Hartung, E., Ebstein, F., Schaefer, M., Tannert, A., Salama, A., Movassaghi, K., Opitz, C., Mages, H.W., Henn, V., Kloetzel, P.-M., Gurka, S., Kroczek, R.A., 2010. Superior antigen cross-presentation and XCR1 expression define human CD11c+CD141+ cells as homologues of mouse CD8+ dendritic cells. The Journal of experimental medicine 207, 1273–1281.

Bachem, A., Hartung, E., Güttler, S., Mora, A., Zhou, X., Hegemann, A., Plantinga, M., Mazzini, E., Stoitzner, P., Gurka, S., Henn, V., Mages, H.W., Kroczek, R.A., 2012. Expression of XCR1 Characterizes the Batf3-Dependent Lineage of Dendritic Cells Capable of Antigen Cross-Presentation. Front. Immun. 3, 1-12

Bain, C.C., Bravo-Blas, A., Scott, C.L., Gomez Perdiguero, E., Geissmann, F., Henri, S., Malissen, B., Osborne, L.C., Artis, D., Mowat, A.M., 2014. Constant replenishment from circulating monocytes maintains the macrophage pool in the intestine of adult mice. Nat Immunol 15, 929–937.

Bain, C.C., Scott, C.L., Uronen-Hansson, H., Gudjonsson, S., Jansson, O., Grip, O., Guilliams, M., Malissen, B., Agace, W.W., Mowat, A.M., 2013. Resident and pro-inflammatory macrophages in the colon represent alternative context-dependent fates of the same Ly6Chi monocyte precursors. Mucosal Immunology 6, 498–510.

Bajana, S., Roach, K., Turner, S., Paul, J., Kovats, S., 2012. IRF4 Promotes Cutaneous Dendritic Cell Migration to Lymph Nodes during Homeostasis and Inflammation. The journal of immunology 189, 3368–3377.

Bancroft, A.J., McKenzie, A.N.J., Grencis, R.K., 1998. A Critical Role for IL-13 in Resistance to Intestinal Nematode Infection. J Immunol 160, 3453–3461.

Barbi, J., Pardoll, D., Pan, F., 2014. Treg functional stability and its responsiveness to the microenvironment. Immunological Reviews 259, 115-139

Barclay, A.N., 2009. Signal regulatory protein alpha (SIRPα)/CD47 interaction and function. Current Opinion in Immunology 21, 47–52.

Barfod, K.K., Roggenbuck, M., Hansen, L.H., Schjørring, S., Larsen, S.T., Sørensen, S.J., Krogfelt, K.A., 2013. The murine lung microbiome in relation to the intestinal and vaginal bacterial communities. BMC Microbiology 2013 13:1 13, 1.

Barnes, M.J., Powrie, F., 2010. Regulatory T Cells Reinforce Intestinal Homeostasis. Immunity 31, 401–411.

Bellinger, D.L., Lorton, D., Brouxhon, S., Felten, S., Felten, D.L., 1996. The significance of vasoactive intestinal polypeptide (VIP) in immunomodulation. Advances in Neuroimmunology 6, 5–27.

Benson, A., Pifer, R., Behrendt, C.L., Hooper, L.V., Yarovinsky, F., 2009. Gut Commensal Bacteria Direct a Protective Immune Response against Toxoplasma gondii. Cell Host & Microbe 6, 187–196.

Bettelli, E., Carrier, Y., Gao, W., Korn, T., Strom, T.B., Oukka, M., Weiner, H.L., Kuchroo, V.K., 2006. Reciprocal developmental pathways for the generation of pathogenic effector TH17 and regulatory T cells. Nature 441, 235–238.

Birchenough, G.M.H., Johansson, M.E.V., Stabler, R.A., Dalgakiran, F., Hansson, G.C., Wren, B.W., Luzio, J.P., Taylor, P.W., 2013. Altered Innate Defenses in the Neonatal Gastrointestinal Tract in Response to Colonization by Neuropathogenic Escherichia coli. Infection and Immunity 81, 3264–3275.

Bogiatzi, S.I., Fernandez, I., Bichet, J.-C., Marloie-Provost, M.-A., Volpe, E., Sastre, X., Soumelis, V., 2007. Cutting Edge: Proinflammatory and Th2 Cytokines Synergize to Induce Thymic Stromal Lymphopoietin Production by Human Skin Keratinocytes. J Immunol 178, 3373–3377.

Bogunovic, M., Ginhoux, F., Helft, J., Shang, L., Hashimoto, D., Greter, M., Liu, K., Jakubzick, C., Ingersoll, M.A., Leboeuf, M., Stanley, E.R., Nussenzweig, M., Lira, S.A., Randolph, G.J., Merad, M., 2009. Origin of the Lamina Propria Dendritic Cell Network. Immunity 31, 513–525.

Bonasio, R., Scimone, M.L., Schaerli, P., Grabie, N., Lichtman, A.H., Andrian, von, U.H., 2006. Clonal deletion of thymocytes by circulating dendritic cells homing to the thymus. Nat Immunol 7, 1092–1100.

Bosco, M.C., Pierobon, D., Blengio, F., Raggi, F., Vanni, C., 2010. Hypoxia modulates the gene expression profile of immunoregulatory receptors in human mDCs: identification of TREM-1 as a novel hypoxic marker in vitro and in vivo. Blood 117, 2625-2639.

Bouchon, A., Dietrich, J., Colonna, M., 2000. Cutting Edge: Inflammatory Responses Can Be Triggered by TREM-1, a Novel Receptor Expressed on Neutrophils and Monocytes. J Immunol 164, 4991–4995.

Bouchon, A., Facchetti, F., Weigand, M.A., Colonna, M., 2001. TREM-1 amplifies inflammation and is a crucial mediator of septic shock. Nature 410, 1103–1107.

Bouloc, A., Bagot, M., Delaire, S., Bensussan, A., Boumsell, L., 2000. Triggering CD101 molecule on human cutaneous dendritic cells inhibits T cell proliferation via IL-10 production. Eur. J. Immunol. 30, 3132–3139.

Bry, L., Falk, P., Huttner, K., Ouellette, A., Midtvedt, T., Gordon, J.I., 1994. Paneth cell differentiation in the developing intestine of normal and transgenic mice. Proceedings of the National Academy of Sciences 91, 10335–10339.

Cannon, J.P., O'Driscoll, M., Litman, G.W., 2012. Specific lipid recognition is a general feature of CD300 and TREM molecules. Immunogenetics 64, 39–47.

Carter, P.B., Collins, F.M., 1974. The route of enteric infection in normal mice. The Journal of experimental medicine 139, 1189–1203.

Cebula, A., Seweryn, M., Rempala, G.A., Pabla, S.S., McIndoe, R.A., Denning, T.L., Bry, L., Kraj, P., Kisielow, P., Ignatowicz, L., 2013. Thymus-derived regulatory T cells contribute to tolerance to commensal microbiota. Nature 497, 258–262.

Cella, M., Fuchs, A., Vermi, W., Facchetti, F., Otero, K., Lennerz, J.K.M., Doherty, J.M., Mills, J.C., Colonna, M., 2008. A human natural killer cell subset provides an innate source of IL-22 for mucosal immunity. Nature 457, 722–725.

Cerovic, V., Bain, C.C., Mowat, A.M., Milling, S.W.F., 2014a. Intestinal macrophages and dendritic cells: what's the difference? Trends in Immunology 35, 270–277.

Cerovic, V., Houston, S.A., Scott, C.L., Aumeunier, A., Yrlid, U., Mowat, A.M., Milling, S.W.F., 2013. Intestinal CD103- dendritic cells migrate in lymph and prime effector T cells. Mucosal Immunology 6, 104–113.

Cerovic, V., Houston, S.A., Westlund, J., Utriainen, L., Davison, E.S., Scott, C.L., Bain, C.C., Joeris, T., Agace, W.W., Kroczek, R.A., Mowat, A.M., Yrlid, U., Milling, S.W., 2014b. Lymph-borne CD8. Mucosal Immunology 8, 1–11.

Cerutti, A., Rescigno, M., 2008. The Biology of Intestinal Immunoglobulin A Responses. Immunity 28, 740–750.

Chieppa, M., Rescigno, M., Huang, A., Germain, R.N., 2006. Dynamic imaging of dendritic cell extension into the small bowel lumen in response to epithelial cell TLR engagement. The Journal of Exp Med 203, 2841-2852.

Chirdo, F., Millington, O., Beacock-Sharp, H., Mowat, A.M., 2005. Immunomodulatory dendritic cells in intestinal lamina propria. European Journal of Immunolgoy 35, 1831–1840.

Clevers, H., 2013. The Intestinal Crypt, A Prototype Stem Cell Compartment. Cell 154, 274–284. d

Coombes, J.L., Siddiqui, K.R.R., Arancibia-Cárcamo, C.V., Hall, J., Sun, C.-M., Belkaid, Y., Powrie, F., 2007. A functionally specialized population of mucosal CD103+ DCs induces Foxp3+ regulatory T cells via a TGF-β– and retinoic acid–dependent mechanism. The Journal of experimental medicine 204, 1757–1764.

Crotty, S., 2011. Follicular Helper CD4 T Cells (TFH). Annu Rev Immunol 29, 621-663

Davila, M.E., Norris, L., Cleary, M.P., Ross, A.C., 1985. Vitamin A during lactation: relationship of maternal diet to milk vitamin A content and to the vitamin A status of lactating rats and their pups. J. Nutr 115, 1033-1041

de Vries, H.E., Hendriks, J.J.A., Honing, H., de Lavalette, C.R., van der Pol, S.M.A., Hooijberg, E., Dijkstra, C.D., van den Berg, T.K., 2002. Signal-Regulatory Protein α-CD47 Interactions Are Required for the Transmigration of Monocytes Across Cerebral Endothelium. J Immunol 168, 5832–5839.

del Rio, M.-L., Rodriguez-Barbosa, J.-I., Kremmer, E., Förster, R., 2007. CD103− and CD103+ Bronchial Lymph Node Dendritic Cells Are Specialized in Presenting and Cross-Presenting Innocuous Antigen to CD4+ and CD8+ T Cells. J Immunol 178, 6861–6866.

Delgado, M.E., Grabinger, T., Brunner, T., 2015. Cell death at the intestinal epithelial front line. FEBS Journal. 1-19

Denning, T.L., Norris, B.A., Medina-Contreras, O., Manicassamy, S., Geem, D., Madan, R., Karp, C.L., Pulendran, B., 2011. Functional Specializations of Intestinal Dendritic Cell and Macrophage Subsets That Control Th17 and Regulatory T Cell Responses Are Dependent on the T Cell/APC Ratio, Source of Mouse Strain, and Regional Localization. The journal of immunology 187, 733–747.

Denning, T.L., Wang, Y.-C., Patel, S.R., Williams, I.R., Pulendran, B., 2007. Lamina propria macrophages and dendritic cells differentially induce regulatory and interleukin 17–producing T cell responses. Nature Immunology 8, 1086–1094.

Desch, A.N., Randolph, G.J., Murphy, K., Gautier, E.L., Kedl, R.M., Lahoud, M.H., Caminschi, I., Shortman, K., Henson, P.M., Jakubzick, C.V., 2011. CD103+ pulmonary dendritic cells preferentially acquire and present apoptotic cell–associated antigen. The Journal of experimental medicine 208, 1789–1797.

Diefenbach, S.G.S.S.C.K.K.O.C.J.C.K.S.L.S.W.P.S.P.A.A., Sanos, S.L., Kallfass, C., Oberle, K., Johner, C., Kirschning, C., Lienenklaus, S., Weiss, S., Staeheli, P., Aichele, P., Diefenbach, A., 2012. Priming of Natural Killer Cells by Nonmucosal Mononuclear Phagocytes Requires Instructive Signals from Commensal Microbiota. Immunity 37, 171–186.

Diehl, G.E., Longman, R.S., Zhang, J.-X., Breart, B., Galan, C., Cuesta, A., Schwab, S.R., Littman, D.R., 2013. Microbiota restricts trafficking of bacteria to mesenteric lymph nodes by CX3CR1hi cells. Nature 494, 1–6.

Dieu, M.-C., Vanbervliet, B., Vicari, A., Bridon, J.-M., Oldham, E., Aït-Yahia, S., Brière, F., Zlotnik, A., Lebecque, S., Caux, C., 1998. Selective Recruitment of Immature and Mature Dendritic Cells by Distinct Chemokines Expressed in Different Anatomic Sites. The Journal of experimental medicine 188, 373–386.

Dillon, S., Agrawal, S., Banerjee, K., Letterio, J., Denning, T.L., Oswald-Richter, K., Kasprowicz, D.J., Kellar, K., Pare, J., van Dyke, T., Ziegler, S., Unutmaz, D., Pulendran, B., 2006. Yeast zymosan, a stimulus for TLR2 and dectin-1, induces regulatory antigen-presenting cells and immunological tolerance. J. Clin. Invest. 116, 916–928.

Dower, K., Ellis, D.K., Saraf, K., Jelinsky, S.A., Lin, L.-L., 2008. Innate Immune Responses to TREM-1 Activation: Overlap, Divergence, and Positive and Negative Cross-Talk with Bacterial Lipopolysaccharide. J Immunol 180, 3520–3534.

Dubuquoy, L., Rousseaux, C., Thuru, X., Peyrin-Biroulet, L., Romano, O., Chavatte, P., Chamaillard, M., Desreumaux, P., 2006. PPARγ as a new therapeutic target in inflammatory bowel diseases. Gut 55, 1341–1349.

Duester, G., 2001. Families of retinoid dehydrogenases regulating vitamin A function. European Journal of Biochemistry 267, 4315–4324.

Dziarski, R., Platt, K.A., Gelius, E., Steiner, H., Gupta, D., 2003. Defect in neutrophil killing and increased susceptibility to infection with nonpathogenic gram-positive bacteria in peptidoglycan recognition protein-S (PGRP-S)–deficient mice. Blood 102, 689–697.

Eberl, G., Lochner, M., 2009. The development of intestinal lymphoid tissues at the interface of self and microbiota. Mucosal Immunology 2, 478–485.

Edelson, B.T., KC, W., Juang, R., Kohyama, M., Benoit, L.A., Klekotka, P.A., Moon, C., Albring, J.C., Ise, W., Michael, D.G., Bhattacharya, D., Stappenbeck, T.S., Holtzman, M.J., Sung, S.S.J., Murphy, T.L., Hildner, K., Murphy, K.M., 2010a. Peripheral CD103+ dendritic cells form a unified subset developmentally related to CD8 + conventional dendritic cells. Journal of Experimental Medicine 207, 823–836.

Farache, J., Koren, I., Milo, I., Gurevich, I., Kim, K.-W., Zigmond, E., Furtado, G.C., Lira, S.A., Shakhar, G., 2013. Luminal Bacteria Recruit CD103+ Dendritic Cells into the Intestinal Epithelium to Sample Bacterial Antigens for Presentation. Immunity 38, 1–15.

Fazilleau, N., Mark, L., McHeyzer-Williams, L.J., McHeyzer-Williams, M.G., 2009. Follicular Helper T Cells: Lineage and Location. Immunity 30, 324–335.

Finkelman, F.D., Katona, I.M., Mosmann, T.R., Coffman, R.L., 1988. IFN-gamma regulates the isotypes of Ig secreted during in vivo humoral immune responses. J Immunol 140, 1022–1027.

Fogg, D.K., Sibon, C., Miled, C., Jung, S., Aucouturier, P., Littman, D.R., Cumano, A., Geissmann, F., 2006. A Clonogenic Bone Marrow Progenitor Specific for Macrophages and Dendritic Cells. Science 311, 83–87.

Fonteneau, J.-F., Larsson, M., Beignon, A.-S., McKenna, K., Dasilva, I., Amara, A., Liu, Y.-J., Lifson, J.D., Littman, D.R., Bhardwaj, N., 2004. Human Immunodeficiency Virus Type 1 Activates Plasmacytoid Dendritic Cells and Concomitantly Induces the Bystander Maturation of Myeloid Dendritic Cells. J. Virol. 78, 5223–5232.

Ford, J.W., McVicar, D.W., 2009. TREM and TREM-like receptors in inflammation and disease. Current Opinion in Immunology 21, 38–46.

Fortin, G., Raymond, M., Van, V.Q., Rubio, M., Gautier, P., Sarfati, M., Franchimont, D., 2009. A role for CD47 in the development of experimental colitis mediated by SIRP +CD103- dendritic cells. Journal of Experimental Medicine 206, 1995–2011.

Francino, M., 2014. Early Development of the Gut Microbiota and Immune Health. Pathogens 3, 769–790.

Fujihashi, K., Dohi, T., Rennert, P.D., Yamamoto, M., Koga, T., Kiyono, H., McGhee, J.R., 2001. Peyer's patches are required for oral tolerance to proteins. Proceedings of the National Academy of Sciences 98, 3310–3315.

Fujimoto, K., Karuppuchamy, T., Takemura, N., Shimohigoshi, M., Machida, T., Haseda, Y., Aoshi, T., Ishii, K.J., Akira, S., Uematsu, S., 2011. A New Subset of CD103+CD8 + Dendritic Cells in the Small Intestine Expresses TLR3, TLR7, and TLR9 and Induces Th1 Response and CTL Activity. The journal of immunology 186, 6287–6295.

Fukaura, H., Kent, S.C., Pietrusewicz, M.J., Khoury, S.J., Weiner, H.L., Hafler, D.A., 1996. Induction of circulating myelin basic protein and proteolipid protein-specific transforming growth factor-beta1-secreting Th3 T cells by oral administration of myelin in multiple sclerosis patients. J. Clin. Invest. 98, 70–77.

Gallegos, A.M., Bevan, M.J., 2004. Central Tolerance to Tissue-specific Antigens Mediated by Direct and Indirect Antigen Presentation. The Journal of experimental medicine 200, 1039–1049.

Gangadharan, D., Lambolez, F., Attinger, A., Wang-Zhu, Y., Sullivan, B.A., Cheroutre, H., 2006. Identification of Pre- and Postselection TCRαβ+ Intraepithelial Lymphocyte Precursors in the Thymus. Immunity 25, 631–641.

Geissmann, F., Manz, M.G., Jung, S., Sieweke, M.H., Merad, M., Ley, K., 2010. Development of Monocytes, Macrophages, and Dendritic Cells. Science 327, 656–661.

Gibot, S., Kolopp-Sarda, M.-N., Béné, M.-C., Bollaert, P.-E., Lozniewski, A., Mory, F., Levy, B., Faure, G.C., 2004. A Soluble Form of the Triggering Receptor Expressed on Myeloid Cells-1 Modulates the Inflammatory Response in Murine Sepsis. The Journal of experimental medicine 200, 1419–1426.

Ginhoux, F., Liu, K., Helft, J., Bogunovic, M., Greter, M., Hashimoto, D., Price, J., Yin, N., Bromberg, J., Lira, S.A., Stanley, E.R., Nussenzweig, M., Merad, M., 2009b. The origin and development of nonlymphoid tissue CD103+ DCs. The Journal of experimental medicine 206, 3115–3130.

Ginhoux, F., Tacke, F., Angeli, V., Bogunovic, M., Loubeau, M., Dai, X.-M., Stanley, E.R., Randolph, G.J., Merad, M., 2006. Langerhans cells arise from monocytes in vivo. Nat Immunol 7, 265–273.

Gonnella, P.A., Chen, Y., Inobe, J.-I., Komagata, Y., Quartulli, M., Weiner, H.L., 1998. In Situ Immune Response in Gut-Associated Lymphoid Tissue (GALT) Following Oral Antigen in TCR-Transgenic Mice. J Immunol 160, 4708–4718.

Gonzalez Rey, E., Delgado, M., 2006. Therapeutic Treatment of Experimental Colitis With Regulatory Dendritic Cells Generated With Vasoactive Intestinal Peptide. Gastroenterology 131, 1799–1811.

Goto, Y., Panea, C., Nakato, G., Cebula, A., Lee, C., Diez, M.G., Laufer, T.M., Ignatowicz, L., Ivanov, I.I., 2014. Segmented Filamentous Bacteria Antigens Presented by Intestinal Dendritic Cells Drive Mucosal Th17 Cell Differentiation. Immunity 40, 1–14.

Green, M.H., Green, J.B., Akohoue, S.A., Kelley, S.K., 2001. Vitamin A Intake Affects the Contribution of Chylomicrons vs. Retinol-Binding Protein to Milk Vitamin A in Lactating Rats. J. Nutr. 131, 1279–1282.

Greter, M., Helft, J., Chow, A., Hashimoto, D., Mortha, A., 2012. GM-CSF Controls Nonlymphoid Tissue Dendritic Cell Homeostasis but Is Dispensable for the Differentiation of Inflammatory Dendritic Cells. Immunity 36, 1031-1046

Gribar, S.C., Sodhi, C.P., Richardson, W.M., Anand, R.J., Gittes, G.K., Branca, M.F., Jakub, A., Shi, X.-H., Shah, S., Ozolek, J.A., Hackam, D.J., 2009. Reciprocal Expression and Signaling of TLR4 and TLR9 in the Pathogenesis and Treatment of Necrotizing Enterocolitis. J Immunol 182, 636–646.

Gubler, U., Chua, A.O., Schoenhaut, D.S., Dwyer, C.M., McComas, W., Motyka, R., Nabavi, N., Wolitzky, A.G., Quinn, P.M., Familletti, P.C., 1991. Coexpression of two distinct genes is required to generate secreted bioactive cytotoxic lymphocyte maturation factor. Proceedings of the National Academy of Sciences 88, 4143–4147.

Guermonprez, P., Valladeau, J., Zitvogel, L., Théry, C., Amigorena, S., 2003. Antigen presentation and T cell stimulation by dendritic cell. Annu Rev Immunol 20, 621-267

Guilliams, M., De Kleer, I., Henri, S., Post, S., Vanhoutte, L., De Prijck, S., Deswarte, K., Malissen, B., Hammad, H., Lambrecht, B.N., 2013. Alveolar macrophages develop from fetal monocytes that differentiate into long-lived cells in the first week of life via GM-CSF. The Journal of experimental medicine 210, 1977–1992.

Guilliams, M., Ginhoux, F., Jakubzick, C., Naik, S.H., Onai, N., Schraml, B.U., Segura, E., Tussiwand, R., Yona, S., 2014. Dendritic cells, monocytes and macrophages: a unified nomenclature based on ontogeny. Nature Publishing Group 14, 571–578.

Hagerbrand, K., Westlund, J., Yrlid, U., Agace, W., Johansson-Lindbom, B., 2015. MyD88 Signaling Regulates Steady-State Migration of Intestinal CD103+ Dendritic Cells Independently of TNF- and the Gut Microbiota. J Immunol 195, 2888–2899.

Hagnerud, S., Manna, P.P., Cella, M., Stenberg, Å., Frazier, W.A., Colonna, M., Oldenborg, P.-A., 2006. Deficit of CD47 Results in a Defect of Marginal Zone Dendritic Cells, Blunted Immune Response to Particulate Antigen and Impairment of Skin Dendritic Cell Migration. The journal of immunology 176, 5772–5778.

Hamada, H., Hiroi, T., Nishiyama, Y., Takahashi, H., Masunaga, Y., Hachimura, S., Kaminogawa, S., Takahashi-Iwanaga, H., Iwanaga, T., Kiyono, H., Yamamoto, H., Ishikawa, H., 2002. Identification of Multiple Isolated Lymphoid Follicles on the Antimesenteric Wall of the Mouse Small Intestine. J Immunol 168, 57–64.

Happel, K.I., Dubin, P.J., Zheng, M., Ghilardi, N., Lockhart, C., Quinton, L.J., Odden, A.R., Shellito, J.E., Bagby, G.J., Nelson, S., Kolls, J.K., 2005. Divergent roles of IL-23 and IL-12 in host defense against Klebsiella pneumoniae. The Journal of experimental medicine 202, 761–769.

Hashi, H., Yoshida, H., Honda, K., Fraser, S., Kubo, H., Awane, M., Takabayashi, A., Nakano, H., Yamaoka, Y., Nishikawa, S.I., 2001. Compartmentalization of Peyer's Patch Anlagen Before Lymphocyte Entry. J Immunol 166, 3702–3709.

Hashiguchi, M., Kobori, H., Ritprajak, P., Kamimura, Y., Kozono, H., Azuma, M., 2008. Triggering receptor expressed on myeloid cell-like transcript 2 (TLT-2) is a counter-receptor for B7-H3 and enhances T cell responses. Proceedings of the National Academy of Sciences 105, 10495–10500.

Hayday, A., Gibbons, D., 2008. Brokering the peace: the origin of intestinal T cells. Mucosal Immunology 1, 172–174.

Heidt, T., Courties, G., Dutta, P., Sager, H.B., Sebas, M., Iwamoto, Y., Sun, Y., Da Silva, N., Panizzi, P., van der Laan, A.M., Swirski, F.K., Weissleder, R., Nahrendorf, M., 2014. Differential Contribution of Monocytes to Heart Macrophages in Steady-State and After Myocardial Infarction. Circulation Research 115, 284–295.

Henri, S., Vremec, D., Kamath, A., Waithman, J., Williams, S., Benoist, C., Burnham, K., Saeland, S., Handman, E., Shortman, K., 2001. The Dendritic Cell Populations of Mouse Lymph Nodes. J Immunol 167, 741–748.

Hoeffel, G., Wang, Y., Greter, M., See, P., Teo, P., Malleret, B., Leboeuf, M., Low, D., Oller, G., Almeida, F., Choy, S.H.Y., Grisotto, M., Renia, L., Conway, S.J., Stanley, E.R., Chan, J.K.Y., Ng, L.G., Samokhvalov, I.M., Merad, M., Ginhoux, F., 2012. Adult Langerhans cells derive predominantly from embryonic fetal liver monocytes with a minor contribution of yolk sac–derived macrophages. The Journal of experimental medicine 209, 1167–1181.

Hooper, L.V., Macpherson, A.J., 2010. Immune adaptations that maintain homeostasis with the intestinal microbiota. Nature Reviews Immunology 10, 159–169.

Hooper, L.V., Stappenbeck, T.S., Hong, C.V., Gordon, J.I., 2003. Angiogenins: a new class of microbicidal proteins involved in innate immunity. Nature Immunology 4, 269–273.

Hooper, L.V., Wong, M.H., Thelin, A., Hansson, L., Falk, P.G., Gordon, J.I., 2001. Molecular Analysis of Commensal Host-Microbial Relationships in the Intestine. Science 291, 881–884.

Hornef, M.W., Fulde, M., 2014. Ontogeny of intestinal epithelial innate immune responses. Front. Immunol. 5, 474.

Housley, W.J., O'Conor, C.A., Nichols, F., Puddington, L., Lingenheld, E.G., Zhu, L., Clark, R.B., 2009. PPARγ regulates retinoic acid-mediated DC induction of Tregs. Journal of Leukocyte Biology 86, 293–301.

Houston, S.A., Cerovic, V., Thomson, C., Brewer, J., Mowat, A.M., Milling, S., 2015. The lymph nodes draining the small intestine and colon are anatomically separate and immunologically distinct. Mucosal Immunology 9, 468-478.

Huang, F.-P., Platt, N., Wykes, M., Major, J.R., Powell, T.J., Jenkins, C.D., MacPherson, G.G., 2000. A Discrete Subpopulation of Dendritic Cells Transports Apoptotic Intestinal Epithelial Cells to T Cell Areas of Mesenteric Lymph Nodes. The Journal of experimental medicine 191, 435–444.

Hubert, F.-X., Kinkel, S.A., Davey, G.M., Phipson, B., Mueller, S.N., Liston, A., Proietto, A.I., Cannon, P.Z.F., Forehan, S., Smyth, G.K., Wu, L., Goodnow, C.C., Carbone, F.R., Scott, H.S., Heath, W.R., 2011. Aire regulates the transfer of antigen from mTECs to dendritic cells for induction of thymic tolerance. Blood 118, 2462–2472.

Iliev, I.D., Mileti, E., Matteoli, G., Chieppa, M., Rescigno, M., 2009a. Intestinal epithelial cells promote colitis-protective regulatory T-cell differentiation through dendritic cell conditioning. Mucosal Immunology 2, 340–350.

Iliev, I.D., Spadoni, I., Mileti, E., Matteoli, G., Sonzogni, A., Sampietro, G.M., Foschi, D., Caprioli, F., Viale, G., Rescigno, M., 2009b. Human intestinal epithelial cells promote the differentiation of tolerogenic dendritic cells. Gut 58, 1481-1489

Inaba, K., Inaba, M., Romani, N., Aya, H., Deguchi, M., Ikehara, S., Muramatsu, S., Steinman, R.M., 1992. Generation of large numbers of dendritic cells from mouse bone marrow cultures supplemented with granulocyte/macrophage colony-stimulating factor. The Journal of experimental medicine 176, 1693–1702.

Ishikawa-Sekigami, T., Kaneko, Y., Okazawa, H., Tomizawa, T., Okajo, J., Saito, Y., Okuzawa, C., Sugawara-Yokoo, M., Nishiyama, U., Ohnishi, H., Matozaki, T., Nojima, Y., 2006. SHPS-1 promotes the survival of circulating erythrocytes through inhibition of phagocytosis by splenic macrophages. Blood 107, 341–348.

Israel, E.J., Patel, V.K., Taylor, S.F., Marshak-Rothstein, A., Simister, N.E., 1995. Requirement for a beta 2-microglobulin-associated Fc receptor for acquisition of maternal IgG by fetal and neonatal mice. J Immunol 154, 6246–6251.

Ivanov, I.I., Atarashi, K., Manel, N., Brodie, E.L., Shima, T., Karaoz, U., Wei, D., Goldfarb, K.C., Santee, C.A., Lynch, S.V., Tanoue, T., Imaoka, A., Itoh, K., Takeda, K., Umesaki, Y., Honda, K., Littman, D.R., 2009. Induction of Intestinal Th17 Cellsby Segmented Filamentous Bacteria. Cell 139, 485–498.

Ivanov, I.I., Frutos, R. de L., Manel, N., Yoshinaga, K., Rifkin, D.B., Sartor, R.B., Finlay, B.B., Littman, D.R., 2008. Specific Microbiota Direct the Differentiation of IL-17-Producing T-Helper Cells in the Mucosa of the Small Intestine. Cell Host & Microbe 4, 337–349.

Ivanov, I.I., McKenzie, B.S., Zhou, L., Tadokoro, C.E., Lepelley, A., Lafaille, J.J., Cua, D.J., Littman, D.R., 2006. The Orphan Nuclear Receptor RORγt Directs the Differentiation Program of Proinflammatory IL-17+ T Helper Cells. Cell 126, 1121–1133.

Iwamura, H., Saito, Y., Sato-Hashimoto, M., Ohnishi, H., Murata, Y., Okazawa, H., Kanazawa, Y., Kaneko, T., Kusakari, S., Kotani, T., Nojima, Y., Matozaki, T., 2011. Essential roles of SIRPÎ± in homeostatic regulation of skin dendritic cells. Immunology Letters 135, 100–107.

Iwata, M., Hirakiyama, A., Eshima, Y., Kagechika, H., Kato, C., Song, S.-Y., 2004. Retinoic Acid Imprints Gut-Homing Specificity on T Cells. Immunity 21, 527–538.

Jackson, J.T., Hu, Y., Liu, R., Masson, F., D'Amico, A., Carotta, S., Xin, A., Camilleri, M.J., Mount, A.M., Kallies, A., Wu, L., Smyth, G.K., Nutt, S.L., Belz, G.T., 2011. Id2 expression delineates differential checkpoints in the genetic program of CD8α+ and CD103+ dendritic cell lineages. EMBO J 30, 2690–2704.

Jaensson, E., Uronen-Hansson, H., Pabst, O., Eksteen, B., Tian, J., Coombes, J.L., Berg, P.L., Davidsson, T., Powrie, F., Johansson-Lindbom, B., Agace, W.W., 2008. Small intestinal CD103+ dendritic cells display unique functional properties that are conserved between mice and humans. Journal of Experimental Medicine 205, 2139–2149.

Jaensson-Gyllenbäck, E., Kotarsky, K., Zapata, F., Persson, E.K., Gundersen, T.E., Blomhoff, R., Agace, W.W., 2011. Bile retinoids imprint intestinal CD103+ dendritic cells with the ability to generate gut-tropic T cells. Mucosal Immunology 4, 438–447.

Janelsins, B.M., Lu, M., Datta, S.K., 2014. Altered inactivation of commensal LPS due to acyloxyacyl hydrolase deficiency in colonic dendritic cells impairs mucosal Th17 immunity. Proceedings of the National Academy of Sciences 111, 373–378.

Jang, M.H., Kweon, M.-N., Iwatani, K., Yamamoto, M., Terahara, K., Sasakawa, C., Suzuki, T., Nochi, T., Yokota, Y., Rennert, P.D., Hiroi, T., Tamagawa, H., Iijima, H., Kunisawa, J., Yuki, Y., Kiyono, H., 2004. Intestinal villous M cells: An antigen entry site in the mucosal epithelium. Proceedings of the National Academy of Sciences 101, 6110–6115.

Jang, M.H., Sougawa, N., Tanaka, T., Hirata, T., Hiroi, T., Tohya, K., Guo, Z., Umemoto, E., Ebisuno, Y., Yang, B.-G., Seoh, J.-Y., Lipp, M., Kiyono, H., Miyasaka, M., 2006. CCR7 Is Critically Important for Migration of Dendritic Cells in Intestinal Lamina Propria to Mesenteric Lymph Nodes. J Immunol 176, 803–810.

Johansson, M.E.V., Ambort, D., Pelaseyed, T., Schütte, A., Gustafsson, J.K., Ermund, A., Subramani, D.B., Holmén-Larsson, J.M., Thomsson, K.A., Bergström, J.H., van der Post, S., Rodriguez-Piñeiro, A.M., Sjövall, H., Bäckström, M., Hansson, G.C., 2011. Composition and functional role of the mucus layers in the intestine. Cell. Mol. Life Sci. 68, 3635–3641.

Johansson, M.E.V., Phillipson, M., Petersson, J., Velcich, A., Holm, L., Hansson, G.C., 2008. The inner of the two Muc2 mucin-dependent mucus layers in colon is devoid of bacteria. Proceedings of the National Academy of Sciences 105, 15064–15069.

Johansson-Lindbom, B., Svensson, M., Pabst, O., Palmqvist, C., Marquez, G., Förster, R., Agace, W.W., 2005. Functional specialization of gut CD103+ dendritic cells in the regulation of tissue-selective T cell homing. The Journal of experimental medicine 202, 1063–1073.

Jung, C., Hugot, J.-P., Barreau, F., 2010. Peyer's Patches: The Immune Sensors of the Intestine. International Journal of Inflammation 2010, 1–12.

Kalinski, P., 2012. Regulation of Immune Responses by Prostaglandin E2. J Immunol 188, 21–28.

Kamanaka, M., Kim, S.T., Wan, Y.Y., Sutterwala, F.S., Lara-Tejero, M., Galán, J.E., Harhaj, E., Flavell, R.A., 2006. Expression of Interleukin-10 in Intestinal Lymphocytes Detected by an Interleukin-10 Reporter Knockin tiger Mouse. Immunity 25, 941–952.

Karsunky, H., Merad, M., Cozzio, A., Weissman, I.L., Manz, M.G., 2003. Flt3 Ligand Regulates Dendritic Cell Development from Flt3+ Lymphoid and Myeloid-committed Progenitors to Flt3+ Dendritic Cells In Vivo. The Journal of experimental medicine 198, 305–313.

Katona, I.M., J F Urban, J., Kang, S.S., Paul, W.E., Finkelman, F.D., 1991. IL-4 requirements for the generation of secondary in vivo IgE responses. J Immunol 146, 4215–4221.

Kawai, O.T., Akira, S., 2009. Cutting Edge: TLR-Dependent Viral. J Immunol 182, 3960-3964

Kawai, T., Akira, S., 2009. The roles of TLRs, RLRs and NLRs in pathogen recognition. Int. Immunol. 21, 317–337.

Kelly, D., Campbell, J.I., King, T.P., Grant, G., Jansson, E.A., Coutts, A.G.P., Pettersson, S., Conway, S., 2003. Commensal anaerobic gut bacteria attenuate inflammation by regulating nuclear-cytoplasmic shuttling of PPAR-γ and RelA. Nat Immunol 5, 104–112.

Kim, Y.S., Ho, S.B., 2010. Intestinal Goblet Cells and Mucins in Health and Disease: Recent Insights and Progress. Curr Gastroenterol Rep 12, 319–330.

King, I.L., Kroenke, M.A., Segal, B.M., 2010. GM-CSF–dependent, CD103+ dermal dendritic cells play a critical role in Th effector cell differentiation after subcutaneous immunization. The Journal of experimental medicine 207, 953–961.

Klebanoff, C.A., Spencer, S.P., Torabi-Parizi, P., Grainger, J.R., Roychoudhuri, R., Ji, Y., Sukumar, M., Muranski, P., Scott, C.D., Hall, J.A., Ferreyra, G.A., Leonardi, A.J., Borman, Z.A., Wang, J., Palmer, D.C., Wilhelm, C., Cai, R., Sun, J., Napoli, J.L., Danner, R.L., Gattinoni, L., Belkaid, Y., Restifo, N.P., 2013. Retinoic acid controls the homeostasis of pre-cDC-derived splenic and intestinal dendritic cells. Journal of Experimental Medicine 210, 1961–1976.

Klesney-Tait, J., Turnbull, I.R., Colonna, M., 2006. The TREM receptor family and signal integration. Nature Immunology 7, 1266–1273.

Kobayashi, T., Walsh, P.T., Walsh, M.C., Speirs, K.M., Chiffoleau, E., King, C.G., Hancock, W.W., Caamano, J.H., Hunter, C.A., Scott, P., Turka, L.A., Choi, Y., 2003. TRAF6 Is a Critical Factor for Dendritic Cell Maturation and Development. Immunity 19, 353–363.

Kramer, D.R., Cebra, J.J., 1995. Early appearance of “natural” mucosal IgA responses and germinal centers in suckling mice developing in the absence of maternal antibodies. J Immunol 154, 2051–2062.

Laouar, Y., Sutterwala, F.S., Gorelik, L., Flavell, R.A., 2005. Transforming growth factor-|[beta]| controls T helper type 1 cell development through regulation of natural killer cell interferon-|[gamma]|. Nature Immunology 6, 600–607.

Larsen, C.P., Ritchie, S.C., Pearson, T.C., Linsley, P.S., Lowry, R.P., 1992. Functional expression of the costimulatory molecule, B7/BB1, on murine dendritic cell populations. The Journal of experimental medicine 176, 1215–1220.

Latour, S., Tanaka, H., Demeure, C., Mateo, V., Rubio, M., Brown, E.J., Maliszewski, C., Lindberg, F.P., Oldenborg, A., Ullrich, A., Delespesse, G., Sarfati, M., 2012. Bidirectional Negative Regulation of Human T and Dendritic Cells by CD47 and Its Cognate Receptor Signal-Regulator Protein-{alpha}: Down-Regulation of IL-12 Responsiveness and Inhibition of Dendritic Cell Activation. The journal of immunology 167, 2547–2554.

Lenschow, D.J., Su, G.H., Zuckerman, L.A., Nabavi, N., Jellis, C.L., Gray, G.S., Miller, J., Bluestone, J.A., 1993. Expression and functional significance of an additional ligand for CTLA-4. Proceedings of the National Academy of Sciences 90, 11054–11058.

Lewis, K.L., Caton, M.L., Bogunovic, M., Greter, M., Grajkowska, L.T., Ng, D., Klinakis, A., Charo, I.F., Jung, S., Gommerman, J.L., Ivanov, I.I., Liu, K., Merad, M., Reizis, B., 2011. Notch2 Receptor Signaling Controls Functional Differentiation of Dendritic Cells in the Spleen and Intestine. Immunity 35, 780–791.

Ley, R.E., Hamady, M., Lozupone, C., Turnbaugh, P.J., Ramey, R.R., Bircher, J.S., Schlegel, M.L., Tucker, T.A., Schrenzel, M.D., Knight, R., Gordon, J.I., 2008. Evolution of Mammals and Their Gut Microbes. Science 320, 1647–1651.

Liu, K., Victora, G.D., Schwickert, T.A., Guermonprez, P., Meredith, M.M., Yao, K., Chu, F.-F., Randolph, G.J., Rudensky, A.Y., Nussenzweig, M., 2009. In Vivo Analysis of Dendritic Cell Development and Homeostasis. Science 324, 392–397.

Luda, K.M., Joeris, T., Persson, E.K., Rivollier, A., Demiri, M., Sitnik, K.M., Pool, L., Holm, J.B., Melo-Gonzalez, F., Richter, L., Lambrecht, B.N., Kristiansen, K., Travis, M.A., Svensson-Frej, M., Kotarsky, K., Agace, W.W., 2016. IRF8 Transcription-Factor-Dependent Classical Dendritic Cells Are Essential for Intestinal T Cell Homeostasis. Immunity 1–16.

Macpherson, A.J., Hunziker, L., McCoy, K., Lamarre, A., 2001. IgA responses in the intestinal mucosa against pathogenic and non-pathogenic microorganisms. Microbes and Infection 3, 1021–1035.

Macpherson, A.J., McCoy, K.D., Johansen, F.-E., Brandtzaeg, P., 2008. The immune geography of IgA induction and function. Mucosal Immunology 1, 11–22.

Macpherson, A.J., Uhr, T., 2004. Induction of Protective IgA by Intestinal Dendritic Cells Carrying Commensal Bacteria. Science 303, 1662–1665.

Maden, M., 2002. Retinoid signalling in the development of the central nervous system. Nat Rev Neurosci 3, 843–853.

Mancino, A., Habbeddine, M., Johnson, E., Luron, L., Bebien, M., Memet, S., Fong, C., Bajenoff, M., Wu, X., Karin, M., Caamano, J., Chi, H., Seed, M., Lawrence, T., 2013. I kappa B kinase alpha (IKKα) activity is required for functional maturation of dendritic cells and acquired immunity to infection. EMBO J 32, 816–828.

Mangan, P.R., Harrington, L.E., O'Quinn, D.B., Helms, W.S., Bullard, D.C., Elson, C.O., Hatton, R.D., Wahl, S.M., Schoeb, T.R., Weaver, C.T., 2006. Transforming growth factor-|[beta]| induces development of the TH17 lineage. Nature 441, 231–234.

Maraskovsky, E., Brasel, K., Teepe, M., Roux, E.R., Lyman, S.D., Shortman, K., McKenna, H.J., 1996. Dramatic increase in the numbers of functionally mature dendritic cells in Flt3 ligand-treated mice: multiple dendritic cell subpopulations identified. The Journal of experimental medicine 184, 1953–1962.

Maslowski, K.M., Vieira, A.T., Ng, A., Kranich, J., Sierro, F., Di Yu, Schilter, H.C., Rolph, M.S., Mackay, F., Artis, D., Xavier, R.J., Teixeira, M.M., Mackay, C.R., 2009. Regulation of inflammatory responses by gut microbiota and chemoattractant receptor GPR43. Nature 461, 1282–1286.

Matozaki, T., Murata, Y., Okazawa, H., Ohnishi, H., 2009. Functions and molecular mechanisms of the CD47-SIRP [alpha] signalling pathway. Trends in Cell Biology 19, 72–80.

Maynard, C.L., Harrington, L.E., Janowski, K.M., Oliver, J.R., Zindl, C.L., Rudensky, A.Y., Weaver, C.T., 2007. Regulatory T cells expressing interleukin 10 develop from Foxp3+ and Foxp3|[minus]| precursor cells in the absence of interleukin 10. Nat Immunol 8, 931–941.

Mayrhofer, G., Pugh, C.W., Barclay, A.N., 1983. The distribution, ontogeny and origin in the rat of Ia-positive cells with dendritic morphology and of Ia antigen in epithelia, with special reference to the intestine. Eur. J. Immunol. 13, 112–122.

Mazmanian, S.K., Liu, C.H., Tzianabos, A.O., Kasper, D.L., 2005. An Immunomodulatory Molecule of Symbiotic Bacteria Directs Maturation of the Host Immune System. Cell 122, 107–118.

Mazzini, E., Massimiliano, L., Penna, G., Rescigno, M., 2014. Oral Tolerance Can Be Establishedvia Gap Junction Transfer of Fed Antigensfrom CX3CR1. Immunity 40, 248–261.

McDole, J.R., Wheeler, L.W., McDonald, K.G., Wang, B., Konjufca, V., Knoop, K.A., Newberry, R.D., Miller, M.J., 2012. Goblet cells deliver luminal antigen to CD103+ dendritic cells in the small intestine. Nature 483, 345–349.

McKenna, H.J., Stocking, K.L., Miller, R.E., Brasel, K., De Smedt, T., Maraskovsky, E., Maliszewski, C.R., Lynch, D.H., Smith, J., Pulendran, B., Roux, E.R., Teepe, M., Lyman, S.D., Peschon, J.J., 2000. Mice lacking flt3 ligand have deficient hematopoiesis affecting hematopoietic progenitor cells, dendritic cells, and natural killer cells. Blood 95, 3489–3497.

Mebius, R.E., Streeter, P.R., Michie, S., Butcher, E.C., Weissman, I.L., 1996. A developmental switch in lymphocyte homing receptor and endothelial vascular addressin expression regulates lymphocyte homing and permits CD4+ CD3- cells to colonize lymph nodes. Proceedings of the National Academy of Sciences 93, 11019–11024.

Medzhitov, R., 2001. Toll-like receptors and innate immunity. Nature Reviews Immunology 1, 135-145.

Mellman, I., Steinman, R.M., 2001. Dendritic cells: specialized and regulated antigen processing machines. Cell 106, 255-258

Merad, M., Sathe, P., Helft, J., Miller, J., Mortha, A., 2013. The Dendritic Cell Lineage: Ontogeny and Function of Dendritic Cells and Their Subsets in the Steady State and the Inflamed Setting. Annu. Rev. Immunol. 31.

Meredith, M.M., Liu, K., Darrasse-Jeze, G., Kamphorst, A.O., Schreiber, H.A., Guermonprez, P., Idoyaga, J., Cheong, C., Yao, K.H., Niec, R.E., Nussenzweig, M.C., 2012. Expression of the zinc finger transcription factor zDC (Zbtb46, Btbd4) defines the classical dendritic cell lineage. Journal of Experimental Medicine 209, 1153–1165.

Miller, J.C., Brown, B.D., Shay, T., Gautier, E.L., Cohain, A., Pandey, G., Leboeuf, M., Elpek, K.G., Helft, J., Hashimoto, D., Chow, A., Price, J., Greter, M., Bogunovic, M., Bellemare-Pelletier, A., Frenette, P.S., Randolph, G.J., Turley, S.J., Merad, M., Jakubzick, C., Best, A.J., Knell, J., Goldrath, A., Miller, J., Brown, B., Jojic, V., Koller, D., Cohen, N., Brennan, P., Brenner, M., Regev, A., Fletcher, A., Elpek, K., Malhotra, D., Turley, S., Jianu, R., Laidlaw, D., Collins, J., Narayan, K., Sylvia, K., Kang, J., Gazit, R., Rossi, D.J., Kim, F., Rao, T.N., Wagers, A., Shinton, S.A., Hardy, R.R., Monach, P., Bezman, N.A., Sun, J.C., Kim, C.C., Lanier, L.L., Heng, T., Kreslavsky, T., Painter, M., Ericson, J., Davis, S., Mathis, D., Benoist, C., 2012. Deciphering the transcriptional network of the dendritic cell lineage. Nat Immunol 13, 888–899.

Mowat, A., 2003. Anatomical basis of tolerance and immunity to intestinal antigens. Nature Reviews Immunology 3, 331–341.

Mowat, A.M., Agace, W.W., 2014. Regional specialization within the intestinal immune system. Nature Reviews Immunology 14, 667–685.

Myers, S.A., DeVries, W.H., Andres, K.R., Gruenthal, M.J., Benton, R.L., Hoying, J.B., Hagg, T., Whittemore, S.R., 2011. CD47 knockout mice exhibit improved recovery from spinal cord injury. Neurobiology of Disease 42, 21–34.

Naik, S.H., Metcalf, D., van Nieuwenhuijze, A., Wicks, I., Wu, L., O'Keeffe, M., Shortman, K., 2006. Intrasplenic steady-state dendritic cell precursors that are distinct from monocytes. Nature Immunology 7, 663–671.

Naik, S.H., Sathe, P., Park, H.-Y., Metcalf, D., Proietto, A.I., Dakic, A., Carotta, S., O'Keeffe, M., Bahlo, M., Papenfuss, A., Kwak, J.-Y., Wu, L., Shortman, K., 2007. Development of plasmacytoid and conventional dendritic cell subtypes from single precursor cells derived in vitro and in vivo. Nat Immunol 8, 1217–1226.

Nakano, H., Yanagita, M., Gunn, M.D., 2001. Cd11c+B220+Gr-1+ Cells in Mouse Lymph Nodes and Spleen Display Characteristics of Plasmacytoid Dendritic Cells. The Journal of experimental medicine 194, 1171–1178.

Neutra, M.R., Frey, A., Kraehenbuhl, J.-P., 1996. Epithelial M Cells: Gateways for Mucosal Infection and Immunization. Cell 86, 345–348.

Newberry, R.D., Lorenz, R.G., 2005. Organizing a mucosal defense. Immunological Reviews 206, 6–21.

Ng, S.C., Kamm, M.A., Stagg, A.J., Knight, S.C., 2010. Intestinal dendritic cells: Their role in bacterial recognition, lymphocyte homing, and intestinal inflammation. Inflamm Bowel Dis 16, 1787–1807.

Niess, J.-H., Brand, S., Gu, X., Landsman, L., Jung, S., McCormick, B.A., Vyas, J.M., Boes, M., Ploegh, H.L., Fox, J.G., Littman, D.R., Reinecker, H.-C., 2005. CX3CR1-Mediated Dendritic Cell Access to the Intestinal Lumen and Bacterial Clearance. Science 307, 254–258.

O'Garra, A., 1998. Cytokines Induce the Development of Functionally Heterogeneous T Helper Cell Subsets. Immunity 8, 275–283.

Ogura, K., Fukunaga, A., Taguchi, K., Nagai, H., Yu, X., 2012. The Rho kinase pathway regulates the migration of dendritic cells through SIRP-α. Journal of Dermatological Science 6, 74-76.

Onai, N., Obata-Onai, A., Schmid, M.A., Ohteki, T., Jarrossay, D., Manz, M.G., 2007. Identification of clonogenic common Flt3+M-CSFR+ plasmacytoid and conventional dendritic cell progenitors in mouse bone marrow. Nat Immunol 8, 1207–1216.

Pabst, O., Mowat, A.M., 2012. Oral tolerance to food protein. Mucosal Immunology 5, 232–239.

Park, H., Li, Z., Yang, X.O., Chang, S.H., Nurieva, R., Wang, Y.-H., Wang, Y., Hood, L., Zhu, Z., Tian, Q., Dong, C., 2005. A distinct lineage of CD4 T cells regulates tissue inflammation by producing interleukin 17. Nat Immunol 6, 1133–1141.

Persson, E.K., Scott, C.L., Mowat, A.M., Agace, W.W., 2013a. Dendritic cell subsets in the intestinal lamina propria: Ontogeny and function. Eur. J. Immunol. n/a–n/a.

Persson, E.K., Uronen-Hansson, H., Semmrich, M., Rivollier, A., Hägerbrand, K., Marsal, J., Gudjonsson, S., Håkansson, U., Reizis, B., Kotarsky, K., Agace, W.W., 2013b. IRF4 Transcription-Factor-Dependent CD103+CD11b+ Dendritic Cells Drive Mucosal T Helper 17 Cell Differentiation. Immunity 38, 1–12.

Pierobon, D., Raggi, F., Cambieri, I., Pelassa, S., Occhipinti, S., Cappello, P., Novelli, F., Musso, T., Eva, A., Castagnoli, C., Varesio, L., Giovarelli, M., Bosco, M.C., 2016. Regulation of Langerhans cell functions in a hypoxic environment. J Mol Med 1–13.

Pott, J., Stockinger, S., Torow, N., Smoczek, A., Lindner, C., McInerney, G., Bäckhed, F., Baumann, U., Pabst, O., Bleich, A., Hornef, M.W., 2012. Age-Dependent TLR3 Expression of the Intestinal Epithelium Contributes to Rotavirus Susceptibility. PLoS Pathogens 8, e1002670.

Raymond, M., Quang Van, V., Rubio, M., Welzenbach, K., Sarfati, M., 2010. Targeting SIRP-α protects from type 2-driven allergic airway inflammation. Eur. J. Immunol. 40, 3510–3518.

Raymond, M., Rubio, M., Fortin, G., Shalaby, K.H., 2009. Selective control of SIRP-α–positive airway dendritic cell trafficking through CD47 is critical for the development of TH 2-mediated allergic inflammation. J Allergy Clin Immunol 1333-1342.

Read, C.B., Kuijper, J.L., Hjorth, S.A., Heipel, M.D., Tang, X., Fleetwood, A.J., Dantzler, J.L., Grell, S.N., Kastrup, J., Wang, C., Brandt, C.S., Hansen, A.J., Wagtmann, N.R., Xu, W., Stennicke, V.W., 2015. Cutting Edge: Identification of Neutrophil PGLYRP1 as a Ligand for TREM-1. The journal of immunology 194, 1417–1421.

Rescigno, M., Urbano, M., Valzasina, B., 2001. Dendritic cells express tight junction proteins and penetrate gut epithelial monolayers to sample bacteria. Nat Immunol 2, 361-367.

Rimoldi, M., Chieppa, M., Salucci, V., Avogadri, F., Sonzogni, A., Sampietro, G.M., Nespoli, A., Viale, G., Allavena, P., Rescigno, M., 2005. Intestinal immune homeostasis is regulated by the crosstalk between epithelial cells and dendritic cells. Nat Immunol 6, 507–514.

Ruane, D., Brane, L., Reis, B.S., Cheong, C., Poles, J., Do, Y., Zhu, H., Velinzon, K., Choi, J.H., Studt, N., Mayer, L., Lavelle, E.C., Steinman, R.M., Mucida, D., Mehandru, S., 2013. Lung dendritic cells induce migration of protective T cells to the gastrointestinal tract. Journal of Experimental Medicine 210, 1871–1888.

Ruckwardt, T.J., Malloy, A.M.W., Morabito, K.M., Graham, B.S., 2014. Quantitative and Qualitative Deficits in Neonatal Lung-Migratory Dendritic Cells Impact the Generation of the CD8+ T Cell Response. PLoS Pathogens 10.

Sainte-Marie, G., 2010. The Lymph Node Revisited: Development, Morphology, Functioning, and Role in Triggering Primary Immune Responses. Anat Rec 293, 320–337.

Saito, Y., Iwamura, H., Kaneko, T., Ohnishi, H., Murata, Y., Okazawa, H., Kanazawa, Y., Sato-Hashimoto, M., Kobayashi, H., Oldenborg, P.A., Naito, M., Kaneko, Y., Nojima, Y., Matozaki, T., 2010. Regulation by SIRP of dendritic cell homeostasis in lymphoid tissues. Blood 116, 3517–3525.

Sallusto, F., Cella, M., Danieli, C., Lanzavecchia, A., 1995. Dendritic cells use macropinocytosis and the mannose receptor to concentrate macromolecules in the major histocompatibility complex class II compartment: downregulation by cytokines and bacterial products. The Journal of experimental medicine 182, 389–400.

Sallusto, F., Lanzavecchia, A., 1994. Efficient presentation of soluble antigen by cultured human dendritic cells is maintained by granulocyte/macrophage colony-stimulating factor plus interleukin 4 and downregulated by tumor necrosis factor alpha. The Journal of experimental medicine 179, 1109–1118.

Sallusto, F., Lanzavecchia, A., Mackay, C.R., 1998. Chemokines and chemokine receptors in T-cell priming and Th1/Th2-mediated responses. Immunology Today 19, 568–574.

Sancho, D., Joffre, O.P., Keller, A.M., Rogers, N.C., Martínez, D., Hernanz-Falcón, P., Rosewell, I., Sousa, C.R.E., 2009. Identification of a dendritic cell receptor that couples sensing of necrosis to immunity. Nature 458, 899–903.

Sancho, D., Mourão-Sá, D., Joffre, O.P., Schulz, O., Rogers, N.C., Pennington, D.J., Carlyle, J.R., Reis e Sousa, C., 2008. Tumor therapy in mice via antigen targeting to a novel, DC-restricted C-type lectin. J. Clin. Invest. 118, 2098–2110.

Sanos, S.L., Bui, V.L., Mortha, A., Oberle, K., Heners, C., Johner, C., Diefenbach, A., 2009. RORγt and commensal microflora are required for the differentiation of mucosal interleukin 22 - producing NKp46+ cells. Nat Immunol 10, 83–91.

Sansonetti, P.J., 2004. War and peace at mucosal surfaces. Nature Reviews Immunology 4, 953–964.

Sato-Hashimoto, M., Saito, Y., Ohnishi, H., Iwamura, H., Kanazawa, Y., Kaneko, T., Kusakari, S., Kotani, T., Mori, M., Murata, Y., Okazawa, H., Ware, C.F., Oldenborg, P.A., Nojima, Y., Matozaki, T., 2011. Signal Regulatory Protein Regulates the Homeostasis of T Lymphocytes in the Spleen. The journal of immunology 187, 291–297.

Satpathy, A.T., Lee, J.S., Ng, D., Manieri, N.A., KC, W., Wu, X., Thomas, S.R., Lee, W.-L., Turkoz, M., McDonald, K.G., Meredith, M.M., Song, C., Guidos, C.J., Newberry, R.D., Ouyang, W., Murphy, T.L., Stappenbeck, T.S., Gommerman, J.L., Nussenzweig, M.C., Colonna, M., Kopan, R., Murphy, K.M., 2013. Notch2-dependent classical dendritic cells orchestrate intestinal immunity to attaching- and-effacing bacterial pathogens. Nature 14, 1–15.

Satpathy, A.T., Wu, X., Albring, J.C., Murphy, K.M., 2012. Re(de)fining the dendritic cell lineage. Nat Immunol 13, 1145–1154.

Schenk, M., Bouchon, A., Birrer, S., Colonna, M., Mueller, C., 2005. Macrophages Expressing Triggering Receptor Expressed on Myeloid Cells-1 Are Underrepresented in the Human Intestine. J Immunol 174, 517–524.

Schenk, M., Bouchon, A., Seibold, F., Mueller, C., 2007. TREM-1–expressing intestinal macrophages crucially amplify chronic inflammation in experimental colitis and inflammatory bowel diseases. J. Clin. Invest. 117, 3097–3106.

Schlitzer, A., Heiseke, A.F., Einwächter, H., Reindl, W., Schiemann, M., Manta, C.-P., See, P., Niess, J.-H., Suter, T., Ginhoux, F., Krug, A.B., 2012. Tissue-specific differentiation of a circulating CCR9− pDC-like common dendritic cell precursor. Blood 119, 6063–6071.

Schlitzer, A., Loschko, J., Mair, K., Vogelmann, R., Henkel, L., Einwächter, H., Schiemann, M., Niess, J.-H., Reindl, W., Krug, A., 2011. Identification of CCR9− murine plasmacytoid DC precursors with plasticity to differentiate into conventional DCs. Blood 117, 6562–6570.

Schlitzer, A., McGovern, N., Teo, P., Zelante, T., Atarashi, K., Low, D., Ho, A.W.S., See, P., Shin, A., Wasan, P.S., Hoeffel, G., Malleret, B., Heiseke, A., Chew, S., Jardine, L., Purvis, H.A., Hilkens, C.M.U., Tam, J., Poidinger, M., Stanley, E.R., Krug, A.B., Renia, L., Sivasankar, B., Ng, L.G., Collin, M., Ricciardi-Castagnoli, P., Honda, K., Haniffa, M., Ginhoux, F., 2013. IRF4 Transcription Factor-Dependent CD11b+ Dendritic Cells in Human and Mouse Control Mucosal IL-17 Cytokine Responses. Immunity 38, 970–983.

Schlitzer, A., Sivakamasundari, V., Chen, J., Sumatoh, H.R.B., Schreuder, J., Lum, J., Malleret, B., Zhang, S., Larbi, A., Zolezzi, F., Renia, L., Poidinger, M., Naik, S., Newell, E.W., Robson, P., Ginhoux, F., 2015. Identification of cDC1- and cDC2-committed DC progenitors reveals early lineage priming at the common DC progenitor stage in the bone marrow. Nat Immunol 16, 718–728.

Schraml, B.U., Reis e Sousa, C., 2015. Defining dendritic cells. Current Opinion in Immunology 32, 13–20.

Schulz, O., Jaensson, E., Persson, E.K., Liu, X., Worbs, T., Agace, W.W., Pabst, O., 2009. Intestinal CD103+, but not CX3CR1+, antigen sampling cells migrate in lymph and serve classical dendritic cell functions. The Journal of experimental medicine 206, 3101–3114.

Scott, C.L., Aumeunier, A.M., Mowat, A.M., 2011. Intestinal CD103+ dendritic cells: master regulators of tolerance? Trends in Immunology 32, 412–419.

Scott, C.L., Bain, C.C., Wright, P.B., Sichien, D., Kotarsky, K., Persson, E.K., Luda, K., Guilliams, M., Lambrecht, B.N., Agace, W.W., Milling, S.W., Mowat, A.M., 2014a. CCR2+CD103− intestinal dendritic cells develop from DC-committed precursors and induce interleukin-17 production by T cells. Mucosal Immunology 8, 327–339.

Scott, C.L., Zangerle Murray, T., Beckham, K., Douce, G., Mowat, A.M., 2014b. Signal regulatory protein alpha (SIRPα) regulates the homeostasis of CD103+CD11b+ DCs in the intestinal lamina propria. European Journal of Immunology 44, 3658-3668.

Sefik, E., Geva-Zatorsky, N., Oh, S., Konnikova, L., Zemmour, D., McGuire, A.M., Burzyn, D., Ortiz-Lopez, A., Lobera, M., Yang, J., Ghosh, S., Earl, A., Snapper, S.B., Jupp, R., Kasper, D., Mathis, D., Benoist, C., 2015. Individual intestinal symbionts induce a distinct population of ROR + regulatory T cells. Science 349, 993–997.

Segal, L.N., Blaser, M.J., 2014. A Brave New World: The Lung Microbiota in an Era of Change. Annals ATS 11, S21–S27.

Siddiqui, K.R.R., Powrie, F., 2008. CD103+ GALT DCs promote Foxp3+ regulatory T cells. Mucosal Immunology 1, S34–S38.

Smith, R.E., 2003. A novel MyD-1 (SIRP-1) signaling pathway that inhibits LPS-induced TNF production by monocytes. Blood 102, 2532–2540.

Snapper, C.M., Finkelman, F.D., Stefany, D., Conrad, D.H., Paul, W.E., 1988a. IL-4 induces co-expression of intrinsic membrane IgG1 and IgE by murine B cells stimulated with lipopolysaccharide. J Immunol 141, 489–498.

Snapper, C.M., Peschel, C., Paul, W.E., 1988b. IFN-gamma stimulates IgG2a secretion by murine B cells stimulated with bacterial lipopolysaccharide. J Immunol 140, 2121–2127.

Soares, L.R.B., Tsavaler, L., Rivas, A., Engleman, E.G., 1998. V7 (CD101) Ligation Inhibits TCR/CD3-Induced IL-2 Production by Blocking Ca2+ Flux and Nuclear Factor of Activated T Cell Nuclear Translocation. J Immunol 161, 209–217.

Sonnenberg, G.F., Fouser, L.A., Artis, D., 2011. Border patrol: regulation of immunity, inflammation and tissue homeostasis at barrier surfaces by IL-22. Nat Immunol 12, 383–390.

Sonnenburg, J.L., Xu, J., Leip, D.D., Chen, C.-H., Westover, B.P., Weatherford, J., Buhler, J.D., Gordon, J.I., 2005. Glycan Foraging in Vivo by an Intestine-Adapted Bacterial Symbiont. Science 307, 1955–1959.

Sozzani, S., Allavena, P., D'Amico, G., Luini, W., Bianchi, G., Kataura, M., Imai, T., Yoshie, O., Bonecchi, R., Mantovani, A., 1998. Cutting Edge: Differential Regulation of Chemokine Receptors During Dendritic Cell Maturation: A Model for Their Trafficking Properties. J Immunol 161, 1083–1086.

Spadoni, I., Iliev, I.D., Rossi, G., Rescigno, M., 2012. Dendritic cells produce TSLP that limits the differentiation of Th17 cells, fosters Treg development, and protects against colitis. Mucosal Immunology 5, 184–193.

Stappenbeck, T.S., Hooper, L.V., Gordon, J.I., 2002. Developmental regulation of intestinal angiogenesis by indigenous microbes via Paneth cells. Proceedings of the National Academy of Sciences 99, 15451–15455.

Stecher, B., Macpherson, A.J., Hapfelmeier, S., Kremer, M., Stallmach, T., Hardt, W.-D., 2005. Comparison of Salmonella enterica Serovar Typhimurium Colitis in Germfree Mice and Mice Pretreated with Streptomycin. Infection and Immunity 73, 3228–3241.

Steege, Ter, J., Buurman, W.A., 1997. The neonatal development of intraepithelial and lamina propria lymphocytes in the murine small intestine. Dev Immunol 5, 121-128 .

Steenwinckel, V., Louahed, J., Lemaire, M.M., Sommereyns, C., Warnier, G., McKenzie, A., Brombacher, F., Van Snick, J., Renauld, J.-C., 2009. IL-9 Promotes IL-13-Dependent Paneth Cell Hyperplasia and Up-Regulation of Innate Immunity Mediators in Intestinal Mucosa. J Immunol 182, 4737–4743.

Stefanidakis, M., Newton, G., Lee, W.Y., Parkos, C.A., Luscinskas, F.W., 2008. Endothelial CD47 interaction with SIRP is required for human T-cell transendothelial migration under shear flow conditions in vitro. Blood 112, 1280–1289.

Steinman, R.M., Cohn, Z.A., 1973. Identification of a novel cell type in peripheral lymphoid organs of mice. The Journal of experimental medicine 137, 1142–1162.

Steinman, R.M., Idoyaga, J., 2010. Features of the dendritic cell lineage - Steinman - 2010 - Immunological Reviews - Wiley Online Library. Immunological Reviews.

Strauch, U.G., Mueller, R.C., Li, X.Y., Cernadas, M., Higgins, J.M.G., Binion, D.G., Parker, C.M., 2001. Integrin αE(CD103)β7 Mediates Adhesion to Intestinal Microvascular Endothelial Cell Lines Via an E-Cadherin-Independent Interaction. J Immunol 166, 3506–3514.

Strobl, H., Knapp, W., 1999. TGF-β1 regulation of dendritic cells. Microbes and Infection 1, 1283–1290.

Sun, C.M., Hall, J.A., Blank, R.B., Bouladoux, N., Oukka, M., Mora, J.R., Belkaid, Y., 2007. Small intestine lamina propria dendritic cells promote de novo generation of Foxp3 T reg cells via retinoic acid. The Journal of experimental medicine 204, 1775–1785.

Suzuki, S., Honma, K., Matsuyama, T., Suzuki, K., Toriyama, K., Akitoyo, I., Yamamoto, K., Suematsu, T., Nakamura, M., Yui, K., Kumatori, A., 2004. Critical roles of interferon regulatory factor 4 in CD11bhighCD8α– dendritic cell development. Proceedings of the National Academy of Sciences 101, 8981–8986.

Szabo, S.J., Kim, S.T., Costa, G.L., Zhang, X., Fathman, C.G., Glimcher, L.H., 2000. A Novel Transcription Factor, T-bet, Directs Th1 Lineage Commitment. Cell 100, 655–669.

Szatmari, I., Pap, A., Rühl, R., Ma, J.-X., Illarionov, P.A., Besra, G.S., Rajnavolgyi, E., Dezso, B., Nagy, L., 2006. PPARγ controls CD1d expression by turning on retinoic acid synthesis in developing human dendritic cells. The Journal of experimental medicine 203, 2351–2362.

Tal, O., Lim, H.Y., Gurevich, I., Milo, I., Shipony, Z., Ng, L.G., Angeli, V., Shakhar, G., 2011. DC mobilization from the skin requires docking to immobilized CCL21 on lymphatic endothelium and intralymphatic crawling. The Journal of experimental medicine 208, 2141–2153.

Tamoutounour, S., Guilliams, M., Montanana Sanchis, F., Liu, H., Terhorst, D., Malosse, C., Pollet, E., Ardouin, L., Luche, H., Sanchez, C., Dalod, M., Malissen, B., Henri, S., 2013. Origins and Functional Specialization of Macrophages and of Conventional and Monocyte-Derived Dendritic Cells in Mouse Skin. Immunity 39, 925–938.

Tamoutounour, S., Henri, S., Lelouard, H., de Bovis, B., de Haar, C., van der Woude, C.J., Woltman, A.M., Reyal, Y., Bonnet, D., Sichien, D., Bain, C.C., Mowat, A.M., Reis e Sousa, C., Poulin, L.F., Malissen, B., Guilliams, M., 2012. CD64 distinguishes macrophages from dendritic cells in the gut and reveals the Th1-inducing role of mesenteric lymph node macrophages during colitis. Eur. J. Immunol. 42, 3150–3166.

Tang, F., Du, Q., Liu, Y.-J., 2010. Plasmacytoid dendritic cells in antiviral immunity and autoimmunity. Sci. China Life Sci. 53, 172–182.

Théry, C., Amigorena, S., 2001. The cell biology of antigen presentation in dendritic cells. Current Opinion in Immunology 13, 45–51.

Thomson, A.W., Knolle, P.A., 2010. Antigen-presenting cell function in the tolerogenic liver environment. Nature Reviews Immunology 10, 753–766.

Tilney, N.L., 1971. Patterns of lymphatic drainage in the adult laboratory rat. Journal of Anatomy 109, 369.

Torow, N., Yu, K., Hassani, K., Freitag, J., Schulz, O., Basic, M., Brennecke, A., Sparwasser, T., Wagner, N., Bleich, A., Lochner, M., Weiss, S., Förster, R., Pabst, O., Hornef, M.W., 2015. Active suppression of intestinal CD4+TCR[alpha][beta]+ T-lymphocyte maturation during the postnatal period. Nat Comms 6.

Tourneur, E., Chassin, C., 2013. Neonatal Immune Adaptation of the Gut and Its Role during Infections. Clinical and Developmental Immunology 2013, 1–17.

Travis, M.A., Reizis, B., Melton, A.C., Masteller, E., Tang, Q., Proctor, J.M., Wang, Y., Bernstein, X., Huang, X., Reichardt, L.F., Bluestone, J.A., Sheppard, D., 2007. Loss of integrin αvβ8 on dendritic cells causes autoimmunity and colitis in mice. Nature 449, 361–365.

Tsai, R.K., Rodriguez, P.L., Discher, D.E., 2010. Blood Cells, Molecules, and Diseases. Blood Cells, Molecules, and Diseases 45, 67–74.

Turfkruyer, M., Rekima, A., Macchiaverni, P., Le Bourhis, L., Muncan, V., van den Brink, G.R., Tulic, M.K., Verhasselt, V., 2015. Oral tolerance is inefficient in neonatal mice due to a physiological vitamin A deficiency. Mucosal Immunology 9, 479–491.

Turnbull, I.R., Gilfillan, S., Cella, M., Aoshi, T., Miller, M., Piccio, L., Hernandez, M., Colonna, M., 2006. Cutting Edge: TREM-2 Attenuates Macrophage Activation. J Immunol 177, 3520–3524.

Turner, J.R., Rill, B.K., Carlson, S.L., Carnes, D., Kerner, R., Mrsny, R.J., Madara, J.L., 1997. Physiological regulation of epithelial tight junctions is associated with myosin light-chain phosphorylation. American Journal of Physiology - Cell Physiology 273, C1378–C1385.

Tussiwand, R., Everts, B., Grajales-Reyes, G.E., Kretzer, N.M., Iwata, A., Bagaitkar, J., Wu, X., Wong, R., Anderson, D.A., Murphy, T.L., Pearce, E.J., Murphy, K.M., 2015. Klf4 Expression in Conventional Dendritic Cells Is Required for T Helper 2 Cell Responses. Immunity 42, 916–928.

Uematsu, S., Fujimoto, K., Jang, M.H., Yang, B.-G., Jung, Y.-J., Nishiyama, M., Sato, S., Tsujimura, T., Yamamoto, M., Yokota, Y., Kiyono, H., Miyasaka, M., Ishii, K.J., Akira, S., 2008. Regulation of humoral and cellular gut immunity by lamina propria dendritic cells expressing Toll-like receptor 5. Nature Immunology 9, 769–776.

Urbain, J., Leo, O., Moser, M., 1998. Regulation of T helper cell differentiation in vivo by soluble and membrane proteins provided by antigen-presenting cells. Eur. J. Immunol 28, 3161-3171.

Van den Broeck, W., Derore, A., Simoens, P., 2006. Anatomy and nomenclature of murine lymph nodes: Descriptive study and nomenclatory standardization in BALB/cAnNCrl mice. Journal of Immunological Methods 312, 12–19.

Van Vu Quang, Lesage, S., Bouguermouh, S., Gautier, P., Rubio, M., Levesque, M., Nguyen, S., Galibert, L., Sarfati, M., 2006. Expression of the self-marker CD47 on dendritic cells governs their trafficking to secondary lymphoid organs. EMBO J 25, 5560–5568.

van Wijk, F., Cheroutre, H., 2009. Intestinal T cells: Facing the mucosal immune dilemma with synergy and diversity. Seminars in Immunology 21, 130–138.

Vander Lugt, B., Khan, A.A., Hackney, J.A., Agrawal, S., Lesch, J., Zhou, M., Lee, W.P., Park, S., Xu, M., DeVoss, J., Spooner, C.J., Chalouni, C., Delamarre, L., Mellman, I., Singh, H., 2013. Transcriptional programming of dendritic cells for enhanced MHC class II antigen presentation. Nat Immunol 15, 161–167.

Varol, C., Vallon-Eberhard, A., Elinav, E., Aychek, T., Shapira, Y., Luche, H., Fehling, H.J., Hardt, W.D., Shakhar, G., Jung, S., 2009. Intestinal lamina propria dendritic cell subsets have different origin and functions. Immunity 31, 502–512.

Veiga-Fernandes, H., Coles, M.C., Foster, K.E., Patel, A., 2007. Tyrosine kinase receptor RET is a key regulator of Peyer's patch organogenesis. Nature.

Veldhoen, M., Hocking, R.J., Atkins, C.J., Locksley, R.M., Stockinger, B., 2006. TGFβ in the Context of an Inflammatory Cytokine Milieu Supports De Novo Differentiation of IL-17-Producing T Cells. Immunity 24, 179–189.

Verjan Garcia, N., Umemoto, E., Saito, Y., Yamasaki, M., Hata, E., Matozaki, T., Murakami, M., Jung, Y.J., Woo, S.Y., Seoh, J.Y., Jang, M.H., Aozasa, K., Miyasaka, M., 2011. SIRP /CD172a Regulates Eosinophil Homeostasis. The journal of immunology 187, 2268–2277.

Vremec, D., Lieschke, G.J., Dunn, A.R., Robb, L., Metcalf, D., Shortman, K., 1997. The influence of granulocyte/macrophage colony-stimulating factor on dendritic cell levels in mouse lymphoid organs. Eur. J. Immunol. 27, 40–44.

Walton, K., He, J., Kelsall, B., Sartor, R., Fisher, N., 2006. Dendritic cells in germ-free and specific pathogen-free mice have similar phenotypes and in vitro antigen presenting function. Immunology Letters 102, 16–24.

Wang, Sen, Villablanca, E.J., De Calisto, J., Gomes, D.C.O., Nguyen, D.D., Mizoguchi, E., Kagan, J.C., Reinecker, H.-C., Hacohen, N., Nagler, C., Xavier, R.J., Rossi-Bergmann, B., Chen, Y.-B., Blomhoff, R., Snapper, S.B., Mora, J.R., 2011. MyD88-Dependent TLR1/2 Signals Educate Dendritic Cells with Gut-Specific Imprinting Properties. J Immunol 187, 141–150.

Washio, K., Kotani, T., Saito, Y., Respatika, D., Murata, Y., Kaneko, Y., Okazawa, H., Ohnishi, H., Fukunaga, A., Nishigori, C., Matozaki, T., 2015. Dendritic cell SIRPα regulates homeostasis of dendritic cells in lymphoid organs. Genes to Cells 20, 451-463.

Waskow, C., Liu, K., Darrasse-Jèze, G., Guermonprez, P., Ginhoux, F., Merad, M., Shengelia, T., Yao, K., Nussenzweig, M., 2008. The receptor tyrosine kinase Flt3 is required for dendritic cell development in peripheral lymphoid tissues. Nat Immunol 9, 676–683.

Watanabe, N., Wang, Y.-H., Lee, H.K., Ito, T., Wang, Y.-H., Cao, W., Liu, Y.-J., 2005. Hassall's corpuscles instruct dendritic cells to induce CD4+CD25+ regulatory T cells in human thymus. Nature 436, 1181–1185.

Weber, B., Saurer, L., Schenk, M., 2011. CX3CR1 defines functionally distinct intestinal mononuclear phagocyte subsets which maintain their respective functions during homeostatic and inflammatory conditions. European Journal of Immunology 41, 773-779.

Weber, B., Schuster, S., Zysset, D., Rihs, S., Dickgreber, N., Schürch, C., Riether, C., Siegrist, M., Schneider, C., Pawelski, H., Gurzeler, U., Ziltener, P., Genitsch, V., Tacchini-Cottier, F., Ochsenbein, A., Hofstetter, W., Kopf, M., Kaufmann, T., Oxenius, A., Reith, W., Saurer, L., Mueller, C., 2014. TREM-1 Deficiency Can Attenuate Disease Severity without Affecting Pathogen Clearance. PLoS Pathogens 10, e1003900.

Weiss, J.M., Bilate, A.M., Gobert, M., Ding, Y., Curotto de Lafaille, M.A., Parkhurst, C.N., Xiong, H., Dolpady, J., Frey, A.B., Ruocco, M.G., Yang, Y., Floess, S., Huehn, J., Oh, S., Li, M.O., Niec, R.E., Rudensky, A.Y., Dustin, M.L., Littman, D.R., Lafaille, J.J., 2012. Neuropilin 1 is expressed on thymus-derived natural regulatory T cells, but not mucosa-generated induced Foxp3+ T reg cells. Journal of Experimental Medicine 209, 1723–1742.

Welty, N.E., Staley, C., Ghilardi, N., Sadowsky, M.J., Igyarto, B.Z., Kaplan, D.H., 2013. Intestinal lamina propria dendritic cells maintain T cell homeostasis but do not affect commensalism. Journal of Experimental Medicine 210, 2011–2024.

Weng, Y., Sun, J., Wu, Q., Pan, J., 2007. Regulatory effects of vasoactive intestinal peptide on the migration of mature dendritic cells. Journal of Neuroimmunology 182, 48–54.

Williams, A.M., Probert, C.S.J., Stepankova, R., Tlaskalova-Hogenova, H., Phillips, A., Bland, P.W., 2006. Effects of microflora on the neonatal development of gut mucosal T cells and myeloid cells in the mouse. Immunology 119, 470–478.

Williams, J.W., Tjota, M.Y., Clay, B.S., Vander Lugt, B., Bandukwala, H.S., Hrusch, C.L., Decker, D.C., Blaine, K.M., Fixsen, B.R., Singh, H., Sciammas, R., Sperling, A.I., 2013. Transcription factor IRF4 drives dendritic cells to promote Th2 differentiation. Nature Communications 4, 1038.

Worbs, T., Bode, U., Yan, S., Hoffmann, M.W., Hintzen, G., Bernhardt, G., Förster, R., Pabst, O., 2006. Oral tolerance originates in the intestinal immune system and relies on antigen carriage by dendritic cells. The Journal of experimental medicine 203, 519–527.

Worthington, J.J., Fenton, T.M., Czajkowska, B.I., Klementowicz, J.E., Travis, M.A., 2012. Regulation of TGFβ in the immune system: An emerging role for integrins and dendritic cells. Immunobiology 217, 1259–1265.

Worthington, J.J., Kelly, A., Smedley, C., Bauché, D., 2015. Integrin αvβ8-Mediated TGF-β Activation by Effector Regulatory T Cells Is Essential for Suppression of T-Cell-Mediated Inflammation. Immunity.

Wu, L., D'Amico, A., Winkel, K.D., Suter, M., Lo, D., Shortman, K., 1998. RelB Is Essential for the Development of Myeloid-Related CD8α– Dendritic Cells but Not of Lymphoid-Related CD8α+ Dendritic Cells. Immunity 9, 839–847.

Yamane, Y., Perez, M., Edelson, R., Agostino, N., 1991. Endocytosis of the TCR/CD3 complex and the class-I major histocompatibility complex in a human T cell line. Cellular Immunology.

Yanagihara, S., Komura, E., Nagafune, J., Watarai, H., Yamaguchi, Y., 1998. EBI1/CCR7 Is a New Member of Dendritic Cell Chemokine Receptor That Is Up-Regulated upon Maturation. J Immunol 161, 3096–3102.

Yen, J.-H., Khayrullina, T., Ganea, D., 2008. PGE2-induced metalloproteinase-9 is essential for dendritic cell migration. Blood 111, 260–270.

Yona, S., Kim, K.-W., Wolf, Y., Mildner, A., Varol, D., Breker, M., Strauss-Ayali, D., Viukov, S., Guilliams, M., Misharin, A., Hume, D.A., Perlman, H., Malissen, B., Zelzer, E., Jung, S., 2012. Fate Mapping Reveals Origins and Dynamics of Monocytes and Tissue Macrophages under Homeostasis. Immunity 38, 1–13.

Yrlid, U., Cerovic, V., Milling, S., Jenkins, C.D., Klavinskis, L.S., MacPherson, G.G., 2006. A distinct subset of intestinal dendritic cells responds selectively to oral TLR7/8 stimulation. European Journal of Immunolgoy 36, 2639–2648.

Zahner, S.P., Kel, J.M., Martina, C.A.E., Brouwers-Haspels, I., van Roon, M.A., Clausen, B.E., 2011. Conditional Deletion of TGF-βR1 Using Langerin-Cre Mice Results in Langerhans Cell Deficiency and Reduced Contact Hypersensitivity. J Immunol 187, 5069–5076.

Zangi, L., Klionsky, Y.Z., Yarimi, L., Bachar-Lustig, E., Eidelstein, Y., Shezen, E., Hagin, D., Ito, Y., Takai, T., Reich-Zeliger, S., Lask, A., Milstein, O., Jung, S., Shinder, V., Reisner, Y., 2012. Deletion of cognate CD8 T cells by immature dendritic cells: a novel role for perforin, granzyme A, TREM-1, and TLR7. Blood 120, 1647–1657.

Zaph, C., Troy, A.E., Taylor, B.C., Berman-Booty, L.D., Guild, K.J., Du, Y., Yost, E.A., Gruber, A.D., May, M.J., Greten, F.R., Eckmann, L., Karin, M., Artis, D., 2007. Epithelial-cell-intrinsic IKK-|[bgr]| expression regulates intestinal immune homeostasis. Nature 446, 552–556.

Zeng, R., Bscheider, M., Lahl, K., Lee, M., Butcher, E.C., 2016. Generation and transcriptional programming of intestinal dendritic cells: essential role of retinoic acid. Mucosal Immunology 9, 183–193.

Zeng, R., Oderup, C., Yuan, R., Lee, M., Habtezion, A., Hadeiba, H., Butcher, E.C., 2012. Retinoic acid regulates the development of a gut-homing precursor for intestinal dendritic cells. Mucosal Immunology 6, 847–856.

Zhang, D.-H., Cohn, L., Ray, P., Bottomly, K., Ray, A., 1997. Transcription Factor GATA-3 Is Differentially Expressed in Murine Th1 and Th2 Cells and Controls Th2-specific Expression of the Interleukin-5 Gene. Journal of Biological Chemistry 272, 21597–21603.

Zheng, W.-P., Flavell, R.A., 1997. The Transcription Factor GATA-3 Is Necessary and Sufficient for Th2 Cytokine Gene Expression in CD4 T Cells. Cell 89, 587–596.